Second order gluonic contributions to physical quantities

Roelof Hamberg

Second order gluonic contributions to physical quantities

Second order gluonic contributions to physical quantities

Proefschrift

ter verkrijging van de graad van Doctor
aan de Rijksuniversiteit te Leiden, op gezag
van de Rector Magnificus Dr. L. Leertouwer,
hoogleraar in de faculteit der godgeleerdheid,
volgens besluit van het College van Dekanen
te verdedigen op donderdag 28 november 1991
te klokke 15.15 uur

door

Roelof Hamberg

geboren te Hardenberg in 1965

Promotiecommissie:

Promotor:	Prof.dr. F.A. Berends
Co–promotor:	Dr. W.L.G.A.M. van Neerven
Overige leden:	Prof.dr. H.J. Habing
	Prof.dr. J. Smith
	Prof.dr. B.Q.P.J. de Wit

Contents

Chapter 1

General introduction

Quantum Chromo Dynamics (QCD) is the commonly accepted theory of the strong interactions. The strong force acts among quarks and gluons, the constituents of hadrons such as protons and neutrons. It is one of the four basic interactions that are known, three of which have been unified in the standard model [1] while the quantum theory of gravity cannot be implemented in this model yet. All these theories have in common that they describe interactions through the exchange of intermediate bosons: gluons in QCD, the photon in QED, W– and Z–bosons in the weak model and gravitons in gravitation. The matter content of these models is constituted by fermions, such as quarks in QCD.

Historically, QCD developed from the quark[1] model. In the early sixties $SU(3)$ symmetry was introduced to classify the observed particles [2]. Accordingly, Gell–Mann and Zweig [3] postulated that hadrons are composite objects, made up of three quarks (baryons) or a quark–antiquark pair (mesons). The three fractionally charged constituents of hadrons are nowadays called up, down and strange quarks. Later on, one established at higher energies the existence of heavier quarks, called charm [4] and bottom [5]. A sixth quark named top can tacitly be assumed to exist, although there is no experimental confirmation for this fact. These different types of quarks are referred to as flavours.

To explain the baryon spectrum in a simple way, one had to assume that the three quarks are in a symmetrical state. However, these constituents are spin–$\frac{1}{2}$ objects obeying Fermi–Dirac statistics and thus, their combined state should be antisymmetric. A solution to this problem was proposed by Greenberg [6], who assumed quarks to obey three–fold parastatistics. The problem was definitely solved by the

[1]The name quark was introduced by M. Gell–Mann, who took it from James Joyce's Finnegan's Wake: 'Three quarks for Muster Mark'.

introduction of the internal quantum number colour and the additional hypothesis that only colour singlet ('colourless') states can occur as physical particles [7]. Also the $\pi^0 \to \gamma\gamma$ decay width [8] and the R–factor, defined in the e^+e^- scattering process [9], give evidence for the existence of three colours.

In 1968 the phenomenon 'scaling' [10] was observed at SLAC in the deep inelastic electron–proton scattering experiment[2] [11]. This means that at high energies the dynamics of this deep inelastic scattering (DIS) process becomes independent of the interaction scale. This fact can only be understood in essentially free field theories. However, when a quantum field theory becomes asymptotically free at high energies, only a minor deviation to scaling behaviour occurs. Non–abelian gauge field theories, formulated already in 1954 by Yang and Mills [12], were shown to exhibit this unique property: the coupling constant vanishes logarithmically for increasing energies [13].

The two concepts colour and local gauge invariance were put together into the (colour) $SU(3)$ gauge field theory QCD. As a consequence eight massless vector bosons emerge, which couple to colour and, because they carry colour themselves, couple also to each other. These bosons are the so–called gluons that 'glue' the quarks together. The gluon self–interactions contribute to the explanation of the experimental observation that neither quarks nor gluons have ever been isolated. This confinement of the hadronic constituents has never been proven rigorously within the context of QCD despite great efforts in the last few decades. It is an outstanding problem that can hopefully be solved by using non–perturbative techniques [14].

In this thesis we will restrict ourselves to perturbative QCD. The vanishing of the strong coupling constant at high energies justifies the application of an expansion around the free field theory in deep inelastic scattering processes. The separation of the hadronic bound state effects and the high energy behaviour of their cross sections can be described by two models. The oldest approach is the operator product expansion [15], which is only applicable to lepton–hadron scattering. The two energy scales of a hadronic cross section (i.e. the interaction scale and the hadron momentum) appear in two separate quantities, the Wilson coefficient and the operator matrix element. The latter is only measurable, whereas the first one can be calculated in the context of perturbative QCD. The second model has a much wider range of applicability. It was introduced by Feynman [16], who called it the parton model. Partons are the constituents of hadrons. According to this model the hadronic cross section is equal to the incoherent sum of partonic cross sections, which are weighted with so–called parton distribution functions (densities). Some years after the introduction

[2]This experiment was awarded the 1990 Nobel prize for physics.

of the parton model the partons were identified with the quarks and gluons of QCD. These two approaches, the operator product expansion and the parton model, are discussed in an introductory way in chapter two of this thesis.

The operator product expansion and the parton model both explained the observed 'scaling' behaviour in the DIS process. Inspired by the success of the parton model, Drell and Yan [17] formulated a mechanism for massive lepton pair production in deep inelastic hadron–hadron scattering processes. According to them the lepton pair is produced by a decaying, highly virtual photon that is created during the annihilation of a parton–antiparton pair from the two hadrons. Due to the success of their description, the production of massive lepton pairs in hadron–hadron scattering experiments is often referred to as the Drell–Yan (DY) process. The DY model predicts scaling of this process too, a fact that was confirmed by experimental data [18].

In spite of the promising models, which put the theory of strong interactions on the level of a predictive theory, consistent with the experiments up to some degree, it was not a satisfactory description of the strong force yet. Some years after the introduction of the parton model, deviations of scaling were observed in the DIS experiments [19]. Moreover, the normalisation constant needed to account for the discrepancy between the experimental DY data and the theoretical predictions, generally called K–factor, was rather large (about 2–3) [18]. In order to solve these problems one calculated higher order corrections (in the strong coupling constant α_s) to cross sections. The determination of higher order corrections is not so trivial, because the appearance of initial state divergences make the partonic cross sections undefined. However, Politzer [20] discovered that these mass singularities, which are due to the masslessness of both quarks and gluons, could be removed by renormalisation of the parton densities. This was true, because the DY and DIS processes contained the same initial state collinear divergences. The renormalisation procedure of the parton densities is called mass factorisation. It is equivalent to the renormalisation of the operator matrix elements, which appear in the operator product expansion.

The mass factorisation procedure yields the parton distribution functions interaction scale dependent. The latter dependence is determined by the anomalous dimensions of the operators, which appear in the operator product expansion. These anomalous dimensions can be calculated from the renormalisation procedure of the operators. However, the renormalisation of the gauge invariant operator that consists of gauge fields (the gluon operator) is not straightforward and has been subject to discussion for many years. Gross and Wilczek [21] discovered that the one loop calculation of the gluon operator yields singularities, which can only be removed by counter terms of some other, new operators. A very important question is whether or not these new counter terms influence the calculation of the anomalous dimension of the gluon operator at higher orders in the loop expansion. Solutions to this problem were proposed by Dixon and Taylor [22], Kluberg–Stern and Zuber [23] and Joglekar and Lee [24], but their work was not transparent and did not provide the definite solution to this problem. This became apparent when two groups actually calculated the two loop anomalous dimensions. The first group determined these quantities in a lightlike axial gauge [25], whereas the second group applied a covariant (the Feynman) gauge [26]. They found different results for the renormalisation constant of the gluon operator. This discrepancy is reconsidered and the problem of calculating the anomalous dimension in the Feynman gauge is solved in chapter three of this thesis.

After the discovery of mass factorisation, one was able to determine first order corrections to the DY cross section [27]. These corrections provided a partial solution for the problem of scaling violation as well as for the large K–factor. Nevertheless, in spite of the improved theoretical predictions in the context of QCD, one disliked the huge size of the first order corrections. The reliability of perturbative QCD becomes questionable when such large corrections appear. Only second order corrections can provide an argument to decide whether perturbative QCD is useless or not. However, it is not easy to calculate higher order subprocesses. Many people have tried to include good estimators for second order terms in order to improve QCD predictions [28], but only the complete calculation can reveal the nature of the perturbation series. This is the subject of chapter four, in which we calculate all second order contributions to the Drell–Yan K–factor.

References

[1] S.L. Glashow, Nucl. Phys. **22** (1961), 579; Phys. Rev. Lett. **14** (1965), 35; S. Weinberg, Phys. Rev. Lett. **19** (1967), 1264; A. Salam and J.C. Ward, Phys. Lett. **13** (1964), 168

[2] M. Gell–Mann, Phys. Rev. **125** (1962), 1067

[3] M. Gell–Mann, Phys. Lett. **8** (1964), 214; G. Zweig, CERN reports TH–401 and TH–412

[4] J.J. Aubert et al., Phys. Rev. Lett. **33** (1974), 1404; J.–E. Augustin et al., Phys. Rev. Lett. **33** (1974), 1406

[5] S.W. Herb et al., Phys. Rev. Lett. **39** (1977), 252; W.R. Innes et al., Phys. Rev. Lett. **39** (1977), 1240

[6] O.W. Greenberg, Phys. Rev. Lett. **13** (1964), 598

[7] M.Y. Han and Y. Nambu, Phys. Rev. **139** (1965), B1006; H. Fritzsch and M. Gell–Mann, Proc. 16th Int. Conf. on High Energy Physics, Chicago–Batavia, 1972, vol. 2, p. 135; M. Gell–Mann, Acta Phys. Austr. Suppl. **9** (1972), 733

[8] J. Steinberger, Phys. Rev. **76** (1949), 1180; J.C. Polkinghorne, Nuovo Cim. **8** (1958), 179, 781; S.L. Adler and W.A. Bardeen, Phys. Rev. **182** (1969), 1517; J.S. Bell and R. Jackiw, Nuovo Cim. **60** (1969), 47; R. Jackiw and K. Johnson, Phys. Rev. **182** (1969), 1459

[9] R. Jost and J.M. Luttinger, Helv. Phys. Acta **23** (1950), 201; T. Appelquist and H. Georgi, Phys. Rev. **D8** (1973), 4000; A. Zee, Phys. Rev. **D8** (1973), 4038

[10] J.D. Bjorken, Phys. Rev. **179** (1969), 1547

[11] D.H. Coward et al., Phys. Rev. Lett. **20** (1968), 292; E.D. Bloom et al., Phys. Rev. Lett. **23** (1969), 930; M. Breidenbach et al., Phys. Rev. Lett. **23** (1969), 935

[12] C.N. Yang and R.L. Mills, Phys. Rev. **96** (1954), 191

[13] H.D. Politzer, Phys. Rev. Lett. **30** (1973), 1346; D.J. Gross and F. Wilczek, Phys. Rev. Lett. **30** (1973), 1343; S. Coleman and D.J. Gross, Phys. Rev. Lett. **31** (1973), 851

[14] K.G. Wilson, Phys. Rev. **D10** (1974), 2445; J.M. Drouffe and C. Itzykson, Phys. Rep. **38C** (1978), 133; A. Hasenfratz and P. Hasenfratz, Ann. Rev. Nucl. Part. Sci. **35** (1985), 559

[15] K.G. Wilson, Cornell Report (1964), unpublished; Phys. Rev. **179** (1969), 1499

[16] R.P. Feynman, Phys. Rev. Lett. **23** (1969), 1415

[17] S.D. Drell and T.M. Yan, Phys. Rev. Lett. **25** (1970), 316; Ann. Phys. **66** (1971), 578

[18] G. Matthiae, Riv. Nuovo Cim. **4–3** (1981), 1; I.R. Kenyon, Rep. Prog. Phys. **45** (1982), 1261

[19] Y. Watanabe et al., Phys. Rev. Lett. **35** (1975), 898; C. Chang et al., Phys. Rev. Lett. **35** (1975), 901

[20] H.D. Politzer, Nucl. Phys. **B129** (1977), 301

[21] D.J. Gross and F. Wilczek, Phys. Rev. **D9** (1974), 980

[22] J.A. Dixon and J.C. Taylor, Nucl. Phys. **B78** (1974), 552; J.C. Taylor, Nucl. Phys. **B33** (1971), 436

[23] H. Kluberg–Stern and J.B. Zuber, Phys. Rev. **D12** (1975), 467

[24] S.D. Joglekar and B.W. Lee, Ann. of Phys. **97** (1976), 160; S.D. Joglekar, Ann. of Phys. **108** (1977), 233; **109** (1977), 210

[25] W. Furmanski and R. Petronzio, Phys. Lett. **97B** (1980), 437

[26] E.G. Floratos, D.A. Ross and C.T. Sachrajda, Nucl. Phys. **B152** (1979), 493; A. Gonzalez–Arroyo and C. Lopez, Nucl. Phys. **B166** (1980), 429; E.G. Floratos, C. Kounnas and R. Lacaze, Nucl. Phys. **B192** (1981), 417

[27] J. Kubar–André and F.E. Paige, Phys. Rev. **D19** (1979), 221; G. Altarelli, R.K. Ellis and G. Martinelli, Nucl. Phys. **B157** (1979), 461; B. Humpert and W.L. van Neerven, Nucl. Phys. **B184** (1981), 225; G. Parisi, Phys. Lett. **90B** (1980), 295

[28] G. Grunberg, Phys. Lett. **95B** (1980), 70, Erratum: **110B** (1982), 501; Phys. Rev. **D29** (1984), 2315; J.H. Christenson et al., Phys. Rev. Lett. **25** (1970), 1523

Chapter 2

Deep inelastic lepton–hadron scattering

2.1 Introduction

Deep inelastic lepton–hadron scattering is an important process, which provides us with information about the structure of hadrons and about the nature of strong interactions at high energies.

In figure 2.1 the deep inelastic scattering (DIS) process

$$\ell_1 + \mathrm{H} \rightarrow \ell_2 + \text{`X'} \tag{2.1.1}$$

is depicted, where the interaction is mediated by one of the vector bosons of the standard model ($V = \gamma$, $\mathrm{W}^{\pm}$ or Z). The symbols ℓ_1 and H refer to the incoming lepton and hadron, respectively. The scattered lepton is denoted by ℓ_2 and 'X' indicates any combination of hadronic states that is allowed by conservation of quantum numbers.

As shown in the figure, q represents the momentum of the vector boson, whereas k_i, p and p_X denote the momenta of ℓ_i, H and X, respectively. The mass of the hadron is M. Furthermore, we introduce some kinematical variables which are frequently used

$$Q^2 = -q^2, \tag{2.1.2}$$

$$\nu = \frac{p\cdot q}{M} \tag{2.1.3}$$

and

$$\tau = -\frac{q^2}{2p\cdot q}, \tag{2.1.4}$$

where ν and τ represent the energy transfer to the hadron in its rest frame and the Bjorken scaling variable, respectively. The inclusive cross section of the DIS process

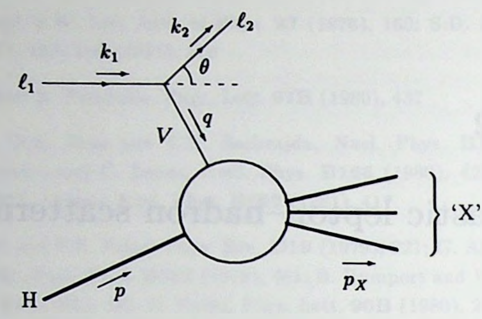

Fig. 2.1. The DIS process.

is obtained by averaging over the initial states and summing the final states, which in the rest frame of the hadron can be expressed by

$$\sigma = \frac{e^4}{4ME_1} \sum_{\ell_2, X} (2\pi)^4 \delta^4(p+q-p_X) \left| \langle \ell_1 | J_\mu^{\text{lepton}} | \ell_2 \rangle \langle \mathrm{H} | J_\nu^{\text{hadron}} | \mathrm{X} \rangle \mathcal{D}^{\mu\nu}(q^2) \right|^2. \quad (2.1.5)$$

The quantity $\mathcal{D}^{\mu\nu}(q^2)$ is the propagator of the vector boson and E_i are the energies of the incoming and outgoing leptons in the rest frame of the hadron. The quantities J_μ^{lepton} and J_ν^{hadron} are the lepton and hadron currents, respectively. The leptonic current is given by the standard model and equals

$$\langle \ell_1 | J_\mu^{\text{lepton}} | \ell_2 \rangle = -i\bar{u}(\ell_2)\gamma_\mu(v + a\gamma_5)u(\ell_1). \quad (2.1.6)$$

In this formula v and a denote the vector and axial parts of the vector boson coupling to the lepton pair, which for any lepton are given by

$$\begin{aligned} v_\ell^\gamma &= q_\ell, & a_\ell^\gamma &= 0, \\ v_\ell^Z &= \frac{1}{2\sin\theta_W\cos\theta_W}(I_3 - 2q_\ell\sin^2\theta_W), & a_\ell^Z &= \frac{-1}{2\sin\theta_W\cos\theta_W} I_3, \\ v_\ell^W &= \frac{1}{2\sqrt{2}\sin\theta_W}, & a_\ell^W &= \frac{-1}{2\sqrt{2}\sin\theta_W}, \end{aligned} \quad (2.1.7)$$

where q_ℓ describes the charge of the lepton (in units of the elementary charge e), θ_W is the weak mixing angle and I_3 denotes the weak isospin of the lepton ($I_3 = \pm\frac{1}{2}$).

The hadronic current is theoretically less well known, but some characteristics are described in the context of perturbative QCD.

The vector boson propagator is usually considered in the convenient Feynman–'t Hooft gauge, where it has the particular form

$$\mathcal{D}_{\mu\nu}(q^2) = \frac{-ig_{\mu\nu}}{q^2 - M_V{}^2}, \tag{2.1.8}$$

where M_V is the mass of the vector boson. The expression for the differential cross section reduces to

$$\frac{d^2\sigma}{dQ^2 d\nu} = \frac{\pi\alpha^2}{\left(q^2 - M_V{}^2\right)^2 E_1{}^2 M} L^{\mu\nu} W_{\mu\nu}, \tag{2.1.9}$$

where $\alpha = e^2/4\pi$ is the fine structure constant. The leptonic tensor $L^{\mu\nu}$ can be calculated in electroweak theory and is equal to

$$L^{\mu\nu} = 4(v^2 + a^2)\left[k_1^\mu k_2^\nu + k_1^\nu k_2^\mu - g^{\mu\nu} k_1 \cdot k_2\right] - 8iva\epsilon^{\mu\nu\sigma\lambda} k_{1\sigma} k_{2\lambda}, \tag{2.1.10}$$

where the lepton masses are neglected and v and a are given in eq. 2.1.7. The last term of eq. 2.1.10 is absent in pure electromagnetic processes due to parity conservation. The hadronic tensor $W_{\mu\nu}$ is given by

$$\begin{aligned} W_{\mu\nu} &\equiv \frac{1}{4\pi} \sum_X (2\pi)^4 \delta^4(q + p - p_X) \langle \mathrm{H}|J_\mu^\dagger(0)|\mathrm{X}\rangle\langle \mathrm{X}|J_\nu(0)|\mathrm{H}\rangle & (2.1.11) \\ &= \frac{1}{4\pi} \int d^4x\, e^{iqx} \langle \mathrm{H}|J_\mu^\dagger(x) J_\nu(0)|\mathrm{H}\rangle \\ &= \frac{1}{4\pi} \int d^4x\, e^{iqx} \langle \mathrm{H}|\left[J_\mu^\dagger(x), J_\nu(0)\right]|\mathrm{H}\rangle. & (2.1.12) \end{aligned}$$

The second line follows from translational invariance, whereas the last equality can be shown to hold by using spectrum conditions (the hadron is stable, this implies $p_X^0 \geq p^0$, from which one can see that the second term of the commutator does not contribute to the integral). The tensor $W_{\mu\nu}$ cannot easily be calculated within the context of a well-known field theory and therefore plays a central role in the theoretical problems concerning the DIS process. The fact that $W_{\mu\nu}$ is the Fourier transform of the expectation value of a causal commutator between one particle states, is very important, as we will see later on.

Lorentz and time-reversal invariance lead to the following expression for this tensor

$$\begin{aligned} W_{\mu\nu}(\tau, Q^2) &= -\left(g_{\mu\nu} - \frac{q_\mu q_\nu}{q^2}\right) F_1(\tau, Q^2) + \\ &\quad + \left(p_\mu - \frac{p\cdot q}{q^2} q_\mu\right)\left(p_\nu - \frac{p\cdot q}{q^2} q_\nu\right) \frac{\tau}{M\nu} F_2(\tau, Q^2) + \\ &\quad - \frac{1}{2} i\epsilon_{\mu\nu\sigma\lambda} p^\sigma q^\lambda \frac{1}{M\nu} F_3(\tau, Q^2), & (2.1.13) \end{aligned}$$

provided we assume that the hadron (weak) current is conserved at high energies. We have chosen dimensionless hadronic structure functions F_i. The decomposition of the hadronic tensor enables us to express the cross section of the DIS process in terms of the structure functions F_i. In the rest frame of the hadron this leads to

$$\frac{d^2\sigma}{dQ^2 d\nu} = \frac{4\pi\alpha^2}{(q^2 - M_V{}^2)^2}\frac{E_2}{E_1 M}\left((v^2 + a^2)\left(2F_1 \sin^2\frac{\theta}{2} + \frac{M}{\nu}F_2\cos^2\frac{\theta}{2}\right)\right.$$
$$\left. + 2va\frac{E_1 + E_2}{\nu}F_3 \sin^2\frac{\theta}{2}\right), \qquad (2.1.14)$$

where θ is the lepton scattering angle (see fig. 2.1). As in the leptonic case (see below 2.1.10) the structure function F_3 drops out in pure electromagnetic processes due to parity conservation.

Bjorken [1] was the first to suggest scale independence for the structure functions in the deep inelastic region. This statement is equivalent to the following claim: if the structure functions, which are dependent on τ and Q^2, are considered in the region of very large Q^2, they will appear to become functions of the variable τ only and their Q^2–dependence will drop out. Immediately after his suggestion, experimental confirmation was found by the electron–proton experiment carried out at SLAC [2]. This confirmation provided a clue for theoretical physicists how to describe the gross features of the hadronic structure tensor. The scale independence of the structure functions could originally be explained in two different, but equivalent ways, i.e. the operator product expansion [3] and the parton model [4]. Both approaches start from the experimentally satisfied condition that Q^2 is very large. In this situation one can study $W_{\mu\nu}$ in the Bjorken limit, which is defined by $Q^2 \to \infty$, while τ stays fixed. Later on, both methods were unified in the context of perturbative QCD. Perturbative QCD can predict interesting properties of certain physical quantities, like scaling deviations which were found [5] a few years after the discovery of scale independence. These deviations can be explained by higher order QCD corrections, which predict the scale evolution of the moments of the hadronic structure functions [6].

In the next section we will discuss the first approach. One might consider the integral representation of $W_{\mu\nu}$ (eq. 2.1.12) and ask which part of the integration region is most important. This leads to a light–cone view of the DIS process and subsequently to the operator product expansion (OPE). Secondly, in section 2.3 we will consider the hadronic states in eq. 2.1.11 as a superposition of pointlike objects. Non–relativistic perturbation theory in an infinite momentum frame together with the neglect of transverse momentum of the constituents lead to the parton model of inelastic scattering processes.

Broken scale invariance is one of the main topics of this thesis. It does not only provide a falsifiable quantity in order to test perturbative QCD, but it also involves the renormalisation of composite objects within a non-abelian field theory, which is still a very complicated problem in theoretical physics.

2.2 The operator product expansion

As we stated in the preceding introduction, the main theoretical problem of the DIS process is the calculation of the structure functions F_i or, equivalently, the calculation of the hadronic structure tensor $W_{\mu\nu}$. Probing the hadron through the exchange of a vector boson with a large momentum, one has a starting point for a theoretical description. In this section we will give the approach of the operator product expansion (OPE), applied to the product of the hadronic currents, which was first proposed by Wilson [3] and later proven to hold in free field theories and some simple interacting field theories [7]. The Callan–Symanzik equation [8], applied to the OPE, yields the scale dependence of the Wilson coefficient functions. This result reveals why one is interested in the renormalisation of the operator matrix elements (OME's). Another important property is the existence of a one–to–one correspondence between the ultraviolet (UV) singularities of the operator renormalisation constants and the mass divergences emerging from the QCD radiative corrections to various parton subprocesses appearing in deep inelastic scattering. This makes the calculation of operator renormalisation constants also relevant within the context of the parton model (see section 2.3).

2.2.1 Light–cone dominance

One way to tackle to the specification of the hadronic tensor $W_{\mu\nu}$ starts at considering the integral representation 2.1.12 in the Bjorken limit, i.e. $Q^2 \to \infty$ and τ fixed. The kinematical variables in the rest frame of the hadron can be parametrised by

$$\begin{aligned} p &= (M,\vec{0}), \\ q &= (q_0,\vec{0}_\perp,q_3). \end{aligned} \tag{2.2.1}$$

From the definition of ν in eq. 2.1.3 it follows $\nu = q_0$. Expressing q_3 in terms of the kinematical variables in the limit $\nu \to \infty$ leads to $q_3 \to \nu + M\tau$. Therefore, the inner product in the exponent of eq. 2.1.12 can be written as

$$q\cdot x = \nu(x_0 - x_3) - M\tau x_3 \tag{2.2.2}$$

The Riemann–Lebesgue theorem [9] tells us that the dominant contributions to the hadronic tensor come from the integration region where the phase of the exponent is stationary. Of course, this is only true if the remaining part of the integrand does not exhibit too large phase fluctuations. Assuming the latter restriction to be satisfied, we meet the stationary phase condition if

$$\begin{aligned} |x_0 - x_3| &= \mathcal{O}\left(\frac{1}{\nu}\right), \\ |x_3| &= \mathcal{O}\left(\frac{1}{M\tau}\right). \end{aligned} \tag{2.2.3}$$

Since the region $x^2 = (x_0 - x_3)(x_0 + x_3) - x_\perp^2 < 0$ is excluded, due to causality of the current commutator in eq. 2.1.12, and $(x_0 - x_3)(x_0 + x_3) = \mathcal{O}(1/M\tau\nu)$ is suppressed by the factor ν, it can be concluded that the contributing $x_\perp$-components

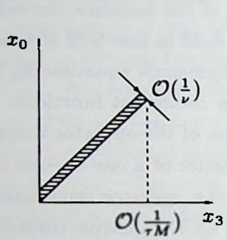

Fig. 2.2. Support of the integrand of $W_{\mu\nu}$.

are also suppressed by a factor $1/\nu$. As a result, in the Bjorken limit the exponent in eq. 2.1.12 becomes stationary in the region

$$0 < x^2 = \mathcal{O}\left(\frac{1}{Q^2}\right). \tag{2.2.4}$$

The support of the integral is sketched in figure 2.2. It shows that the tensor $W_{\mu\nu}$ only receives contributions coming from the light–cone region of the commutator of the two hadronic currents. This is called light–cone dominance [10].

2.2.2 The Wilson hypothesis

In this section we will formulate the operator product expansion, which is an adequate tool to handle the product of the two currents, showing up in the expression for the hadronic tensor $W_{\mu\nu}$ in eq. 2.1.12. As we will see, this product can be expanded in a more manageable form.

The original version of Wilson's hypothesis [3] stated that a product of two operators, that becomes singular when the distance between the points at which the operators act approaches zero, can be written as

$$A(x)B(0) \stackrel{x_\mu \to 0}{\longrightarrow} \sum_{i=0}^{n} C_i(x) O_i(0). \tag{2.2.5}$$

In this formula, the O_i constitute a finite set of n local operators, which can be constructed by means of the fundamental fields of the theory. The operators are understood to be regular at $x = 0$. The whole singular behaviour at the right-hand side of eq. 2.2.5 can be attributed to the quantities C_i (the so-called Wilson coefficients). These quantities have to be interpreted in a distributional sense (generalised functions [9]). The operator product expansion was proven by Zimmermann [7] within perturbation theory through application of the BPHZ method.

Operator product expansions, like in eq. 2.2.5, can be formulated for several types of products, like the time-ordered product, or a commutator of two operators. In fact, the whole idea has its origin in Wick's normal ordering theorem [11], which relates the time-ordered product of two operators to a normal ordered product and a singular distribution. For instance, for two fields ϕ it says

$$T\left(\phi(x)\phi(0)\right) = \underbrace{\phi(x)\phi(0)}\, \mathbb{1} + :\phi(x)\phi(0):, \tag{2.2.6}$$

where $\mathbb{1}$ and $:\phi(x)\phi(0):$ are regular operators, while the contraction $\underbrace{\phi(x)\phi(0)}$ is a singular function (the Feynman propagator).

However, we need a light-cone expansion rather than a short distance expansion for the current commutator in eq. 2.1.12 (see section 2.2.1). Therefore, we want to express the product of two hadronic (weak) currents near the light-cone. It can be proven (in free field, ϕ^4 and Yukawa theories), that such an expansion exists. It can be written like

$$A(x)B(0) \stackrel{x^2 \to 0}{\longrightarrow} \sum_{i=0}^{\infty} C_i(x^2) O_i(0), \tag{2.2.7}$$

where the C_i denote the Wilson coefficients, which are singular as $x^2 \to 0$. Note that there are now infinitely many operators. This is due to the fact, that such an expansion involves more than one quantity which becomes asymptotic [7]. In the Bjorken limit of the scattering process under consideration this amounts to taking the limit of $Q^2 \to \infty$ and $p \cdot q \to \infty$.

We want to exemplify such an expansion here by considering the electromagnetic current of free fermions,

$$J_\mu(x) =: \overline{\psi}(x)\gamma_\mu\psi(x): . \tag{2.2.8}$$

The time–ordered product of two such currents can be written as (using the Wick expansion)

$$T\left(J_\mu(x)J_\nu(0)\right) = -\frac{1}{\pi^4}\frac{g_{\mu\nu}x^2 - 2x_\mu x_\nu}{\left(x^2 - i\epsilon\right)^4}1 + \frac{i}{2\pi^2}\frac{x^\lambda}{\left(x^2 - i\epsilon\right)^2}$$
$$\times \sum_{m=0}^{\infty}\left(1 - (-1)^m\right) x_{\mu_1}\ldots x_{\mu_m}\left(s_{\mu\lambda\nu\sigma}O^{\sigma\mu_1\ldots\mu_m}(0) - i\epsilon_{\mu\lambda\nu\sigma}O_5^{\sigma\mu_1\ldots\mu_m}(0)\right)$$
$$+ \text{ non–singular terms}, \tag{2.2.9}$$

where we made use of the identity $\gamma_\mu\gamma_\lambda\gamma_\nu = s_{\mu\lambda\nu\sigma}\gamma^\sigma - i\epsilon_{\mu\lambda\nu\sigma}\gamma^\sigma\gamma^5$, with $s_{\mu\lambda\nu\sigma} = g_{\mu\lambda}g_{\nu\sigma} + g_{\mu\sigma}g_{\nu\lambda} - g_{\mu\nu}g_{\lambda\sigma}$. The operators are defined by

$$\begin{aligned} O^{\sigma\mu_1\ldots\mu_m}(y) &= \frac{1}{m!}:\overline{\psi}(y)\gamma^\sigma\partial^{\mu_1}\ldots\partial^{\mu_m}\psi(y):, \\ O_5^{\sigma\mu_1\ldots\mu_m}(y) &= \frac{1}{m!}:\overline{\psi}(y)\gamma^\sigma\gamma^5\partial^{\mu_1}\ldots\partial^{\mu_m}\psi(y):. \end{aligned} \tag{2.2.10}$$

The expansion 2.2.9 is exact in free field theory. It is clear that the sum in eq. 2.2.9 only extends to infinity in the light–cone limit and not in the short distance limit.

2.2.3 The operator product expansion applied to structure functions

In the DIS process, the product of two hadronic currents is important. It is convenient (see previous section) to consider the time–ordered product of these two currents, though this is not necessary. The corresponding hadronic quantity can be identified with the forward virtual Compton scattering amplitude and is related to $W_{\mu\nu}$ by the optical theorem. It can be written as follows

$$T_{\mu\nu} = \frac{i}{2}\int d^4x\, e^{iqx}\langle \mathrm{H}|T\left(J_\mu(x)J_\nu(0)\right)|\mathrm{H}\rangle. \tag{2.2.11}$$

This tensor can be expressed in structure functions T_i, analogous to the decomposition of $W_{\mu\nu}$ into functions F_i. The optical theorem relates these structure functions by

$$\mathrm{Im}\, T_i(\tau, Q^2) = \pi F_i(\tau, Q^2). \tag{2.2.12}$$

This theorem makes it possible to derive the following dispersion relation:

$$\begin{aligned} T_i(\tau, Q^2) &= \frac{1}{\pi}\int_0^1 d\tau'\,\frac{\mathrm{Im}\, T_i(\tau', Q^2)}{\tau' - \tau} = \int_0^1 d\tau'\,\frac{F_i(\tau', Q^2)}{\tau' - \tau} \\ &= \sum_{m=1}^{\infty}\frac{1}{\tau^m}\int_0^1 d\tau'\,(\tau')^{m-1}F_i(\tau', Q^2), \end{aligned} \tag{2.2.13}$$

which can be used later on in order to derive a simple relation for the moments of F_i. In view of the decomposition in structure functions, the operator product expansion takes the following form

$$\frac{1}{2}iT\left(J_\mu(x)J_\nu(0)\right) \overset{x^2\to 0}{\longrightarrow} \sum_{m,j}\Big[-i^m \left(g_{\mu\nu} - \Box^{-1}\partial_\mu\partial_\nu\right)\partial_{\mu_1}\ldots\partial_{\mu_m}C_{j,1}^{(m)}(x^2)$$
$$-\frac{1}{2}i^m\left(g_{\mu\mu_1} - \Box^{-1}\partial_\mu\partial_{\mu_1}\right)\left(g_{\nu\mu_2} - \Box^{-1}\partial_\nu\partial_{\mu_2}\right)\partial_{\mu_3}\ldots\partial_{\mu_m}\Box C_{j,2}^{(m)}(x^2)$$
$$+\frac{1}{2}i^{m+1}\epsilon_{\mu\nu\lambda\mu_1}\partial^\lambda\partial_{\mu_2}\ldots\partial_{\mu_m}C_{j,3}^{(m)}(x^2)\Big]\, O_j^{\mu_1\ldots\mu_m}(0). \tag{2.2.14}$$

The summation index j runs over the set of possible operators in the model, while the sum over m extends to infinity. Dimensional analysis shows that the strength of the singularities of the functions $C_j^{(m)}$ depends on the twist of the operators $O_j^{\mu_1\ldots\mu_m}$, which is defined as

$$\tau_j \equiv \dim O_j^{\mu_1\ldots\mu_m} - \text{spin } O_j^{\mu_1\ldots\mu_m} = \dim O_j^{\mu_1\ldots\mu_m} - m. \tag{2.2.15}$$

The singularities become stronger as the twists of the operators lower. The operators with lowest twist are the most important ones (here $\tau_j = 2$). Operators with higher twist lead to suppression factors $p^2/Q^2 = M^2/Q^2$ in the structure functions T_i and F_i. Therefore, only the lowest twist operators are contributing in the expansion 2.2.14.

In the special case of QCD, all twist–2 operators can be classified according to their flavour group representation. They represent two classes:

1. The non–singlet quark operator

$$O_{q,r}^{\mu_1\ldots\mu_m}(x) = \frac{i^{m-1}}{2}\mathcal{S}\left[\overline{\psi}(x)\gamma^{\mu_1}D^{\mu_2}\ldots D^{\mu_m}(1\pm\gamma_5)\frac{\lambda_r}{2}\psi(x)\right] + \text{trace terms}. \tag{2.2.16}$$

2. The singlet quark and gluon operators

$$O_{q}^{\mu_1\ldots\mu_m}(x) = \frac{i^{m-1}}{2}\mathcal{S}\left[\overline{\psi}(x)\gamma^{\mu_1}D^{\mu_2}\ldots D^{\mu_m}(1\pm\gamma_5)\psi(x)\right] + \text{trace terms} \tag{2.2.17}$$

and

$$O_{g}^{\mu_1\ldots\mu_m}(x) = \frac{i^{m-2}}{2}\mathcal{S}\left[F_\alpha^{\alpha\mu_1}(x)D^{\mu_2}\ldots D^{\mu_{m-1}}F^{\alpha\alpha\mu_m}(x)\right] + \text{trace terms}. \tag{2.2.18}$$

Here S denotes the symmetrisation of the operators in their Lorentz indices μ_i and the trace terms are necessary to make these operators traceless. The λ_r in eq. 2.2.16 refer to matrices in flavour space, whereas the index a in eq. 2.2.18 stands for the colour index. These properties follow from the fact that according to Wilson's hypothesis, it is sufficient to consider the operators which belong to irreducible representations of the internal $(SU(3)_F,\ SU(3)_C)$ and the external (conformal) group.

Returning to the general case of eq. 2.2.14, the matrix elements of the operators $O_j^{\mu_1 \ldots \mu_m}$ can be expressed in the following way

$$\langle \mathrm{H}|O_j^{\mu_1 \ldots \mu_m}|\mathrm{H}\rangle = A_j^{(m)}(p^2)(p^{\mu_1} \ldots p^{\mu_m} + \text{ trace terms}), \tag{2.2.19}$$

since the operators are completely traceless and symmetric (they are in an irreducible representation of the Lorentz group, as we noticed already in the specific case of QCD operators). Using the expression of the matrix elements of the operators, one can take the Fourier transform of the OPE (eq. 2.2.14) like in eq. 2.2.11. In leading twist the structure functions T_i become equal to

$$T_i(\tau, Q^2) = \sum_{m,j} \left(\frac{1}{2\tau}\right)^m \tilde{C}_{j,i}^{(m)}(Q^2) A_j^{(m)}(p^2), \tag{2.2.20}$$

upon defining the Fourier transforms of the coefficients $C_{j,i}^{(m)}$ as

$$\tilde{C}_{j,i}^{(m)}(Q^2) = \left(Q^2\right)^m \int d^4x\, e^{iqx} C_{j,i}^{(m)}(x^2). \tag{2.2.21}$$

The optical theorem enables us to relate the expressions from eq. 2.2.20 to the hadronic structure functions F_i. The combination of the dispersion relation 2.2.13 and eq. 2.2.20 yields the following sum rules

$$F_i^{(m)}(Q^2) \equiv \int_0^1 d\tau\, \tau^{m-1} F_i(\tau, Q^2) = \frac{1}{2^m} \sum_j \tilde{C}_{j,i}^{(m)}(Q^2) A_j^{(m)}(p^2), \tag{2.2.22}$$

where $F_i^{(m)}$ is called the Mellin transform of $F_i(\tau)$. The expression states that the moments (Mellin transforms) of the structure functions F_i are related to the Wilson coefficients of the leading operators with spin m which show up in the OPE 2.2.14. The operator matrix elements (OME) are uncalculable, because of the lack of a suitable non–perturbative method in QCD. However, the coefficients $\tilde{C}_{j,i}^{(m)}$ can be calculated in perturbative QCD. One simply considers the moments of the hadronic structure function and the OME in the case of quarks and gluons. The coefficients are obtained by matching the tensor structures on both sides. The lowest order calculation in QCD shows scaling of the structure functions in the Bjorken limit. Higher order corrections to these matrix elements involve the renormalisation of the operators that occur in the OPE. This renormalisation procedure will cause a Q^2-evolution of the coefficients that is determined by the renormalisation group equation. The discussion of Q^2-dependences will be the subject of the next section.

2.2.4 Callan–Symanzik equation for operator matrix elements

At the end of the previous section, it was made clear that the moments of structure functions are connected to the Wilson coefficients of the operators from the product expansion. This was considered in the most general case, in which $A_j^{(m)}(p^2)$ belonged to the expectation value of an operator between hadronic states. However, like in the case of the parton model, the OPE is usually embedded in QCD.

The Lagrangian of QCD contains quarks, gluons and, in a general covariant gauge, ghosts. The quantised theory involves the construction of states, built out of the physical particles. Bearing this in mind, we introduce as an analogy of eq. 2.2.19 the following operator matrix element

$$\langle p,j|O_i^{\mu_1\cdots\mu_m}|p,j\rangle = p^{\mu_1}\ldots p^{\mu_m}\mathcal{A}_{ij}^{(m)}(p^2) + \text{ trace terms,} \tag{2.2.23}$$

where i,j indicate particle types and $O_i^{\mu_1\cdots\mu_m}$ is one of the twist–2 operators in QCD (see eqs. 2.2.16–2.2.18). The matrix element is considered to be renormalised. The moments of the structure functions can be generalised to equivalent quantities, belonging to processes with QCD particles. In view of eq. 2.2.22 we introduce the following equation at the particle level

$$\mathcal{F}_j^{(m)}\left(g(\mu^2),\frac{Q^2}{p^2}\right) = \sum_i \tilde{C}_i^{(m)}\left(g(\mu^2),\frac{Q^2}{\mu^2}\right)\mathcal{A}_{ij}^{(m)}\left(g(\mu^2),\frac{p^2}{\mu^2}\right), \tag{2.2.24}$$

where all dependences are explicitly shown, but where the index that labels the structure functions is left out. The index j labels a particle type in this equation! The variables g and μ^2 are introduced; they denote the renormalised coupling constant and the scale at which the renormalisation took place, respectively. Notice that in principle there are two scales. The first one is the scale that appears in the argument of the renormalised coupling constant $g(\mu^2)$. The second one is the operator renormalisation scale, which scales the momentum p^2 in eq. 2.2.24. The latter can be identified with the mass factorisation scale (cf. eq. 2.3.6). For convenience, we will put the two scales equal to each other. All functions in eq. 2.2.24 are dimensionless (at least at the twist–2 level), which enables us to give the dependences on momenta as quotients.

The operator matrix element that occurs in eq. 2.2.24 has the following multiplicative renormalisation property

$$\hat{\mathcal{A}}_{ij}^{(m)}(\hat{g},p^2) = \sum_k Z_{ik}^{(m)}(g(\mu^2))\mathcal{A}_{kj}^{(m)}\left(g(\mu^2),\frac{p^2}{\mu^2}\right), \tag{2.2.25}$$

where the hatted quantities denote the unrenormalised (bare) ones. In the literature one often replaces matrix elements by vacuum expectation values of time–ordered products in which the particle fields are included. This leads to another formulation of renormalisation properties, which includes the anomalous dimensions of the particle fields as well. However, the equality that will be given for the coefficients $\tilde{\mathcal{C}}_i^{(m)}$ (see eq. 2.2.29) is not changed by this procedure.

Since the bare, unrenormalised quantities are independent of the scale μ, one can derive the following renormalisation group equations (or Callan–Symanzik equations) for the structure functions and the operator matrix elements

$$\left(\mu\frac{\partial}{\partial\mu}+\beta(g)\frac{\partial}{\partial g}\right)\mathcal{F}_j^{(m)}\left(g(\mu^2),\frac{Q^2}{p^2}\right)=0, \tag{2.2.26}$$

$$\sum_k\left[\left(\mu\frac{\partial}{\partial\mu}+\beta(g)\frac{\partial}{\partial g}\right)\delta_{ik}+\gamma_{ik}^{(m)}\right]\mathcal{A}_{kj}^{(m)}\left(g(\mu^2),\frac{p^2}{\mu^2}\right)=0, \tag{2.2.27}$$

where the following abbreviations have been introduced

$$\beta(g(\mu^2))\equiv\mu\frac{\partial g(\mu^2)}{\partial\mu},\qquad \gamma\equiv\mu\frac{\partial\ln Z}{\partial\mu}. \tag{2.2.28}$$

The quantities β and γ are the well–known β–function and the general definition of an anomalous dimension, respectively, where in the latter case Z denotes a general renormalisation constant. Combining the two differential equations, one can deduce for the Wilson coefficients

$$\left[\left(\mu\frac{\partial}{\partial\mu}+\beta(g)\frac{\partial}{\partial g}\right)\delta_{ik}-\gamma_{ik}^{(m)}\right]\tilde{\mathcal{C}}_i^{(m)}\left(g(\mu^2),\frac{Q^2}{\mu^2}\right)=0. \tag{2.2.29}$$

It is convenient to introduce a logarithmic variable

$$t\equiv\frac{1}{2}\ln\left(\frac{\mu^2}{Q^2}\right). \tag{2.2.30}$$

Subsequently, we can write the Callan–Symanzik (CS) equation for the Wilson coefficients as follows

$$\left[\left(\frac{\partial}{\partial t}+\beta(g(t))\frac{\partial}{\partial g}\right)\delta_{ik}-\gamma_{ik}^{(m)}\right]\tilde{\mathcal{C}}_i^{(m)}(g(t),t)=0. \tag{2.2.31}$$

By solving the following set of equations for the coupling constant g,

$$\begin{aligned} \frac{dg(t)}{dt} &= \beta(g(t)), \\ g(0) &= g_0, \end{aligned} \tag{2.2.32}$$

it is possible to make the implicit t–dependence of g in the Wilson coefficient explicit. This is the procedure of introducing a running coupling constant, in which the actual value of g_0 is extracted from experiment. When the solution of eq. 2.2.32 (the running coupling constant) is substituted into the expression for the Wilson coefficients, the β–term drops out of the CS equation and the latter is equally well described by

$$\frac{d}{dt}\bar{C}_k^{(m)}(g_0,t) = \gamma_{ik}^{(m)}(g_0,t)\bar{C}_i^{(m)}(g_0,t), \tag{2.2.33}$$

where the t–dependence is explicit and the corresponding partial and total derivatives can be interchanged. The solution can formally be written as

$$\bar{C}_k^{(m)}(g_0,t) = \left[T\exp\left\{\int_{t_0}^{t} dt'\,\gamma(g_0,t')\right\}\right]_{ik}^{(m)} \bar{C}_i^{(m)}(g_0,t_0), \tag{2.2.34}$$

where T–ordering is necessary, because the matrices γ do not commute in general. Another way to solve the CS equations is obtained by a solution for t in terms of the coupling constant g. In that case, the formal expression reads

$$\bar{C}_k^{(m)}(g,t_0) = \left[T\exp\left\{\int_{g_0}^{g} dg'\,\frac{\gamma(g',t_0)}{\beta(g',t_0)}\right\}\right]_{ik}^{(m)} \bar{C}_i^{(m)}(g_0,t_0). \tag{2.2.35}$$

In both cases the expressions for the coefficients reveal that the scale dependence is governed by the anomalous dimensions $\gamma_{ik}^{(m)}$. The calculation of these quantities

$$\gamma_{ik}^{(m)} = \mu\frac{\partial}{\partial\mu}\left[\ln Z^{(m)}\right]_{ik} \tag{2.2.36}$$

at higher orders involves the renormalisation of the operators of the OPE. In the case of identical quantum numbers the matrix Z_{ik} gets off–diagonal non–zero elements and mixing of operators occurs. A discussion of operator mixing and renormalisation at one loop is given by several authors [6]. We want to study this complication in detail in chapter 3, specified to the case of mixing between gluon and ghost operators. This is not entirely the same problem as genuine operator mixing (because ghost operators do not appear in the Wilson expansion), but it should be studied in order to perform renormalisation of the gluon operator in a covariant gauge.

2.3 The parton model

The parton model [4] is an alternative approach to study deep inelastic structure functions. In this model hadrons are considered to be complex syntheses of underlying constituents, the so–called partons. However, the interactions between these partons only show up in a set of measurable quantities, i.e. the parton distribution functions. Theoretically, these functions are just a set of parameters. When a collision takes place, the partons are considered to be observed in a frozen state; effectively, the parton model deals with them as if they were free particles. This enables us to consider the scattering process as a weighted, incoherent sum of parton scattering processes, cross sections of which are calculable within a dynamical theory describing the partons, such as QCD. The idea is shown in figure 2.3. The infinite momentum

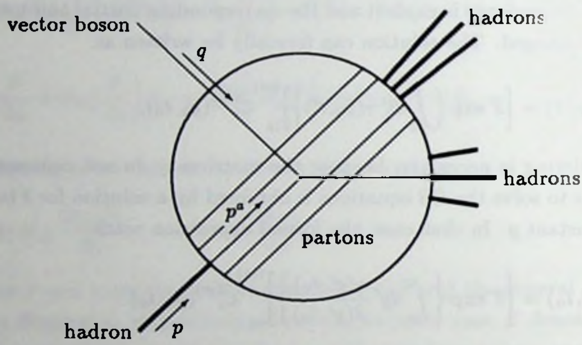

Fig. 2.3. The parton picture of deep inelastic scattering.

frame technique and the assumption of negligible transverse momenta of the partons provide a justification for the parton model. Moreover, the lowest order results reproduce those of the operator product expansion.

In the next section we will show that already a very simple assumption about the nature of partons reproduces some important, experimentally verified phenomena. Higher order QCD corrections will contain collinear divergences, which make mass factorisation necessary. This technique is the subject of the last subsection and it will be shown that anomalous dimensions enter the discussion again.

2.3.1 A simple parton model

A hadron is described by a set of distribution functions $f_a^{\mathrm{H}}(\xi)$, which give the probability of finding a parton a, which carries a momentum fraction ξ of its parent hadron. Due to infinite momentum frame arguments, ξ can only take values in the range $0 < \xi < 1$. According to this definition, the hadronic structure tensor takes the form

$$W_{\mu\nu}(\tau, Q^2) = \frac{1}{4\pi}\sum_a \int_0^1 d\xi \int_0^1 dx\, f_a^{\mathrm{H}}(\xi)\, \mathcal{W}_{\mu\nu}^a(x, Q^2)\, \delta(\tau - \xi x), \tag{2.3.1}$$

where $\mathcal{W}_{\mu\nu}^a$ denotes the parton structure tensor, belonging to the subprocess of parton a. The argument of the hadronic tensor, τ, is replaced by x, which is the equivalent of the Bjorken scaling variable at the parton level. Using $p^a = \xi p$ (p^a is the momentum of the incoming parton, cf. fig. 2.3), we must have $\xi x = \tau$, which is expressed by the δ-function.

Let us assume that the electromagnetic parton current takes the simple form

$$\langle a|j_\mu^a(x)|a\rangle = -ie_a\bar{u}^a\gamma_\mu u^a, \tag{2.3.2}$$

where the partons are considered to be spin-$\frac{1}{2}$ particles and e_a is the charge of the parton. For the lowest order contribution to the parton structure tensor one finds

$$\mathcal{W}_{\mu\nu}^a(x, Q^2) = \frac{2\pi e_a^2}{q\cdot p^a}\delta(1-x)\left[2p_\mu^a p_\nu^a + p_\mu^a q_\nu + q_\mu p_\nu^a - g_{\mu\nu} q\cdot p^a\right]. \tag{2.3.3}$$

Substitution of the expression 2.3.3 into eq. 2.3.1 reveals, after projection onto the structure functions F_1 and F_2 (F_3 is absent in this pure electromagnetic example),

$$\begin{aligned} F_1(\tau, Q^2) &= \tfrac{1}{2}\sum_a e_a^2 f_a^{\mathrm{H}}(\tau), \\ F_2(\tau, Q^2) &= \sum_a e_a^2 f_a^{\mathrm{H}}(\tau). \end{aligned} \tag{2.3.4}$$

As we can infer from these results, the lowest order calculations predict the following features:

- The Callan–Gross relation [12] holds: $F_2 = 2F_1$.
- The structure functions are scale–independent.

In general, higher order contributions to the DIS process will spoil both properties. Due to mass singularities the higher order calculations of $\mathcal{W}_{\mu\nu}^a$ involve the introduction of Q^2–dependences of the distribution functions f_a^{H}. These dependences are controlled by the same quantities (anomalous dimensions of composite operators) as the Q^2–dependences of the coefficients $\bar{C}_i^{(m)}(Q^2)$ discussed in section 2.2. Singularities are the subject of the next section.

2.3.2 QCD corrections within the parton model

The simple parton model, as described in the previous section, is nowadays supported by the gauge field theory QCD to describe the partons, which are identified with quarks and gluons. QCD is an asymptotic free theory, which means that the coupling constant decreases towards zero if energies increase. Therefore, at high energies one can apply QCD perturbatively to calculate cross sections. Moreover, the running coupling constant provides an argument for the issue, why the parton model is not in total contradiction with the fact, that free quarks have never been observed.

The calculation of higher order corrections to parton structure functions involves phase space and loop integrals. As these integrals are not always well defined, one should introduce a regulator to be able to calculate them. We will choose dimensional regularisation, i.e. we perform our calculations in $n = 4 + \varepsilon$ instead of 4 dimensions. The singularities, appearing in the integrals, will manifest themselves as ε^{-i} terms (where i is a positive integer). These poles can be classified according to their origin.

Firstly, divergences show up in loop integrals where the loop momentum goes to infinity. These are called ultraviolet (UV) divergences; they are removed by coupling constant renormalisation. Secondly, if the integration momentum goes to zero, one may encounter infrared poles. According to the Bloch–Nordsieck theorem [13], these singularities cancel if both virtual and bremsstrahlung diagrams are considered. Thirdly, collinear divergences can occur. This happens when the momenta of two massless particles become parallel. A propagator $[(p-k)^2]^{-1}$ can be expressed in that case by

$$(p-k)^2 = -2|\vec{p}||\vec{k}|(1-\cos\theta) \xrightarrow{\theta\to 0} -|\vec{p}||\vec{k}|\theta^2, \tag{2.3.5}$$

which gives rise to a singularity in both phase space and loop integrals.

In quantum field theory there exists a very powerful theorem due to Kinoshita, Lee and Nauenberg [14], which determines the mass singular behaviour of a given quantity. It states that when the mass of one of the particles goes to zero the quantity is finite, provided one sums over all initial and final states which are degenerate in energy or mass. The latter means that they are experimentally indistinguishable. In the case of parton structure functions this condition is met for the final states only, because we consider an inclusive process. Therefore, we can conclude that the divergences, left over in the final expression for a parton structure function after renormalisation of the coupling constant, are initial state collinear divergences. These singularities are removed by renormalisation of the parton densities, a procedure which is usually called mass factorisation [15].

The wide range of applicability of the parton model finds its origin in the mass factorisation theorem, which states that mass singularities have a universal character, i.e. they are process independent. This implies that the parton model can also be used to describe other processes, like the Drell–Yan process, a deep inelastic hadron–hadron scattering process in which a lepton pair is produced [16]. Such a theoretical description is not possible in the framework of the operator product expansion, because one does not have light–cone dominance in this case. QCD corrections to the Drell–Yan process will be the subject of chapter 4.

As in the case of coupling constant renormalisation, mass factorisation will introduce a new, arbitrary mass scale. Unfactorised quantities cannot depend on this mass scale. This implies the formulation of renormalisation group equations on splitting functions and correction terms, which is the subject of the next section.

2.3.3 Mass factorisation and the renormalisation group

The mass factorisation theorem, applied to the parton structure functions, which can be deduced from the parton tensor in eq. 2.3.1, will give rise to a completely parallel discussion as can be found in section 2.2.4. The precise statement of this mass factorisation theorem is that after coupling constant renormalisation and cancellation of IR divergences, the parton structure functions can be written as

$$\begin{aligned} \mathcal{F}_a\left(x, g(\mu^2), \frac{Q^2}{p^2}\right) &= \sum_b \int_0^1 dx_1 \int_0^1 dx_2\, \delta(x - x_1 x_2) \\ &\times \Gamma_{ba}\left(x_1, g(\mu^2), \frac{\mu^2}{p^2}\right) \Delta_b\left(x_2, g(\mu^2), \frac{Q^2}{\mu^2}\right), \end{aligned} \tag{2.3.6}$$

where p^2 represents the mass singularity originating from the incoming parton a. Note that we have suppressed the index of the structure function. The singular splitting functions Γ_{ba} are universal and the functions Δ_b are free of collinear divergences. The parameter μ is the so–called mass factorisation scale, which is arbitrarily chosen. For convenience we have put it equal to the renormalisation scale (see the discussion below eq. 2.2.24). It is immediately clear, that the parton structure function cannot explicitly depend on the mass factorisation scale μ. This fact gives rise to the formulation of a renormalisation group equation (RGE), applied to these structure functions. It is convenient to express eq. 2.3.6 in terms of the moments of all occurring quantities, i.e.

$$\mathcal{F}_a^{(m)}\left(g(\mu^2), \frac{Q^2}{p^2}\right) = \sum_b \Gamma_{ba}^{(m)}\left(g(\mu^2), \frac{\mu^2}{p^2}\right) \Delta_b^{(m)}\left(g(\mu^2), \frac{Q^2}{p^2}\right), \tag{2.3.7}$$

where the Mellin transform $f^{(m)}$ of a function $f(x)$ is defined by

$$f^{(m)} = \int_0^1 dx\, x^{m-1} f(x). \tag{2.3.8}$$

The RGE for the functions Δ_b (DIS correction terms) becomes

$$\left[\left(\mu\frac{\partial}{\partial\mu} + \beta(g(\mu^2))\frac{\partial}{\partial g}\right)\delta_{ab} - \gamma_{ba}^{(m)}\right]\Delta_b^{(m)}\left(g(\mu^2), \frac{Q^2}{\mu^2}\right) = 0, \tag{2.3.9}$$

where we have introduced the quantities $\gamma_{bc}^{(m)}$ by

$$\mu\frac{\mathrm{d}}{\mathrm{d}\mu}\Gamma_{ba}^{(m)} = -\gamma_{bc}^{(m)}\Gamma_{ca}^{(m)}. \tag{2.3.10}$$

These quantities are found to be the same anomalous dimensions which appeared in section 2.2.4 in the scale dependences of operators. The equation for the DIS correction function is exactly the same as the one for the Wilson coefficient. It means that the solution can be stated immediately for the splitting functions as well as for the correction terms. The result for the correction term is

$$\Delta_b^{(m)}(g_0, t) = \left[T\exp\left\{\int_{t_0}^{t} dt'\,\gamma(g_0, t')\right\}\right]_{ab}^{(m)}\Delta_a^{(m)}(g_0, t_0), \tag{2.3.11}$$

where the logarithmic variable t is introduced in exactly the same way as before in eq. 2.2.30. Furthermore, the running coupling constant is introduced in the above equation. This makes the t–dependence of the correction term explicit (see the discussion in section 2.2.4).

The parton structure functions $\mathcal{F}_a$ are combined with the parton densities to give the hadronic structure functions (see eq. 2.3.1). If one now introduces scale dependent parton density functions in terms of the old ones by

$$f_a^{(m)}(t) = \Gamma_{ab}^{(m)}\left(g(t, g_0), t\right) f_b^{(m)}, \tag{2.3.12}$$

the collinear divergences will be absorbed in these new parton density functions and the correction term Δ_b becomes finite. The scale dependence of the parton distributions is determined by the so–called Altarelli–Parisi equations [17]

$$\frac{\mathrm{d}}{\mathrm{d}t}f_a^{(m)}(t) = -\gamma_{ab}^{(m)} f_b^{(m)}(t). \tag{2.3.13}$$

The densities can be evaluated for any t once they are measured at a certain experimental value of Q^2. The moments of the hadronic structure function can eventually be written as

$$F^{(m)}(g_0, t) = \sum_a f_a^{(m)}(g_0, t)\Delta_a^{(m)}(g_0, t_0). \tag{2.3.14}$$

The DIS correction terms are really correction terms, because if the choice $\mu^2 = Q^2$ is made, these expressions will only depend on the scale Q via the running coupling constant. This means that in lowest order the correction term cannot depend on Q.

The status of eq. 2.3.14 is completely the same as the one of eq. 2.2.22 in the operator product expansion. The correction terms Δ can be identified with the Wilson coefficients $\tilde{C}$ and the parton densities f with the operator matrix elements A. Since in both cases the dependence on Q^2 is completely contained in one expression, the actual evolution of this dependence should be parallel. This explains why the anomalous dimensions play the same role in the OPE as well as in the parton model. A beautiful property of the operator matrix elements is that its ultraviolet divergences are uniquely related to its collinear divergences. This enables one to use the pole terms ε^{-i} of the renormalisation constants of the matrix elements as splitting functions in the factorisation procedure of dimensionally regularised on-shell cross sections.

For the Drell–Yan process one can formulate a similar set of equalities [15]. This process is a 'crossing' of the DIS process, i.e.

$$\begin{array}{l} H_1 + H_2 \to V + \text{'X'} \\ \qquad\qquad\quad \lfloor\!\!\longrightarrow \ell_1 + \ell_2 . \end{array} \tag{2.3.15}$$

The formulation of the mass factorisation theorem in this case reveals an equation for the parton structure functions, analogous to eq. 2.3.6, which is given by

$$\mathcal{W}_{ab}\left(x, g(\mu^2), \frac{Q^2}{p_1{}^2}, \frac{Q^2}{p_2{}^2}\right) = \sum_{cd} \int_0^1 dx_1 \int_0^1 dx_2 \int_0^1 dx_3\, \delta(x - x_1 x_2 x_3)$$
$$\times\, \Gamma_{ca}\left(x_1, g(\mu^2), \frac{\mu^2}{p_1{}^2}\right) \Gamma_{db}\left(x_2, g(\mu^2), \frac{\mu^2}{p_2{}^2}\right) \Delta_{cd}\left(x_3, g(\mu^2), \frac{Q^2}{\mu^2}\right), \tag{2.3.16}$$

where the scales $p_1{}^2$ and $p_2{}^2$ indicate the mass divergences of the two incoming particles. Note that in the actual calculation in chapter 4 the partons are set on-shell. In that case the collinear singularities reappear as pole terms ε^{-i}. The equivalent of eq. 2.3.14 in this case is

$$W^{(m)}(g_0, t) = \sum_{a,b} f_a^{(m)}(g_0, t) f_b^{(m)}(g_0, t) \Delta_{ab}^{(m)}(g_0, t_0), \tag{2.3.17}$$

where $W^{(m)}$ are the moments of the hadronic structure function and $\Delta_{ab}^{(m)}$ denote the Drell–Yan correction terms. The calculation of these quantities is the subject of chapter 4.

References

[1] J.D. Bjorken, Phys. Rev. **179** (1969), 1547

[2] W.K.H. Panofsky, Proc. 14th Int. Conf. on High Energy Physics, Vienna, 1968, CERN, Scientific Information Service, p. 23

[3] K.G. Wilson, Cornell Report (1964), unpublished; Phys. Rev. **179** (1969), 1499

[4] R.P. Feynman, Phys. Rev. Lett. **23** (1969), 1415

[5] Y. Watanabe et al., Phys. Rev. Lett. **35** (1975), 898; C. Chang et al., Phys. Rev. Lett. **35** (1975), 901

[6] D.J. Gross and F. Wilczek, Phys. Rev. D8 (1973), 3633; D9 (1974), 980; H. Georgi and H.D. Politzer, Phys. Rev. D9 (1974), 416; H.D. Politzer, Phys. Rep. 14C (1974), 129

[7] R.A. Brandt, Ann. Phys. **44** (1967), 221; R.A. Brandt and G. Preparata, Nucl. Phys. **B27** (1971), 541; W. Zimmermann, Ann. Phys. **77** (1973), 570; R. Jackiw, R. van Royen and G.B. West, Phys. Rev. **D2** (1970), 2473

[8] C.G. Callan, Phys. Rev. **D2** (1970), 1541; K. Symanzik, Comm. Math. Phys. 18 (1970), 227

[9] M.J. Lighthill, 'Introduction to Fourier analysis and generalised functions', Cambridge University Press, 1958

[10] B.L. Ioffe, Phys. Lett. **30B** (1969), 123

[11] G.C. Wick, Phys. Rev. **80** (1950), 268

[12] C.G. Callan and D.J. Gross, Phys. Rev. Lett. **22** (1969), 156

[13] F. Bloch and A. Nordsieck, Phys. Rev. **52** (1937), 54

[14] T. Kinoshita, J. Math. Phys. **3** (1962), 650; T.D. Lee and M. Nauenberg, Phys. Rev. **133** (1964), B1549; N. Nakanishi, Prog. Theor. Phys. **19** (1958), 159

[15] H.D. Politzer, Nucl. Phys. **B129** (1977), 301; D. Amati, R. Petronzio and G. Veneziano, Nucl. Phys. **B140** (1978), 54; S.B. Libby and G. Sterman, Phys. Rev. **D18** (1978), 3252, 4737; A.H. Mueller, Phys. Rev. **D18** (1978), 3705; J.C. Collins and G. Sterman, Nucl. Phys. **B185** (1981), 172; J.C. Collins, D.E. Soper and G. Sterman, Nucl. Phys. **B261** (1985), 104; G.T. Bodwin, Phys. Rev. **D31** (1985), 2616

[16] S.D. Drell and T.M. Yan, Phys. Rev. Lett. **25** (1970), 316; Ann. Phys. **66** (1971), 578

[17] G. Altarelli and G. Parisi, Nucl. Phys. **B126** (1977), 298

Chapter 3

The anomalous dimension of the gluon operator

3.1 Introduction

One of the most important successes of the theory of perturbative QCD is the prediction of the scale dependence of the structure functions, measured in deep inelastic lepton–hadron scattering. From these deep inelastic structure functions one can infer the parton distribution functions (densities), which therefore become scale dependent too. The parton densities have been used as input for many other deep inelastic (hard) processes, leading to a wealth of predictions, which can be tested by experiment. As has been shown in the introductional chapter, the scale evolution of the structure functions is determined by the anomalous dimensions of composite operators. These operators appear in the (Wilson) operator product expansion (OPE) of the current commutator, the Fourier transform of which defines the hadronic structure tensor showing up in the calculation of the deep inelastic lepton–hadron scattering cross section. Using renormalisation group methods, one can derive a one–to–one correspondence between the coefficients of the scale violating terms and the aforementioned anomalous dimensions.

Immediately after the discovery of asymptotic freedom in non–abelian gauge field theories and in particular in QCD, the renormalisation of these operators was carried out up to the one loop level. To clarify our discussion and the findings in the literature, the operators showing up in QCD can be divided in two classes according to their representation of the flavour group:

1. <u>The non–singlet quark operator</u>

$$O_{q,r}^{\mu_1\ldots\mu_m}(x) = \frac{i^{m-1}}{2}\mathcal{S}\left[\overline{\psi}(x)\gamma^{\mu_1}D^{\mu_2}\ldots D^{\mu_m}(1\pm\gamma_5)\frac{\lambda_r}{2}\psi(x)\right] + \text{trace terms.} \tag{3.1.1}$$

2. The singlet quark and gluon operators

$$O_{q}^{\mu_1\cdots\mu_m}(x) = \frac{i^{m-1}}{2}\mathcal{S}\left[\bar{\psi}(x)\gamma^{\mu_1}D^{\mu_2}\ldots D^{\mu_m}(1\pm\gamma_5)\psi(x)\right] + \text{trace terms} \tag{3.1.2}$$

and

$$O_{g}^{\mu_1\cdots\mu_m}(x) = \frac{i^{m-2}}{2}\mathcal{S}\left[F_{a}^{\alpha\mu_1}(x)D^{\mu_2}\ldots D^{\mu_{m-1}}F^{a\alpha\mu_m}(x)\right] + \text{trace terms.} \tag{3.1.3}$$

Here $\mathcal{S}$ denotes the symmetrisation of the operators in their Lorentz indices μ_i and the trace terms are necessary to make these operators traceless. The λ_r in eq. 3.1.1 refer to matrices in flavour space, whereas the index a in eq. 3.1.3 stands for the colour index. The matrix γ_5 is added in case one does not average over the spin of the quark field. These properties follow from the fact that according to Wilson's hypothesis the operators belong to irreducible representations of the internal flavour and colour $SU(3)$ and the external (conformal) groups.

One of the consequences of Wilson's theorem is that operators, which belong to the same irreducible representation, like the two in class 2, mix under renormalisation. This property follows from the phenomenon that the renormalisation constant of a given operator receives contributions from virtual corrections to all other operators belonging to the same representation as the original one. In this way the operator renormalisation constant becomes a matrix. This feature is common for all renormalisable theories. However, as has been discovered for the first time by Gross and Wilczek [1], in gauge theories a second type of mixing occurs. In this case the locally gauge invariant (physical) operator 3.1.3 mixes with gauge variant (unphysical) operators. They consist of products of gauge fields as well as ghost fields, and are hereafter called alien and ghost operators, respectively. Therefore, this phenomenon already appears without the presence of quark fields and the corresponding operators in eqs. 3.1.1 and 3.1.2.

The origin of this feature, which is characteristic for Yang–Mills field theories as well as gravity, was explained for the first time by Dixon and Taylor in [2]. They showed that the renormalised effective Lagrangian is invariant under a more general type of gauge transformations as the bare effective Lagrangian. The latter is invariant under the usual local gauge transformations. In this way they could construct the gauge variant operators order by order in the coupling constant, which are needed to render the theory renormalisable. This construction was put on a more general footing in [3] by using BRST techniques. Unfortunately, the insight gained by the work done in the references [2, 3] was not sufficient enough to lead to an unambiguous prescription for the computation of the anomalous dimension of the gauge invariant operator beyond the one loop level. This became apparent in the calculation of the second order anomalous dimension of the gluon operator in 3.1.3 carried out in [4] by using a covariant (actually the Feynman) gauge. Their result was not in agreement with the calculation done in a physical (axial) gauge presented in [5].

This would lead to the conclusion that the anomalous dimension of a physical (gauge invariant) operator is gauge dependent, which is of course unacceptable. The issue, which anomalous dimension is correct, was decided in favour of the results obtained by the axial gauge calculation [6]. As has been pointed out in [7], the anomalous dimensions of the quark and gluon operators satisfy a relation, which is derived from supersymmetry. The 'axial gauge' result satisfies this relation in contrast to the covariant one. However, to our opinion the status of this ambiguity is still unsatisfactory for the following reasons:

1. The anomalous dimension of the gluon operator is a physical quantity, which determines the scale evolution of the parton and in particular the gluon distribution function, and therefore, no uncertainty concerning its status can be accepted.

2. The equality of the results, obtained from calculations in different gauges, should directly follow from a proper application of the rules given in quantum field theory, without having recourse to arguments derived from supersymmetry.

3. The axial gauge chosen in [5] is a lightlike one. As is pointed out in [8], this singular gauge leads to an unrenormalisable field theory by power counting. Therefore, its result would be suspect, if it did not satisfy the supersymmetric relation mentioned above.

In this chapter we will show that the result for the anomalous dimension obtained in the axial gauge is correct and can also be derived from a covariant (here Feynman) gauge calculation. The main reason for the discrepancy between our work and the covariant gauge calculations in [4] can be attributed to the fact that the renormalisation of the gauge variant operators leads to a counter term corresponding to the physical operator in eq. 3.1.3. The latter counter term is needed for the computation of the anomalous dimension and was neglected in the previous work. The last feature does not show up when the gauge variant operators are calculated in the axial gauge, as is shown in [9]. In this case, the mixing matrix gets the Jordan form and hence, the unphysical anomalous dimensions cannot affect the physical one corresponding to the operator in eq. 3.1.3.

This chapter will be organised as follows. In section 3.2 we present the one loop calculation of the operator matrix element. It will become clear, that the gluon operator cannot be renormalised in a simple way by multiplicative renormalisation. We will reformulate the problem in section 3.3, where we rely heavily upon the findings in [2, 3, 10]. In section 3.4, we present the calculation of the unrenormalised matrix elements of the physical as well as the unphysical operators and show their renormalisation. Our conclusions and some final remarks will be given in section 3.5. Feynman rules will be given in appendix 3A and the technical details of the one and two loop integrals will be discussed in the appendices 3B and 3C, respectively. Appendix 3D contains some long expressions which are needed in the calculations in section 3.4.

3.2 One loop corrections to the gluon operator

The gluon operator has the same quantum numbers as the flavour singlet quark operator. Therefore, the renormalisation procedure involves mixing between these operators. However, as stated already in the introduction, another kind of mixing occurs when the renormalisation of the gluon operator is considered. This phenomenon is present even if the quark operator is absent. Therefore, in order to simplify our discussion, we will limit ourselves to pure gauge field theories and leave out the quark operators from now on.

The presence of this kind of mixing (i.e. mixing of the gluon operator and new gauge dependent operators, which are built out of gauge fields) can beautifully be observed at first order in the loop expansion by comparing renormalisations of the gluon operator in two different gauges, i.e. the axial and the covariant gauge. Axial gauge fixing terms do not give rise to the introduction of ghost terms in the Lagrangian; hence, there will be no mixing with possible ghost operators in that case. This does not imply that the renormalisation procedure cannot give rise to new, unphysical operators, but these new structures can easily be distinguished from the original gluon operator. Furthermore, Crewther [9] showed that the renormalisation of the latter is not affected by the introduction of unphysical operators. On the contrary, the covariant gauge does exhibit the property, that counter terms which involve ghost fields and new structures with gluon fields must be introduced during renormalisation. In this case the renormalisation matrix is as such, that the new operators can influence the determination of the anomalous dimension of the gluon operator in higher orders.

The quantity that we want to calculate is the physical operator matrix element. This is a S-matrix element, the external states of which are put on mass shell and contracted with physical polarisations. However, the calculation of such a quantity is not possible in the case of external gluons, because if the gluons would be put on-shell, there is no mass scale left in the Feynman integrals. Since we are interested in the anomalous dimension of the operator only, we will consider the renormalisation of the one particle irreducible (1PI) Green's function.

3.2.1 Introduction of the gluon operator

We consider the pure Yang-Mills field Lagrangian (without fermions), which is given by

$$\mathcal{L}_{YM} = -\tfrac{1}{4}F^a_{\mu\nu}F^{a\mu\nu} + \mathcal{L}_{GF} + \mathcal{L}_{FP}, \tag{3.2.1}$$

where $\mathcal{L}_{GF}$ is a gauge fixing term and $\mathcal{L}_{FP}$ the Faddeev-Popov ghost term. In a covariant gauge fixing their expressions are given by

$$\begin{aligned} \mathcal{L}_{GF} &= -\tfrac{1}{2\alpha}(\partial^\mu A^a_\mu)^2, \\ \mathcal{L}_{FP} &= -\xi^a\partial^\mu D^{ab}_\mu\omega^b, \end{aligned} \tag{3.2.2}$$

where ξ^a and ω^b are the (anti)ghost fields. The indices a and b denote colour indices, whereas α is called the gauge parameter. In the so-called axial gauge, the ghost term decouples from the physical sector of the theory and the gauge fixing term is given by

$$\mathcal{L}_{GF} = -\tfrac{1}{2\alpha}(n^\mu A^a_\mu)^2, \tag{3.2.3}$$

where n^μ is an arbitrary vector. In this case, one usually takes the limit $\alpha \to 0$, which is necessary to render the theory renormalisable by power counting [8]. The Feynman rules for the gluon propagator, which follow from these gauge fixing terms, are given in appendix 3A.1. The field strength and the covariant derivative are defined by

$$F^a_{\mu\nu} = \partial_\mu A^a_\nu - \partial_\nu A^a_\mu + g f^{abc}A^b_\mu A^c_\nu, \tag{3.2.4}$$

$$D^{ab}_\mu = \delta^{ab}\partial_\mu - g f^{abc}A^c_\mu, \tag{3.2.5}$$

where f^{abc} are the structure constants of the colour gauge group and g is the strong coupling constant.

Using path integral methods the introduction of the flavour singlet gluon operator (see eq. 3.1.3) proceeds by adding a new source to the action, which is coupled to the gluon operator (see also section 3.3). Since we are only interested in the coefficient $\mathcal{A}_{gg}^{(m)}(p^2)$ of the matrix element of the gluon operator, given in eq. 2.2.23, the source is chosen in such a way that the trace terms drop out. This can be achieved if the form of the current is equal to

$$J_{\mu_1 \ldots \mu_m} = \Delta_{\mu_1} \ldots \Delta_{\mu_m}, \tag{3.2.6}$$

where the vector Δ is taken to be lightlike: $\Delta^2 = 0$. The exact form of the bare Lagrangian, which is the starting point of the discussion, becomes

$$\begin{aligned} \mathcal{L} &= \mathcal{L}_{\mathrm{YM}} + \frac{i^{m-2}}{2} \Delta^{\mu_1} \ldots \Delta^{\mu_m} F^{a_1}_{\alpha\mu_1} D^{a_1 a_2}_{\mu_2} \ldots D^{a_{m-2} a_{m-1}}_{\mu_{m-1}} F^{a_{m-1}\alpha}{}_{\mu_m} \delta^{a a_{m-1}} \\ &= \mathcal{L}_{\mathrm{YM}} + \tfrac{1}{2} F_\alpha D^{m-2} F^\alpha \equiv \mathcal{L}_{\mathrm{YM}} + O_g, \end{aligned} \tag{3.2.7}$$

where we introduced the following simplifying notation in the last line

$$F_\alpha = \Delta^\beta F_{\alpha\beta}, \quad D = i\Delta^\alpha D_\alpha. \tag{3.2.8}$$

A trace taken in colour space is always implicitly understood. Whenever ambiguities cannot occur, colour indices are suppressed (like in the last line of eq. 3.2.7).

The central issue of the next two sections is the renormalisation of the gluon operator. This problem cannot be solved at the level of real operator matrix elements (with on–shell external legs). Therefore, the central quantity will be the amputated, one particle irreducible (1PI) Green's function, called Γ_{O_g}. This quantity can be deduced from the vacuum expectation value

$$\langle 0| T \left(A^a_\mu(p) O_g(0) A^b_\nu(-p) \right) |0\rangle \tag{3.2.9}$$

by amputating the external legs. The operator $O_g(0)$ in this expression is defined in eq. 3.2.7. As the expectation value of all connected graphs will be renormalised by the factor $Z_A Z_O$, the 1PI Green's function Γ_{O_g} will be renormalised by the factor $Z_A^{-1} Z_O$, where Z_A and Z_O denote the gluon field and gluon operator renormalisation constants, respectively. Therefore, we will have to multiply the results for Γ_{O_g} by the factor Z_A in order to obtain Z_O.

Since the external fields of the Green's function under study are kept off–shell, the quantity will not be gauge independent. However, the renormalisation constant Z_O corresponds to a gauge invariant operator, i.e. O_g. Therefore, it does not depend on any gauge parameter. This remark does not hold for additional operators, which must be introduced in the Lagrangian.

3.2.2 The axial gauge calculation

In spite of the fact that the gluon propagator in the axial gauge has a quite complicated expression (compared to its form in a covariant gauge, cf. eqs. 3A.2 and 3A.4), we present the calculation of the 1PI Green's function in this gauge up to second order in g (one loop). The physical motivation for this effort is the form of the renormalisation matrix in this gauge. Crewther [9] showed that the one loop result of the 1PI Green's function will contain more terms than the physical operator only. However, the counter terms of these new operators, which have to be introduced in the Lagrangian, will not be needed for the renormalisation of the gluon operator. Therefore, we will not compute them in this section.

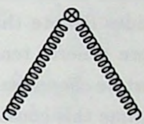

Fig. 3.1. The lowest order contribution to the 1PI Green's function.

The quantity we want to calculate is the 1PI Green's function, which is multiplied by the wave function renormalisation constant Z_A. This quantity can be denoted up to $\mathcal{O}(g^2)$ in the following way

$$
\begin{aligned}
Z_A \hat{\Gamma}_{O_g,\mu\nu} &= \frac{1+(-1)^m}{2}\delta^{ab}(\Delta\cdot p)^m Z_A \\
&\quad \times \int_0^1 dx\, x^{m-1}\left\{\mathcal{A}^{(0)}_{\mu\nu}(x,p) + \frac{\hat{\alpha}_s}{4\pi}S_\epsilon C_A \mathcal{A}^{(1)}_{\mu\nu}(x,p)\right\} \\
&= \frac{1+(-1)^m}{2}\delta^{ab}(\Delta\cdot p)^m Z^{(m)}_{gg} \\
&\quad \times \int_0^1 dx\, x^{m-1}\left\{\mathcal{M}^{(0)}_{\mu\nu}(x,p) + \frac{\alpha_s}{4\pi}C_A \mathcal{M}^{(1)}_{\mu\nu}(x,p)\right\}, \qquad (3.2.10)
\end{aligned}
$$

where $\mathcal{A}^{(i)}_{\mu\nu}(x,p)$ and $\mathcal{M}^{(i)}_{\mu\nu}(x,p)$ stand for the $\mathcal{O}(\alpha_s^i)$ unrenormalised and renormalised parts of the 1PI Green's function, respectively. Further, $\alpha_s = g^2/4\pi$ represents the strong coupling constant. The first equation is given in terms of unrenormalised quantities (like the hatted $\hat{\alpha}_s$ and the unrenormalised gauge parameter), while the second is expressed in renormalised ones. Some factors could already be factored out of the $\mathcal{O}(g^2)$ contribution to the 1PI Green's function. The spherical factor S_ϵ that originates from the dimensionally regularised loop integrals, is given by

$$S_\varepsilon = \exp\left\{\frac{\varepsilon}{2}\left[\gamma_E - \ln 4\pi\right]\right\}, \tag{3.2.11}$$

where γ_E is the Euler constant and ε is defined by the dimension $n = 4 + \varepsilon$. The eigenvalue of the quadratic Casimir operator in the adjoint representation is represented by C_A. It is equal to N in the case of a $SU(N)$ gauge group. Note that up to this order we do not need coupling constant renormalisation, because the zeroth order Green's function is independent of g.

Each first term on the right-hand side of eq. 3.2.10 represents the zeroth order contribution, which is also shown in fig. 3.1. These expressions are given by

$$\mathcal{A}^{(0)}_{\mu\nu}(x,p) = \mathcal{M}^{(0)}_{\mu\nu}(x,p) = O^1_{\mu\nu}(p)\delta(1-x), \tag{3.2.12}$$

where the tensor $O^1_{\mu\nu}(p)$ can be found in eq. 3.2.17 (cf. also appendix 3A.3). The second terms on the right-hand sides denote the one loop contribution to the 1PI Green's function, which has a more general tensor structure. The gluon operator renormalisation constant[1] $Z^{(m)}_{gg}$ must be chosen as such, that the first order expression $\mathcal{M}^{(1)}_{\mu\nu}(x,p)$ is finite. One can determine this constant by considering the combination

$$\mathcal{A}^{(1)}_{\mu\nu}(x,p) + Z^{(1)}_A \mathcal{A}^{(0)}_{\mu\nu}(x,p) = \mathcal{M}^{(1)}_{\mu\nu}(x,p) + Z^{1,(m)}_{gg}\mathcal{M}^{(0)}_{\mu\nu}(x,p), \tag{3.2.13}$$

where $Z^{(1)}_A$ and $Z^{1,(m)}_{gg}$ are the first order terms from the following expansions of the renormalisation constants

$$Z_A = 1 + \sum_{i=1}^{\infty}\left(\frac{\alpha_s}{4\pi}\right)^i S^i_\varepsilon C_A{}^i Z^{(i)}_A, \tag{3.2.14}$$

$$Z^{(m)}_{gg} = 1 + \sum_{i=1}^{\infty}\left(\frac{\alpha_s}{4\pi}\right)^i S^i_\varepsilon C_A{}^i Z^{i,(m)}_{gg}. \tag{3.2.15}$$

The quantity $\mathcal{A}^{(1)}_{\mu\nu}(x,p)$ denotes the one loop contribution to the unrenormalised Green's function and has to be calculated. It can be written as

$$\mathcal{A}^{(1)}_{\mu\nu}(x,p) = \sum_{i=1}^{2}\mathcal{A}^{(1)}_{i,\mu\nu}(x,p), \tag{3.2.16}$$

where the quantity $\mathcal{A}^{(1)}_{i,\mu\nu}(x,p)$ corresponds to the i-th Feynman diagram in fig. 3.2 (i=1,2).

The possible Lorentz structure of the quantities $\mathcal{A}^{(1)}_{i,\mu\nu}(x,p)$ can be explored before calculating anything. A regular base for these tensor structures, which contain the vectors p, Δ and n, consists of seven elements. We will choose a set and label the elements by $O^i_{\mu\nu}$. The first one belongs to the physical operator (cf. appendix 3A.3), whereas only the last three tensors contain the vector n. We introduce the tensors as follows

---

[1]The two indices gg indicate that the quantity Z_{gg} refers to a gluon–gluon transition.

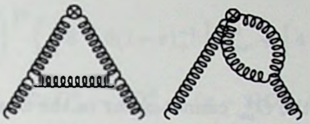

Fig. 3.2. The one loop contributions to the 1PI Green's function. The second diagram appears twice, because the blob can also occur on the other side.

$$O^1_{\mu\nu}(p) = g_{\mu\nu} - \frac{p_\mu\Delta_\nu + \Delta_\mu p_\nu}{\Delta\cdot p} + \frac{\Delta_\mu\Delta_\nu p^2}{(\Delta\cdot p)^2}, \tag{3.2.17}$$

$$O^2_{\mu\nu}(p) = \frac{p_\mu p_\nu}{p^2} - \frac{p_\mu\Delta_\nu + \Delta_\mu p_\nu}{\Delta\cdot p} + \frac{\Delta_\mu\Delta_\nu p^2}{(\Delta\cdot p)^2}, \tag{3.2.18}$$

$$O^3_{\mu\nu}(p) = -\frac{1}{2}\frac{p_\mu\Delta_\nu + \Delta_\mu p_\nu}{\Delta\cdot p} + \frac{\Delta_\mu\Delta_\nu p^2}{(\Delta\cdot p)^2}, \tag{3.2.19}$$

$$O^4_{\mu\nu}(p) = \frac{1}{2}\frac{p_\mu\Delta_\nu + \Delta_\mu p_\nu}{\Delta\cdot p} + \frac{\Delta_\mu\Delta_\nu p^2}{(\Delta\cdot p)^2}, \tag{3.2.20}$$

$$O^5_{\mu\nu}(p) = \frac{p_\mu p_\nu}{p^2} - \frac{p_\mu n_\nu + n_\mu p_\nu}{n\cdot p} + \frac{n_\mu n_\nu p^2}{(n\cdot p)^2}, \tag{3.2.21}$$

$$O^6_{\mu\nu}(p) = \frac{n_\mu n_\nu p^2}{n\cdot p)^2} - \frac{(n_\mu\Delta_\nu + \Delta_\mu n_\nu)p^2}{(\Delta\cdot p)(n\cdot p)} + \frac{\Delta_\mu\Delta_\nu p^2}{(\Delta\cdot p)^2} \tag{3.2.22}$$

and

$$O^7_{\mu\nu}(p) = -\frac{1}{2}\frac{p_\mu n_\nu + n_\mu p_\nu}{n\cdot p} + \frac{n_\mu n_\nu p^2}{(n\cdot p)^2}. \tag{3.2.23}$$

These tensors, the last three of which cannot be present in a covariant gauge calculation, obey the following relations

$$p^\mu O^{1,2,5,6}_{\mu\nu} = 0, \quad p^\mu O^{3,4,7}_{\mu\nu} \neq 0, \tag{3.2.24}$$

$$p^\mu p^\nu O^{3,7}_{\mu\nu} = 0, \quad p^\mu p^\nu O^4_{\mu\nu} \neq 0. \tag{3.2.25}$$

The residual gauge symmetry of the Green's functions in a gauge field theory after fixing the gauge, i.e. BRST symmetry, is usually expressed in terms of Ward–Takahashi (WT) identities[2]. The least restrictive WT identity, first used by 't Hooft, expresses the property of a Green's function, that it becomes zero when all the external gauge particle lines are contracted with their own momenta. In our case this is expressed by

---

[2]Sometimes also called Slavnov–Taylor identities.

$$p^\mu p^\nu \hat{\Gamma}_{O_g,\mu\nu} = 0. \tag{3.2.26}$$

Hence, it follows that

$$p^\mu p^\nu \mathcal{A}^{(1)}_{\mu\nu}(x,p) = 0, \tag{3.2.27}$$

from which we infer that the $O^4_{\mu\nu}$ cannot occur in the final answer (see eq. 3.2.25).

In the axial gauge there exists also a stronger WT identity, which states that the Green's function already becomes equal to zero if only one of the external gluon lines is contracted with its momentum. This property is expressed by

$$p^\mu \hat{\Gamma}_{O_g,\mu\nu} = p^\nu \hat{\Gamma}_{O_g,\mu\nu} = 0, \tag{3.2.28}$$

from which it follows that

$$p^\mu \mathcal{A}^{(1)}_{\mu\nu}(x,p) = p^\nu \mathcal{A}^{(1)}_{\mu\nu}(x,p) = 0. \tag{3.2.29}$$

Therefore, the tensors $O^3_{\mu\nu}$ and $O^7_{\mu\nu}$ must be absent too (see equation 3.2.24).

Furthermore, we expect that the tensors $O^{2,5,6}_{\mu\nu}$ do not appear in the one loop result accompanied by singularities in ε, because these structures are non-local. The presence of such pole terms would make the Lagrangian non-renormalisable. Our final conclusion concerning the Lorentz structure of the Green's function is that the only possible tensor structure of the ε^{-1}-terms of the one loop result is $O^1_{\mu\nu}$, i.e. the structure of the gluon operator at lowest order.

The actual calculation of the quantities $\mathcal{A}^{(1)}_{i,\mu\nu}(x,p)$ in the general axial gauge is rather difficult. Therefore, we only determine the UV singular behaviour of the integrals, which shows up like a ε^{-1} term. These singularities can be determined without too much effort. A general vector n does not only complicate the integrals, it also causes the introduction of a cascade of factors $(\Delta{\cdot}n)^i$ where $i = 0,1,2,\ldots,m$. The complete treatment of these factors is difficult, but luckily enough at the same time unnecessary, because counter terms proportional to $(\Delta{\cdot}n)^i$ only produce $(\Delta{\cdot}n)^j$ terms with $j \geq i$ in higher order calculations [9]. For this reason they do not affect the renormalisation of the physical operator indicated by $O^1_{\mu\nu}$. Since we are only interested in the renormalisation of the latter we suppress the terms $(\Delta{\cdot}n)^i$ for $i > 0$ by putting $\Delta{\cdot}n = 0$ in the calculation. After some non-trivial algebra we find

$$\mathcal{A}^{(1)}_{1,\mu\nu}(x,p) = \frac{1}{\varepsilon}\left(\frac{-p^2}{\mu^2}\right)^{\frac{1}{2}\varepsilon} \Big\{ \Big[8 + 8x^2 - 8x - 8x^{-1} \Big] O^1_{\mu\nu} + \Big[16x^2 - 4 - 16x \Big] O^3_{\mu\nu}$$
$$+ 4\frac{(n{\cdot}p)^2}{p^2 n^2} \Big[-xO^2_{\mu\nu} + 2xO^3_{\mu\nu} + xO^5_{\mu\nu} + (2-x)O^6_{\mu\nu} - 2xO^7_{\mu\nu} \Big] \Big\} \tag{3.2.30}$$

and

$$\mathcal{A}^{(1)}_{2,\mu\nu}(x,p) = \frac{1}{\varepsilon}\left(\frac{-p^2}{\mu^2}\right)^{\frac{1}{2}\epsilon} \Big\{ \left[\, 8 - 8(1-x)_+^{-1} \,\right] O^1_{\mu\nu} + \left[\, 4 + 16x - 16x^2 \,\right] O^3_{\mu\nu}$$

$$+ 4\frac{(n\cdot p)^2}{p^2 n^2} \left[\, x O^2_{\mu\nu} - 2x O^3_{\mu\nu} - x O^5_{\mu\nu} + (x-2) O^6_{\mu\nu} + 2x O^7_{\mu\nu} \,\right] \Big\}, \qquad (3.2.31)$$

where the tensors $O^i_{\mu\nu}$ are given in eqs. 3.2.17–3.2.23. The parameter μ is an arbitrary mass scale, which expresses the mass dimension of the coupling constant. The distribution $(1-x)_+^{-1}$, appearing in eq. 3.2.31, is a regular distribution in the following sense:

$$\int_0^1 dx\,(1-x)_+^{-1+a\epsilon} f(x) = \int_0^1 dx\,(1-x)^{-1+a\epsilon}\{f(x) - f(1)\}, \qquad (3.2.32)$$

where $f(x)$ is a general 'test' function, which is regular in $x = 1$.

The renormalisation constant of the gluon operator is determined by the sum of the expressions 3.2.30 and 3.2.31 and the inclusion of the effect of wave function renormalisation. The first order coefficient of the latter quantity in this gauge is given by

$$Z^{(1)}_A = \frac{1}{\varepsilon}\left[\, -\frac{22}{3} \,\right], \qquad (3.2.33)$$

where the common one loop factors were suppressed (see eq. 3.2.14). The total UV singular result in the x-language is equal to (see eq. 3.2.10)

$$\left(\frac{-p^2}{\mu^2}\right)^{-\frac{1}{2}\epsilon} \mathcal{A}^{(1)}_{\mu\nu}(x,p) + Z^{(1)}_A \mathcal{A}^{(0)}_{\mu\nu}(x,p) =$$

$$\frac{1}{\varepsilon}\Big\{\, 16 + 8x^2 - 8x - 8x^{-1} - 8(1-x)_+^{-1} - \frac{22}{3}\delta(1-x) \,\Big\} O^1_{\mu\nu}(p), \qquad (3.2.34)$$

where the last term of the left–hand side of the above equation represents the wave function renormalisation constant at first order. The factor $(-p^2/\mu^2)^{-\epsilon/2}$ is introduced for notational convenience; it does not affect the pole structure. It is clear that this expression is independent of the axial gauge vector n. As the expression 3.2.34 is the only contribution to the physical operator renormalisation constant, this must be a quantity which is generally gauge independent. This does clearly not hold for the non–pole terms, as we will see in the next section where we calculate the above quantity up to constant terms in the covariant gauge.

When the inner product $\Delta\cdot n$ is put equal to zero, it is sufficient to introduce a single counter term of the same form as the original gluon operator in order to render the one loop result finite. Renormalisation in the $\overline{\text{MS}}$ scheme implies that this counter term is given by

$$-\frac{1}{\varepsilon}\frac{\alpha_s}{4\pi}S_\varepsilon C_A O_g$$
$$\times \int_0^1 dx\, x^{m-1}\left[\, 16+8x^2-8x-8x^{-1}-8(1-x)_+^{-1}-\tfrac{22}{3}\delta(1-x)\,\right], \quad (3.2.35)$$

where $\alpha_s = g^2/4\pi$ is the renormalised coupling constant (cf. eq. 3.2.10) and the physical gluon operator O_g is defined in eq. 3.2.7. The $\overline{\text{MS}}$ scheme distinguishes itself from the MS scheme by the additional constant $\gamma_E - \ln 4\pi$, which appears in the argument of the exponent in eq. 3.2.11. The first order contribution $Z_{gg}^{1,(m)}$ to the renormalisation matrix element Z_{gg} follows from eqs. 3.2.13 and 3.2.34. Expanding the anomalous dimension γ_{gg} of the gluon operator in a power series

$$\gamma_{gg}^{(m)} = \sum_{i=0}^{\infty}\left(\frac{\alpha_s}{4\pi}\right)^{i+1}\gamma_{gg}^{i,(m)}, \quad (3.2.36)$$

the lowest order coefficient equals

$$\gamma_{gg}^{0,(m)} = C_A\mu\frac{\partial}{\partial\mu}Z_{gg}^{1,(m)}$$
$$= C_A\left[\frac{16}{m}+\frac{8}{m+2}-\frac{8}{m+1}-\frac{8}{m-1}+\sum_{i=1}^{m-1}\frac{8}{i}-\frac{22}{3}\right]. \quad (3.2.37)$$

Since for $m = 2$ the gluon operator becomes equal to the stress energy–momentum tensor, it follows from energy–momentum conservation that eq. 3.2.37 satisfies the relation

$$\gamma_{gg}^{0,(2)} = 0. \quad (3.2.38)$$

This identity is a special example of the general property that conserved quantities have a zero anomalous dimension.

The calculations of the complicated one loop integrals in the general axial gauge can be facilitated by making a more suitable choice for the vector n. For instance, the integrals become considerably easier when the vector n is lightlike, i.e. $n^2 = 0$. Furthermore, the tensor structure of the quantities $\mathcal{A}_{i,\mu\nu}^{(1)}(x,p)$ can be reduced to the first four tensors $O_{\mu\nu}^i$, given in eqs. 3.2.17–3.2.20, by choosing the axial gauge fixing vector n proportional to the vector Δ defined in eq. 3.2.7. However, there is prize to be paid since such a gauge fixing term yields a Lagrangian, which is not renormalisable by power counting [8]. Moreover, one will encounter a new kind of divergences in the Feynman integrals, the so–called gauge singularities. Nevertheless, we will present the expressions $\mathcal{A}^{(1)}_{i,\mu\nu}(x,p)$ in this case, because one of the two available two loop anomalous dimensions has been calculated in this gauge [5].

If $n \propto \Delta$ the expressions $\mathcal{A}^{(1)}_{i,\mu\nu}(x,p)$ are given by

$$\mathcal{A}^{(1)}_{1,\mu\nu}(x,p) = \left(\frac{-x(1-x)p^2}{\mu^2}\right)^{\frac{1}{2}\varepsilon} \Big\{ \frac{1}{\varepsilon}\Big[\, 16 + 8x^2 - 8x - 8x^{-1} - 8(1-x)_+^{-1}$$
$$+ 8\delta(1-x)\ln\delta \Big] + 8 + 4x^2 - 4x - 4x^{-1} - 4(1-x)_+^{-1}$$
$$+ \Big[\, 2\ln^2\delta + 4\ln\delta + 4\zeta(2) \Big]\, \delta(1-x) \Big\}\, O^1_{\mu\nu}(p) + \Big[\, 2 + 8x^2 - 8x \Big]\, O^2_{\mu\nu}(p)$$
$$+ \Big\{ \frac{1}{\varepsilon}\Big[\, 16x^2 - 8x \Big] + 8x^2 - 4x \Big\}\, O^3_{\mu\nu}(p) \qquad (3.2.39)$$

and

$$\mathcal{A}^{(1)}_{2,\mu\nu}(x,p) = \left(\frac{-x(1-x)p^2}{\mu^2}\right)^{\frac{1}{2}\varepsilon} \Big\{ \frac{1}{\varepsilon}\Big[\, 8x - 16x^2 \Big]\, 4x - 8x^2 \Big\}\, O^3_{\mu\nu}(p). \qquad (3.2.40)$$

The parameter δ is a gauge regulator, which is used to distinguish gauge singular contributions from real UV divergences. It appears in the gluon propagator (see eq. 3A.2) by replacing

$$n\cdot k \to n\cdot(k + \delta p), \qquad (3.2.41)$$

where p is the external momentum and k is an arbitrary loop momentum. In appendix 3B the loop integrals are shown. They reveal why such a regulator should be used, especially at the boundaries of the integral over x.

The effect of wave function renormalisation is almost the same as in eq. 3.2.34, except for the presence of a $\ln\delta$ term. The calculation of Z_A at first order renders the following gauge singular expression

$$Z^{(1)}_A = \frac{1}{\varepsilon}\Big[-\frac{22}{3} - 8\ln\delta \Big], \qquad (3.2.42)$$

where the same quantities were factorised as in eq. 3.2.33. The final sum of the contributions is equal to

$$\left(\frac{-x(1-x)p^2}{\mu^2}\right)^{-\frac{1}{2}\varepsilon} \mathcal{A}^{(1)}_{\mu\nu}(x,p) + Z^{(1)}_A \mathcal{A}^{(0)}_{\mu\nu}(x,p) = \Big\{ \frac{1}{\varepsilon}\Big[\, 16 + 8x^2 - 8x - 8x^{-1}$$
$$- 8(1-x)_+^{-1} - \frac{22}{3}\delta(1-x) \Big] + \Big[\, 4\zeta(2) + 4\ln\delta + 2\ln^2\delta \Big]\, \delta(1-x) + 8 + 4x^2$$
$$- 4 - 4x^{-1} - 4(1-x)_+^{-1} \Big\}\, O^1_{\mu\nu}(p) + \Big[\, 2 + 8x^2 - 8x \Big]\, O^2_{\mu\nu}(p), \qquad (3.2.43)$$

where the tensors $O^i_{\mu\nu}$ can be found in eqs. 3.2.17–3.2.18. The factor in front of $\mathcal{A}^{(1)}_{\mu\nu}(x,p)$ was again introduced for notational convenience. Note the structure $O^2_{\mu\nu}(p)$ has no infinities and $O^3_{\mu\nu}(p)$ vanishes in the sum of contributions to the one loop calculation. The first two structures satisfy the relation $p^\mu O^{1,2}_{\mu\nu}(p) = 0$, whereas $O^3_{\mu\nu}(p)$ does not. Hence, the one loop calculation in the lightlike gauge satisfies the restriction imposed by the WT identity 3.2.28. Furthermore, in order to render the one loop result finite, it is sufficient to introduce a single counter term of the same form as the original gluon operator. This is not entirely analogous with the case of a general gauge vector n (cf. eq. 3.2.35). There the inner product $\Delta \cdot n$ was put equal to zero by hand, otherwise the operators with the structures $(\Delta \cdot n)^i$ had to be renormalised too.

From eq. 3.2.43 it is clear why the specific gauge regularisation by means of an additional parameter δ was necessary. Due to the singular gauge fixing (we choose $n^2 = 0$!), there is a gauge singular behaviour of the result near x equal to 1. Moreover, the presence of the $\ln \delta$ terms in the final expression 3.2.43 means that the Green's function does depend on the regularisation of the gauge singularities. The calculation of the anomalous dimension is not affected at least up to the one loop level. However, one can only hope that this also happens for the two loop calculation done in [5].

In spite of the nice and straightforward calculation in the lightlike axial gauge with $n_\mu \propto \Delta_\mu$, it must be remarked that there exists another problem due to this gauge choice. The Lorentz structures with n_μ and Δ_μ cannot be distinguished. We tried to calculate the case where $n^2 = 0$ and $\Delta \cdot n = 0$, but without the assumption $n_\mu \propto \Delta_\mu$. In the final answer, not only the $O^1_{\mu\nu}$ term, but also other structures exhibit singular behaviour. We cannot think of a satisfactory explanation for this phenomenon.

3.2.3 The covariant gauge calculation

In this section we present the results of the one loop calculation of the 1PI Green's function in a general covariant gauge. The relevant quantity is given in eq. 3.2.10. The Feynman diagrams that contribute are the same (see fig. 3.2) and the Feynman rules are given in appendix 3A. In this calculation it is not necessary to introduce additional regulators like has been done in the lightlike axial gauge, because the gauge singularities are harmless and do not affect the pole structure[3].

In a general covariant gauge the quantities $\mathcal{A}^{(1)}_{i,\mu\nu}(x,p)$ (see eq. 3.2.16) are given

[3]We have checked this by recalculation of the integrals with the introduction of regulator masses.

by

$$\mathcal{A}^{(1)}_{1,\mu\nu}(x,p) = \left(\frac{-x(1-x)p^2}{\mu^2}\right)^{\frac{1}{2}\varepsilon} \Big\{ \frac{1}{\varepsilon}\big[\, 8 + 8x^2 - 12x - 8x^{-1} + 2(1-\alpha)\delta(1-x) \,\big]$$
$$+ 6 + 4x^2 - 4x - 4x^{-1} + \big[\, (1-x)^{-1}_{+} - 2 + \delta(1-x) \,\big](1-\alpha) \Big\} O^{1}_{\mu\nu}(p)$$
$$+ \big[\, 2 + 8x^2 - 8x - (1-\alpha)x^{-1} \,\big] O^{2}_{\mu\nu}(p)$$
$$+ \Big\{ \frac{1}{\varepsilon}\big[\, 16x^2 - 12x + 4x^{-1} - 4(1-\alpha) \,\big]$$
$$- 2 + 8x^2 - 4x + 2x^{-1} - 2(1-\alpha) \Big\} O^{3}_{\mu\nu}(p)$$
$$+ \frac{1}{\varepsilon}\big[\, 2 - 2x \,\big] O^{4}_{\mu\nu}(p) \qquad (3.2.44)$$

and

$$\mathcal{A}^{(1)}_{2,\mu\nu}(x,p) = \left(\frac{-x(1-x)p^2}{\mu^2}\right)^{\frac{1}{2}\varepsilon} \Big\{ \frac{1}{\varepsilon}\big[\, 8 + 4x - 8(1-x)^{-1}_{+}$$
$$- [4 + (1-\alpha)]\delta(1-x) \,\big] + \big[\, 2 - 2(1-x)^{-1}_{+} \,\big](1-\alpha)$$
$$+ \big[\, 4 - 4\zeta(2) + (1-\alpha) - \tfrac{1}{2}(1-\alpha)^2 \,\big]\delta(1-x) \Big\} O^{1}_{\mu\nu}(p)$$
$$+ \Big\{ \frac{1}{\varepsilon}\big[\, 12x - 4 - 16x^2 + 4(1-\alpha) \,\big] - 8x^2 + 4x + 2(1-\alpha) \Big\} O^{3}_{\mu\nu}(p)$$
$$+ \frac{1}{\varepsilon}\big[\, 2x - 2 \,\big] O^{4}_{\mu\nu}(p), \qquad (3.2.45)$$

where the tensors $O^{i}_{\mu\nu}$ are given in eqs. 3.2.17–3.2.20. The first coefficient of Z_A in the covariant gauge is given by

$$Z^{(1)}_{A} = \frac{1}{\varepsilon}\big[\, -\tfrac{10}{3} - (1-\alpha) \,\big], \qquad (3.2.46)$$

which is explicitly dependent on the gauge parameter α. The sum of the contributions is equal to

$$\left(\frac{-x(1-x)p^2}{\mu^2}\right)^{-\frac{1}{2}\varepsilon} \mathcal{A}^{(1)}_{\mu\nu}(x,p) + Z^{(1)}_{A}\mathcal{A}^{(0)}_{\mu\nu}(x,p) = \Big\{ \frac{1}{\varepsilon}\big[\, 16 + 8x^2 - 8x - 8x^{-1}$$
$$- 8(1-x)^{-1}_{+} - \tfrac{22}{3}\delta(1-x) \,\big] + 6 + 4x^2 - 4x - 4x^{-1} - (1-\alpha)(1-x)^{-1}_{+}$$
$$+ \big[\, \tfrac{67}{9} - 4\zeta(2) + (1-\alpha) - \tfrac{1}{4}(1-\alpha)^2 \,\big]\delta(1-x) \Big\} O^{1}_{\mu\nu}(p)$$

$$+\left[2+8x^2-8x-(1-\alpha)x^{-1}\right]O^2_{\mu\nu}(p)$$

$$+\left\{\frac{1}{\varepsilon}\left[4x^{-1}-4\right]-2+2x^{-1}\right\}O^3_{\mu\nu}(p). \tag{3.2.47}$$

Comparing the above expression with the one given in eq. 3.2.43, where we used the lightlike axial gauge, the pole term corresponding to $O^1_{\mu\nu}(p)$ is left unchanged. It means that the anomalous dimension γ_{gg} is not altered (at this order) by changing from an axial gauge calculation to the covariant one. The tensor structure $O^4_{\mu\nu}(p)$, which doesn't satisfy the WT identity 3.2.26, drops out (see eq. 3.2.25).

However, there are a few differences with respect to the axial gauge calculation. Firstly, the finite terms which are proportional to the tensors $O^{1,2}_{\mu\nu}(p)$, are different due to gauge effects. This feature is not important, because it just entails a shift of finite terms and it does not influence the physically important UV singular behaviour. Nevertheless, it is interesting to see that the constant terms of eq. 3.2.47 are explicitly dependent on the gauge parameter α. It means that the non–pole part of the Green's function is not gauge independent, even when we include the effect of wave function renormalisation. This is important, because it entails the renormalisation of the gauge parameter when we treat the two loop calculation. Notice that in the covariant gauge the renormalisation constant for the gauge parameter α is equal to the wave function renormalisation constant Z_A. Secondly, in the final result appears the tensor $O^3_{\mu\nu}(p)$, which satisfies relation 3.2.26, but not 3.2.28. Moreover, its coefficient shows an UV singular behaviour, represented by ε^{-1} (see eq. 3.2.47). Due to this structure a new operator has to be introduced in the Lagrangian, the matrix element of which removes its divergence. We will call this gauge variant operator the <u>alien operator</u>. At lowest order it has the following form (where we use the notation of eq. 3.2.8)

$$O_a=\left[(\partial^\alpha A-\partial A^\alpha)\partial^{m-2}\partial_\alpha A\right], \tag{3.2.48}$$

and its Feynman rule is proportional to the tensor structure $O^3_{\mu\nu}(p)$, given in eq. 3.2.19. The counter term, which must be included in the Lagrangian, is given by

$$-\frac{1}{\varepsilon}\frac{\alpha_s}{4\pi}S_\varepsilon C_A\,\frac{(1+(-1)^m)}{m(m-1)}O_a\equiv-\frac{\alpha_s}{4\pi}S_\varepsilon C_A Z^{1,(m)}_{ga}O_a, \tag{3.2.49}$$

where Z_{ga} is the renormalisation constant belonging to the gluon–alien transition, which is expanded in the same way as Z_{gg} (cf. eq. 3.2.15). The first order result becomes finite if one calculates the Green's function in which <u>both</u> operators, the gluon and the alien one, are inserted. Then one observes that we can write the bare Green's function as a sum of two renormalised Green's functions in the following way

$$Z_A \hat{\Gamma}_{O_g,\mu\nu} = Z_{gg}^{(m)} \Gamma_{O_g,\mu\nu} + Z_{ga}^{(m)} \Gamma_{O_a,\mu\nu}. \quad (3.2.50)$$

The new WT identity, which is valid in the covariant gauge, couples the contribution of $O^3_{\mu\nu}(p)$ to the Green's function of the operator sandwiched between ghost fields. Instead of eq. 3.2.28 we have in this case

$$p_\nu \hat{\Gamma}^{\mu\nu}_{O_g} = \hat{\tilde{\Gamma}}^{\mu}_{O_g}, \quad (3.2.51)$$

where the right–hand side denotes the 1PI Green's function of the gluon operator with external ghost fields. It can be written at lowest order in the coupling constant as follows

$$\hat{\tilde{\Gamma}}_{O_g,\mu} = \frac{1+(-1)^m}{2} \delta^{ab} (\Delta \cdot p)^m \int_0^1 dx\, x^{m-1} \left\{ \frac{\hat{\alpha}_s}{4\pi} S_\varepsilon C_A \mathcal{A}^{(1)}_\mu(x,p) \right\}. \quad (3.2.52)$$

The expression $\mathcal{A}^{(1)}_\mu(x,p)$ is given by the graph in fig. 3.3. The Feynman rule of the amputated ghost–gluon vertex, that is indicated by a dot and only one ghost line, is altered (with respect to the normal ghost–gluon vertex) in the sense that one leaves out the outgoing momentum. This reveals the Lorentz index ν (see figure 3.3). An extra feature is the multiplication with the orthogonal projection operator $p^2 g_{\mu\nu} - p_\mu p_\nu$, which is explained by J.C. Taylor in [10]. The WT identity 3.2.51 holds for connected diagrams, but here it can be applied without any modifications, because the external self–energy diagram does not contribute.

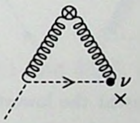

Fig. 3.3. WT diagram which represents the lowest order contribution to the right–hand side of eq. 3.2.51. The dot indicates the amputated ghost vertex, which does not have the outgoing momentum like the normal ghost–gluon vertex. The × represents the multiplication with the orthogonal projection operator $p^2 g_{\mu\nu} - p_\mu p_\nu$.

The quantity $\mathcal{A}^{(1)}_\mu(x,p)$ is given by

$$\mathcal{A}^{(1)}_\mu(x,p) = \left(\frac{-x(1-x)p^2}{\mu^2} \right)^{\frac{1}{2}\varepsilon} \left\{ \frac{1}{\varepsilon} \left[2x^{-1} - 2 \right] - 1 + x^{-1} \right\} \left(\frac{p^2 \Delta_\mu}{\Delta \cdot p} - p_\mu \right), \quad (3.2.53)$$

which is in agreement with the contribution of $O^3_{\mu\nu}(p)$ to the gluon operator Green's function that we calculated in eq. 3.2.47 in view of the equality

$$p^\nu O^3_{\mu\nu}(p) = \frac{1}{2}\left(\frac{p^2\Delta_\mu}{\Delta\cdot p} - p_\mu\right). \tag{3.2.54}$$

From the WT identity in eq. 3.2.51 it follows that in addition to the counter term for the alien operator (see eq. 3.2.49), we also have to introduce one for the ghost operator, which in lowest order in g is given by

$$O_\omega = -\xi\partial^m\omega, \tag{3.2.55}$$

where ξ and ω are the (anti)ghost fields. The counter term corresponding to O_ω, which has to be included in the Lagrangian, equals

$$-\frac{1}{\varepsilon}\frac{\alpha_s}{4\pi}S_\varepsilon C_A\frac{(1+(-1)^m)}{m(m-1)}O_\omega \equiv -\frac{\alpha_s}{4\pi}S_\varepsilon C_A Z^{1,(m)}_{g\omega}O_\omega, \tag{3.2.56}$$

up to the lowest order in the renormalised coupling constant α_s. This counter term is introduced in order to get a finite Green's function, which has two external ghost lines. The contributing graphs to this 1PI Green's function are shown in fig. 3.4. Because of the relation between $\hat{\hat{\Gamma}}_{O_{g,\mu}}$ and $\hat{\Gamma}_{O_\omega}$, which in lowest order equals the contribution

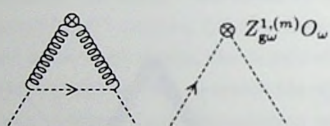

Fig. 3.4. Diagrams which represent the lowest order contribution to the 1PI Green's function with two external ghost lines. The expression for the diagram on the left can be deduced from eq. 3.2.53 by replacing the factor $p^2\Delta_\mu/\Delta p - p_\mu$ by 1. The diagram on the right is due to the introduced counter term for the ghost operator (cf. eq. 3.2.56).

of eq. 3.2.56 (shown in the second diagram of fig. 3.4), and the WT identity expressed by eq. 3.2.51, we have the following equality in terms of the renormalisation constants

$$Z^{(m)}_{ga} = Z^{(m)}_{g\omega}. \tag{3.2.57}$$

Renormalisation of the gluon operator in the covariant gauge at higher orders involves mixing between these three operators that we have seen up to now at least.

Already at this moment, it can be seen that we will need the newly discovered alien and ghost operators up to order g^3 in the Lagrangian to perform a correct two loop calculation. The actual form of the operators at this order cannot easily be guessed by covariantisation of the derivatives or by introduction of the non-abelian field strength in 3.2.48. The determination of the correct Lagrangian is the subject of the next section.

3.3 One loop renormalisation of the action to order g^3

In the previous section it became clear that the gluon operator is not multiplicatively renormalised. In other words, the divergent expressions, which one finds at the one loop level, do not have the same form as the original ones. Hence, in order to achieve finiteness of the theory, one must introduce new counter terms in the Lagrangian. The problem under study is the calculation of the two loop contributions to the renormalisation factor of the gluon operator, which is $\mathcal{O}(g^4)$ in the coupling constant. This makes it obligatory to determine the new counter terms (due to one loop calculations) up to $\mathcal{O}(g^3)$. Fourth order terms are excluded, because they cannot contribute to a Green's function with 2 external legs.

In this section we want to calculate these terms. In order to justify the connection between new gluon (alien) operators and ghost operators, we use the general idea of BRST invariance.

3.3.1 BRST invariance

The Lagrangian, given by eqs. 3.2.1 and 3.2.2, is invariant under the rigid BRST transformations

$$\begin{aligned} \delta A^a_\mu &= D^{ab}_\mu \omega^b \lambda, \\ \delta\omega^a &= -\tfrac{1}{2} g f^{abc}\omega^b\omega^c\lambda, \\ \delta\xi^a &= -\tfrac{1}{\alpha}(\partial^\mu A^a_\mu)\lambda, \end{aligned} \tag{3.3.1}$$

where λ is a x-independent infinitesimal anti-commuting constant. The invariance can equally well be expressed by

$$\mathcal{G}\mathcal{L} = 0, \tag{3.3.2}$$

where

$$\mathcal{G} = (D^{ab}_\mu\omega^b)\frac{\delta}{\delta A^a_\mu} - \tfrac{1}{2} g f^{abc}\omega^b\omega^c\frac{\delta}{\delta\omega^a} - \tfrac{1}{\alpha}(\partial^\mu A^a_\mu)\frac{\delta}{\delta\xi^a}. \tag{3.3.3}$$

Following Zinn–Justin [11], we introduce sources K and L for the BRST variations of the gluon and the ghost fields, which results in the following action

$$S[A,\xi,\omega,K,L] = \int d^4x \, \left(\mathcal{L}[A,\xi,\omega] + K^{a\mu} D_\mu^{ab}\omega^b - \tfrac{1}{2} g L^a f^{abc}\omega^b\omega^c\right). \tag{3.3.4}$$

The Lagrangian $\mathcal{L}[A,\xi,\omega]$ is taken from eqs. 3.2.1 and 3.2.2. The generating functional of connected Green's functions W is defined by

$$\begin{aligned} & e^{iW}[j,\rho,\sigma,K,L,J] = \\ & \int [dA][d\omega][d\xi] \, \exp\left[iS + i\int d^4x \, \left(j^{a\mu}A_\mu^a + \xi^a\rho^a + \sigma^a\omega^a + J_{\mu_1\ldots\mu_m}O_g^{\mu_1\ldots\mu_m}\right)\right], \end{aligned} \tag{3.3.5}$$

where j, ρ and σ are sources for the fields, in order to be able to define expectation values, and $J_{\mu_1\ldots\mu_m}O_g^{\mu_1\ldots\mu_m}$ represents the introduction of the gluon operator. The Legendre transformation of the functional W, with respect to the sources of the fields, gives the generating functional Γ of the one particle irreducible (1PI) vertices. In order to keep the notation limited, we do not introduce new variables for the expectation values of the fields. The actual meaning of A, ξ and ω should be contextually clear at any moment. We have

$$\Gamma[A,\xi,\omega,K,L,J] = W[j,\rho,\sigma,K,L,J] - \int d^4x \, (j^{a\mu}A_\mu^a + \xi^a\rho^a + \sigma^a\omega^a). \tag{3.3.6}$$

We are now able to formulate two equalities, which we want to maintain at all orders in the loop expansion of Γ. These are the equation of motion for the antighost field,

$$\frac{\delta\tilde{\Gamma}}{\delta\xi^a} = \partial^\mu \frac{\delta\tilde{\Gamma}}{\delta K^{a\mu}}, \tag{3.3.7}$$

and the WT identity, which expresses BRST invariance of the action,

$$\frac{\delta\tilde{\Gamma}}{\delta A_\mu^a}\frac{\delta\tilde{\Gamma}}{\delta K^{a\mu}} = \frac{\delta\tilde{\Gamma}}{\delta\omega^a}\frac{\delta\tilde{\Gamma}}{\delta L^a}, \tag{3.3.8}$$

where $\tilde{\Gamma}$ is defined by

$$\tilde{\Gamma} = \Gamma - \int d^4x \, \mathcal{L}_{\mathrm{GF}}, \tag{3.3.9}$$

which is manifestly gauge invariant.

We are interested in Green's functions with one single insertion of the gluon operator. Therefore, it is natural to differentiate eqs. 3.3.7 and 3.3.8 with respect to the source $J_{\mu_1\ldots\mu_m}$ and set $J_{\mu_1\ldots\mu_m} = 0$. This action will give us the generating functional of 1PI Green's functions with one operator insertion, which obeys the relations

$$\frac{\delta\tilde{\Gamma}^{\mu_1\cdots\mu_m}}{\delta\xi^a} = \partial^\mu \frac{\delta\tilde{\Gamma}^{\mu_1\cdots\mu_m}}{\delta K^{a\mu}}, \tag{3.3.10}$$

$$\frac{\delta\tilde{\Gamma}}{\delta A^a_\mu}\frac{\delta\tilde{\Gamma}^{\mu_1\cdots\mu_m}}{\delta K^{a\mu}} + \frac{\delta\tilde{\Gamma}^{\mu_1\cdots\mu_m}}{\delta A^a_\mu}\frac{\delta\tilde{\Gamma}}{\delta K^{a\mu}} = \frac{\delta\tilde{\Gamma}}{\delta\omega^a}\frac{\delta\tilde{\Gamma}^{\mu_1\cdots\mu_m}}{\delta L^a} + \frac{\delta\tilde{\Gamma}^{\mu_1\cdots\mu_m}}{\delta\omega^a}\frac{\delta\tilde{\Gamma}}{\delta L^a}, \tag{3.3.11}$$

where

$$\tilde{\Gamma}^{\mu_1\cdots\mu_m} = \left.\frac{\delta\tilde{\Gamma}}{\delta J_{\mu_1\ldots\mu_m}}\right|_{J_{\mu_1\ldots\mu_m}=0}. \tag{3.3.12}$$

Applying these equations to the case, where $\tilde{\Gamma}$ has already been expressed in renormalised fields (therefore being finite), the one loop divergent part of $\tilde{\Gamma}^{\mu_1\cdots\mu_m}$ must satisfy the following restrictions

$$\frac{\delta\left(\tilde{\Gamma}^{\mu_1\cdots\mu_m}\right)_1^{\text{div}}}{\delta\xi^a} = \partial^\mu \frac{\delta\left(\tilde{\Gamma}^{\mu_1\cdots\mu_m}\right)_1^{\text{div}}}{\delta K^{a\mu}}, \tag{3.3.13}$$

$$\mathcal{G}_0\left(\tilde{\Gamma}^{\mu_1\cdots\mu_m}\right)_1^{\text{div}} = \left[-\frac{\delta\tilde{\Gamma}}{\delta A^a_\mu}\frac{\delta}{\delta K^{a\mu}} + \frac{\delta\tilde{\Gamma}}{\delta\omega^a}\frac{\delta}{\delta L^a}\right]\left(\tilde{\Gamma}^{\mu_1\cdots\mu_m}\right)_1^{\text{div}}, \tag{3.3.14}$$

where we introduced $\mathcal{G}_0$, the generator of BRST transformations in the (A,ω) sector,

$$\mathcal{G}_0 = (D^{ab}_\mu\omega^b)\frac{\delta}{\delta A^a_\mu} - \tfrac{1}{2}gf^{abc}\omega^b\omega^c\frac{\delta}{\delta\omega^a}. \tag{3.3.15}$$

Because the relations 3.3.13 and 3.3.14 are valid, we can write down new invariance transformations of the action with <u>all</u> operators (the old gluon operator as well as the new ones). The action that is meant here can be expressed by

$$\mathcal{L}[A,\xi,\omega] + J_{\mu_1\ldots\mu_m}\sum_i O_i^{\mu_1\cdots\mu_m}, \tag{3.3.16}$$

where i runs over the set $\{\text{g},\text{a},\omega\}$. The gauge fixing term $\mathcal{L}_{\text{GF}}$ is left out. The new transformations are given by

$$\begin{aligned}
\delta A^a_\mu &= \left(D^{ab}_\mu\omega^b + J_{\mu_1\ldots\mu_m}\frac{\delta\left(\tilde{\Gamma}^{\mu_1\cdots\mu_m}\right)_1^{\text{div}}}{\delta K^{a\mu}}\right)\lambda,\\
\delta\omega^a &= \left(-\tfrac{1}{2}gf^{abc}\omega^b\omega^c + J_{\mu_1\ldots\mu_m}\frac{\delta\left(\tilde{\Gamma}^{\mu_1\cdots\mu_m}\right)_1^{\text{div}}}{\delta L^a}\right)\lambda,\\
\delta\xi^a &= -\tfrac{1}{\alpha}(\partial_\mu A^{\mu a})\lambda.
\end{aligned} \tag{3.3.17}$$

The invariance of the complete system under the transformations 3.3.17 must be present, because the derivatives with respect to the sources K and L <u>are</u> the BRST variations of the fields A and ω, respectively. One can also show, by plain algebra, that the new action is invariant up to the first order in the current $J_{\mu_1\ldots\mu_m}$ under the transformations 3.3.17.

3.3.2 Construction of the renormalised action

The outstanding question is how the new action is expressed in terms of the renormalised fields. If we can give an answer to this question, we have a Lagrangian at hand from which we can calculate all counter terms at the two loop level. The beautiful fact is that we have found an invariance of this new action, in spite of the fact that we do not know the action itself. However, if we can invent a transformation on the field A as such, that the new field A' obeys old transformation laws, we know that $\mathcal{L} + J_{\mu_1\cdots\mu_m} O_g^{\mu_1\cdots\mu_m}$ in terms of A' is invariant. Substituting the new field (in terms of the old field) into the action renders an action, which is invariant under transformations 3.3.17. One should also carry this procedure through for the ghost field, but we do not present that here, because it does not influence the calculation under study.

The programme is as follows. Firstly, we will consider the general form of the expression

$$J_{\mu_1\cdots\mu_m} \frac{\delta\left(\tilde{\Gamma}^{\mu_1\cdots\mu_m}\right)_1^{\text{div}}}{\delta K^{a\mu}} \equiv Q^a_\mu. \tag{3.3.18}$$

It will appear that the quantity Q^a_μ is precisely the extension of the gauge transformation that is presented by Dixon and Taylor [2]. Secondly, a transformation on the field A is given in such a way that the transformed field obeys the old BRST transformation law. Thirdly, we substitute this new field in the Lagrangian. The resulting expression for the Lagrangian must be invariant under transformations 3.3.17.

Consider the quantity Q^a_μ. One can state the following about it:

- It has a colour index a and a Lorentz index μ.
- Its dimension is 2.
- The expression must have ghost number 1, because it belongs to a BRST transformation, which means that one ω field must be present.
- The previous two arguments and the fact that the current $J_{\mu_1\cdots\mu_m}$ has dimension $-(m-2)$ demand that an object (consisting of gluon fields, derivatives, etc.) of dimension $m-1$ must be added.
- The parameters, appearing in Q^a_μ, must be dimensionless, because we want the theory to be renormalisable.
- The gluon operator only couples to gluon fields, which means that all diagrams with more pairs of external ghost lines are convergent by power counting.

- The form of the current $J_{\mu_1\ldots\mu_m}$ is given in eq. 3.2.6. This form restricts the possible Lorentz structures severely.

From these conditions one can deduce the most general form for Q^a_μ:

$$Q^a_\mu = \eta\Delta_\mu\partial^{m-1}\omega^a + gf^{abc}\Delta_\mu\sum_{i=1}^{m-2}\eta_i(\partial^i\omega^c)(\partial^{m-2-i}A^b) + \mathcal{O}(g^2). \tag{3.3.19}$$

The determination of this form involved the additional restriction that the new transformations 3.3.17 should be nilpotent. This fixes the specific colour factor f^{abc} and restricts the values of η_i. These parameters must satisfy

$$\eta_i + \eta_{m-1-i} = \eta\begin{pmatrix} m-2 \\ i \end{pmatrix}, \tag{3.3.20}$$

while η_0 must be absent.

Looking at the definition of Q^a_μ in eq. 3.3.18, one can easily see that η must be $\mathcal{O}(g^2)$. In the same way one can observe that the extra term in $\delta\omega^a$ in eq. 3.3.17 is $\mathcal{O}(g^4)$. We do not consider this quantity, because its effect is beyond the scope of our problem. The parameters η and η_i follow from the calculation of 3.3.18, i.e. the divergent part of the Feynman graphs with one operator and one amputated K-vertex insertion. The actual determination of these parameters is performed in the next section.

Subsequently, we want to find a transformation on the field A, which involves the current $J_{\mu_1\ldots\mu_m}$, such that the transformed field obeys the BRST transformation laws 3.3.1. The new field will be implicitly expressed in terms of the old field as

$$A^a_\mu = A^{a\prime}_\mu + R^a_\mu(A'). \tag{3.3.21}$$

From the requirement $\delta A^{a\prime}_\mu = D^{ab}_\mu\omega^b\lambda$ (where D involves the new field A') follows

$$\left(\frac{\delta R^a_\mu}{\delta A^b_\nu}D^{bc}_\nu - gf^{abc}R^b_\mu\right)\omega^c = Q^a_\mu. \tag{3.3.22}$$

The polynomial R^a_μ obeys a similar set of conditions as Q^a_μ. It must have the same dimension and quantum numbers as the field A^a_μ, and the coupling to the current $J_{\mu_1\ldots\mu_m}$ must be present. The most simple way to find a general parametrisation[4] (in view of the restriction 3.3.22) is to take Q^a_μ (see eq. 3.3.19) and replace each term $\partial_\mu\omega^a$ by A^a_μ. One arrives at the expression

$$R^a_\mu = \kappa\Delta_\mu\partial^{m-2}A^a - gf^{abc}\Delta_\mu\sum_{i=1}^{m-2}\kappa_i(\partial^{i-1}A^b)(\partial^{m-2-i}A^c) + \mathcal{O}(g^2). \tag{3.3.23}$$

[4]We do not know whether eq. 3.3.22 has always a solution. At least up to order g we find one.

The restriction 3.3.22 determines the parameters κ and κ_i to be equal to

$$\kappa = \eta, \quad 2\kappa_i = \eta_i - \eta \binom{m-2}{i}. \tag{3.3.24}$$

From the discussion below eq. 3.3.20 we infer that a field redefinition of the ghost field starts at $\mathcal{O}(g^4)$. This will not give rise to contributing counter terms in the Lagrangian to our problem. However, if one wants to carry through the whole renormalisation programme, it is necessary to take care of these terms, too.

The final step to construct the new Lagrangian is the substitution of the new field into the old Lagrangian. Up to the relevant order the inverse of relation 3.3.21 is simply

$$A_\mu^{a\prime} = A_\mu^a - R_\mu^a(A). \tag{3.3.25}$$

We substitute this expression into $\mathcal{L}[A', \xi, \omega] + J_{\mu_1 \cdots \mu_m} O_{\rm g}^{\mu_1 \cdots \mu_m}$, where we understand the Lagrangian <u>without</u> gauge fixing term. One should leave out $\mathcal{L}_{\rm GF}$, because the invariance transformations 3.3.17 are valid for $\tilde{\Gamma}$, which is defined in eq. 3.3.9 as the generating functional without the gauge fixing term. The substitution procedure gives us the Lagrangian, expressed in renormalised quantities

$$\begin{aligned} \mathcal{L} = & -\tfrac{1}{4} Z_A F_{\mu\nu} F^{\mu\nu} - \tfrac{1}{2\alpha}(\partial^\mu A_\mu)^2 - Z_\omega \xi \partial^\mu D_\mu \omega + Z_{\rm gg} O_{\rm g} \\ & + \eta F^\alpha D_\alpha \partial^{m-2} A - g f^{abc} F_\alpha^a \sum_{i=1}^{m-2} \kappa_i \partial^\alpha [(\partial^{i-1} A^b)(\partial^{m-2-i} A^c)] \\ & - \eta \xi \partial^m \omega - g f^{abc} \xi^a \sum_{i=1}^{m-2} \eta_i \partial [(\partial^{m-2-i} A^b)(\partial^i \omega^c)], \end{aligned} \tag{3.3.26}$$

where the second and third lines constitute the generalisations of the alien and the ghost operators given in eqs. 3.2.48 and 3.2.55, i.e.

$$O_{\rm a} = F^\alpha D_\alpha \partial^{m-2} A - g f^{abc} F_\alpha^a \sum_{i=1}^{m-2} \frac{\kappa_i}{\eta} \partial^\alpha [(\partial^{i-1} A^b)(\partial^{m-2-i} A^c)], \tag{3.3.27}$$

$$O_\omega = -\xi \partial^m \omega - g f^{abc} \xi^a \sum_{i=1}^{m-2} \frac{\eta_i}{\eta} \partial [(\partial^{m-2-i} A^b)(\partial^i \omega^c)]. \tag{3.3.28}$$

The constant η, as it was used in this section, can be related to $Z_{\rm ga}^{1,(m)}$, which was defined in eq. 3.2.49. At lowest order in the coupling constant we recover the operators $O_{\rm a}$ and O_ω, given in eqs. 3.2.48 and 3.2.55. The notation applied in the above expressions is defined in eq. 3.2.8, but for convenience we give the rules here again

$$\begin{aligned} F_\alpha = \Delta^\beta F_{\alpha\beta} \quad &, \quad D = i\Delta^\alpha D_\alpha, \\ A = \Delta^\alpha A_\alpha \quad &, \quad \partial = i\Delta^\alpha \partial_\alpha. \end{aligned} \tag{3.3.29}$$

Colour indices are suppressed in those cases where no ambiguities can occur. From this new Lagrangian one can calculate the Feynman rules, corresponding to the new operators. They are given in appendix 3A.4.

3.3.3 The calculation of η and η_i

In this section we present the calculation of the parameters η and η_i. As we apply dimensional regularisation throughout this thesis, these quantities are calculated in $n = 4 + \varepsilon$ dimensions. From the definition of Q^a_μ in eq. 3.3.18 it is clear that we can determine η and η_i by considering one loop graphs, which are 1PI and which have one insertion of the operator O_g. Furthermore, they have one amputated K–vertex insertion coming from the non–abelian part of $(D_\mu\omega)^a$, as can be seen in eq. 3.3.4. The Feynman rule of such a vertex is equal to the one of the gluon–ghost vertex, but without the momentum of the outgoing ghost. The relevant diagram for the calculation of η was already given in fig. 3.3, but in this case the projection operator $\times$ is not considered. The diagrams for η_i are shown in fig. 3.5.

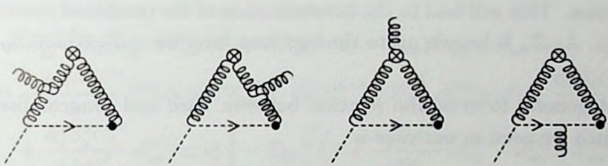

Fig. 3.5. One loop 1PI graphs which contribute to η_i. They have one operator O_g insertion (indicated by $\otimes$) as well as one amputated K–vertex (indicated by $\bullet$).

The expressions, due to the diagrams for η_i, contain non–local terms of the form

$$\sum_{i=1}^{m-2} \frac{1}{i}(\Delta\cdot p_1)^i(\Delta\cdot p_2)^{m-2-i}, \tag{3.3.30}$$

which however cancel in the sum of the 4 diagrams (cf. eq. 3A.17). Further, the diagrams for η_i are dependent on the gauge fixing parameter α, but this dependence also disappears in the final sum. We find that η and η_i are equal to

$$\eta = -\frac{g^2}{(4\pi)^2} C_A \frac{1+(-1)^m}{\varepsilon}\frac{1}{m(m-1)}, \tag{3.3.31}$$

$$\eta_i = \eta\left[\frac{1}{4}(-1)^i + \frac{3}{4}\binom{m-2}{i-1} + \frac{1}{4}\binom{m-2}{i}\right], \tag{3.3.32}$$

where η can be straightforwardly identified with the renormalisation constant $Z_{ga}^{1,(m)}$ of the alien operator O_a (see eq. 3.2.49) and therefore also with the one corresponding to the ghost operator, $Z_{g\omega}^{1,(m)}$, which was given in eq. 3.2.56. This result is identical to what Dixon and Taylor found in [2], except for the factor $\frac{1}{4}$ that accompanies $(-1)^i$ in the expression for η_i. Notice that the η_i satisfy the relation imposed by nilpotency of the BRST variations 3.3.17, which was given in eq. 3.3.20.

We have arrived at an expression for the Lagrangian, which is renormalised at the one loop level up to sufficiently high order to perform the two loop calculation of the 1PI Green's function.

3.4 Results of the two loop calculations

In this section we show the two loop renormalisation of the gluon operator. We perform the calculation in the Feynman gauge, i.e. the covariant gauge with $\alpha = 1$ (see eq. 3A.4). In order to do this calculation we use the Lagrangian, which is one loop renormalised up to $\mathcal{O}(g^3)$ (see eq. 3.3.26), to calculate all contributions to the 1PI Green's function. This will lead to the determination of the combined renormalisation factor $Z_A^{-1} Z_O$. As Z_A is known up to the two loop level we can extract Z_O from this result.

The most general form of the relation between bare and renormalised Green's functions which we need in our case is

$$Z_A \begin{pmatrix} \hat{\Gamma}_{O_g} \\ \hat{\Gamma}_{O_a} \\ \hat{\Gamma}_{O_\omega} \end{pmatrix} = \begin{pmatrix} Z_{gg} & Z_{ga} & Z_{g\omega} \\ Z_{ag} & Z_{aa} & Z_{a\omega} \\ Z_{\omega g} & Z_{\omega a} & Z_{\omega\omega} \end{pmatrix} \begin{pmatrix} \Gamma_{O_g} \\ \Gamma_{O_a} \\ \Gamma_{O_\omega} \end{pmatrix}, \tag{3.4.1}$$

where Γ_{O_i} denotes the 1PI Green's function with two external gluon fields and an operator O_i insertion. This equation is the starting point of our discussion, in which we will calculate the order α_s^2 contributions to Z_{gg} and Z_{ga}.

Let us consider the renormalised Green's function that contains one gluon operator insertion. Because the renormalised Lagrangian contains more operators we have

$$Z_A \hat{\Gamma}_{O_g} = Z_{gg} \Gamma_{O_g} + Z_{ga} \Gamma_{O_a} + Z_{g\omega} \Gamma_{O_\omega}, \tag{3.4.2}$$

where the operator renormalisation constants are defined in eqs. 3.2.49 and 3.2.56. Hence, the renormalised Green's function can be denoted as

$$\Gamma_{O_g} = Z_{gg}^{-1} \left(Z_A \hat{\Gamma}_{O_g} - Z_{ga} \Gamma_{O_a} - Z_{g\omega} \Gamma_{O_\omega} \right). \tag{3.4.3}$$

As the two renormalisation constants Z_{ga} and $Z_{\mathrm{g}\omega}$ are equal to each other (cf. eqs. 3.2.49 and 3.2.56), we need to consider the sum $\Gamma_{O_{\mathrm{a}}} + \Gamma_{O_\omega}$ only. In view of the general renormalisation matrix 3.4.1 we have the following equality

$$Z_A\left(\hat{\Gamma}_{O_{\mathrm{a}}} + \hat{\Gamma}_{O_\omega}\right) = (Z_{\mathrm{ag}} + Z_{\omega\mathrm{g}})\,\Gamma_{O_{\mathrm{g}}} + (Z_{\mathrm{aa}} + Z_{\omega\mathrm{a}})\,\Gamma_{O_{\mathrm{a}}} + (Z_{\mathrm{a}\omega} + Z_{\omega\omega})\,\Gamma_{O_\omega}. \quad (3.4.4)$$

As we will see later on, the first sum of renormalisation constants on the right-hand side vanishes:[5]

$$Z_{\mathrm{ag}} + Z_{\omega\mathrm{g}} = 0. \quad (3.4.5)$$

Using this property and the knowledge that off-diagonal renormalisation constants and Γ_{O_ω} are $\mathcal{O}(\alpha_s)$, we can invert relation 3.4.4 into

$$\Gamma_{O_{\mathrm{a}}} + \Gamma_{O_\omega} = (Z_A - (Z_{\mathrm{aa}} - 1) - Z_{\omega\mathrm{a}})\,\hat{\Gamma}_{O_{\mathrm{a}}} + \hat{\Gamma}_{O_\omega}, \quad (3.4.6)$$

which is valid up to order α_s. This result can be inserted into eq. 3.4.3, yielding (cf. eq. 3.2.10)

$$\begin{aligned}
\Gamma_{O_{\mathrm{g}}} &= Z_{\mathrm{gg}}^{-1}\left[Z_A\hat{\Gamma}_{O_{\mathrm{g}}} - Z_{\mathrm{ga}}(Z_A - (Z_{\mathrm{aa}} - 1) - Z_{\omega\mathrm{a}})\,\hat{\Gamma}_{O_{\mathrm{a}}} - Z_{\mathrm{g}\omega}\hat{\Gamma}_{O_\omega}\right] \\
&= \frac{1+(-1)^m}{2}\delta^{ab}(\Delta\cdot p)^m Z_{\mathrm{gg}}^{-1}\int_0^1 dx\, x^{m-1}\Big\{ Z_A\Big[\mathcal{A}^{(0)}_{\mu\nu}(x,p) + \frac{\hat{\alpha}_s S_\epsilon C_A}{4\pi}\mathcal{A}^{(1)}_{\mu\nu}(x,p) \\
&\quad + \frac{\hat{\alpha}_s^2 S_\epsilon^2 {C_A}^2}{(4\pi)^2}\mathcal{A}^{(2)}_{\mu\nu}(x,p)\Big] - Z_{\mathrm{ga}}\Big[\Big(1 + \frac{\alpha_s S_\epsilon C_A}{4\pi}(Z_A^{(1)} - Z_{\mathrm{aa}}^{(1)} - Z_{\omega\mathrm{a}}^{(1)})\Big)\mathcal{B}^{(0)}_{\mu\nu}(x,p) \\
&\quad + \frac{\hat{\alpha}_s S_\epsilon C_A}{4\pi}\mathcal{B}^{(1)}_{\mu\nu}(x,p)\Big] - Z_{\mathrm{g}\omega}\frac{\hat{\alpha}_s S_\epsilon C_A}{4\pi}\mathcal{C}^{(1)}_{\mu\nu}(x,p)\Big\} \\
&= \frac{1+(-1)^m}{2}\delta^{ab}(\Delta\cdot p)^m \int_0^1 dx\, x^{m-1}\Big\{ \mathcal{M}^{(0)}_{\mu\nu}(x,p) + \frac{\alpha_s C_A}{4\pi}\mathcal{M}^{(1)}_{\mu\nu}(x,p) \\
&\quad + \frac{\alpha_s^2 {C_A}^2}{(4\pi)^2}\mathcal{M}^{(2)}_{\mu\nu}(x,p)\Big\}, \qquad (3.4.7)
\end{aligned}$$

where $\mathcal{A}^{(0)}_{\mu\nu}(x,p)$ and $\mathcal{M}^{(0)}_{\mu\nu}(x,p)$ are defined in eq. 3.2.12. In the above expression $\mathcal{B}^{(0)}_{\mu\nu}(x,p)$ is the zero loop contribution of the alien operator, which is equal to

$$\mathcal{B}^{(0)}_{\mu\nu}(x,p) = 2O^3_{\mu\nu}(p)\delta(1-x). \quad (3.4.8)$$

The unrenormalised one loop contributions $\mathcal{B}^{(1)}_{\mu\nu}(x,p)$ and $\mathcal{C}^{(1)}_{\mu\nu}(x,p)$ come from the alien and the ghost operator insertions. The one loop contribution $\mathcal{B}^{(1)}_{\mu\nu}(x,p)$ due to

[5]This fact is established at first order in α_s, but it must be true in all orders, because these renormalisation constants can not affect the physical renormalisation constant Z_{gg}.

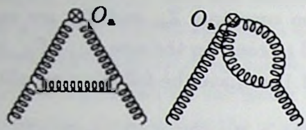

Fig. 3.6. The one loop contributions coming from the alien operator. The Feynman rules which correspond to the operator insertion can be found in appendix 3A.4.

the alien operator can be obtained from the diagrams given in fig. 3.6. Its expression in the Feynman gauge is

$$B^{(1)}_{\mu\nu}(x,p) = \left(\frac{-x(1-x)p^2}{\mu^2}\right)^{\frac{1}{2}\varepsilon} \Bigg(\Big\{ \frac{1}{\varepsilon}\big[\,2x - 2x^2\,\big] + 2 - 4x^{-1} \Big\} O^1_{\mu\nu}(p)$$
$$+ \big[\,4 - 2x^2 + 2x\,\big]\, O^2_{\mu\nu}(p)$$
$$+ \Big\{ \frac{1}{\varepsilon}\big[\,2 + 2x^2 - 5x + 4x^{-1} - 6(1-x)^{-1}_{+} - \tfrac{3}{2}\delta(1-x)\,\big]$$
$$- \tfrac{5}{2} + 2x^{-1} + \big[\,\tfrac{4}{3} - 3\zeta(2)\,\big]\,\delta(1-x) \Big\} O^3_{\mu\nu}(p) + \tfrac{1}{2} O^4_{\mu\nu}(p) \Bigg). \qquad (3.4.9)$$

Note that the quantities Z_{ag} and Z_{aa} at first order are the pole terms ε^{-1} belonging

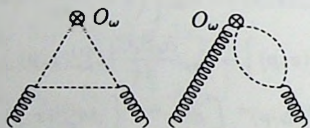

Fig. 3.7. The one loop contributions coming from the ghost operator. The Feynman rules which correspond to the operator insertion can be found in appendix 3A.4.

to the $O^1_{\mu\nu}$ and $2O^3_{\mu\nu}$ structures, respectively.

The quantity $C^{(1)}_{\mu\nu}(x,p)$ denotes the one loop contribution of the ghost operator. Its expression can be calculated from the diagrams given in fig. 3.7 and its result in the Feynman gauge is

$$C^{(1)}_{\mu\nu}(x,p) = \left(\frac{-x(1-x)p^2}{\mu^2}\right)^{\frac{1}{2}\varepsilon} \Bigg(\Big\{ \frac{1}{\varepsilon}\big[\,2x^2 - 2x\,\big] \Big\} O^1_{\mu\nu}(p) + \big[\,2x^2 - 2x\,\big]\, O^2_{\mu\nu}(p)$$

$$+\left\{ \frac{1}{\varepsilon}\left[5x - 2 - 2x^2 + \tfrac{1}{6}\delta(1-x) \right] + \tfrac{1}{2} - \tfrac{2}{9}\delta(1-x) \right\} O^3_{\mu\nu}(p)$$

$$- \tfrac{1}{2}O^4_{\mu\nu}(p) \Big) . \tag{3.4.10}$$

The first order contributions to the quantities $Z_{\omega g}$ and $Z_{\omega a}$ are determined by the pole terms ε^{-1} belonging to the $O^1_{\mu\nu}$ and $2O^3_{\mu\nu}$ structures, respectively. Note the pole terms proportional to $O^1_{\mu\nu}$ cancel in the sum of the two expressions $\mathcal{B}^{(1)}_{\mu\nu}$ and $\mathcal{C}^{(1)}_{\mu\nu}$ above. This is equivalent to the fact that these new operators do not influence the double pole structure of the physical contribution to the two loop calculation (cf. eq. 3.4.5).

The pole terms proportional to $2O^3_{\mu\nu}$ in eqs. 3.4.9 and 3.4.10 are elements of the anomalous dimension matrix. We will indicate these with indices a and ω, originating from the alien and the ghost operators, respectively. They are given by

$$\gamma^{0,(m)}_{aa} = C_A \left[\frac{1}{m} + \frac{1}{m+2} - \frac{5}{2(m+1)} + \frac{2}{m-1} - \sum_{i=1}^{m-1} \frac{3}{i} - \frac{3}{4} \right] \tag{3.4.11}$$

and

$$\gamma^{0,(m)}_{\omega a} = C_A \left[\frac{5}{2(m+1)} - \frac{1}{m} - \frac{1}{m+2} + \frac{1}{12} \right] . \tag{3.4.12}$$

The unrenormalised quantity $\mathcal{A}^{(1)}_{\mu\nu}(x,p)$ in expression 3.4.7 is taken from the one loop covariant gauge calculation:

$$\mathcal{A}^{(1)}_{\mu\nu}(x,p) = \mathcal{A}^{(1)}_{1,\mu\nu}(x,p) + \mathcal{A}^{(1)}_{2,\mu\nu}(x,p), \tag{3.4.13}$$

where the two terms on the right-hand side are given in eqs. 3.2.44 and 3.2.45, respectively.

Our object is to calculate the second order quantities $Z^{2,(m)}_{gg}$ and $Z^{2,(m)}_{ga}$, which render the total expression finite at second order in the coupling constant α_s. The expansion of such operator renormalisation constants can be found in eq. 3.2.15. In order to achieve the correct expressions for these renormalisation constants, it is necessary to express the lower order contributions to the 1PI Green's function in renormalised quantities. In order to do this we need the following renormalisation constants

$$Z_g = 1 + \sum_{i=1}^{\infty} \left(\frac{\alpha_s}{4\pi}\right)^i S^i_\varepsilon {C_A}^i Z^{(i)}_g , \tag{3.4.14}$$

$$Z_A = Z_\alpha = 1 + \sum_{i=1}^{\infty} \left(\frac{\alpha_s}{4\pi}\right)^i S^i_\varepsilon {C_A}^i Z^{(i)}_A , \tag{3.4.15}$$

where the constants Z_g, Z_A and Z_α represent the coupling constant, the wave function and the gauge parameter renormalisation constants, respectively. Notice that we have factorised the renormalised coupling constant α_s, the spherical factor S_ε (see eq. 3.2.11) and the universal colour factor C_A as usual. The coefficients which are relevant for our calculation are given by

$$Z_g^{(1)} = \Big[\, \tfrac{11}{3} \,\Big] \frac{1}{\varepsilon} \equiv \beta_0 \frac{1}{\varepsilon}, \tag{3.4.16}$$

$$Z_A^{(1)} = Z_\alpha^{(1)} = \Big[-\tfrac{10}{3} - (1-\alpha) \Big] \frac{1}{\varepsilon} \equiv \gamma_A^0 \frac{1}{\varepsilon} \tag{3.4.17}$$

and

$$Z_A^{(2)} = \Big[-\tfrac{25}{3} + \tfrac{5}{6}(1-\alpha) + (1-\alpha)^2 \Big] \frac{1}{\varepsilon^2} + \Big[-\frac{23}{4} - \tfrac{15}{8}(1-\alpha) + \tfrac{1}{4}(1-\alpha)^2 \Big] \frac{1}{\varepsilon}. \tag{3.4.18}$$

For completeness the above expressions are given for general α, the renormalised gauge fixing parameter. Note that the double pole term of $Z_A^{(2)}$ (denoted by $Z_A^{(2)}\,[\varepsilon^{-2}]$) can be expressed in lower order quantities through application of the renormalisation group equations:

$$\begin{aligned} Z_A^{(2)}\left[\varepsilon^{-2}\right] &= \frac{1}{2}\left(2Z_g^{(1)} + Z_\alpha^{(1)}\alpha\frac{\mathrm{d}}{\mathrm{d}\alpha} + Z_A^{(1)}\right) Z_A^{(1)} \\ &= \frac{1}{2\varepsilon^2}\left(\left(\gamma_A^0\right)^2 + 2\beta_0\gamma_A^0 + \gamma_A^0\right). \end{aligned} \tag{3.4.19}$$

Furthermore, we will need the renormalisation constants of the operators. These factors can be inferred from eqs. 3.2.47, 3.4.9 and 3.4.10, where the ε^{-1} terms represent the first order renormalisations of the gluon operator (proportional to $O^1_{\mu\nu}(p)$) and the alien operator (proportional to $2O^3_{\mu\nu}(p)$). The ghost operator has the same renormalisation constant as the alien operator. We will consider these quantities in the x–language, i.e. at the level of $\mathcal{A}^{(2)}_{\mu\nu}(x,p)$. This will lead to contributions which are convolutions of one loop results (like the complete expression 3.2.47), instead of simple multiplications. The inserted operator renormalisation constants have the following forms

$$Z_{gg}^{(1)}(x) = \frac{1}{\varepsilon}\Big[\, 16 + 8x^2 - 8x - 8x^{-1} - 8(1-x)_+^{-1} - \tfrac{22}{3}\delta(1-x) \,\Big], \tag{3.4.20}$$

$$Z_{ga}^{(1)}(x) = Z_{g\omega}^{(1)}(x) = \frac{1}{\varepsilon}\Big[\, 2x^{-1} - 2 \,\Big], \tag{3.4.21}$$

$$Z_{aa}^{(1)}(x) = \frac{1}{\varepsilon}\Big[\, 1 + x^2 - \tfrac{5}{2}x + 2x^{-1} - 3(1-x)_+^{-1} - \tfrac{49}{12}\delta(1-x) \,\Big], \tag{3.4.22}$$

$$Z^{(1)}_{\omega a}(x) = \frac{1}{\varepsilon}\left[\, \tfrac{5}{2}x - 1 - x^2 + \tfrac{1}{12}\delta(1-x) \,\right], \tag{3.4.23}$$

where the connection between the x–dependent and the m–dependent quantities is as follows

$$Z^{i,(m)} = \int_0^1 dx\, x^{m-1} Z^{(i)}(x). \tag{3.4.24}$$

From the above it follows that the renormalised second order contribution to the Green's function, $\mathcal{M}^{(2)}_{\mu\nu}(x,p)$, given in eq. 3.4.7, can be expressed in the following way

$$\begin{aligned}
\mathcal{M}^{(2)}_{\mu\nu} \;=\;& \mathcal{A}^{(2)}_{\mu\nu} + \left[\, 2Z^{(1)}_g + Z^{(1)}_A + Z^{(1)}_A \alpha\frac{\mathrm{d}}{\mathrm{d}\alpha} \,\right] \mathcal{A}^{(1)}_{\mu\nu} - Z^{(1)}_{g\omega} \otimes \mathcal{C}^{(1)}_{\mu\nu} \\
& - Z^{(1)}_{ga} \otimes \left[\, \mathcal{B}^{(1)}_{\mu\nu} - \left(\, Z^{(1)}_{aa} + Z^{(1)}_{a\omega} - Z^{(1)}_A \,\right) \otimes \mathcal{B}^{(0)}_{\mu\nu} \,\right] \\
& - Z^{(1)}_{gg} \otimes \left[\, \mathcal{A}^{(1)}_{\mu\nu} - \left(\, Z^{(1)}_{gg} - Z^{(1)}_A \,\right) \otimes \mathcal{A}^{(0)}_{\mu\nu} - Z^{(1)}_{ga} \otimes \mathcal{B}^{(0)}_{\mu\nu} \,\right] \\
& + \left[\, Z^{(2)}_A - Z^{(2)}_{gg} \,\right] \otimes \mathcal{A}^{(0)}_{\mu\nu} - Z^{(2)}_{ga} \otimes \mathcal{B}^{(0)}_{\mu\nu},
\end{aligned} \tag{3.4.25}$$

where we used the Z–factors given in eqs. 3.4.16–3.4.23 and left the x–dependences out. The convolution operator $\otimes$ is defined by

$$(f \otimes g)(x) = \int_0^1 dx_1 \int_0^1 dx_2\, \delta(x - x_1 x_2) f(x_1) g(x_2), \tag{3.4.26}$$

where f and g are arbitrary functions. In the expression 3.4.25 there are 3 unknown parts. Firstly, the contribution of all 1PI two loop graphs that is denoted by $\mathcal{A}^{(2)}_{\mu\nu}(x,p)$, which was also defined in eq. 3.4.7. Secondly, the second order of the gluon operator renormalisation $Z^{(2)}_{gg}(x)$, which is the central object of our calculation. Thirdly, the renormalisation constant $Z^{(2)}_{ga}(x)$.

First, we give the result of all the 1PI two loop diagrams which are shown in fig. 3.8. The Feynman rules and a general description of the calculation of two loop integrals are given in appendices 3A and 3C, respectively. In the Feynman gauge we find the following result

$$\begin{aligned}
\mathcal{A}^{(2)}_{\mu\nu}(x,p) = \left(\frac{-p^2}{\mu^2}\right)^{\varepsilon} \Bigg(\bigg\{ \frac{1}{\varepsilon} \Big[\Big[\, & \tfrac{136}{3}\zeta(2) + 20\zeta(3) - \tfrac{683}{12} \,\Big] \delta(1-x) \\
& - 4\left[\, 16x - 6x^2 + 4x^{-1} + 5(1-x)^{-1} + (1+x)^{-1} \,\right] \ln^2 x - 16\left[\, 6 + x^2 + 3x \right. \\
& \left. - x^{-1} - (1-x)^{-1} \,\right] \ln x \ln(1-x) - 8\left[\, 4 + 2x^2 - (1-x)^{-1} - (1+x)^{-1} \,\right] \zeta(2) \\
& - \tfrac{4}{3}\left[\, 88 - 10x^2 + 73x + 28x^{-1} - 34(1-x)^{-1} \,\right] \ln x + 48\left[\, x - 2 - x^2 + x^{-1} \right.
\end{aligned}$$

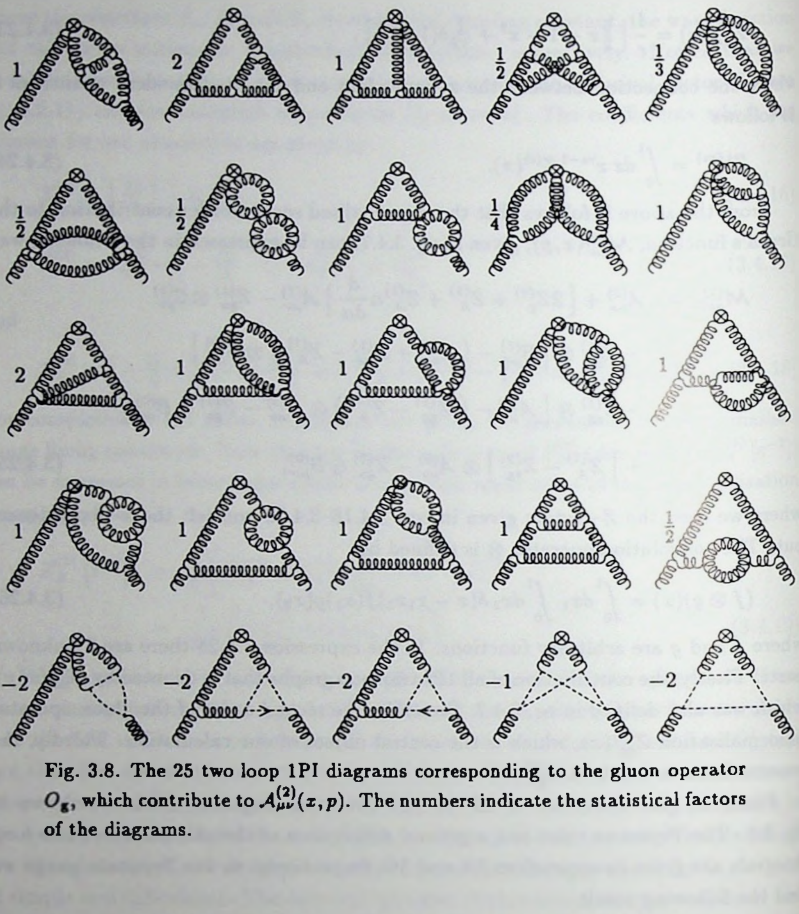

Fig. 3.8. The 25 two loop 1PI diagrams corresponding to the gluon operator O_g, which contribute to $\mathcal{A}^{(2)}_{\mu\nu}(x,p)$. The numbers indicate the statistical factors of the diagrams.

$$
\begin{aligned}
&+ (1-x)^{-1} \Big] \ln^2(1-x) - 16 \Big[2 + x^2 + x + x^{-1} - (1+x)^{-1} \Big] \ln x \ln(1+x) \\
&+ \tfrac{8}{3} \Big[15x^2 - 16 - 7x - 15x^{-1} + 17(1-x)^{-1} \Big] \ln(1-x) \\
&- 64 \Big[1 + x \Big] \operatorname{Li}_2(1-x) - 16 \Big[2 + x^2 + x + x^{-1} - (1+x)^{-1} \Big] \operatorname{Li}_2(-x) \\
&+ \tfrac{2}{9} + \tfrac{40}{9} x^2 + \tfrac{458}{9} x - \tfrac{148}{9} x^{-1} - \tfrac{526}{9} (1-x)^{-1} \Big]
\end{aligned}
$$

$$
\begin{aligned}
&+\frac{1}{\varepsilon^2}\Big[\,\big[\,21-32\zeta(2)\,\big]\,\delta(1-x)-32\,\big[\,3x-x^2+x^{-1}+(1-x)^{-1}\,\big]\ln x \\
&+64\,\big[\,x-2-x^2+x^{-1}+(1-x)^{-1}\,\big]\ln(1-x)-\tfrac{80}{3}+56x^2-\tfrac{104}{3}x \\
&-56x^{-1}+\tfrac{184}{3}(1-x)^{-1}\Big]\Big\}\,O^1_{\mu\nu}(p) \\
&+\frac{1}{\varepsilon}\Big[-8\,\big[\,1+16x\,\big]\ln x-16\,\big[\,1+4x^2-4x\,\big]\ln(1-x) \\
&-\tfrac{164}{3}+\tfrac{248}{3}x^2-\tfrac{160}{3}x+6x^{-1}\Big]\,O^2_{\mu\nu}(p) \\
&+\Big\{\,\frac{1}{\varepsilon}\Big[\,\big[\,\tfrac{15}{2}+7x^{-1}\,\big]\ln^2 x+2\,\big[\,15-4x^{-1}\,\big]\ln x\ln(1-x) \\
&+4\,\big[\,1+x^{-1}\,\big]\ln x\ln(1+x)+\big[\,\tfrac{110}{3}+4x+\tfrac{56}{3}x^{-1}\,\big]\ln x \\
&+\tfrac{32}{3}\,\big[\,1-x^{-1}\,\big]\ln^2(1-x)+\big[\,\tfrac{8}{3}x^2-4-8x+\tfrac{28}{3}x^{-1}\,\big]\ln(1-x) \\
&+2\,\big[\,1+x^{-1}\,\big]\zeta(2)+2\,\big[\,14-3x^{-1}\,\big]\,\mathrm{Li}_2(1-x)+4\,\big[\,1+x^{-1}\,\big]\,\mathrm{Li}_2(-x) \\
&-1+\tfrac{8}{3}x^2-\tfrac{67}{3}x+\tfrac{62}{3}x^{-1}\Big]+\frac{1}{\varepsilon^2}\Big[\,2\,\big[\,5+6x^{-1}\,\big]\ln x \\
&+22\,\big[\,1-x^{-1}\,\big]\ln(1-x)-12+\tfrac{8}{3}x^2-8x+\tfrac{52}{3}x^{-1}\Big]\Big\}\,O^3_{\mu\nu}(p)\,\Big)\,. \qquad (3.4.27)
\end{aligned}
$$

The tensors $O^i_{\mu\nu}$ are given in eqs. 3.2.17–3.2.19. Notice that the tensor $O^4_{\mu\nu}$ is absent. As in the case of the one loop calculations, this is due to 't Hooft's WT identity 3.2.26 that states

$$p^\mu p^\nu \mathcal{A}^{(2)}_{\mu\nu}(x,p)=0, \qquad (3.4.28)$$

a property that should be maintained at the renormalised level:

$$p^\mu p^\nu \mathcal{M}^{(2)}_{\mu\nu}(x,p)=0. \qquad (3.4.29)$$

The WT identity 3.2.51 relates the coefficient of $O^3_{\mu\nu}$ to the set of all two loop graphs, which have external ghost fields and an amputated ghost vertex in them (cf. fig. 3.3). As was already remarked in section 3.2 below eq. 3.2.51, this WT identity only holds for connected graphs. Therefore, in order to check the equality one has to take into account the one loop graphs with an external self–energy insertion. We have calculated the ghost diagrams, and the contribution of the alien operator in eq. 3.4.27 is in agreement with their expressions.

Furthermore, we observe that the term proportional to $O^2_{\mu\nu}$ has a single pole term ε^{-1} only. This term will vanish due to coupling constant and gauge parameter renormalisation.

In order to check whether the overlapping divergences cancel, i.e. divergences of the form $\varepsilon^{-1}\ln(-p^2/\mu^2)$, we have considered the sum of all contributions to $\mathcal{M}^{(2)}_{\mu\nu}(x,p)$, which are proportional to $(-p^2/\mu^2)^{\varepsilon/2}$. This part of the second order finite 1PI Green's function is equal to

$$\left[\, 2Z^{(1)}_g + Z^{(1)}_A + Z^{(1)}_A \alpha\frac{\mathrm{d}}{\mathrm{d}\alpha} - Z^{(1)}_{gg} \,\right] \otimes \mathcal{A}^{(1)}_{\mu\nu} - Z^{(1)}_{ga} \otimes \mathcal{B}^{(1)}_{\mu\nu} - Z^{(1)}_{g\omega} \otimes \mathcal{C}^{(1)}_{\mu\nu}. \qquad (3.4.30)$$

The explicit expression can be found in appendix 3D, in which we also present the non-trivial convolutions of the above expression separately. We observe that the double poles ε^{-2} of eq. 3D.4 and the ones of expression 3.4.27 are related by a factor -2 and thus, the overlapping divergences are cancelled against each other. Furthermore, the contributions of the form $O^2_{\mu\nu}$ disappear in the sum of the two loop graphs and the above convolutions. This is in accordance with the non-renormalisability of such an operator.

The part of $\mathcal{M}^{(2)}_{\mu\nu}(x,p)$ (see eq. 3.4.25) that does not depend on $(-p^2/\mu^2)^{\varepsilon/2}$ is given by

$$\begin{aligned}
&\left[\, Z^{(1)}_{gg} \otimes \left(\, Z^{(1)}_{gg} - Z^{(1)}_A \,\right) + Z^{(2)}_A \,\right] \otimes \mathcal{A}^{(0)}_{\mu\nu} \\
&\quad + Z^{(1)}_{ga} \otimes \left[\, Z^{(1)}_{gg} + Z^{(1)}_{aa} + Z^{(1)}_{a\omega} - Z^{(1)}_A \,\right] \otimes \mathcal{B}^{(0)}_{\mu\nu} = Z^{(2)}_A \otimes \mathcal{A}^{(0)}_{\mu\nu} \\
&\quad - Z^{(1)}_{gg} \otimes \mathcal{A}^{(1)}_{\mu\nu}\left[\varepsilon^{-2}\right] - Z^{(1)}_{ga} \otimes \mathcal{B}^{(1)}_{\mu\nu}\left[\varepsilon^{-2}\right] - Z^{(1)}_{g\omega} \otimes \mathcal{C}^{(1)}_{\mu\nu}\left[\varepsilon^{-2}\right]. \qquad (3.4.31)
\end{aligned}$$

The first term on the right-hand side in the above expression can be straightforwardly deduced from eq. 3.4.18, whereas the remaining terms in the last line denote the double pole parts of the convolutions, which can be found in eqs. 3D.1, 3D.2 and 3D.3.

It has now become straightforward to determine the remaining unknown parts of expression eq. 3.4.25, which are given by $Z^{(2)}_{gg}\otimes\mathcal{A}^{(0)}_{\mu\nu}$ and $Z^{(2)}_{ga}\otimes\mathcal{B}^{(0)}_{\mu\nu}$. From the finiteness of $\mathcal{M}^{(2)}_{\mu\nu}(x,p)$ it follows that the renormalisation matrix elements Z_{gg} (gluon–gluon transition) and Z_{ga} (gluon–alien transition) can be written as follows:

$$\begin{aligned}
Z^{(m)}_{gg} &= 1 + \frac{\alpha_s}{4\pi}\frac{\gamma^{0,(m)}_{gg}}{\varepsilon} + \left(\frac{\alpha_s}{4\pi}\right)^2 \left[\frac{\gamma^{0,(m)}_{gg}}{2\varepsilon^2}\left[\, 2\beta_0 + \gamma^{0,(m)}_{gg} \,\right] + \frac{\gamma^{1,(m)}_{gg}}{2\varepsilon}\right] \\
&= \int_0^1 dx\, x^{m-1}\left[\delta(1-x) + \frac{\alpha_s}{4\pi} Z^{(1)}_{gg}(x) + \left(\frac{\alpha_s}{4\pi}\right)^2 Z^{(2)}_{gg}(x)\right] \qquad (3.4.32)
\end{aligned}$$

and

$$Z_{ga}^{(m)} = \frac{\alpha_s}{4\pi}\frac{\gamma_{ga}^{0,(m)}}{\varepsilon} + \left(\frac{\alpha_s}{4\pi}\right)^2 \left[\frac{\gamma_{ga}^{0,(m)}}{2\varepsilon^2}\left[\,2\beta_0 - \gamma_A^0 + \gamma_{gg}^{0,(m)} + \gamma_{aa}^{0,(m)} + \gamma_{\omega a}^{0,(m)}\,\right] + \frac{\gamma_{ga}^{1,(m)}}{2\varepsilon}\right] = \int_0^1 dx\, x^{m-1}\left[\frac{\alpha_s}{4\pi} Z_{ga}^{(1)}(x) + \left(\frac{\alpha_s}{4\pi}\right)^2 Z_{ga}^{(2)}(x)\right]. \qquad (3.4.33)$$

The structure of the double pole terms follows from the renormalisation group equations. The lowest order contribution to the anomalous dimension of the gluon operator, $\gamma_{gg}^{0,(m)}$, can be found in eq. 3.2.37, whereas the lowest order anomalous dimensions of the gluon–alien $\gamma_{ga}^{0,(m)}$, the alien–alien $\gamma_{aa}^{0,(m)}$ and the ghost–alien $\gamma_{\omega a}^{0,(m)}$ transitions can be found in eqs. 3.2.49, 3.4.11 and 3.4.12, respectively. The x–dependent renormalisation constants $Z_{gg}^{(1)}(x)$ and $Z_{ga}^{(1)}(x)$ were given in eqs. 3.4.20 and 3.4.21, respectively.

Finally, the second order coefficients of the anomalous dimensions can be extracted from the presented expressions. They are given by

$$\begin{aligned}\gamma_{gg}^{1,(m)} = \int_0^1 dx\, x^{m-1}\Big\{ &-\left[\,\tfrac{64}{3} + 24\zeta(3)\,\right]\delta(1-x) - 32\left[\,1+x\,\right]\ln^2 x \\ &- 8\left[\,2 + x^2 + x + x^{-1} - (1+x)^{-1}\,\right]\left[\,4\,\mathrm{Li}_2(-x) + 4\ln x\ln(1+x) - \ln^2 x \right.\\ &\left. + 2\zeta(2)\,\right] - 8\left[\,2 + x^2 - x - x^{-1} - (1-x)^{-1}\,\right]\left[\,4\ln x\ln(1-x) - \ln^2 x \right.\\ &\left. + 2\zeta(2)\,\right] + \tfrac{8}{3}\left[\,25 + 44x^2 - 11x\,\right]\ln x + \tfrac{100}{9} + \tfrac{436}{9}x - \tfrac{536}{9}(1-x)^{-1}\Big\}\end{aligned} \qquad (3.4.34)$$

and

$$\begin{aligned}\gamma_{ga}^{1,(m)} = \int_0^1 dx\, x^{m-1}\Big\{ &\tfrac{11}{2}\ln^2 x + \left[\,\tfrac{8}{3}x^2 - 18 - 4x + 4x^{-1}\,\right]\ln x \\ &+ \left[\,1 + x^{-1}\,\right]\left[\,4\,\mathrm{Li}_2(-x) + 4\ln x\ln(1+x) - \ln^2 x + 2\zeta(2)\,\right] \\ &+ \left[\,1 - x^{-1}\,\right]\left[\,4\ln x\ln(1-x) - 2\ln^2 x - 8\,\mathrm{Li}_2(1-x) + 10\zeta(2) \right.\\ &\left. - \tfrac{5}{2}\ln^2(1-x) - \tfrac{20}{3}\ln(1-x)\,\right] - \tfrac{97}{9} - \tfrac{20}{9}x^2 + 3x + 10x^{-1}\Big\}.\end{aligned} \qquad (3.4.35)$$

The $\mathcal{O}(\alpha_s^2)$ contribution to the anomalous dimension of the gluon operator, $\gamma_{gg}^{1,(m)}$, is in agreement with the result of the calculation of Furmanski and Petronzio [5].

If we perform the x–integration explicitly, we get the anomalous dimensions in the m–language. The results are as follows:

$$\gamma_{gg}^{1,(m)} = 16S_3(m-1) - 32S_{1,2}(m-1) - 32S_{2,1}(m-1) \qquad (3.4.36)$$

$$+ 32\left[S_2(m-1) - \tfrac{1}{2}\zeta(2) + 1 \right]\left[\frac{1}{m-1} - \frac{2}{m} + \frac{1}{m+1} - \frac{1}{m+2} \right]$$

$$+ S_1(m-1)\left[\tfrac{536}{9} + 16\zeta(2) \right] - \tfrac{64}{3} - 8\zeta(3) - \frac{116}{9m} - \frac{104}{3m^2} - \frac{192}{m^3}$$

$$+ \frac{436}{9(m+1)} - \frac{8}{3(m+1)^2} - \frac{32}{(m+1)^3} + \frac{24}{m+2} - \frac{208}{3(m+2)^2} - \frac{64}{(m+2)^3}$$

$$+ (-1)^m \Big[16S_{\tilde{3}}(m-1) - 32S_{1,\tilde{2}}(m-1) - 16\zeta(2)S_1(m-1)$$

$$+ 32\left[S_{\tilde{2}}(m-1) + \tfrac{1}{2}\zeta(2) \right]\left[\frac{1}{m-1} - \frac{2}{m} + \frac{1}{m+1} - \frac{1}{m+2} \right] + 8\zeta(3) \Big]$$

and

$$\gamma_{ga}^{1,(m)} = \frac{1}{m(m-1)}\left[\tfrac{5}{2}S_1^2(m-1) - \tfrac{19}{2}S_2(m-1) - \tfrac{20}{3}S_1(m-1) + 2\zeta(2) \right]$$

$$- S_1(m-1)\left[\frac{4}{(m-1)^2} + \frac{1}{m^2} \right] + \frac{10}{m-1} - \frac{4}{(m-1)^2} + \frac{2}{(m-1)^3}$$

$$- \frac{97}{9m} + \frac{74}{3m^2} + \frac{20}{m^3} + \frac{3}{m+1} + \frac{4}{(m+1)^2} - \frac{20}{9(m+2)} - \frac{8}{3(m+2)^2}$$

$$- \frac{2(-1)^m}{m(m-1)}\left[2S_{\tilde{2}}(m-1) + \zeta(2) \right]. \qquad (3.4.37)$$

In these formulas the functions S are defined recursively as follows

$$S_{n,a_1,\ldots,a_k}(m-1) = \sum_{i=1}^{m-1} \frac{1}{i^n} S_{a_1,\ldots,a_k}(i), \qquad (3.4.38)$$

$$S_{\tilde{n},a_1,\ldots,a_k}(m-1) = \sum_{i=1}^{m-1} \frac{(-1)^i}{i^n} S_{a_1,\ldots,a_k}(i), \qquad (3.4.39)$$

$$S_n(m-1) = \sum_{i=1}^{m-1} \frac{1}{i^n}, \qquad (3.4.40)$$

$$S_{\tilde{n}}(m-1) = \sum_{i=1}^{m-1} \frac{(-1)^i}{i^n}, \qquad (3.4.41)$$

where $a_1, \ldots, a_k$ can have tildes or not. The Riemann zeta's can be expressed in these sums too: $\zeta(n) = S_n(\infty)$.

Note the second moment of the anomalous dimension of the gluon operator remains zero at this order, i.e.

$$\gamma_{gg}^{1,(2)} = 0. \qquad (3.4.42)$$

It is a consequence of conservation of energy–momentum, as has already been mentioned in section 3.2 (cf. eq. 3.2.38).

3.5 Discussion and conclusions

In this chapter we have described the renormalisation of the gluon operator. It appeared to be a non-trivial problem that involves many steps and considerations, which can go wrong or which are easily overlooked. We will discuss these items in this section.

Already at the level of one loop, the renormalisation of the gluon operator exhibits some peculiarities. In the axial gauge new operators appear, which are proportional to $(\Delta\cdot n)^i$ with $i > 0$. However, as the factor $\Delta\cdot n$ can never appear in the numerator, the renormalisation matrix of the complete set of operators has an upper triangular form. This means that a counter term proportional to $(\Delta\cdot n)^i$ never can give rise to an operator with the factor $(\Delta\cdot n)^j$, where $j < i$. Therefore, the additional operators cannot affect the physical anomalous dimension. One can circumvent the whole item of new operators in this gauge by choosing $n \propto \Delta$. This is also the gauge in which Furmanski and Petronzio [5] performed their calculations. The most severe problems of the latter gauge are its non-renormalisability (by power counting) and the presence of gauge singularities [8]. We observed that these pitfalls do not influence the lowest order calculation of the anomalous dimension. Therefore, it could not be excluded that the two loop result of Furmanski and Petronzio is right.

The one loop covariant gauge calculation is even more interesting. Here one cannot circumvent the introduction of new operators in the procedure of the renormalisation of the gluon operator. It appeared that one has to introduce a new operator in the Lagrangian in order to cancel divergences of the Green's function Γ_{O_g}. This is analogue to what happened in the axial gauge, but in the latter case one could choose n in such a way, that the effect disappears. In the covariant gauge this is not possible! The calculation of a single Green's function yields already two renormalisation constants, one of which cannot belong to the physical operator. We have called the other one the alien operator. The previous remarks also indicate the difference with genuine operator mixing. To determine the renormalisation matrix in the latter case one should calculate as many Green's functions as there are entries in the renormalisation matrix.

It is wrong to consider the renormalisation of the gluon operator only, if one wants to calculate Z_{gg}. One also needs to compute the renormalisation of the other operators in the Lagrangian, since these operators yield counter terms which have the same structure as the gluon operator. Moreover, it is not sufficient to know the counter term of the lowest order alien operator to perform renormalisation at second order.

The residual gauge invariance (BRST invariance) of the action after gauge fixing is a property that we do not want to spoil during renormalisation. Therefore, the introduction of yet another operator in the Lagrangian, the ghost operator, is inevitable. The same symmetry property also accounts for the form of the higher order contributions to the alien and the ghost operators. Only if these structures are included up to $\mathcal{O}(g^3)$ the renormalisation procedure becomes sensible. The construction of the higher order operator terms was described in section 3.3.

Floratos, Lacaze and Kounnas [6] were probably not aware of these complications, or they were misled by the proposition of Joglekar and Lee [3], which implied the possible choice of a base of operators as such, that 'mixing' of the non-physical operators with the physical one can be ignored. This proposition does not imply that one can forget about all other operators in the Lagrangian. It just states that it is possible to introduce a linear combination of the gluon, alien and ghost operators, which is multiplicatively renormalised. Also Dixon and Taylor [2] consider the problem of mixing. As far as we understand, they only claim that the renormalisation constant of the alien operator is not relevant for the Callan–Symanzik equation, or, equivalently, it does not appear in the operator product expansion. This can be explained as follows: if the 1PI Green's function is changed into a physical matrix element by putting external legs on shell and contracting them with physical polarisation vectors, the alien operator will totally disappear.

We want to criticise the work of Floratos et al. on some more subjects. As we deduce from the description of their calculation in [4, 6], they included the counter terms by subtracting divergent subintegrals from the two loop integrals. This is a very risky procedure, because the would-be consistency check on the cancellation of overlapping divergences has implicitly been fulfilled. Moreover, their modified loop integrals would render every theory finite, renormalisable as well as non-renormalisable ones. However, it turns out that the difference between their and our result cannot be explained only by the fact that they ignored the contributions of the alien and ghost operators to the anomalous dimension. This consolidates the suspicion of their method to determine the integrals. The last remark we want to make is about the renormalisation of the gauge parameter. In the Feynman gauge the inclusion of this effect can easily be forgotten. The Landau gauge ($\alpha = 0$) is the only case where it can really be ignored.

We have performed a successful calculation of the two loop anomalous dimension of the gluon operator in the Feynman gauge. The determination of the contributions is far from trivial and the renormalisation procedure is one of the most involved that we know of. Nevertheless, the lightlike axial gauge result of Furmanski and Petronzio is now reproduced in a covariant gauge. The latter is a more reliable gauge, because it is shown to be renormalisable. Furthermore, the gauge singularities can be suppressed by choosing the gauge parameter equal to one, i.e. the Feynman gauge. Therefore, the problem of the right anomalous dimension of the gluon operator is solved by our calculation.

Appendices

3A Feynman rules

This appendix will contain the most important Feynman rules that are used in the calculation of operator matrix elements. It is divided into four parts; subsequently, the gluon propagator, the vertices, the gluon operator and the new alien and ghost operators are described. Metric and related conventions are according to Bjorken and Drell [12]. All momenta are incoming.

3A.1 The gluon propagator

The gluon propagator is used in two different gauges. In the axial gauge we have the gauge fixing term

$$-\frac{1}{2\alpha}(n\cdot A^a)^2, \tag{3A.1}$$

with $\alpha = 0$. Additionally, one can choose n_μ to be lightlike, i.e. $n^2 = 0$. This simplifies the calculation, because one complicated term of the propagator disappears. The propagator has the form (for general n and α)

$$\mathcal{D}_g^{\mu\nu}(p) = \frac{i\delta^{ab}}{p^2}\left(-g^{\mu\nu} + \frac{n^\mu p^\nu + p^\mu n^\nu}{n\cdot p} - \frac{n^2 p^\mu p^\nu - \alpha p^2 n^\mu n^\nu}{(n\cdot p)^2}\right). \tag{3A.2}$$

In the general covariant gauge, where we have the gauge fixing term

$$-\frac{1}{2\alpha}(\partial^\mu A_\mu^a)^2, \tag{3A.3}$$

the propagator is expressed by

$$\mathcal{D}_g^{\mu\nu}(p) = \frac{i\delta^{ab}}{p^2}\left(-g^{\mu\nu} + (1-\alpha)\frac{p^\mu p^\nu}{p^2}\right). \tag{3A.4}$$

Several choices for α have special names: $\alpha = 0$ is called the Landau gauge, $\alpha = 1$ the Feynman gauge, $\alpha = 3$ the Yennie gauge and $\alpha = \infty$ the unitary gauge.

3A.2 Vertices in QCD

In the calculation of Green's functions one encounters three types of vertices. We will give their expressions here and use the convention that all momenta are incoming.

The first vertex is the 3–gluon vertex. It is given by

$$V^{abc}_{\mu\nu\lambda}(p,q,k) = g f^{abc}\Big[(q-k)_\mu g_{\nu\lambda} + (k-p)_\nu g_{\lambda\mu} + (p-q)_\lambda g_{\mu\nu}\Big]. \tag{3A.5}$$

Secondly, we have the 4–gluon vertex. Its expression has the following form

$$\begin{aligned} V^{abcd}_{\mu\nu\lambda\sigma}(p,q,k,s) = -ig^2\Big[& f^{abe}f^{cde}(g_{\mu\lambda}g_{\nu\sigma} - g_{\mu\sigma}g_{\nu\lambda}) \\ & + f^{ace}f^{bde}(g_{\mu\nu}g_{\lambda\sigma} - g_{\mu\sigma}g_{\nu\lambda}) + f^{ade}f^{bce}(g_{\mu\nu}g_{\lambda\sigma} - g_{\mu\lambda}g_{\nu\sigma})\Big]. \end{aligned} \tag{3A.6}$$

The last and most simple vertex is the ghost–gluon vertex, which is given by

$$V^{abc}_{\mu}(p,q,k) = -g f^{abc} k_\mu, \tag{3A.7}$$

where the third argument of $V^{abc}_\mu(p,q,k)$ represents the outgoing ghost and the first argument the gluon field. Remember that every ghost loop requires an additional factor -1.

3A.3 The gluon operator

The gluon operator, which is given by eq. 3.1.3, gives rise to vertices with 2 legs up to vertices with $m+2$ legs. The first three Feynman rules for such vertices are given here. The operator is contracted with the current given in eq. 3.2.6.

The vertex with two legs is proportional to the structure $O^1_{\mu\nu}(p)$ given in eq. 3.2.17. It is given by

$$O^{ab}_{\mu\nu}(p,-p) = \frac{1+(-1)^m}{2}\delta^{ab}O^{(2)}_{\mu\nu}(p), \tag{3A.8}$$

where

$$\begin{aligned} O^{(2)}_{\mu\nu}(p) &= (\Delta\cdot p)^m O^1_{\mu\nu}(p) \\ &= (\Delta\cdot p)^{m-2}\Big[g_{\mu\nu}(\Delta\cdot p)^2 - (p_\mu\Delta_\nu + \Delta_\mu p_\nu)\Delta\cdot p + p^2\Delta_\mu\Delta_\nu\Big]. \end{aligned} \tag{3A.9}$$

This function obeys the equality (cf. eq. 3.2.24)

$$p^\mu O^{(2)}_{\mu\nu}(p) = 0. \tag{3A.10}$$

The 3–leg vertex is given by

$$O^{abc}_{\mu\nu\lambda}(p,q,k) = -ig\frac{1+(-1)^m}{2} f^{abc} O^{(3)}_{\mu\nu\lambda}(p,q,k), \tag{3A.11}$$

where

$$\begin{aligned}
O^{(3)}_{\mu\nu\lambda}(p,q,k) = & \Big[(\Delta_\nu g_{\lambda\mu} - \Delta_\lambda g_{\mu\nu})\Delta\cdot p + \Delta_\mu(p_\nu \Delta_\lambda - p_\lambda \Delta_\nu) \Big] (\Delta\cdot p)^{m-2} \\
& + \Delta_\nu \Big[\Delta\cdot p\, q_\mu \Delta_\nu + \Delta\cdot q\, p_\nu \Delta_\mu - \Delta\cdot p\, \Delta\cdot q\, g_{\mu\nu} - p\cdot q\, \Delta_\mu \Delta_\nu \Big] \\
& \qquad \times \sum_{i=0}^{m-3} (-\Delta\cdot p)^i (\Delta\cdot q)^{m-3-i} \\
& + \left\{ \begin{array}{c} p \to q \to k \to p \\ \mu \to \nu \to \lambda \to \mu \end{array} \right\} + \left\{ \begin{array}{c} p \to k \to q \to p \\ \mu \to \lambda \to \nu \to \mu \end{array} \right\}.
\end{aligned} \tag{3A.12}$$

This function is related to the lowest order function by

$$p^\mu O^{(3)}_{\mu\nu\lambda}(p,q,k) = O^{(2)}_{\nu\lambda}(q) - O^{(2)}_{\nu\lambda}(k). \tag{3A.13}$$

At last, we give the 4-leg vertex denoted by

$$\begin{aligned}
O^{abcd}_{\mu\nu\lambda\sigma}(p,q,k,s) = & \, g^2 \frac{1+(-1)^m}{2} \Big\{ f^{abe} f^{cde} O^{(4)}_{\mu\nu\lambda\sigma}(p,q,k,s) \\
& - f^{ace} f^{bde} O^{(4)}_{\mu\lambda\nu\sigma}(p,k,q,s) + f^{ade} f^{bce} O^{(4)}_{\mu\sigma\nu\lambda}(p,s,q,k) \Big\},
\end{aligned} \tag{3A.14}$$

where

$$\begin{aligned}
O^{(4)}_{\mu\nu\lambda\sigma}(p,q,k,s) = & \, \Delta_\nu \Delta_\lambda \Big\{ -g_{\mu\sigma}(\Delta\cdot k + \Delta\cdot s)^{m-2} \\
& + \Big[s_\mu \Delta_\sigma - \Delta\cdot s\, g_{\mu\sigma} \Big] \sum_{i=0}^{m-3} (\Delta\cdot k + \Delta\cdot s)^i (\Delta\cdot s)^{m-3-i} \\
& - \Big[p_\sigma \Delta_\mu - \Delta\cdot p\, g_{\mu\sigma} \Big] \sum_{i=0}^{m-3} (-\Delta\cdot p)^i (\Delta\cdot k + \Delta\cdot s)^{m-3-i} \\
& + \Big[\Delta\cdot p\, \Delta\cdot s\, g_{\mu\sigma} + p\cdot s\, \Delta_\mu \Delta_\sigma - \Delta\cdot s\, p_\sigma \Delta_\mu - \Delta\cdot p\, s_\mu \Delta_\sigma \Big] \\
& \qquad \times \sum_{i=0}^{m-4} \sum_{j=0}^{i} (-\Delta\cdot p)^{m-4-i} (\Delta\cdot k + \Delta\cdot s)^{i-j} (\Delta\cdot s)^j \Big\} \\
& + \left\{ \begin{array}{c} p \leftrightarrow q \\ \mu \leftrightarrow \nu \end{array} \right\} + \left\{ \begin{array}{c} k \leftrightarrow s \\ \lambda \leftrightarrow \sigma \end{array} \right\} + \left\{ \begin{array}{c} p \leftrightarrow q,\ k \leftrightarrow s \\ \mu \leftrightarrow \nu,\ \lambda \leftrightarrow \sigma \end{array} \right\}.
\end{aligned} \tag{3A.15}$$

The function $O^{(4)}$ is coupled to the function belonging to the 3–leg vertex as follows

$$p^\mu O^{(4)}_{\mu\nu\lambda\sigma}(p,q,k,s) = O^{(3)}_{\nu\lambda\sigma}(-k-s,k,s) - O^{(3)}_{\nu\lambda\sigma}(q,k,s). \tag{3A.16}$$

The sums in these Feynman rules can be simplified as follows

$$\sum_{i=0}^{m-3} A^i B^{m-3-i} = \frac{A^{m-2}}{A-B} + \frac{B^{m-2}}{B-A} \tag{3A.17}$$

and

$$\begin{aligned}\sum_{i=0}^{m-4}\sum_{j=0}^{i} A^j B^{i-j} C^{m-4-i} &= \frac{1}{A-B}\sum_{i=0}^{m-3} A^i C^{m-3-i} + \frac{1}{B-A}\sum_{i=0}^{m-3} B^i C^{m-3-i} \\ &= \frac{A^{m-2}}{(A-B)(A-C)} + \frac{B^{m-2}}{(B-A)(B-C)} + \frac{C^{m-2}}{(C-A)(C-B)}.\end{aligned} \tag{3A.18}$$

Note the sums are completely symmetric in all their arguments. The single sum disappears for $m = 2$, while the double sum gives zero for $m = 2, 3$.

3A.4 The alien and the ghost operator

This section will contain the Feynman rules, which are used in the calculation of the counter terms to the 1PI Green's function of the gluon operator at the two loop level.

Firstly, we need the first two orders of the alien operator (which only contains gluon fields), that can be calculated from expression 3.3.27. The lowest order form can be deduced from the one loop calculation and is also traceable in the Lagrangian of eq. 3.3.26. It is given by

$$O^{ab}_{\mu\nu}(p,-p) = 2\delta^{ab}(\Delta\cdot p)^m O^3_{\mu\nu}(p), \tag{3A.19}$$

where the tensor structure $O^3_{\mu\nu}(p)$ is given in eq. 3.2.19.

The Feynman rule for the alien operator vertex with three legs can be deduced too, and has the form

$$O^{abc}_{\mu\nu\lambda}(p,q,k) = -igf^{abc}O^{(3)}_{\mu\nu\lambda}(p,q,k), \tag{3A.20}$$

where

$$\begin{aligned}O^{(3)}_{\mu\nu\lambda}(p,q,k) = \Big[&\Delta_\mu\Delta_\nu(q_\lambda - p_\lambda) + \Delta_\mu\Delta_\lambda(p_\nu - k_\nu) + g_{\nu\lambda}\Delta_\mu(\Delta\cdot k - \Delta\cdot q)\Big] \\ &\times(\Delta\cdot p)^{m-2} - \tfrac{1}{4}\Delta_\nu\Delta_\lambda(\Delta_\mu p^2 - p_\mu\Delta\cdot p)\sum_{i=1}^{m-3}\Big[(-\Delta\cdot q)^i(\Delta\cdot k)^{m-3-i} \\ &- 3(-\Delta\cdot k)^i(\Delta\cdot p)^{m-3-i} - 3(-\Delta\cdot p)^i(\Delta\cdot q)^{m-3-i}\Big] \\ &+\left\{\begin{matrix} p\to q\to k\to p \\ \mu\to\nu\to\lambda\to\mu\end{matrix}\right\} + \left\{\begin{matrix} p\to k\to q\to p \\ \mu\to\lambda\to\nu\to\mu\end{matrix}\right\}.\end{aligned} \tag{3A.21}$$

The actual factors in this expression follow from η_i (see eq. 3.3.32).

Secondly, we need the first two orders of the ghost operator (eq. 3.3.28). The lowest order vertex with two ghost legs is given by

$$O^{ab}(p,-p) = -\delta^{ab}(\Delta\cdot p)^m, \tag{3A.22}$$

while the first order vertex with two ghost legs and a gluon leg is given by

$$O^{abc}_\mu(p,q,k) = igf^{abc}O^{(3)}_\mu(p,q,k), \tag{3A.23}$$

where

$$O^{(3)}_\mu(p,q,k) = \Delta_\mu \Big[\tfrac{1}{2}(\Delta\cdot k)^{m-1} + \tfrac{1}{4}(\Delta\cdot q - 3\Delta\cdot k)(\Delta\cdot q)^{m-2} + \tfrac{1}{4}(\Delta\cdot k - \Delta\cdot q)(\Delta\cdot p)^{m-2} - \tfrac{3}{4}(\Delta\cdot k)^2 \sum_{i=1}^{m-3}(\Delta\cdot k)^i(-\Delta\cdot q)^{m-3-i} \Big]. \tag{3A.24}$$

The last argument of the expression $O^{(3)}_\mu(p,q,k)$ corresponds to the outgoing ghost field, whereas the first argument represents the gluon field.

3B One loop integrals for the operator Green's functions

In this appendix we will present some useful formulae for calculating the Green's functions at one loop in two gauges, the axial and the covariant one. Only axial gauge type integrals are given, because the covariant gauge types follow from these by taking special values for some parameters. The loop integrals are presented for two cases. Firstly, we will consider the case of a lightlike axial gauge, $n^2 = 0$. The corresponding integrals can easily be calculated exactly. Secondly, we will discuss some aspects of integrals which appear in the case of the general axial gauge fixing, i.e. $n^2 \neq 0$.

The UV divergences that determine the anomalous dimension, are regulated by n–dimensional integration, where $n = 4 + \varepsilon$. Other divergences, like gauge singularities and infrared infinities, are regulated by mass parameters whenever necessary.

3B.1 The case $n^2 = 0$

The most general scalar integral one should consider is given by

$$I^m_{\alpha\beta\gamma} = \int \frac{d^n k}{(2\pi)^n} \frac{(\Delta\cdot k)^m}{(k^2+\lambda p^2)^\alpha((p-k)^2+\lambda p^2)^\beta(n\cdot k + \delta\, n\cdot p)^\gamma}, \tag{3B.1}$$

where we introduced a regulator λ for the infrared and collinear region of the loop momentum k and a regulator δ for the gauge singularities (which only show up in the case $n^2 = 0$). For $n^2 = 0$, one can show for all α, β, γ and $\lambda/\delta = 0$

$$I^m_{\alpha 0\gamma} = I^m_{0\beta\gamma} = 0. \tag{3B.2}$$

This result holds irrespective of additional inner products in the numerator, because it is deduced from the absence of a mass scale. In all other cases we can use the following expression

$$I^m_{\alpha\beta\gamma} = i\frac{1}{(4\pi)^{\frac{1}{2}n}}\frac{\Gamma(\alpha+\beta+\gamma-\frac{n}{2})}{\Gamma(\alpha)\Gamma(\beta)}\left(-p^2\right)^{\epsilon/2}\left(p^2\right)^{2-\alpha-\beta}(n\cdot p)^{-\gamma} \tag{3B.3}$$
$$\times\sum_{i=0}^{m}\binom{m}{i}\left(-\frac{p^2\,\Delta\cdot n}{2n\cdot p}\right)^i(\Delta\cdot p)^{m-i}\frac{\Gamma(\alpha+\beta-\frac{n}{2}-i)}{\Gamma(\alpha+\beta-\frac{n}{2})}\frac{\Gamma(\gamma+i)}{\Gamma(\gamma)}$$
$$\times\int_0^1 dx\, x^{\beta-1+m-i}(1-x)^{\alpha-1}(x+\delta)^{-\gamma-i}(x(1-x)+\lambda)^{\frac{1}{2}-\alpha-\beta+i}.$$

If one substitutes

$$\frac{\Gamma(\gamma+i)}{\Gamma(\gamma)} = \begin{cases} 1 & i=0 \\ \prod_{j=1}^{i}(\gamma+j-1) & i>0 \end{cases}, \tag{3B.4}$$

the formula is valid for all γ (including $\gamma < 0$). The case $n_\mu \propto \Delta_\mu$ is particularly convenient, because then only the first term of the sum contributes. If we do not make this choice, the factors $m\ldots(m-i-1)$ from the binomial can be removed by partial integration in the integral over x. The integrals, which show up in the covariant gauge calculation, are determined by putting γ equal to zero.

3B.2 The case $n^2 \neq 0$

In the integrals of the axial gauge type we have now n^2 to provide an extra scale. The regulators λ and δ are left out here, because n^2 serves automatically as a regulator. It turns out that in this case

$$I^m_{\alpha 0\gamma} = 0, \tag{3B.5}$$
$$I^m_{0\beta\gamma} \neq 0. \tag{3B.6}$$

The complete calculation of the general integral 3B.1 is tedious. For instance, the parameter integral that remains after the loop momentum integration, contains in the case of $I^m_{\alpha\beta\gamma}$ a term, which is quadratic in two integration variables. However, if one only wants to know the UV singular behaviour of the integrals, the situation is more prospective. After projection of the integrals with $k_{\mu_1}\ldots k_{\mu_i}$ in the numerator onto scalar integrals, one can show by power counting that $I^m_{\alpha\beta\gamma}$ is UV finite.

To find the UV divergences of the integrals $I^m_{0\beta\gamma}$, one should be very careful. Not only the Γ-functions coming from the loop momentum integration give rise to possible

UV divergences, but also the remaining integrals over Feynman parameters can cause UV poles. This feature becomes apparent in the following parameter integral, which occurs after application of the Feynman trick and performing the loop momentum integration,

$$\int_0^1 dx\, x^{-c-2}(1-x)^c\left[\frac{1-x}{x}n\cdot p-\left(\frac{1-x}{2x}\right)^2 n^2\right]^{\frac{1}{2}\varepsilon-d} =$$
$$\left(-\frac{n^2}{4}\right)^{\frac{1}{2}\varepsilon-d}\left(-\frac{4n\cdot p}{n^2}\right)^{c-2d+1+\varepsilon} B(2d-c-1-\varepsilon, c-d+1+\frac{\varepsilon}{2}), \tag{3B.7}$$

where c and d are integers, and the B-function, which is defined as

$$B(\alpha,\beta)=\frac{\Gamma(\alpha)\Gamma(\beta)}{\Gamma(\alpha+\beta)}, \tag{3B.8}$$

can give rise to real UV poles. This becomes clear if one considers the sign of the offset ε, which appears in the Γ-functions.

3C Two loop contributions to the operator Green's function

In this appendix we want to give a general treatment of the two loop calculation needed to obtain the second order contribution to the anomalous dimension (see section 3.4). All the consecutive steps in the calculation that are described here, have been programmed in FORM, a computer language allowing algebraic manipulations[6].

The diagrams that contribute are given in figure 3.8 and the Feynman rules that serve as building blocks can be found in appendix 3A.

The colour structure (due to the gauge group $SU(N)$) is rather trivial. If we introduce matrices C^a in the following way

$$f^{abc}=-i[C^a]_{bc}, \tag{3C.1}$$

it is straightforward to show that only 3 possible combinations of such matrices can occur in the calculation, i.e.

$$\sum_{s,t}[C^sC^tC^sC^s]_{ab} = \sum_{s,t}[C^sC^sC^tC^t]_{ab}=C_A{}^2\delta_{ab}, \tag{3C.2}$$
$$\sum_{s,t}[C^sC^tC^sC^t]_{ab} = \tfrac{1}{2}C_A{}^2\delta_{ab}. \tag{3C.3}$$

[6]FORM is a symbolic manipulation programme written by J.A.M. Vermaseren (NIKHEF-H, Amsterdam).

The Lorentz structure of the diagrams can be projected onto the 4 combinations $O^i_{\mu\nu}$, given in eqs. 3.2.17–3.2.20. The projection operators $P^i_{\mu\nu}$ can be easily found by solving the equation

$$P^i_{\mu\nu} O^{j\mu\nu} = \delta^{ij} \tag{3C.4}$$

on a certain basis (e.g. the $O^i_{\mu\nu}$ themselves), which reveals amongst others the relation

$$P^1_{\mu\nu} = \frac{1}{n-2} O^1_{\mu\nu}. \tag{3C.5}$$

Application of these projections on a diagram gives us its contribution in terms of scalar integrals. Parametrising the integrals in a suitable way, the scalar integrals have the general form

$$\int \frac{d^n k_1}{(2\pi)^n} \frac{d^n k_2}{(2\pi)^n} \frac{(\Delta\cdot k_1)^a (\Delta\cdot k_2)^b (p\cdot k_2)^i (k_1\cdot k_2)^j}{{k_1}^{2\alpha} {k_2}^{2\beta} (p-k_1)^{2\gamma} (p-k_2)^{2\delta} (k_1-k_2)^{2\epsilon}}, \tag{3C.6}$$

where

$$a, b = 0, 1, \ldots, m, \tag{3C.7}$$

$$i, j = 0, 1, 2. \tag{3C.8}$$

The parameters $\alpha, \beta, \gamma, \delta$ and ϵ are non–negative, except when $\delta = 0$: in that case α might be smaller than zero. The exponents i and j cannot be unequal to zero at the same time (because the integral is zero in that case). The factors $\Delta\cdot k_1$ and $\Delta\cdot k_2$ can occur to any power, because they occur in the sums of the Feynman rules in a complicated way (see appendix 3A, eqs. 3A.17 and 3A.18).

The first step in calculating these integrals consists of the elimination of the factors $p\cdot k_2$ and $k_1\cdot k_2$ in the numerator when $\delta = 0$ or $\epsilon = 0$, respectively. A convenient method to do this is given by the Passarino–Veltman reduction in n dimensions.

Consider the case where $i > 0$. The integral with i inner products $p\cdot k_2$ can be written as

$$\int \frac{d^n k_1}{(2\pi)^n} \frac{(\Delta\cdot k_1)^a p_{\mu_1}\ldots p_{\mu_i}}{{k_1}^{2\alpha}(p-k_1)^{2\gamma}} \int \frac{d^n k_2}{(2\pi)^n} \frac{(\Delta\cdot k_2)^b {k_2}^{\mu_1}\ldots {k_2}^{\mu_i}}{{k_2}^{2\beta}(k_1-k_2)^{2\epsilon}} \tag{3C.9}$$

and the only 'external' momenta with respect to the k_2–integration are k_1 and Δ. The easiest way to obtain the k_2–integral is by projecting onto all possible $\mu_1 \ldots \mu_i$ structures with the aid of orthogonal projective momenta [13], e.g.

$$P_1{}^\mu = k_1{}^\mu, \tag{3C.10}$$

$$P_2{}^\mu = \Delta^\mu - \frac{\Delta\cdot k_1}{{k_1}^2} k_1{}^\mu, \tag{3C.11}$$

and the projection operator, which projects onto the metric tensor,

$$P^{\mu\nu} = \frac{1}{n-2}\left(g^{\mu\nu} - \frac{P_1{}^\mu P_1{}^\nu}{P_1{}^2} - \frac{P_2{}^\mu P_2{}^\nu}{P_2{}^2}\right). \tag{3C.12}$$

These quantities satisfy

$$P_i \cdot P_j = \delta_{ij} P_i^2, \tag{3C.13}$$

$$P_i{}^\mu P_{\mu\nu} = 0, \tag{3C.14}$$

$$P^{\mu\nu} P_{\mu\nu} = n-2. \tag{3C.15}$$

It follows that we can replace the inner products by[7]

$$(p\cdot k_2)^2 \rightarrow \frac{p_\mu p_\nu P^{\mu\nu} k_{2\alpha} k_{2\beta} P^{\alpha\beta}}{n-2} + \frac{(p\cdot P_1)^2 (k_2\cdot P_1)^2}{P_1{}^4} \tag{3C.16}$$

$$+ \frac{(p\cdot P_2)^2 (k_2\cdot P_2)^2}{P_2{}^4} + \frac{2(p\cdot P_1)(p\cdot P_2)(k_2\cdot P_1)(k_2\cdot P_2)}{P_1{}^2 P_2{}^2}, \tag{3C.17}$$

$$p\cdot k_2 \rightarrow \frac{(p\cdot P_1)(k_2\cdot P_1)}{P_1{}^2} + \frac{(p\cdot P_2)(k_2\cdot P_2)}{P_2{}^2}. \tag{3C.18}$$

All the inner products, present in the integral after this projection, can be written in terms of propagators. In the case of the $k_1 \cdot k_2$ terms, the role of p and k_1 is interchanged.

The operation leaves us with the general integrals

$$I^{abcde}_{\alpha\beta\gamma\delta\epsilon} = \int \frac{d^n k_1}{(2\pi)^n} \frac{d^n k_2}{(2\pi)^n} \frac{(\Delta\cdot k_1)^a (\Delta\cdot k_2)^b (\Delta\cdot p - \Delta\cdot k_1)^c (\Delta\cdot p - \Delta\cdot k_2)^d (\Delta\cdot k_1 - \Delta\cdot k_2)^e}{k_1{}^{2\alpha} k_2{}^{2\beta} (p-k_1)^{2\gamma} (p-k_2)^{2\delta} (k_1-k_2)^{2\epsilon}}, \tag{3C.19}$$

where we have introduced the parameters c, d and e for convenience, because if one applies the equalities given in eqs. 3A.17 and 3A.18, the corresponding combinations of inner products can occur with a power $m-2$ in the numerator, or in the denominator with a single power. Irrespective of their numerators, we know that the following integrals are zero due to the absence of a mass scale:

$$I_{\alpha\beta\gamma00} = I_{\alpha\beta0\delta0} = I_{\alpha\beta00\epsilon} = I_{\alpha0\gamma\delta0} = I_{\alpha0\gamma0\epsilon} = I_{0\beta\gamma\delta0} = I_{0\beta0\delta\epsilon} = I_{00\gamma\delta\epsilon} = 0. \tag{3C.20}$$

The integrals, which have 5 different denominators, are UV finite and will not be considered here. So we have

$$I_{\alpha\beta\gamma\delta\epsilon} = \mathcal{O}(1), \quad \text{if} \quad \alpha,\beta,\gamma,\delta,\epsilon > 0. \tag{3C.21}$$

However, in appendix 4C we will give a method to determine these integrals too.

[7] It will appear that in the case of the general covariant gauge one also needs to replace $(p\cdot k_2)^3$.

There are only two different integrals left, which we can write in terms of Feynman parameter integrals in the following way

$$I^{abcde}_{\alpha\beta\gamma\delta 0} = -\frac{1}{(4\pi)^n}\left(-p^2\right)^e (p^2)^{4-\alpha-\beta-\gamma-\delta}(\Delta\cdot p)^{a+b+c+d+e}\times$$
$$\frac{\Gamma(\alpha+\gamma-\frac{n}{2})}{\Gamma(\alpha)\Gamma(\gamma)}\frac{\Gamma(\beta+\delta-\frac{n}{2})}{\Gamma(\beta)\Gamma(\delta)}\int_0^1 dx\, x^{a+\frac{1}{2}n-\alpha-1}(1-x)^{c+\frac{1}{2}n-\gamma-1}$$
$$\times\int_0^1 dy\, y^{b+\frac{1}{2}n-\beta-1}(1-y)^{d+\frac{1}{2}n-\delta-1}(x-y)^e, \tag{3C.22}$$

$$I^{abcde}_{\alpha\beta\gamma 0\epsilon} = -\frac{1}{(4\pi)^n}\left(-p^2\right)^e (p^2)^{4-\alpha-\beta-\gamma-\epsilon}(\Delta\cdot p)^{a+b+c+d+e}\times$$
$$\frac{\Gamma(\alpha+\beta+\gamma+\epsilon-n)}{\Gamma(\alpha+\beta+\epsilon-\frac{n}{2})\Gamma(\gamma)}\frac{\Gamma(\beta+\delta-\frac{n}{2})}{\Gamma(\beta)\Gamma(\delta)}\int_0^1 dx\, x^{a+b+e+n-\alpha-\beta-\epsilon-1}(1-x)^{c+\frac{1}{2}n-\gamma-1}$$
$$\times\int_0^1 dy\, y^{b+\frac{1}{2}n-\beta-1}(1-y)^{e+\frac{1}{2}n-\epsilon-1}(1-xy)^d, \tag{3C.23}$$

where the UV singularities are already visible in the Γ–functions. It is clear from eq. 3C.23 that the case $\alpha < 0,\ \delta = 0$ is not exceptional. The parameter integrals can be brought into a standard form by the simple transformations $x \to 1-x$, $x \leftrightarrow y$ and $y \to 1-y$ and the more complicated transformations in the following 2 cases.

- When a factor $(xy)^m$ or $(1-xy)^m$ is present, one can introduce the following variables

$$x' = xy,\qquad y' = \frac{x(1-y)}{1-xy}, \tag{3C.24}$$

  in terms of which the integrals have the following form

$$\int_0^1 dx\int_0^1 dy\,(xy)^m x^\alpha(1-x)^\beta y^\gamma(1-y)^\delta =$$
$$\int_0^1 dx'\,(x')^{m+\gamma}(1-x')^{\beta+\delta+1}$$
$$\times\int_0^1 dy'\,(y')^\beta(1-y')^\delta(1-(1-x')y')^{\alpha-\gamma-\delta-1}, \tag{3C.25}$$

$$\int_0^1 dx\int_0^1 dy\,(1-xy)^m x^\alpha(1-x)^\beta y^\gamma(1-y)^\delta =$$
$$\int_0^1 dx'\,(x')^{m+\beta+\delta+1}(1-x')^\gamma$$
$$\times\int_0^1 dy'\,(y')^\beta(1-y')^\delta(1-x'y')^{\alpha-\gamma-\delta-1}. \tag{3C.26}$$

- In the case of a factor $(x-y)^m$, the integral can be split up into two parts, depending on $x-y>0$ or $x-y<0$. The following transformations bring the two parts into the standard form

$$x-y>0 \ : \ x'=x-y, \qquad y'=\frac{y}{1-x+y}, \tag{3C.27}$$

$$x-y<0 \ : \ x'=y-x, \qquad y'=\frac{1-y}{1-x+y}. \tag{3C.28}$$

The integral becomes, in terms of these variables,

$$\begin{aligned}
&\int_0^1 dx \int_0^1 dy\,(x-y)^m x^\alpha (1-x)^\beta y^\gamma (1-y)^\delta = \\
&\quad \int_0^1 dx'\,(x')^{m+\alpha}(1-x')^{\beta+\gamma+1} \\
&\quad \times \int_0^1 dy'\,(y')^\gamma (1-y')^\beta (1-(1-x')y')^\delta \left(1+\frac{1-x'}{x'}y'\right)^\alpha \\
&\quad + \int_0^1 dx'\,(-1)^m (x')^{m+\beta}(1-x')^{\alpha+\delta+1} \\
&\quad \times \int_0^1 dy'(y')^\delta (1-y')^\alpha (1-(1-x')y')^\gamma \left(1+\frac{1-x'}{x'}y'\right)^\beta .
\end{aligned} \tag{3C.29}$$

As a consequence, the general form of the parameter integrals is as such, that the parameter m only occurs in the x–integral.

The next and last step of the calculation of the loop integrals consists of explicit integration over the Feynman parameter y and, if x^m is absent, integration over x. One should take care of the fact that, in order to obtain the correct behaviour for $x=1$, the factors $(1-x)^{-1+a\epsilon}$ must be treated exactly. This means that the y–integration should neither produce $\ln^i(1-x)$ terms nor any other terms which are singular near $x=1$. Therefore, the y-integration is described here for those cases, which cause trouble, if they are not given special care.

- Factors $1-xy$ in the denominator. Analytic continuation yields the following result

$$\begin{aligned}
&\int_0^1 dy\, y^\alpha (1-y)^\beta (1-xy)^\gamma \qquad (\gamma=-1,-2,\ldots) \\
&\quad = \frac{B(-\beta-\gamma,\beta+\gamma+1)}{B(-\alpha-\beta-\gamma-1,\alpha+\beta+\gamma+2)} \\
&\qquad \times \int_0^1 dy\, y^\alpha (1-y)^{-\alpha-\beta-\gamma-2}(1-(1-x)y)^\gamma
\end{aligned}$$

$$+ x^{-\alpha-\beta-1}(1-x)^{\beta+\gamma+1}B(\beta+1,-\beta-\gamma-1)$$

$$\times F(\alpha,\gamma+1;\beta+\gamma+2;1-x). \quad (3C.30)$$

The second term, which contains the hypergeometric function F [14], can be expressed in powers of x and $1-x$. The first term results in functions, which are regular near $x=1$. If the x integration must be carried out too (so if x^m is absent), one should also avoid x^{-1} terms (the functions from the first term of eq. 3C.30 are generally not regular near $x=0$). This can be obtained by suitable transformations $x \leftrightarrow y$ or $x \to 1-x$ before applying the above transformations.

- A factor $x-y$ in the denominator. Analytic continuation of the hypergeometric function yields the following equality

$$\int_0^1 dy\, y^\alpha(1-y)^\beta(x-y)^{-1}$$
$$= \frac{B(1-\beta,\beta)}{B(-\alpha-\beta,\alpha+\beta+1)}\int_0^1 dy\, y^{-\alpha-\beta-1}(1-y)^\alpha(1-(1-x)y)^{-1}$$
$$+ B(-\beta,\beta+1)x^\alpha(x-1)^\beta. \quad (3C.31)$$

The second part of this expression has an imaginary part, which we do not consider, because we only need the principal value of the integral. It means that we drop the imaginary part of the analytic continuation of $(x-1)^{a\epsilon}$

$$(x-1)^{a\epsilon} = (1-x)^{a\epsilon}\left[\frac{B(1+a\epsilon,1-a\epsilon)}{B(1+2a\epsilon,1-2a\epsilon)} - \frac{i\pi a\epsilon}{B(1+a\epsilon,1-a\epsilon)}\right]. \quad (3C.32)$$

The integrals without x^m can be treated by applying recursive relations to them. If we define

$$I_\delta^{\alpha,\beta} = \int_0^1 dx \int_0^1 dy\, x^\delta (xy)^{\alpha-1}[(1-x)(1-y)]^{\beta-1}(x-y)^{-1}, \quad (3C.33)$$

where $\delta = 0,1,2,\ldots$, one can prove the following properties, which solve all cases

$$I_\delta^{\alpha,\beta} = I_{\delta-2}^{\alpha+1,\beta} + B(\alpha+\delta-1,\beta)B(\alpha,\beta), \quad (3C.34)$$
$$I_1^{\alpha,\beta} = \tfrac{1}{2}B(\alpha,\beta)^2, \quad (3C.35)$$
$$I_0^{\alpha,\beta} = 0. \quad (3C.36)$$

3D Convolutions

In this section we will present some useful convolutions of first order results which are needed in order to determine the second order gluon operator renormalisation constant.

The convolution of the first order gluon operator renormalisation constant, given in eq. 3.4.20, and the complete first order result which can be inferred from eqs. 3.2.44 and 3.2.45, is the most difficult one to calculate. In the Feynman gauge the result is as follows

$$
\begin{aligned}
-(Z^{(1)}_{gg} \otimes \mathcal{A}^{(1)}_{\mu\nu})(x,p) = \left(\frac{-p^2}{\mu^2}\right)^{\frac{1}{2}\varepsilon} & \Bigg(\Big\{ \frac{1}{\varepsilon}\Big[\big[\tfrac{88}{3} - \tfrac{88}{3}\zeta(2) - 32\zeta(3) \big] \delta(1-x) \\
&+ 16 \big[3x - x^2 + x^{-1} + (1-x)^{-1} \big] \ln x^2 + 64 \big[1 + x \big] \ln x \ln(1-x) + \tfrac{8}{3} \big[46 \\
&+ 11x^2 + 3[\text{illegible}]x + 23x^{-1} - 11(1-x)^{-1} \big] \ln x + 48 \big[2 + x^2 - x - (1-x)^{-1} \\
&- x^{-1} \big] \ln(1-x)^2 + \tfrac{8}{3} \big[4 - 21x^2 + 13x + 21x^{-1} - 11(1-x)^{-1} \big] \ln(1-x) \\
&+ 64 \big[1 + x \big] \operatorname{Li}_2(1-x) - \tfrac{92}{3} - \tfrac{184}{9}x^2 - \tfrac{32}{3}x + \tfrac{400}{9}x^{-1} + 32(1-x)^{-1} \Big] \\
&+ \frac{1}{\varepsilon^2}\Big[\big[64\zeta(2) - \tfrac{88}{3} \big] \delta(1-x) + 64 \big[3x - x^2 + x^{-1} + (1-x)^{-1} \big] \ln x \\
&+ 128 \big[2 + x^2 - x - x^{-1} - (1-x)^{-1} \big] \ln(1-x) - \tfrac{32}{3} - 144x^2 + \tfrac{304}{3}x \\
&+ 144x^{-1} - \tfrac{272}{3}(1-x)^{-1} \Big] \Big\} O^1_{\mu\nu}(p) + \frac{1}{\varepsilon}\Big[16 \big[1 + 4x^2 - 4x \big] \ln(1-x) \\
&+ 16 \big[1 + 8x \big] \ln x + \tfrac{116}{3} - \tfrac{344}{3}x^2 + \tfrac{256}{3}x + \tfrac{16}{3}x^{-1} \Big] O^2_{\mu\nu}(p) \\
&+ \Big\{ \frac{1}{\varepsilon}\Big[-8 \big[1 + x^{-1} \big] \ln x^2 - 32 \ln x \ln(1-x) - 16 \big[1 - x^{-1} \big] \ln^2(1-x) \\
&- \tfrac{4}{3} \big[41 - 2x^2 + 6x + 23x^{-1} \big] \ln x + \tfrac{4}{3} \big[7 - 2x^2 + 6x - 11x^{-1} \big] \ln(1-x) \\
&- 16 \big[3 - x^{-1} \big] \operatorname{Li}_2(1-x) + 16 \big[1 - x^{-1} \big] \zeta(2) + 8 - \tfrac{44}{9}x^2 + \tfrac{76}{3}x \\
&- \tfrac{256}{9}x^{-1} \Big] + \frac{1}{\varepsilon^2}\Big[-32 \big[1 + x^{-1} \big] \ln x - 32 \big[1 - x^{-1} \big] \ln(1-x) \\
&+ \tfrac{152}{3} - \tfrac{16}{3}x^2 + 16x - \tfrac{184}{3}x^{-1} \Big] \Big\} O^3_{\mu\nu}(p) \Bigg) . \qquad \text{(3D.1)}
\end{aligned}
$$

The tensor $O^4_{\mu\nu}(p)$ is absent in this expression, which could be expected, because the tensor structure of the expression is determined by $\mathcal{A}^{(1)}_{\mu\nu}(x,p)$, which should obey the

WT identity 3.2.26.

The two convolutions, which arise from the one loop renormalisation of the alien and the ghost operator, lead to the following expressions:

$$
\begin{aligned}
-(Z^{(1)}_{ga} \otimes B^{(1)}_{\mu\nu})(x,p) = \left(\frac{-p^2}{\mu^2}\right)^{\frac{1}{2}\epsilon} & \Bigg(\Bigg\{ \frac{1}{\varepsilon}\Bigg[\Big[\tfrac{1}{3}x^2 - 4 - x - 8x^{-1} \Big] \ln x + \Big[1 + \tfrac{1}{3}x^2 \\
& - x - \tfrac{1}{3}x^{-1} \Big] \ln(1-x) + \tfrac{29}{3} - \tfrac{5}{9}x^2 + \tfrac{7}{3}x - \tfrac{103}{9}x^{-1} \Bigg] + \frac{1}{\varepsilon^2}\Big[2 + \tfrac{2}{3}x^2 - 2x \\
& - \tfrac{2}{3}x^{-1} \Big] \Bigg\} O^1_{\mu\nu}(p) + \frac{1}{\varepsilon}\Big[-8\ln x + 10 + \tfrac{2}{3}x^2 - 2x - \tfrac{26}{3}x^{-1} \Big] O^2_{\mu\nu}(p) \\
& + \Bigg\{ \frac{1}{\varepsilon}\Bigg[2\Big[1 + x^{-1} \Big] \ln x^2 + 4\Big[1 + x^{-1} \Big] \ln x \ln(1-x) - 6\Big[1 - x^{-1} \Big] \zeta(2) \\
& - 3\Big[1 - x^{-1} \Big] \ln^2(1-x) + \Big[11 - \tfrac{1}{3}x^2 + \tfrac{5}{2}x + 8x^{-1} \Big] \ln x + \Big[\tfrac{5}{2}x - 6 - \tfrac{1}{3}x^2 \\
& + \tfrac{23}{6}x^{-1} \Big] \ln(1-x) + 2\Big[5 - x^{-1} \Big] \operatorname{Li}_2(1-x) - \tfrac{9}{2} + \tfrac{5}{9}x^2 - \tfrac{41}{6}x + \tfrac{97}{9}x^{-1} \Bigg] \\
& + \frac{1}{\varepsilon^2}\Bigg[8\Big[1 + x^{-1} \Big] \ln x - 12\Big[1 - x^{-1} \Big] \ln(1-x) - 15 - \tfrac{2}{3}x^2 + 5x \\
& + \tfrac{32}{3}x^{-1} \Bigg] \Bigg\} O^3_{\mu\nu}(p) + \frac{1}{\varepsilon}\Big[-\ln x + 1 - x^{-1} \Big] O^4_{\mu\nu}(p) \Bigg)
\end{aligned}
\tag{3D.2}
$$

and

$$
\begin{aligned}
-(Z^{(1)}_{g\omega} \otimes C^{(1)}_{\mu\nu})(x,p) = \left(\frac{-p^2}{\mu^2}\right)^{\frac{1}{2}\epsilon} & \Bigg(\Bigg\{ \frac{1}{\varepsilon}\Bigg[\Big[x - \tfrac{1}{3}x^2 \Big] \ln x + \Big[x - 1 - \tfrac{1}{3}x^2 \\
& + \tfrac{1}{3}x^{-1} \Big] \ln(1-x) + \tfrac{7}{3} + \tfrac{5}{9}x^2 - \tfrac{7}{3}x - \tfrac{5}{9}x^{-1} \Bigg] - \frac{1}{\varepsilon^2}\Big[2 + \tfrac{2}{3}x^2 - 2x \\
& - \tfrac{2}{3}x^{-1} \Big] \Bigg\} O^1_{\mu\nu}(p) + \frac{1}{\varepsilon}\Big[-2 - \tfrac{2}{3}x^2 + 2x + \tfrac{2}{3}x^{-1} \Big] O^2_{\mu\nu}(p) \\
& + \Bigg\{ \frac{1}{\varepsilon}\Bigg[\ln x^2 + 2\ln x \ln(1-x) + 2\operatorname{Li}_2(1-x) - \Big[3 - \tfrac{1}{3}x^2 + \tfrac{5}{2}x \Big] \ln x \\
& + \Big[2 + \tfrac{1}{3}x^2 - \tfrac{5}{2}x + \tfrac{1}{6}x^{-1} \Big] \ln(1-x) - \tfrac{95}{18} - \tfrac{5}{9}x^2 + \tfrac{41}{6}x - x^{-1} \Bigg] \\
& + \frac{1}{\varepsilon^2}\Big[4\ln x + \tfrac{13}{3} + \tfrac{2}{3}x^2 - 5x \Big] \Bigg\} O^3_{\mu\nu}(p) + \frac{1}{\varepsilon}\Big[\ln x - 1 + x^{-1} \Big] O^4_{\mu\nu}(p) \Bigg).
\end{aligned}
\tag{3D.3}
$$

In these expressions we used the Feynman gauge expressions, which can be found in eqs. 3.4.9, 3.4.10 and 3.4.21. In this case the tensor $O^4_{\mu\nu}$ only vanishes in the sum of the two contributions. Further, the double pole ε^{-2} that belongs to the structure $O^1_{\mu\nu}$ does not receive any contribution from the sum of the alien and ghost graphs. As a result of this fact, the overlapping divergences of $\mathcal{M}^{(2)}_{\mu\nu}(x,p)$ (see eq. 3.4.25) which are proportional to $O^1_{\mu\nu}(p)$, would also cancel in the case one leaves out the last two lines of the Lagrangian 3.3.26. The cancellation of these divergent terms, which are of the form $\varepsilon^{-1}\ln(-p^2/\mu^2)$, is indispensable in order to be able to renormalise the gluon operator. Nevertheless, the renormalisability of the alien operator does depend on the inclusion of the two convolutions, given in eqs. 3D.2 and 3D.3.

Finally, we give the complete explicit contribution to the finite 1PI Green's function which is used in order to check whether the overlapping divergences cancel. In the Feynman gauge it is given by

$$\Big[\,2Z_g^{(1)} + Z_A^{(1)} + Z_A^{(1)}\alpha\frac{\mathrm{d}}{\mathrm{d}\alpha} - Z_{gg}^{(1)}\,\Big]\otimes A^{(1)}_{\mu\nu} - Z^{(1)}_{ga}\otimes B^{(1)}_{\mu\nu} - Z^{(1)}_{gw}\otimes C^{(1)}_{\mu\nu} = \left(\frac{-p^2}{\mu^2}\right)^{\frac{1}{2}\varepsilon}$$

$$\times\Bigg(\bigg\{\frac{1}{\varepsilon}\Big[\Big[\,52 - \tfrac{112}{3}\zeta(2) - 32\zeta(3)\,\Big]\delta(1-x) + 64\Big[\,1+x\,\Big]\ln x\ln(1-x)$$

$$+\,48\Big[\,2 + x^2 - x - x^{-1} - (1-x)^{-1}\,\Big]\ln^2(1-x) + 64\Big[\,1+x\,\Big]\,\mathrm{Li}_2(1-x)$$

$$+\,16\Big[\,3x - x^2 + x^{-1} + (1-x)^{-1}\,\Big]\ln x^2 + \tfrac{4}{3}\Big[\,113 + 34x^2 + 62x + 28x^{-1}$$

$$-\,34(1-x)^{-1}\,\Big]\ln x + \tfrac{8}{3}\Big[\,4 - 21x^2 + 13x + 21x^{-1} - 11(1-x)^{-1}\,\Big]\ln(1-x)$$

$$+\,\tfrac{16}{3} - \tfrac{40}{9}x^2 - \tfrac{80}{3}x + \tfrac{148}{9}x^{-1} + \tfrac{86}{3}(1-x)^{-1}\,\Big] + \frac{1}{\varepsilon^2}\Big[\Big[\,64\zeta(2) - 42\,\Big]\delta(1-x)$$

$$+\,64\Big[\,3x - x^2 + x^{-1} + (1-x)^{-1}\Big]\ln x + 128\Big[\,2 + x^2 - x^{-1} - (1-x)^{-1}$$

$$-\,x\,\Big]\ln(1-x) + \tfrac{160}{3} - 112x^2 + \tfrac{208}{3}x + 112x^{-1} - \tfrac{368}{3}(1-x)^{-1}\,\Big]\bigg\}\,O^1_{\mu\nu}(p)$$

$$+\,\frac{1}{\varepsilon}\Big[\,8\Big[\,1+16x\,\Big]\ln x + 16\Big[\,1 + 4x^2 - 4x\,\Big]\ln(1-x) + \tfrac{164}{3} - \tfrac{248}{3}x^2 + \tfrac{160}{3}x$$

$$-\,6x^{-1}\,\Big]\,O^2_{\mu\nu}(p) + \bigg\{\frac{1}{\varepsilon}\Big[-2\Big[\,13 - 2x^{-1}\,\Big]\ln x\ln(1-x) - \Big[\,5 + 6x^{-1}\,\Big]\ln x^2$$

$$-\,19\Big[\,1 - x^{-1}\,\Big]\ln^2(1-x) - 2\Big[\,18 - 7x^{-1}\,\Big]\,\mathrm{Li}_2(1-x) + 10\Big[\,1 - x^{-1}\,\Big]\zeta(2)$$

$$+\,\tfrac{4}{3}\Big[\,2x^2 - 41 - 6x - 11x^{-1}\,\Big]\ln x + \tfrac{8}{3}\Big[\,3x - 1 - x^2 - x^{-1}\,\Big]\ln(1-x)$$

$$-\,\tfrac{88}{9} - \tfrac{44}{9}x^2 + \tfrac{76}{3}x - \tfrac{32}{3}x^{-1}\,\Big] + \frac{1}{\varepsilon^2}\Big[-44\Big[\,1 - x^{-1}\,\Big]\ln(1-x)$$

$$-\,4\Big[\,5 + 6x^{-1}\,\Big]\ln x + 24 - \tfrac{16}{3}x^2 + 16x - \tfrac{104}{3}x^{-1}\,\Big]\bigg\}\,O^3_{\mu\nu}(p)\Bigg). \qquad \text{(3D.4)}$$

References

[1] D.J. Gross and F. Wilczek, Phys. Rev. **D9** (1974), 980

[2] J.A. Dixon and J.C. Taylor, Nucl. Phys. **B78** (1974), 552

[3] S.D. Joglekar and B.W. Lee, Ann. of Phys. **97** (1976), 160; S.D. Joglekar, Ann. of Phys. **108** (1977), 233; **109** (1977), 210

[4] E.G. Floratos, D.A. Ross and C.T. Sachrajda, Nucl. Phys. **B152** (1979), 493; A. Gonzalez-Arroyo and C. Lopez, Nucl. Phys. **B166** (1980), 429

[5] W. Furmanski and R. Petronzio, Phys. Lett. **97B** (1980), 437

[6] E.G. Floratos, C. Kounnas and R. Lacaze, Nucl. Phys. **B192** (1981), 437

[7] I. Antoniadis and E.G. Floratos, Nucl. Phys. **B191** (1981), 217

[8] W. Kummer, Acta Phys. Austr. **41** (1975), 315; W. Konetschny and W. Kummer, Nucl. Phys. **B100** (1975), 106; **B108** (1976), 397; **B124** (1977), 145; W. Kainz, W. Kummer and M. Schweda, Nucl. Phys. **B79** (1974), 484; R.J. Crewther, in 'Weak and electromagnetic interactions at high energy', edited by M. Levy et al., Plenum, New York, 1976, p. 345

[9] R.J. Crewther, 'Asymptotic behaviour in quantum field theory', CERN report TH-2119

[10] J.C. Taylor, Nucl. Phys. **B33** (1971), 436

[11] J. Zinn-Justin, in 'International Summer Institute on Theoretical Physics', Bonn, 1974

[12] J.D. Bjorken and S.D. Drell, 'Relativistic Quantum Mechanics', McGraw-Hill, New York, 1964

[13] W.J.P. Beenakker, thesis, University of Leiden, 1989, chapter III

[14] H. Bateman, 'Higher transcendental functions', McGraw-Hill, New York, 1953, volume I; L. Lewin, 'Polylogarithms and Associated Functions', North-Holland, 1983; R. Barbieri, J.A. Mignaco and E. Remiddi, Nuovo Cim. **11A** (1972), 824; A. Devoto and D.W. Duke, Riv. Nuovo Cim. **7-6** (1984), 1

Chapter 4

The Drell–Yan K–factor

4.1 Introduction

The theoretical justification for perturbative strong interaction corrections to the parton model [1] and their summation by renormalisation group techniques in the framework of QCD lead to a wealth of radiative corrections to numerous processes (for a review see [2]). The most interesting outcome of these calculations was that some of the corrections turned out to be rather large. This can mainly be attributed to the considerable size of the running coupling constant $\alpha_s(R^2)$, which decreases slowly as R^2 grows. Because of these large corrections one can question the predictive power of perturbative QCD. However, experiments show that there is a considerable discrepancy between the predictions of the Born approximation and the experimental data. Nowadays, it is commonly accepted that the ratio between the measured cross section and the Born approximation, generally called K–factor, can be explained by including the higher order corrections. For most processes only first order corrections have been calculated. They give a reasonable agreement with the experimental data. Nevertheless, corrections beyond the order α_s are needed for practical as well as for theoretical reasons.

The practical reason is that the statistics in the ongoing and future experiments will improve so that the higher order corrections might become noticeable. This is expected because the size of the various K– and R–factors can become rather large. It is also interesting to see how the K–factors will behave at very large energies, which are characteristic for future accelerators, like LHC and SSC. Here we expect processes with gluons in the initial state to play a very important role. From the theoretical point of view higher order corrections are interesting because we can learn something about the behaviour of the perturbation series, in particular about its convergence.

One also wants to know by which terms the series is dominated. An example of such a striking term is the soft gluon part of the K-factor, which is present in reactions with one or more gluons in the final state. Knowledge about these dominant parts can provide us with useful information about which techniques are needed for their resummation. Another possibility to improve the perturbation series is the choice of a suitable mass factorisation and renormalisation scale. These scales can for instance be determined in the optimised perturbation theory. Examples are the principle of minimal sensitivity (PMS) [3] and the method of fastest asymptotic convergence (FAC) [4]. The drawback of these approaches is that they are based on extrapolations of the lowest order terms, ignoring the effects coming from higher order corrections. Moreover, we expect that cross sections, calculated in higher order of α_s, will be less sensitive to variations in the factorisation and renormalisation scales than the lowest order ones.

In this chapter we will present the full order α_s^2 correction to inclusive massive lepton pair production (Drell–Yan process). The first experiment to study this reaction was carried out by the Columbia–BNL group [5] in 1970. From that time onwards this process called the attention of many experimentalists as well as theorists in elementary particle physics. Before the $p\overline{p}$ collider at CERN became operational in the beginning of the eighties all experiments were of the fixed target type. One of the aims was to study the structure of hadrons. When the Drell–Yan reaction takes place at relatively low energies ($\sqrt{S} < 20$ GeV) the hadrons are probed by a highly virtual timelike photon, which is experimentally observed through its decay into a massive lepton pair. Therefore, this process is complementary to deep inelastic lepton–proton scattering where the exchanged photon is spacelike. An advantage of massive lepton pair production is that it allows us to study the structure of unstable particles, like pions or kaons. This is not possible in deep inelastic lepton–hadron scattering where the target particles (like the proton or the bound neutron) have to be stable. On the other hand the latter process provides us with much better statistics. Both reactions belong to the class of the so–called hard processes, which means that at increasing energies all kinematical variables get large while their ratios stay fixed. In such a case one can apply the methods of perturbative QCD.

The first successful description of massive lepton pair production in the context of the parton model (lowest order QCD) was given by Drell and Yan [6]. Later on, this production mechanism, called Drell–Yan (DY) after their inventors, was supplemented by perturbative QCD. Using renormalisation group methods and the mass factorisation theorem, for which an all order proof exists [7], one can compute

QCD corrections to this process. Between 1978 and 1980 the first order α_s corrections were performed by many groups [8]–[13]. At the same time (1979) the NA3 group [14] found a discrepancy between the data and the zeroth order parton model, a result which was confirmed by other fixed target experiments (for a review see [15]). Later on a second confirmation came from the p$\overline{\text{p}}$ colliders at CERN and FERMILAB [16]. At the energies of these machines, exceeding those of fixed target experiments by two orders of magnitude, the lepton pair is produced through the W– and Z–bosons. Comparison of the data with the theory revealed that the discrepancy, generally represented by the so–called experimental K–factor, could be rather well explained by the existing order α_s corrections. In spite of this success one might question the reliability of perturbation theory, as the corrections turned out to be rather large ($\sim$ 70% at fixed target energies and $\sim$ 30% for the $Sp\overline{p}S$). Therefore, higher order corrections are necessary to put the order α_s predictions on a firmer ground.

Unlike other QCD processes the DY reaction seems to be one of the few cases where the calculation of the order α_s^2 corrections is feasible, a property it shares with deep inelastic lepton–hadron scattering. This is because the maximum number of particles appearing in the final state of the parton subprocesses, which contribute to these two reactions does not exceed three. Notice that the most complicated parts of these calculations are the many body phase space integrals. If there are more than three particles in the final state the number of these integrals as well as their complexity get completely out of control. In the case of collinear finite processes like R, defined in the reaction $e^+ + e^- \rightarrow$ 'X', the situation is a little better. The optical theorem, which relates this quantity to the absorptive part of a two point function, makes it even possible to calculate its radiative corrections up to order α_s^3 [17]. Another example is the order α_s^2 correction to the two jet cross section of the same process [18] although here the used methods resemble those used in the DY calculation.

However, note that in the last two cases no mass factorisation is involved, hence, these quantities only depend on the chosen scheme for the strong coupling constant. Therefore, one can study their dependence on the renormalisation scale only. In deep inelastic lepton–hadron scattering and the DY process we also have to perform mass factorisation rendering the Wilson coefficient dependent on two separate scales. In this way the DY K–factor provides us with a beautiful opportunity to investigate the dependence on the mass factorisation as well as on the renormalisation scale. Finally, notice that in order to obtain the order α_s^2 correction to the K–factor, we need the two loop corrected splitting functions to remove the collinear divergences from the parton cross sections. This is the first time that the higher order splitting functions show up in a perturbative calculation.

This chapter will be organised as follows. In section 4.2 we present the results of the complete order α_s^2 correction to the DY K-factor, which is calculated in the $\overline{\rm MS}$ scheme. The latter refers to coupling constant renormalisation as well as mass factorisation. In particular we have included the contribution of the hard gluon radiation to the $q\bar{q}$ process and the order α_s correction to the qg reaction, which were not presented previously. In section 4.3 we discuss the effect of the higher order corrections on heavy vector boson production at current and future accelerators. The long expressions for the hadronic structure function and the DY correction terms, not presented in section 4.2, can be found in appendices 4A and 4B, respectively. A partial but powerful check on the DY correction terms will be presented in appendix 4C.

4.2 The Drell–Yan deep inelastic scattering process

4.2.1 The DY formalism and first order corrections

Massive lepton pair production in hadronic collisions proceeds through the following reaction

$$\begin{aligned} {\rm H}_1 + {\rm H}_2 \to\ & V + \text{`X'} \\ & \llcorner\!\!\longrightarrow \ell_1 + \ell_2, \end{aligned} \tag{4.2.1}$$

where V is one of the vector bosons of the standard model (γ, Z or W), which subsequently decays into a lepton pair (ℓ_1, ℓ_2). The symbol 'X' denotes any inclusive final hadronic state allowed by conservation of quantum numbers. The colour averaged inclusive cross section is given by

$$\frac{d\sigma^V}{dQ^2} = \tau\ \sigma_V(Q^2, M_V{}^2)\ W_V(\tau, Q^2), \tag{4.2.2}$$

where $\tau = Q^2/S$. The quantity σ_V is the pointlike cross section (see eqs. 4A.1–4A.3). The variables $\sqrt{S}$ and $\sqrt{Q^2}$ stand for the C.M. energy of the incoming hadrons H_1, H_2 and the invariant mass of the dilepton pair, respectively. The hadronic structure function is represented by $W_V(\tau, Q^2)$. According to the DY mechanism it can be written as

$$W_V(\tau, Q^2) \;=\; \sum_{i,j} \int_0^1 dx_1 \int_0^1 dx_2 \int_0^1 dx\, \delta(\tau - x x_1 x_2)$$

$$\times\, PD^V_{ij}(x_1, x_2, M^2)\, \Delta_{ij}(x, Q^2, M^2). \tag{4.2.3}$$

The functions $PD^V_{ij}(x_1, x_2, M^2)$ stand for the usual combination of parton distribution functions, which depend on the mass factorisation scale M. The indices i and j refer to the type of the incoming partons. Furthermore, the PD^V_{ij} contain all the information on the coupling of the quarks to the vector bosons, such as the quark charges, the Weinberg angle θ_W and the Cabibbo angle θ_C (the other angles and phases of the Kobayashi–Maskawa (KM) matrix are neglected). The explicit way in which the functions PD^V_{ij} combine with the correction terms Δ_{ij} is given in eq. 4A.21. Notice that the parton distribution functions not only depend on the mass factorisation scale M, but also on the renormalisation scale R, because the calculation of their scale dependence originates from operator renormalisation (= mass factorisation) as well as from coupling constant renormalisation. However, in the existing parametrisations of the parton distribution functions the two scales M and R are always set to be equal. Also the DY correction term $\Delta_{ij}(x, Q^2, M^2)$ (Wilson coefficient) depends on both scales. This can be seen by expanding the DY correction term in a power series in the running coupling constant $\alpha_s(R^2)$

$$\Delta_{ij}(x, Q^2, M^2) = \sum_{n=0}^{\infty} \alpha_s^n(R^2) \Delta_{ij}^{(n)}(x, Q^2, M^2, R^2). \tag{4.2.4}$$

When $\alpha_s(R^2)$ is expanded in a power series in $\alpha_s(M^2)$ the explicit R–dependence in eq. 4.2.4 drops out.

The DY correction term Δ_{ij} can be obtained from the DY partonic structure function $\mathcal{W}_{ij}$ through mass factorisation

$$\begin{aligned} \mathcal{W}_{ij}(z, Q^2, M^2, \varepsilon) &= \sum_{k,l} \int_0^1 dx_1 \int_0^1 dx_2 \int_0^1 dx\, \delta(z - x x_1 x_2) \\ &\qquad \times \Gamma_{ki}(x_1, M^2, \varepsilon) \Gamma_{lj}(x_2, M^2, \varepsilon) \Delta_{kl}(x, Q^2, M^2), \end{aligned} \tag{4.2.5}$$

where $\mathcal{W}_{ij}$ is determined by the parton subprocess

$$i + j \to V + \text{'X'} \tag{4.2.6}$$

and Γ_{ki} represents the transition function (parton $i \to$ parton k). In eq. 4.2.5 we assume that coupling constant renormalisation has already been performed (cf. eq. 2.3.16). Like the DY correction term presented in eq. 4.2.4 the quantities $\mathcal{W}$ and Γ can be expanded in a power series in the renormalised coupling constant $\alpha_s(R^2)$ and therefore implicitly depend on the chosen renormalisation scale R. The collinear

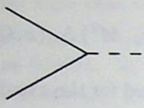

Fig. 4.1. The Born contribution to the subprocess $q+\bar{q}\rightarrow V$.

divergences present in $\mathcal{W}$ and Γ are handled using dimensional regularisation and manifest themselves as pole terms of the type ε^{-i} ($\varepsilon \equiv n-4$).

The parton subprocesses contributing to the DY cross section up to second order in α_s are listed in table 4.1.

figure		Drell-Yan subprocesses			
4.1	α_s^0:	$q+\bar{q}$	$\rightarrow$	V	
4.2	α_s^1:	$q+\bar{q}$	$\rightarrow$	V	(one loop correction)
4.3		$q+\bar{q}$	$\rightarrow$	$V+g$	
4.3		$q(\bar{q})+g$	$\rightarrow$	$V+q(\bar{q})$	
4.4	α_s^2:	$q+\bar{q}$	$\rightarrow$	V	(two loop correction)
4.5		$q+\bar{q}$	$\rightarrow$	$V+g$	(one loop correction)
4.6		$q+\bar{q}$	$\rightarrow$	$V+g+g$	
4.5		$q(\bar{q})+g$	$\rightarrow$	$V+q(\bar{q})$	(one loop correction)
4.6		$q(\bar{q})+g$	$\rightarrow$	$V+q(\bar{q})+g$	
4.7,4.8		$q+\bar{q}$	$\rightarrow$	$V+q+\bar{q}$	
4.8,4.9		$q(\bar{q})+q(\bar{q})$	$\rightarrow$	$V+q(\bar{q})+q(\bar{q})$	
4.6		$g+g$	$\rightarrow$	$V+q+\bar{q}$	

Table 4.1. List of Drell Yan processes up to $\mathcal{O}(\alpha_s^2)$.

In zeroth order in α_s the only parton subprocess is given by quark–antiquark ($q\bar{q}$) annihilation (see fig. 4.1) and the resulting expression for $\mathcal{W}$ is given by

$$\mathcal{W}_{q\bar{q}}^{(0)} = \delta(1-x). \tag{4.2.7}$$

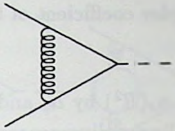

Fig. 4.2. The one loop correction to the process $q + \overline{q} \to V$.

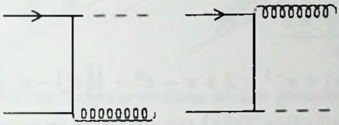

Fig. 4.3. Diagrams contributing to the subprocess $q + \overline{q} \to V + g$. The graphs corresponding to the subprocess $q(\overline{q}) + g \to V + q(\overline{q})$ can be obtained from those presented in this figure via crossing.

The first order corrections, calculated using dimensional regularisation, can be found in [8, 12]. The order α_s correction to the $q\overline{q}$ process receives contributions from virtual (fig. 4.2) as well as real gluon (fig. 4.3) graphs. Further the qg subprocess (fig. 4.3), showing up for the first time in this order, has to be computed too. The partonic structure functions can be expressed in the following form

$$\mathcal{W}^{(1)}_{q\overline{q}} = \frac{\hat{\alpha}_s}{4\pi} S_\varepsilon \left(\frac{Q^2}{\mu^2}\right)^{\frac{1}{2}\varepsilon} \left\{ \frac{2}{\varepsilon} P^0_{qq} + w^0_{q\overline{q}} + \varepsilon\, \bar{w}^0_{q\overline{q}} \right\} \tag{4.2.8}$$

and

$$\mathcal{W}^{(1)}_{qg} = \mathcal{W}^{(1)}_{\overline{q}g} = \frac{\hat{\alpha}_s}{4\pi} S_\varepsilon \left(\frac{Q^2}{\mu^2}\right)^{\frac{1}{2}\varepsilon} \left\{ \frac{1}{2\varepsilon} P^0_{qg} + w^0_{qg} + \varepsilon\, \bar{w}^0_{qg} \right\}, \tag{4.2.9}$$

where S_ε is defined by

$$S_\varepsilon = \exp\left\{ \frac{\varepsilon}{2} \left[\gamma_E - \ln 4\pi \right] \right\}. \tag{4.2.10}$$

Here $\hat{\alpha}_s$ stands for the unrenormalised strong coupling constant. It is related to the renormalised running coupling constant $\alpha_s(R^2)$ in the following way

$$\frac{\hat{\alpha}_s}{4\pi} = \frac{\alpha_s(R^2)}{4\pi} \left(1 + \frac{\alpha_s(R^2)}{4\pi} \frac{2\beta_0}{\varepsilon} S_\varepsilon \left(\frac{R^2}{\mu^2}\right)^{\frac{1}{2}\varepsilon} + \mathcal{O}(\alpha_s^2(R^2)) \right). \tag{4.2.11}$$

The constant β_0 is the lowest order coefficient of the β-function, equal to

$$\beta_0 = \tfrac{11}{3}C_A - \tfrac{2}{3}n_f. \tag{4.2.12}$$

In the following we will denote $\alpha_s(R^2)$ by α_s and refer to R as the renormalisation scale. The residues of the collinear divergences are given by the Altarelli–Parisi splitting functions P^n_{ij} [19]. In lowest order they are

$$P^0_{qq} = 4C_F\Big[\,2\mathcal{D}_0(x) - 1 - x + \tfrac{3}{2}\delta(1-x)\,\Big], \tag{4.2.13}$$

$$P^0_{qg} = 8T_f\Big[\,(1-x)^2 + x^2\,\Big], \tag{4.2.14}$$

$$P^0_{gq} = 4C_F\frac{(1-x)^2+1}{x}, \tag{4.2.15}$$

$$P^0_{gg} = 8C_A\Big[\,\mathcal{D}_0(x) + x^{-1} - 2 + x - x^2 + \tfrac{11}{12}\delta(1-x)\,\Big] - \tfrac{4}{3}n_f\delta(1-x). \tag{4.2.16}$$

The definition of the distribution $\mathcal{D}_i(x)$ can be found in appendix 4B (eq. 4B.5). The $SU(N)$ Casimir operators are given by

$$C_A = N, \quad C_F = \frac{N^2-1}{2N}, \tag{4.2.17}$$

where N is the number of colours. The number of flavours is indicated by n_f and T_f $(=\frac{1}{2})$ is the normalisation corresponding to the fundamental representation. For completeness we have also presented P^0_{gq} and P^0_{gg} since they will be needed later on. The calculation of the non-pole terms in eqs. 4.2.8 and 4.2.9 yields the expressions

$$\frac{\alpha_s}{4\pi}w^0_{q\bar{q}} = \Delta^{(1)}_{q\bar{q}}(M^2 = Q^2), \tag{4.2.18}$$

$$\frac{\alpha_s}{4\pi}w^0_{qg} = \Delta^{(1)}_{qg}(M^2 = Q^2), \tag{4.2.19}$$

$$\begin{aligned}\bar{w}^0_{q\bar{q}} = {}& C_F\Big\{\,8\mathcal{D}_2(x) - 6\zeta(2)\mathcal{D}_0(x) + (1+x)\Big[-4\ln^2(1-x) + 3\zeta(2)\Big] \\ &+ \frac{1+x^2}{1-x}\Big[-4\ln x\ln(1-x) + \ln^2 x\Big] + 4(1-x) \\ &+ \delta(1-x)\Big[16 - \tfrac{21}{2}\zeta(2)\Big]\Big\},\end{aligned} \tag{4.2.20}$$

$$\begin{aligned}\bar{w}^0_{qg} = {}& T_f\Big\{\,\tfrac{1}{2}(1+2x^2-2x)\Big[\ln^2\Big(\frac{(1-x)^2}{x}\Big) - 3\zeta(2)\Big] \\ &+ \tfrac{1}{2}(1-7x^2+6x)\ln\Big(\frac{(1-x)^2}{x}\Big) - 3 + 7x^2 - 4x\Big\}.\end{aligned} \tag{4.2.21}$$

The functions $w^0_{q\bar{q}}$ and w^0_{qg} are equal to the DY correction terms $\Delta^{(1)}_{q\bar{q}}$ and $\Delta^{(1)}_{qg}$ (see eqs. 4B.2 and 4B.17, respectively) provided the latter are calculated in the $\overline{\text{MS}}$ mass factorisation scheme. The ε-parts $\bar{w}^0_{q\bar{q}}$ and $\bar{w}^0_{qg}$ are also given, as we will need them for the order α_s^2 calculations.

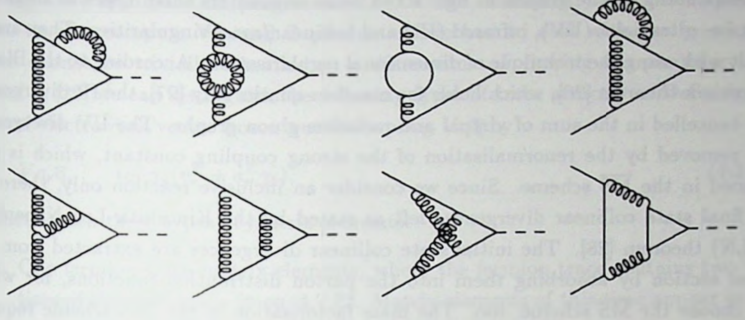

Fig. 4.4. The two loop corrections to the process $q + \bar{q} \to V$.

4.2.2 Second order corrections

In second order of α_s the set of possible parton–parton reactions is completed by the qq and gg subprocesses. This exhausts all possible combinations of i and j in W_{ij}. A part of them has already been presented in the literature. The first calculation was done for the qq process [20] (see figs. 4.8 and 4.9). Its results also hold for the $q\bar{q}$ scattering subprocess where a gluon is exchanged between the quark and the antiquark line. Thereafter, the soft and virtual gluon contributions from the $q\bar{q}$ process with two gluons or a quark pair in the final state were determined [21]–[24] (see figs. 4.4, 4.5, 4.6 and 4.7). Finally, we recently finished the computation of the gg subprocess [25] (see fig. 4.6). All calculations mentioned above have been performed in the DIS mass factorisation scheme. However, the results can easily be transformed to the $\overline{\rm MS}$ scheme. The latter procedure only requires the knowledge of the DY partonic cross sections, whereas in the DIS scheme one also has to calculate the deep inelastic partonic structure functions. In both schemes the following reactions were missing until now:

a. the hard gluon contribution to the $q\bar{q}$ subprocess (figs. 4.5, 4.6 and 4.7),

b. the order α_s correction to the qg subprocess (figs. 4.6 and 4.7) and

c. all possible interference terms between the various $q\bar{q} \to q\bar{q}V$ subprocesses (figs. 4.7, 4.8 and 4.9).

In order to complete the α_s^2 correction to the DY process we include these missing pieces, which is the main goal of this chapter. The calculation of the subprocesses listed in table 4.1 can be outlined as follows. While computing the cross sections corresponding to the graphs in figs. 4.1–4.9 one encounters three types of singularities, i.e. ultraviolet (UV), infrared (IR) and collinear/mass singularities. They are all dealt with using the technique of dimensional regularisation. According to the Bloch–Nordsieck theorem [26], which holds for massless quarks only [27], the IR divergences are cancelled in the sum of virtual and radiative gluon graphs. The UV divergences are removed by the renormalisation of the strong coupling constant, which is performed in the $\overline{\text{MS}}$ scheme. Since we consider an inclusive reaction only, there are no final state collinear divergences left as stated by the Kinoshita–Lee–Nauenberg (KLN) theorem [28]. The initial state collinear divergences are extracted from the cross section by absorbing them into the parton distribution functions, for which we choose the $\overline{\text{MS}}$ scheme, too. The mass factorisation in the DIS scheme requires the computation of the partonic deep inelastic structure functions for the Vq and Vg subprocesses. The calculation of these structure functions is of the same level of complexity as the one encountered in the DY process and will therefore not be considered here.

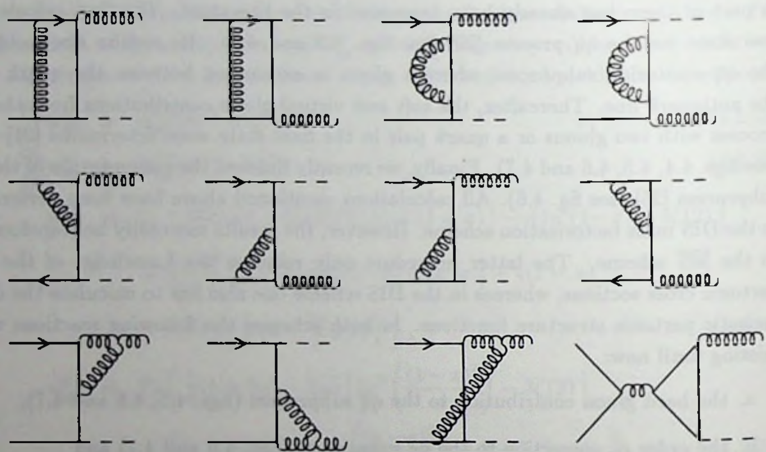

Fig. 4.5. The one loop corrections to the process $q+\overline{q} \to V+g$. The diagrams corresponding to the one loop correction to the subprocess $q(\overline{q})+g \to V+q(\overline{q})$ can be obtained via crossing.

The calculation of the squared amplitudes was performed in n dimensions using the algebraic manipulation programmes REDUCE[1], SCHOONSCHIP[2] and FORM[3]. Since we also compute W– and Z–production we had to deal with the γ_5–matrix, which cannot be trivially extended to n dimensions. Following the procedure discussed in [29] we can distinguish the following types of trace structures. Defining the general electroweak vector boson quark coupling $Vq\overline{q}$ by

$$Vq_r\overline{q}_s: \quad ig_V\gamma_\mu(v_r^V + a_r^V\gamma_5), \tag{4.2.22}$$

we distinguish three types of matrix elements:

1. One fermion trace matrix elements, where the fermion trace contains two vertices of the form given in eq. 4.2.22. Matrix elements of this type appear in the computation of the graphs in figs. 4.1–4.6 and in the interference terms $A\overline{C}$, $A\overline{D}$, $B\overline{C}$, $B\overline{D}$, $C\overline{E}$, $C\overline{F}$, $D\overline{E}$ and $D\overline{F}$ in figs. 4.7–4.9.

2. Two fermion trace matrix elements, where one of the traces contains both vertices of the form (4.2.22). They appear in the terms $A\overline{A}$, $B\overline{B}$, $C\overline{C}$, $D\overline{D}$, $E\overline{E}$ and $F\overline{F}$ in figs. 4.7–4.9.

3. Two fermion trace matrix elements, in which each trace contains one vertex of the type given above. Contributions of these type originate from the combinations $A\overline{B}$, $C\overline{D}$ and $E\overline{F}$ in figs. 4.7–4.9.

Traces of types 1 and 2 can be performed by anticommuting the γ_5 with all Dirac matrices γ_μ so that the matrix element is proportional to the one obtained for a virtual photon ($V = \gamma$) multiplied by ${v_r}^2 + {a_r}^2$. Traces of type 3 have to be dealt with more care. However, since the partonic structure functions $\mathcal{W}$ corresponding to the combinations mentioned in item 3 are manifestly collinearly finite the trace can be calculated in four dimensions. In this case the vector–vector ($v_r v_s$) and the axial–axial ($a_r a_s$) parts of the matrix element are in general not equal to each other.

After having computed the traces we have to integrate the matrix elements over all internal loop and final state momenta, which is the most difficult part of the calculation. In this chapter we take all partons to be massless. The case of massive

---

[1] A.C. Hearn, 'Reduce User's Manual', The Rand corporation, Santa Monica, CA, 1985.

[2] SCHOONSCHIP is an algebraic manipulation programme written by M. Veltman, see H. Strubbe, Comput. Phys. Comm. 8 (1974), 1.

[3] FORM (version 1.0) is a symbolic manipulation programme written by J.A.M. Vermaseren (NIKHEF-H, Amsterdam).

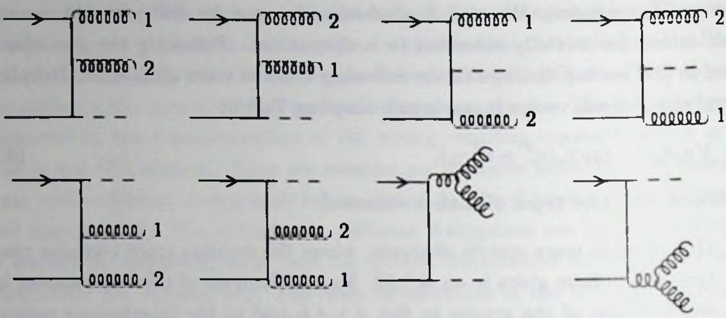

Fig. 4.6. Diagrams contributing to the subprocess $q + \overline{q} \rightarrow V + g + g$. The graphs corresponding to the subprocess $q(\overline{q})+g \rightarrow V+q(\overline{q})+g$ can be obtained from those presented in this figure via crossing. By crossing two pairs of lines one can obtain the diagrams corresponding to the subprocess $g+g \rightarrow V+q+\overline{q}$.

quarks (e.g. when heavy flavours are produced in the final state) will be discussed at the end section 4.2.3. Even if the partons are massless the integrals are very numerous and far from trivial. This in particular holds for the two loop integrals appearing in the quark form factor (fig. 4.4) and the three body phase space integrals showing up in the calculation of the graphs in figs. 4.6–4.9. Some of them even have to be expanded up to order ε^4.

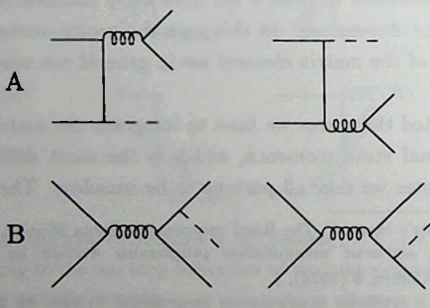

Fig. 4.7. Annihilation graphs contributing to the subprocess $q + \overline{q} \rightarrow V + q + \overline{q}$.

Starting with the two loop graphs in fig. 4.4 we had to evaluate 107 different types of scalar integrals [30]. Note that they are not linearly independent. The irreducible set contains 36 elements only and can be found in [31]. Apart from one misprint in the scalar integral corresponding to diagram 4C in the appendix of [31], we agree with their result. The final result for the quark form factor is presented in eq. 2.49 of [21] (see also appendix A of [23]). This result agrees with the one quoted in [18]. Finally, we would like to comment on the vertex graph in fig. 4.4 containing the triangle fermion loop. This graph only contributes in the case of Z–production with massive quarks in the loop. Notice that one always has to sum over all flavours in a quark family in order to cancel the anomaly arising from this type of graph.

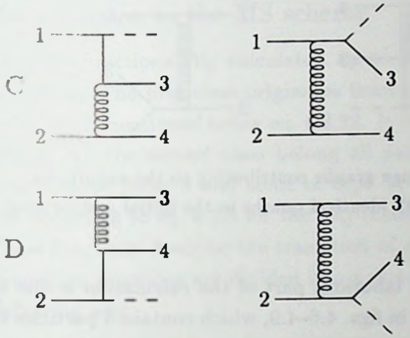

Fig. 4.8. Gluon exchange graphs contributing to the subprocesses $q+\overline{q} \to V + q + \overline{q}$ and $q + q \to V + q + q$.

The two body phase space integrals emerging from fig. 4.5 constitute the easiest part of the calculation. They can be expressed in the following way

$$\int dPS^{(2)}\, |\mathcal{M}|^2 = \frac{(16\pi)^{1-\frac{1}{2}n}}{\Gamma(\frac{1}{2}n-1)} \left(\frac{s-Q^2}{s}\right)^{n-3} s^{\frac{1}{2}n-2} \int_0^{\pi} d\theta\, (\sin\theta)^{n-3}\, |\mathcal{M}|^2, \qquad (4.2.23)$$

where s is the C.M. energy of the incoming partons and θ is the angle between one of the incoming partons and the outgoing one. The amplitude $|\mathcal{M}|^2$ contains all one loop integrals. The scalar loop integrals can be found in appendix F of [24]. It turned out that we had to evaluate 89 integrals of the kind in eq. 4.2.23, which however do not form an independent set. Distinguishing them in soft (singular at $s = Q^2$) and hard (regular at $s = Q^2$) gluon integrals we count 8 and 81, respectively. Again the graph containing the fermion loop in fig. 4.5 only contributes in the case of Z–production with a massive quark loop. Like for the two loop diagram of fig. 4.4 one has to sum over the members of a quark family in order to cancel the anomaly.

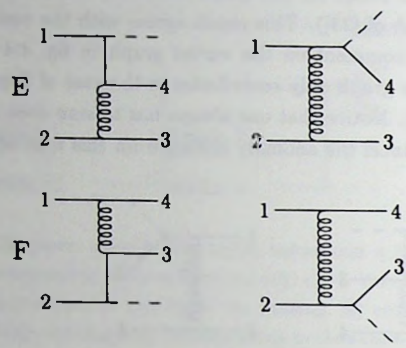

Fig. 4.9. Gluon exchange graphs contributing to the subprocess $q + q \to V + q + q$ with identical quarks in the initial and/or final state.

The most difficult and laborious part of the calculation is due to the purely radiative subprocesses given in figs. 4.6–4.9, which contain 3 particles in the final state. They involve the calculation of the three body phase space integrals of the form

$$\int dPS^{(3)} = \frac{1}{(4\pi)^n}\frac{s^{1-\frac{1}{2}n}}{\Gamma(n-3)}\int_0^\pi d\theta \int_0^\pi d\phi\,(\sin\theta)^{n-3}(\sin\phi)^{n-4}\int_{Q^2}^{s} ds_1 \times \int_{sQ^2/s_1}^{s+Q^2-s_1} ds_2\left[(s_1 s_2 - sQ^2)(s+Q^2-s_1-s_2)\right]^{\frac{1}{2}n-2}. \qquad (4.2.24)$$

This expression has been derived in the C.M. frame of the incoming partons, where s_i denotes the invariant mass of the vector boson combined with one of the final state partons i. In many cases it is more convenient to evaluate the three particle phase space integrals in other Lorentz frames, like the C.M. frame of the two outgoing partons [21, 23, 24, 32] or the C.M. frame of the vector boson and one of the outgoing partons [33]. In order to perform the angular integrations the matrix element $|\mathcal{M}|^2$ has to be decomposed in such a way that only two factors contain the angular variables θ and ϕ. The angular integrals are of the form

$$I_n^{(i,j)} = \int_0^\pi d\theta \int_0^\pi d\phi \frac{(\sin\theta)^{n-3}(\sin\phi)^{n-4}}{(a+b\cos\theta)^i(A+B\cos\theta+C\sin\theta\cos\phi)^j}, \qquad (4.2.25)$$

where a, b, A, B and C are functions of the kinematical invariants s, Q^2, s_1 and s_2. These integrals can be found in appendix C of [34]. For $n = 4+\varepsilon$ and either $a^2 \neq b^2$ or $A^2 \neq B^2 + C^2$ the expressions are very cumbersome, let alone when both $a^2 \neq b^2$ and $A^2 \neq B^2+C^2$. Fortunately the latter case can be avoided by choosing an appropriate frame. The partial fractioning of $|\mathcal{M}|^2$ leads to 217 three body phase space integrals each of them containing four integration variables. We did not bother to see how they could be reduced to a linearly independent set. Among these integrals only 10 were of the soft gluon type (singular at $s = Q^2$); they can be found in appendix G of [24]. Some other 3–body phase space integrals are listed in appendix A of [25].

4.2.3 Mass factorisation in the $\overline{\rm MS}$ scheme

The partonic structure functions $\mathcal{W}_{ij}$ calculated up to second order in α_s can be divided into two classes. The first class originates from the matrix elements corresponding to types 1 and 2 mentioned below eq. 4.2.22. It contains all $\mathcal{W}_{ij}$ which have collinear divergences. To the second class belong all partonic structure functions, which are collinearly finite (type 3 and some of type 1). In order to perform the mass factorisation according to eq. 4.2.5 for the $\mathcal{W}_{ij}$ (class I) we need the transition functions Γ_{ij}. These functions describe the transition of a parton j into a parton i. The qq and q$\overline{\rm q}$ transition functions are divided into a non–singlet (NS) and a singlet (S) part in the following way

$$\Gamma_{{\rm q}_r{\rm q}_s} = \delta_{rs}\,\Gamma^{\rm NS}_{\rm qq} + \Gamma^{\rm S}_{{\rm q}_r{\rm q}_s}, \tag{4.2.26}$$

$$\Gamma_{{\rm q}_r\bar{\rm q}_s} = \delta_{rs}\,\Gamma^{\rm NS}_{{\rm q}\bar{\rm q}} + \Gamma^{\rm S}_{{\rm q}_r\bar{\rm q}_s}, \tag{4.2.27}$$

where the indices r and s refer to the flavour of the (anti)quark. As the expressions for the transition functions do not explicitly depend on the flavours, we will suppress the flavour indices from now on. In the $\overline{\rm MS}$ mass factorisation scheme the Γ_{ij} can be expressed in terms of the Altarelli–Parisi splitting functions as follows

$$\begin{aligned}\Gamma^{\rm NS}_{\rm qq} &= \Gamma^{\rm NS}_{\bar{\rm q}\bar{\rm q}} = 1 + \frac{\hat{\alpha}_s}{4\pi}\left(\frac{M^2}{\mu^2}\right)^{\frac{1}{2}\varepsilon}\left[\,\frac{1}{\varepsilon}P^0_{\rm qq}\,\right] \\ &\quad + \left(\frac{\hat{\alpha}_s}{4\pi}\right)^2\left(\frac{M^2}{\mu^2}\right)^{\varepsilon}\left[\,\frac{1}{2\varepsilon^2}(P^0_{\rm qq}\otimes P^0_{\rm qq} - 2\beta_0 P^0_{\rm qq}) + \frac{1}{2\varepsilon}P^{1,{\rm NS}}_{\rm qq}\,\right],\end{aligned} \tag{4.2.28}$$

$$\Gamma^{\rm NS}_{{\rm q}\bar{\rm q}} = \Gamma^{\rm NS}_{\bar{\rm q}{\rm q}} = \left(\frac{\hat{\alpha}_s}{4\pi}\right)^2\left(\frac{M^2}{\mu^2}\right)^{\varepsilon}\left[\,\frac{1}{2\varepsilon}P^{1,-}_{\rm qq}\,\right], \tag{4.2.29}$$

$$\Gamma^{\rm S}_{\rm qq} = \Gamma^{\rm S}_{{\rm q}\bar{\rm q}} = \left(\frac{\hat{\alpha}_s}{4\pi}\right)^2\left(\frac{M^2}{\mu^2}\right)^{\varepsilon}\left[\,\frac{1}{4\varepsilon^2}P^0_{\rm qg}\otimes P^0_{\rm gq} + \frac{1}{4\varepsilon}P^{1,{\rm S}}_{\rm qq}\,\right], \tag{4.2.30}$$

$$\Gamma^{S}_{q\bar{q}} = \Gamma^{S}_{qq} = \left(\frac{\hat{\alpha}_s}{4\pi}\right)^2 \left(\frac{M^2}{\mu^2}\right)^{\epsilon} \Big[\frac{1}{4\varepsilon^2} P^0_{qg} \otimes P^0_{gq} + \frac{1}{4\varepsilon} P^{1,S}_{qq} \Big], \tag{4.2.31}$$

$$\Gamma_{qg} = \Gamma_{\bar{q}g} = \frac{\hat{\alpha}_s}{4\pi}\left(\frac{M^2}{\mu^2}\right)^{\frac{1}{2}\epsilon} \Big[\frac{1}{2\varepsilon} P^0_{qg} \Big] + \left(\frac{\hat{\alpha}_s}{4\pi}\right)^2 \left(\frac{M^2}{\mu^2}\right)^{\epsilon} \Big[\frac{1}{4\varepsilon^2} (P^0_{qg} \otimes P^0_{gg}$$

$$+ P^0_{qq} \otimes P^0_{qg} - 2\beta_0 P^0_{qg}) + \frac{1}{4\varepsilon} P^1_{qg} \Big], \tag{4.2.32}$$

$$\Gamma_{gq} = \Gamma_{g\bar{q}} = \left(\frac{\hat{\alpha}_s}{4\pi}\right) \left(\frac{M^2}{\mu^2}\right)^{\frac{1}{2}\epsilon} \Big[\frac{1}{\varepsilon} P^0_{gq} \Big], \tag{4.2.33}$$

$$\Gamma_{gg} = 1 + \left(\frac{\hat{\alpha}_s}{4\pi}\right) \left(\frac{M^2}{\mu^2}\right)^{\frac{1}{2}\epsilon} \Big[\frac{1}{\varepsilon} P^0_{gg} \Big], \tag{4.2.34}$$

where M is the mass factorisation scale. To obtain the above expressions in terms of the renormalised coupling constant $\alpha_s(R^2)$, one has to perform coupling constant renormalisation (see eq. 4.2.11). Notice that at $\mathcal{O}(\alpha_s^2)$ the transition functions Γ^{S}_{qq} and $\Gamma^{S}_{q\bar{q}}$ are equal, which is not necessarily true at higher orders. The convolution symbol $\otimes$ is defined by

$$(f \otimes g)(x) = \int_0^1 dx_1 \int_0^1 dx_2\, \delta(x - x_1 x_2) f(x_1) g(x_2). \tag{4.2.35}$$

The lowest order Altarelli–Parisi splitting functions have already been listed in eqs. (4.2.13)–(4.2.16) and the expression for β_0 can be found in eq. 4.2.12. In the next-to-leading order we need P^1_{qg} and the singlet (S) as well as the non-singlet (NS) part of P^1_{qq}. They can be obtained from eqs. 16 and 17 in [35] (see also [36]–[39]). Since we use a little different notation we will list them here below

$$P^{1,NS}_{qq} = n_f C_F \Big\{ \delta(1-x) \Big[-\tfrac{2}{3} - \tfrac{16}{3}\zeta(2) \Big] - \tfrac{80}{9}\mathcal{D}_0(x) - \tfrac{8}{3}\frac{1+x^2}{1-x}\ln x$$
$$- \tfrac{8}{9} + \tfrac{88}{9}x \Big\} + C_F^2 \Big\{ \delta(1-x) \Big[3 - 24\zeta(2) + 48\zeta(3) \Big]$$
$$- 16\frac{1+x^2}{1-x}\ln x \ln(1-x) - 4(1+x)\ln^2 x - 8(2x + 3(1-x)^{-1})\ln x$$
$$- 40(1-x) \Big\} + C_A C_F \Big\{ \delta(1-x) \Big[\tfrac{17}{3} + \tfrac{88}{3}\zeta(2) - 24\zeta(3) \Big]$$
$$+ (\tfrac{536}{9} - 16\zeta(2))\mathcal{D}_0(x) + 4\frac{1+x^2}{1-x}\ln^2 x + 8(1+x)\zeta(2)$$
$$- \tfrac{4}{3}(5 + 5x - 22(1-x)^{-1})\ln x + \tfrac{4}{9}(53 - 187x) \Big\}, \tag{4.2.36}$$

$$P^{1,S}_{qq} = 8 C_F T_f \Big\{ -2(1+x)\ln^2 x + (2 + 10x + \tfrac{16}{3}x^2)\ln x$$
$$+ \tfrac{40}{9}x^{-1} - 4 + 12x - \tfrac{112}{9}x^2 \Big\}, \tag{4.2.37}$$

$$P^{1,-}_{qq} = 8C_F(C_F - \tfrac{1}{2}C_A)\Big\{ \frac{1+x^2}{1+x}\Big[\ln^2 x - 4\ln x \ln(1+x) - 4\,\mathrm{Li}_2(-x) - 2\zeta(2)\Big]$$
$$+ 2(1+x)\ln x + 4(1-x)\Big\}, \tag{4.2.38}$$

$$P^1_{qg} = -8C_F T_f\Big\{ 2(1-2x+2x^2)\Big[2\ln x\ln(1-x) + 2\zeta(2) - \ln^2(1-x)\Big]$$
$$-(1-2x+4x^2)\ln^2 x - 8x(1-x)\ln(1-x) - (3-4x+8x^2)\ln x$$
$$-14+29x-20x^2\Big\} - 8C_A T_f\Big\{ -(1+2x+2x^2)\Big[\ln^2 x - 4\ln x\ln(1-x)$$
$$-4\,\mathrm{Li}_2(-x) - 2\zeta(2)\Big] + (1-2x+2x^2)\Big[2\ln^2(1-x) - 2\zeta(2)\Big]$$
$$+(3+6x+2x^2)\ln^2 x + 8x(1-x)\ln(1-x) - \tfrac{2}{3}(3+24x+44x^2)\ln x$$
$$-\tfrac{2}{9}(20x^{-1} - 18 + 225x - 218x^2)\Big\}. \tag{4.2.39}$$

The relation between the anomalous dimension of the composite operators denoted by $\gamma_{ij}^{(m)}$ and the splitting functions P_{ij} is given through a Mellin transformation

$$\gamma_{ij}^{k,(m)} = -\int_0^1 dx\, x^{m-1}\, P^k_{ij}(x). \tag{4.2.40}$$

In the literature the expressions $\gamma^{1,\mathrm{NS}}_{qq} + (-1)^m\gamma^{1,-}_{qq}$ stand for the non-singlet anomalous dimension. The singlet anomalous dimensions we need for our calculation are given by $\gamma^{1,\mathrm{NS}}_{qq} + (-1)^m\gamma^{1,-}_{qq} + \gamma^{1,\mathrm{S}}_{qq}$ and γ^1_{qg}, respectively. The reason that the splitting functions P^k_{qg} in eqs. 4.2.30–4.2.32 are multiplied by an extra factor $\frac{1}{2}$ can be attributed to the fact that the corresponding anomalous dimensions γ^k_{qg} receive contributions from the quark as well as the antiquark. The same applies to $P^{1,\mathrm{S}}_{qq}$ in eqs. 4.2.30 and 4.2.31. Notice that the splitting functions P^k_{gq} and P^k_{gg} are only needed up to first order in α_s since the vector boson V does not couple directly to the gluon.

For the mass factorisation of $\mathcal{W}_{ij}$ it is convenient to split $\mathcal{W}_{qq}$, $\mathcal{W}_{q\bar{q}}$, Δ_{qq} and $\Delta_{q\bar{q}}$ into non–singlet and singlet parts as has been done for the transition functions (see eqs. 4.2.26 and 4.2.27). Then the mass singular partonic structure functions can be classified as

1. $\mathcal{W}^{(2),\mathrm{NS}}_{q\bar{q}}$, which gets contributions from the graphs in figs. 4.4, 4.5, 4.6 and A$\overline{\text{A}}$, A$\overline{\text{C}}$ and A$\overline{\text{D}}$ in figs. 4.7 and 4.8.
2. $\mathcal{W}^{(2),\mathrm{S}}_{q\bar{q}}$. It receives contributions from C$\overline{\text{C}}$ and D$\overline{\text{D}}$ in fig. 4.8. Likewise $\mathcal{W}^{(2),\mathrm{S}}_{qq}$, which is determined by C$\overline{\text{C}}$, D$\overline{\text{D}}$, E$\overline{\text{E}}$ and F$\overline{\text{F}}$ in figs. 4.8 and 4.9.

3. $\mathcal{W}^{(2),\mathrm{NS}}_{\mathrm{qq}}$, which receives its contributions from $\mathrm{C\overline{E}}$ and $\mathrm{D\overline{F}}$ (see figs. 4.8 and 4.9).

4. $\mathcal{W}^{(2)}_{\mathrm{qg}}$. It gets contributions from the graphs in figs. 4.5 and 4.6.

5. $\mathcal{W}^{(2)}_{\mathrm{gg}}$, which receives contributions from the graphs in fig. 4.6.

Since the partonic structure functions $\mathcal{W}_{ij}$ satisfy the mass factorisation theorem, the unrenormalised and mass singular expressions can be written as follows (where S_ε is defined in eq. 4.2.10)

$$\mathcal{W}^{(2),\mathrm{NS}}_{\mathrm{q\bar q}} = \Gamma^{\mathrm{NS}}_{\mathrm{qq}}\Gamma^{\mathrm{NS}}_{\mathrm{\bar q\bar q}}\Delta^{\mathrm{NS}}_{\mathrm{q\bar q}} = \left(\frac{\hat\alpha_s}{4\pi}\right)^2 S_\varepsilon^2\left(\frac{Q^2}{\mu^2}\right)^\varepsilon\left\{\frac{1}{\varepsilon^2}\left[2P^0_{\mathrm{qq}}\otimes P^0_{\mathrm{qq}} - 2\beta_0 P^0_{\mathrm{qq}}\right]\right. \quad (4.2.41)$$

$$\left. +\frac{1}{\varepsilon}\left[P^{1,\mathrm{NS}}_{\mathrm{qq}} + 2P^0_{\mathrm{qq}}\otimes w^0_{\mathrm{q\bar q}} - 2\beta_0 w^0_{\mathrm{q\bar q}}\right] + 2P^0_{\mathrm{qq}}\otimes \bar w^0_{\mathrm{q\bar q}} - 2\beta_0\bar w^0_{\mathrm{q\bar q}} + w^{1,\mathrm{NS}}_{\mathrm{q\bar q}}\right\},$$

$$\mathcal{W}^{(2),\mathrm{S}}_{\mathrm{q\bar q}} = \mathcal{W}^{(2),\mathrm{S}}_{\mathrm{qq}}$$

$$= \Gamma^{\mathrm{NS}}_{\mathrm{qq}}\Gamma^{\mathrm{NS}}_{\mathrm{\bar q\bar q}}\Delta^{\mathrm{S}}_{\mathrm{q\bar q}} + \Gamma^{\mathrm{NS}}_{\mathrm{qq}}\Gamma^{\mathrm{S}}_{\mathrm{\bar q q}}\Delta^{\mathrm{NS}}_{\mathrm{q\bar q}} + \Gamma^{\mathrm{S}}_{\mathrm{qq}}\Gamma^{\mathrm{NS}}_{\mathrm{\bar q\bar q}}\Delta^{\mathrm{NS}}_{\mathrm{q\bar q}} + \Gamma_{\mathrm{gq}}\Gamma^{\mathrm{NS}}_{\mathrm{\bar q\bar q}}\Delta_{\mathrm{qg}} + \Gamma_{\mathrm{g\bar q}}\Gamma^{\mathrm{NS}}_{\mathrm{qq}}\Delta_{\mathrm{qg}}$$

$$= \left(\frac{\hat\alpha_s}{4\pi}\right)^2 S_\varepsilon^2\left(\frac{Q^2}{\mu^2}\right)^\varepsilon\left\{\frac{1}{2\varepsilon^2}P^0_{\mathrm{qg}}\otimes P^0_{\mathrm{gq}} + \frac{1}{\varepsilon}\left[\frac{1}{2}P^{1,\mathrm{S}}_{\mathrm{qq}} + 2P^0_{\mathrm{gq}}\otimes w^0_{\mathrm{qg}}\right]\right.$$

$$\left. + 2P^0_{\mathrm{gq}}\otimes\bar w^0_{\mathrm{qg}} + w^{1,\mathrm{S}}_{\mathrm{q\bar q}}\right\}, \quad (4.2.42)$$

$$\mathcal{W}^{(2),\mathrm{NS}}_{\mathrm{qq}} = \Gamma^{\mathrm{NS}}_{\mathrm{qq}}\Gamma^{\mathrm{NS}}_{\mathrm{qq}}\Delta^{\mathrm{NS}}_{\mathrm{qq}} + \Gamma^{\mathrm{NS}}_{\mathrm{qq}}\Gamma_{\mathrm{\bar q q}}\Delta^{\mathrm{NS}}_{\mathrm{q\bar q}} + \Gamma_{\mathrm{\bar q q}}\Gamma^{\mathrm{NS}}_{\mathrm{qq}}\Delta^{\mathrm{NS}}_{\mathrm{\bar q q}}$$

$$= \left(\frac{\hat\alpha_s}{4\pi}\right)^2 S_\varepsilon^2\left(\frac{Q^2}{\mu^2}\right)^\varepsilon\left\{\frac{1}{\varepsilon}P^{1,-}_{\mathrm{qq}} + w^{1,\mathrm{NS}}_{\mathrm{qq}}\right\}, \quad (4.2.43)$$

$$\mathcal{W}^{(2)}_{\mathrm{qg}} = \Gamma^{\mathrm{NS}}_{\mathrm{qq}}\Gamma_{\mathrm{\bar q g}}\Delta^{\mathrm{NS}}_{\mathrm{q\bar q}} + \Gamma^{\mathrm{NS}}_{\mathrm{qq}}\Gamma_{\mathrm{gg}}\Delta_{\mathrm{qg}}$$

$$= \left(\frac{\hat\alpha_s}{4\pi}\right)^2 S_\varepsilon^2\left(\frac{Q^2}{\mu^2}\right)^\varepsilon\left\{\frac{1}{\varepsilon^2}\left[\frac{3}{4}P^0_{\mathrm{qq}}\otimes P^0_{\mathrm{qg}} + \frac{1}{4}P^0_{\mathrm{gg}}\otimes P^0_{\mathrm{qg}} - \frac{1}{2}\beta_0 P^0_{\mathrm{qg}}\right]\right.$$

$$+ \frac{1}{\varepsilon}\left[\frac{1}{4}P^1_{\mathrm{qg}} - 2\beta_0 w^0_{\mathrm{qg}} + \frac{1}{2}P^0_{\mathrm{qg}}\otimes w^0_{\mathrm{q\bar q}} + (P^0_{\mathrm{qq}} + P^0_{\mathrm{gg}})\otimes w^0_{\mathrm{qg}}\right]$$

$$\left. - 2\beta_0\bar w^0_{\mathrm{qg}} + \frac{1}{2}P^0_{\mathrm{qg}}\otimes\bar w^0_{\mathrm{q\bar q}} + (P^0_{\mathrm{qq}} + P^0_{\mathrm{gg}})\otimes\bar w^0_{\mathrm{qg}} + w^1_{\mathrm{qg}}\right\}, \quad (4.2.44)$$

$$\mathcal{W}^{(2)}_{\mathrm{gg}} = 2\Gamma_{\mathrm{qg}}\Gamma_{\mathrm{\bar q g}}\Delta^{\mathrm{NS}}_{\mathrm{q\bar q}} + 2\Gamma_{\mathrm{qg}}\Gamma_{\mathrm{gg}}\Delta_{\mathrm{qg}} + 2\Gamma_{\mathrm{\bar q g}}\Gamma_{\mathrm{gg}}\Delta_{\mathrm{\bar q g}} + \Gamma_{\mathrm{gg}}\Gamma_{\mathrm{gg}}\Delta_{\mathrm{gg}}$$

$$= \left(\frac{\hat\alpha_s}{4\pi}\right)^2 S_\varepsilon^2\left(\frac{Q^2}{\mu^2}\right)^\varepsilon\left\{\frac{1}{2\varepsilon^2}P^0_{\mathrm{qg}}\otimes P^0_{\mathrm{qg}} + \frac{2}{\varepsilon}P^0_{\mathrm{qg}}\otimes w^0_{\mathrm{qg}}\right.$$

$$\left. + 2P^0_{\mathrm{qg}}\otimes\bar w^0_{\mathrm{qg}} + w^1_{\mathrm{gg}}\right\}. \quad (4.2.45)$$

In the above equations $\hat{\alpha}_s$ is the unrenormalised strong coupling constant, which has to be renormalised using the relation in eq. 4.2.11. The UV divergences are due to the loop diagrams appearing in the calculation of $\mathcal{W}_{q\bar{q}}^{(2),NS}$ and $\mathcal{W}_{qg}^{(2)}$. Notice that the gg subprocess can be made finite by using the lowest order splitting function P_{qg}^0 only. The various non–pole terms w_{ij}^1 are equal to

$$\left(\frac{\alpha_s}{4\pi}\right)^2 w_{q\bar{q}}^{1,NS} = \Delta_{q\bar{q}}^{(2)}(M^2 = Q^2, R^2 = Q^2), \tag{4.2.46}$$

$$\left(\frac{\alpha_s}{4\pi}\right)^2 w_{q\bar{q}}^{1,S} = 2\Delta_{q\bar{q},C\bar{C}}^{(2)}(M^2 = Q^2), \tag{4.2.47}$$

$$\left(\frac{\alpha_s}{4\pi}\right)^2 w_{qq}^{1,NS} = 2\Delta_{qq,C\bar{E}}^{(2)}(M^2 = Q^2), \tag{4.2.48}$$

$$\left(\frac{\alpha_s}{4\pi}\right)^2 w_{qg}^{1} = \Delta_{qg}^{(2)}(M^2 = Q^2, R^2 = Q^2), \tag{4.2.49}$$

$$\left(\frac{\alpha_s}{4\pi}\right)^2 w_{gg}^{1} = \Delta_{gg}^{(2)}(M^2 = Q^2). \tag{4.2.50}$$

The expressions for the DY correction terms $\Delta_{ij}^{(2)}$, calculated in the $\overline{\rm MS}$ scheme, can be found in appendix 4B (see eqs. 4B.7, 4B.21, 4B.24, 4B.18 and 4B.28, respectively).

The remaining contributions to $\mathcal{W}_{ij}$ (class II), which are not collinearly divergent, do not need mass factorisation. They originate from the combinations of the graphs $B\bar{B}$, $B\bar{C}$, $B\bar{D}$, $C\bar{D}$, $C\bar{F}$, $D\bar{E}$ and $E\bar{F}$ in figs. 4.7–4.9. In the case of Z–production also the combination $A\bar{B}$ contributes. It vanishes if one sums over all flavours in one family unless the final state quarks are massive. This situation is akin to the virtual graphs in figs. 4.4 and 4.5 except that here no anomaly term appears. The class II partonic structure functions $\mathcal{W}_{ij}$ are equal to the DY correction terms Δ_{ij} (see appendix 4B), which implies that they are scheme independent at least up to order α_s^2.

Summarising the content of this section we conclude that the calculation of the order α_s^2 correction to the inclusive DY cross section has been completed now in the $\overline{\rm MS}$ scheme. As already has been mentioned in the previous section there is another popular scheme to present the correction terms to various QCD processes, i.e. the DIS scheme. In our case this requires the calculation of the deep inelastic partonic structure functions $\mathcal{F}_q^{(2)}$ and $\mathcal{F}_g^{(2)}$, which is as laborious as the calculation of the DY structure functions $\mathcal{W}_{ij}$. A part of this work has already been published in the literature. The soft plus virtual gluon part of $\mathcal{F}_q^{(2)}$ is given in [23]. The part of $\mathcal{F}_q^{(2)}$ due to the DIS counterparts of the diagrams A in fig. 4.7 can be found in [24]. Ten years ago the contribution to $\mathcal{F}_q^{(2)}$ corresponding to the graphs obtained by crossing the diagrams in figs. 4.8 and 4.9 were calculated in [20]. Left over are the hard gluon part of $\mathcal{F}_q^{(2)}$ coming from the diagrams found by crossing the vector boson and a quark in figs. 4.5 and 4.6 and the full order α_s^2 contribution to $\mathcal{F}_g^{(2)}$. The graphs for the latter can be found by appropriate crossings in figs. 4.5 and 4.6. Their calculation will be presented in the near future. In principle we also need the three loop contribution to the anomalous dimensions γ_{ij} in eq. 4.2.40. The coefficients of the perturbative expansion in the running coupling constant $\alpha_s(Q^2)$ of the renormalisation group improved Wilson coefficient are only scheme independent if Δ_{ij}^k as well as γ_{ij}^{k+1} are known (see [36, 40]).

Finally, we want to comment on heavy flavour production in the DY process. In this chapter we assume all heavy flavours to be massless. This in particular is a crude assumption for top quark production. A part of this problem is investigated in [41] where the contributions due to triangle graphs of figs. 4.4 and 4.5 have been calculated in the case of heavy quarks. The calculation reveals a correction of 0.025% for $q\overline{q} \to Zg$ and 0.005% for $qg \to Zq$ at CERN collider energies coming from the last graph of fig. 4.5. The contribution of the two loop triangle graph in fig. 4.4 is larger and amounts to 0.73% at most. These corrections become even smaller at larger energies. They never exceed the contributions coming from the smallest subprocess calculated above (qq scattering) and can therefore be completely neglected. Still missing are the production mechanisms $q + \overline{q} \to Q + \overline{Q} + V$ due to graphs A and B in fig. 4.7 and $g + g \to Q + \overline{Q} + V$ in fig. 4.6. Their contributions will have to be calculated, but we expect that they are small.

4.3 Total cross sections for W– and Z–production

4.3.1 Introduction

In this section we will show results for vector boson production and compare them with the most recent data from the UA2 and CDF experiments. The total inclusive cross section is given by (see eq. 4.2.2)

$$\sigma_{\rm total}(S) = \int dQ^2\, \tau\, \sigma_V(Q^2, M_V{}^2)\, W_V(\tau, Q^2). \tag{4.3.1}$$

The pointlike cross section $\sigma_V(Q^2, M_V{}^2)$ for $V = \gamma$, Z, W is explicitly given in eqs. 4A.1–4A.3. The hadronic structure function $W_V(\tau, Q^2)$ can be obtained from eq. 4.2.3 by combining the various combinations of the parton distribution functions indicated by PD_{ij}^V with the DY correction terms Δ_{ij} discussed in the previous section. The explicit expression can be found in eq. 4A.21. For our subsequent discussions it is convenient to rewrite W_V in the following way

$$W_V(\tau, Q^2) = \sum_{i,j} \int_\tau^1 \frac{dx}{x} \Phi_{ij}(x, M^2)\, \Delta_{ij}(\frac{\tau}{x}, Q^2, M^2), \tag{4.3.2}$$

where Φ_{ij} denotes the parton flux, which is defined by

$$\Phi_{ij}(x, M^2) = \int_x^1 \frac{dy}{y} PD_{ij}^V(y, \frac{x}{y}, M^2). \tag{4.3.3}$$

At high energies the total cross section is dominated by W– and Z–production. Since the widths of these vector bosons are small compared to their masses, the integral in eq. 4.3.1 can be performed using the narrow width approximation. The integration becomes trivial and its result for σ_{total} is given by the expressions in eqs. 4A.10 and 4A.11.

We will now present the DY cross section and its K–factor for both $p\bar{p}$ and pp collisions at the current and future high energy colliders. The C.M. energies under consideration are $\sqrt{S} = 0.63$ TeV ($Sp\bar{p}S$), $\sqrt{S} = 1.8$ TeV (Tevatron), $\sqrt{S} = 16$ TeV (LHC) and $\sqrt{S} = 40$ TeV (SSC). For the electroweak parameters we take the following values : $M_Z = 91$ GeV, $M_W = 80$ GeV, $G_F = 1.166 \cdot 10^{-5}$ GeV^{-2} (Fermi constant), $\sin^2\theta_W = 0.227$ and $\sin^2\theta_C = 0.05$. Further we assume the top quark to be heavier than the W. For the running coupling constant, determined in the $\overline{\text{MS}}$ scheme, we adopt the expression in eq. 10 of [42], which is corrected up to two loops with the heavy flavour thresholds included. The number of flavours n_f is chosen to be five and the QCD scale parameter Λ is given below. Since the DY correction terms are calculated in the $\overline{\text{MS}}$ scheme we need the parton distribution functions in the same scheme. Here we have taken the HMRS parametrisations [43, 44], which are indicated by HMRSE$_+$, HMRSE, HMRSE$_-$ ($\Lambda = 100$ MeV) and HMRSB ($\Lambda = 190$ MeV). Furthermore, to make a comparison of the various independent parametrisation sets we also used the parton distribution functions given in tables I2 and I4 of [45], which we will refer to as MTE ($\Lambda = 155$ MeV) and MTB ($\Lambda = 194$ MeV), respectively. Unless stated otherwise, all results are obtained using the HMRSB parametrisation. The renormalisation scale R is always taken to be equal to the mass factorisation scale M (see the comment above eq. 4.2.4), for which we have chosen the canonical value $\sqrt{Q^2}$. Since the total cross section is calculated in the narrow width approximation this implies that $M = M_V$ (vector boson mass). The dependence of the cross section on the chosen mass factorisation scale will be discussed at the end of this section. All numerical results in this chapter are produced by our Fortran programme ZWPROD.

For the discussion of the various contributions to the Drell–Yan correction term it is convenient to introduce the K–factor. In this chapter the theoretical K–factor is defined as follows

$$K_{th} = \sum_{n=0}^{\infty} K^{(n)}, \tag{4.3.4}$$

where $K^{(n)}$ is the $\mathcal{O}(\alpha_s^n)$ contribution to the K-factor, which is given by

$$K^{(n)} = \frac{W^{(n)}(\tau, Q^2)}{W^{(0)}(\tau, Q^2)} = \frac{\sigma^{(n)}}{\sigma^{(0)}}. \tag{4.3.5}$$

The functions $W^{(n)}(\tau, Q^2)$ and $\sigma^{(n)}$ are the $\mathcal{O}(\alpha_s^n)$ correction to the hadronic structure function $W_V(\tau, Q^2)$ and cross section, respectively. They originate from the $\mathcal{O}(\alpha_s^n)$ contribution to Δ_{ij} in eq. 4.2.4. The order α_s^i corrected K-factor is defined by

$$K_i = \sum_{n=0}^{i} K^{(n)} = \frac{\sigma_i}{\sigma_0}, \tag{4.3.6}$$

where σ_i is the $\mathcal{O}(\alpha_s^i)$ corrected DY cross section and σ_0 the Born contribution.

In the discussion of the results we will try to answer the following questions:

1. How large is the $\mathcal{O}(\alpha_s^2)$ contribution to the K-factor ($K^{(2)}$) compared with the $\mathcal{O}(\alpha_s)$ one ($K^{(1)}$)?

2. What is the relative contribution of the four different subprocesses $q\bar{q}$, qg, qq and gg to the $\mathcal{O}(\alpha_s^2)$ part of the DY cross section?

3. How does the cross section depend on the various parametrisations chosen for the parton distribution functions?

4. How does the cross section depend on the different choices made for the factorisation scale M and the renormalisation scale R?

The same type of questions can also be raised in the case of other processes, like heavy flavour production [34, 46, 47], direct photon production [48] or jet production [49]. Note that the answers to the first question and to a lesser extent to the second and third one very heavily depend on the chosen renormalisation and mass factorisation schemes (we use the $\overline{\text{MS}}$ scheme) and the scales R and M. A change of schemes at a fixed value for M and R alters the coefficients in the perturbation series of the Wilson coefficient. The same happens if in a given scheme M or R is varied. This leads to an increase or decrease of the higher order corrections with respect to the lower order ones. It also entails a redistribution of the contributions, coming from the various production mechanisms, to the Wilson coefficient. Therefore, an investigation of the problems 1, 2 and 3 only makes sense if the schemes and scales are specified. In this chapter we have chosen the $\overline{\text{MS}}$ scheme and have taken $R = M = M_V$, unless mentioned otherwise.

4.3.2 The α_s^2 contributions to the K–factor

Starting with W–production at $p\overline{p}$ colliders we show in fig. 4.10 the $\mathcal{O}(\alpha_s)$ and $\mathcal{O}(\alpha_s^2)$ corrections to the DY K–factor for 0.5 TeV $< \sqrt{S} <$ 50 TeV. Here the K–factor originates from eqs. 4.3.5 and 4.3.6 where the total cross section stands for the sum of production of W^+ and W^-. The figure reveals that the $\mathcal{O}(\alpha_s^2)$ contribution to the K–factor, i.e. $K^{(2)}$, gets negative for $\sqrt{S} >$ 2.7 TeV, which implies $K_2 < K_1$ for high energies. Moreover, $K^{(2)}$ is much smaller than $K^{(1)}$ so that the first order corrected cross section σ_1 is hardly modified over the whole energy range. The same phenomenon is also observed for pp collisions where $K^{(2)} < 0$ for $\sqrt{S} >$ 2.0 TeV (see fig. 4.10). The same behaviour of the K–factor is also observed when other

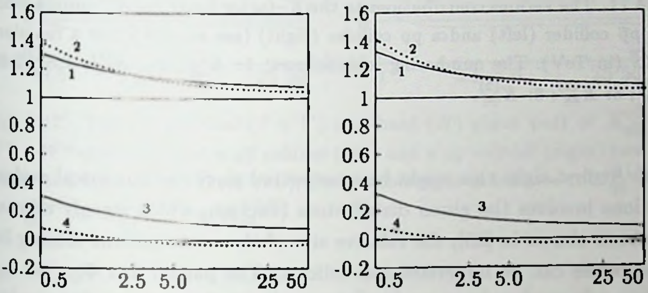

Fig. 4.10. The K–factor for $W^+ + W^-$–production at a $p\overline{p}$ collider (left) and a pp collider (right) (see eqs. 4.3.5 and 4.3.6), plotted as a function of $\sqrt{S}$ (in TeV). The numbering is as follows: 1: K_1; 2: K_2; 3: $K^{(1)}$; 4: $K^{(2)}$.

parametrisations of the parton distribution functions are used, like HMRSE, MTE or MTB. The property that $K^{(2)}$ gets negative at very large energies can be wholly attributed to the qg subprocess. Notice that the latter leads to a negative correction over the whole energy range, hence, the positive contribution of the $q\overline{q}$ subprocess is always compensated (see fig. 4.11). Remember that the $\mathcal{O}(\alpha_s)$ part of the qg subprocess is negative too, but in this case its absolute value is always smaller than the one computed for the $q\overline{q}$ reaction at the same order of α_s.

The separate contributions to the K–factor coming from the four subprocesses are shown in fig. 4.11. From this figure we infer that the K–factor is dominated by the $q\overline{q}$ and qg subprocesses. A striking result of our calculations is the small contribution of gg fusion to the K–factor, in particular when we compare it to the

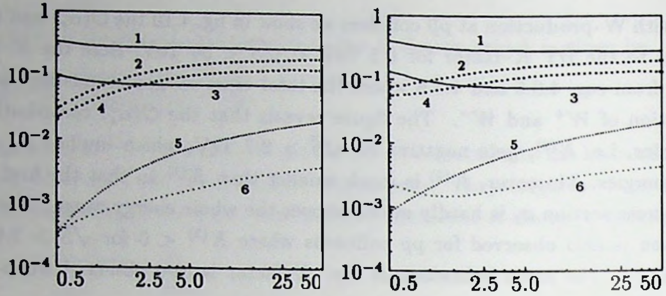

Fig. 4.11. The various contributions to the K–factor for $W^+ + W^-$-production at a $p\bar{p}$ collider (left) and a pp collider (right) (see eq. 4.3.5), as a function of $\sqrt{S}$ (in TeV). The numbering is as follows: 1: $K^{(1)}_{q\bar{q}}$; 2: $-K^{(1)}_{qg}$; 3: $K^{(2)}_{q\bar{q}}$; 4: $-K^{(2)}_{qg}$; 5: $K^{(2)}_{gg}$; 6: $K^{(2)}_{qq}$.

qg process. At first sight this might be unexpected since the numerical evaluation of both reactions involves the gluon distribution function, which steeply rises at small x. As has been shown in [25], the relative size of the contributions coming from the four subprocesses can be understood as follows. The parton flux Φ_{ij} (see eq. 4.3.3) steeply rises as $x \to 0$, whereas it sharply decreases for $x \to 1$. This implies that $x \sim \tau$ is the relevant integration region in eq. 4.3.2. Therefore, the cross section will heavily depend on the behaviour of $\Delta_{ij}(\tau/x, Q^2, M^2)$ near $x = \tau$. The functional form of $\Delta_{ij}(x, Q^2, M^2)$ near $x = 1$ for the various subprocesses is given in appendix 4B.6. Qualitatively they behave like (see eqs. 4B.29–4B.46)

$$\Delta_{q\bar{q}} \overset{x \to 1}{\simeq} a_i \mathcal{D}_i(x) + b_i \ln^i(1-x) + c\,\delta(1-x) + d, \tag{4.3.7}$$

$$\Delta_{qg} \overset{x \to 1}{\simeq} a_i \ln^i(1-x) + b, \tag{4.3.8}$$

$$\Delta_{qq} \overset{x \to 1}{\simeq} (1-x)^a \ln^2(1-x), \quad (a > 0), \tag{4.3.9}$$

$$\Delta_{gg} \overset{x \to 1}{\simeq} (1-x)^b \ln^2(1-x), \quad (b > 0). \tag{4.3.10}$$

The vanishing of the last two correction terms near $x = 1$ is caused by the absence of gluons in the final state. In that case the three body phase space integrals do not contribute at the boundary of phase space. Now one can understand why the contributions from qq and gg are small compared to those from $q\bar{q}$ and qg. The Drell–Yan correction term Δ_{gg} tends to suppress the fast rise of the gg flux, whereas Δ_{qg} enhances the behaviour of the qg flux. However, notice that the suppression of the DY correction term near $x = 1$ is more and more compensated at higher energies, due to the faster growth of the gg flux relative to the other fluxes, as can be seen in fig. 4.11.

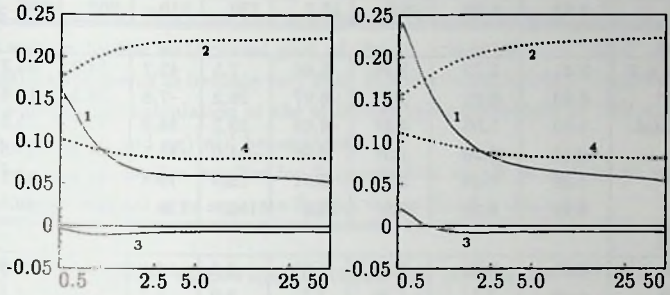

Fig. 4.12. The soft+virtual $(S+V)$ and hard (H) gluon part of $K^{(i)}_{q\bar{q}}$ for $W^+ + W^-$–production at a p$\bar{\rm p}$ collider (left) and a pp collider (right) (see eq. 4.3.5), as a function of $\sqrt{S}$ (in TeV). The numbering is as follows: 1: $K^{(1),S+V}_{q\bar{q}}$; 2: $K^{(1),H}_{q\bar{q}}$; 3: $K^{(2),S+V}_{q\bar{q}}$; 4: $K^{(2),H}_{q\bar{q}}$.

We also want to comment on the contributions coming from the distributions $\mathcal{D}_i(x)$ and $\delta(1-x)$ in eq. 4.3.7. The coefficients of these functions can be determined by a soft gluon approximation, which means that only the contributions coming from soft and virtual gluons are taken into account. As is known from the literature, in the DIS scheme (with $M = R = M_V$) the dominant part of the K–factor can be attributed to the soft/virtual piece of the Drell–Yan correction terms (see table 4.2). However, in the $\overline{\rm MS}$ scheme (also with $M = R = M_V$) this is no longer true. This can be seen in fig. 4.12, where we have split the contribution to $K^{(i)}_{q\bar{q},{\rm NS}}$ into a soft/virtual ($K^{(i),S+V}_{q\bar{q}}$) and a hard ($K^{(i),H}_{q\bar{q}}$) part, as described in appendix 4B (see below eq. 4B.7). From this figure we infer that in $\overline{\rm MS}$ the hard part is much larger than the soft/virtual piece. Moreover, in the DIS scheme the main contribution to $K^{(i),S+V}_{q\bar{q}}$ can be traced back to the $\delta(1-x)$ function. In the $\overline{\rm MS}$ scheme, however, the $\mathcal{D}_i(x)$ dominate the $S+V$–part. The above discussion implies that the exponentiation of the soft/virtual gluon contribution only makes sense in the DIS scheme. These observations illustrate very nicely that the answer to the question, which reaction or production mechanism is dominant, depends very much on the chosen schemes and scales.

As a further illustration of this fact we have made a comparison between the $\overline{\rm MS}$

W$^+$ + W$^-$-production (nb)								
	$Sp\overline{p}S$		Tevatron		LHC		SSC	
	$\overline{\text{MS}}$	DIS	$\overline{\text{MS}}$	DIS	$\overline{\text{MS}}$	DIS	$\overline{\text{MS}}$	DIS
Born								
$q\overline{q}$	4.93	4.90	16.0	15.7	120.	119.	262.	260.
$\mathcal{O}(\alpha_s)$								
$q\overline{q}$, $S+V$	0.61	1.79	1.16	5.66	7.5	42.7	14.8	93.3
$q\overline{q}$, H	0.93	-0.21	3.41	-0.97	26.2	-7.8	58.3	-17.8
$q\overline{q}$, total	1.54	1.58	4.57	4.69	33.7	34.9	73.1	75.5
qg	-0.18	-0.10	-1.57	-0.98	-21.0	-15.5	-48.3	-37.8
$\sigma^{(1)}$	1.36	1.48	3.00	3.71	12.7	19.4	24.8	37.7
σ_1	6.29	6.38	19.0	19.4	132.	138.	287.	298.
$\mathcal{O}(\alpha_s^2)$								
$q\overline{q}$, $S+V$	-0.05	0.59	-0.12	1.87	-0.8	14.1	-1.8	30.8
$q\overline{q}$, H	0.49	?.?	1.35	?.?	9.9	?.?	21.5	?.?
$q\overline{q}$, total	0.44	?.?	1.23	?.?	9.1	?.?	19.7	?.?
qg	-0.13	?.?	-1.06	?.?	-14.9	?.?	-33.5	?.?
gg	0.0022	0.0006	0.043	0.020	1.5	1.1	4.4	3.6
$qq+\overline{q}\overline{q}$	0.0021	0.0013	0.016	0.025	0.4	1.0	1.0	2.6
$\sigma^{(2)}$	0.31	?.?	0.23	?.?	-3.9	?.?	-8.4	?.?

Table 4.2. Comparison of $\overline{\text{MS}}$ and DIS scheme results at $Sp\overline{p}S$, Tevatron, LHC and SSC. In both sets of results we used the MTB parton densities parametrisations.

and DIS scheme results in table 4.2. For the DIS parton distribution function we have chosen the one given in table I3 of [45] ($\Lambda = 194$ MeV), which is the DIS scheme counterpart of MTB. Notice that the Born cross section for $\overline{\text{MS}}$ is always slightly larger than the one obtained in the DIS scheme. Although the $\mathcal{O}(\alpha_s)$ contributions to the soft/virtual and hard gluon parts depend heavily on the chosen scheme, the total $q\overline{q}$ result is hardly affected by this choice. For the $\mathcal{O}(\alpha_s)$ qg subprocess this dependence is stronger and we find that the $\overline{\text{MS}}$ result is always more negative than the one obtained for DIS. Contrary to the Born cross section we find that the $\mathcal{O}(\alpha_s)$ corrected cross section in DIS is slightly larger than in $\overline{\text{MS}}$. From table 4.2 we infer that the difference is about 5%. In the DIS scheme the second order contribution to the K-factor from the hard gluon part of the $q\overline{q}$ subprocess is only partially known and no $\mathcal{O}(\alpha_s^2)$ result exists for the qg process. Therefore, we have put in table

4.2 a question mark in the entries corresponding to these subprocesses. At second order we find that the numerical results for those DY correction terms, which are known for both the DIS and the $\overline{\text{MS}}$ scheme, depend considerably on the chosen mass factorisation procedure. Furthermore, assuming that the scheme dependence of $\sigma^{(2)}$ is comparable to that of $\sigma^{(1)}$, we find that in the DIS scheme only for the $Sp\overline{p}S$ ($\sqrt{S} = 0.63$ TeV) one can approximate the second order contribution to the cross section by the soft/virtual part of the $q\overline{q}$ subprocess. At higher energies this approximation seems to become very bad. In order to make a full comparison between both schemes the calculation of the still missing contributions in DIS (i.e. the hard gluon part of $q\overline{q}$ and qg) will be necessary.

The same discussion applies for Z–production at $p\overline{p}$ as well as at pp colliders, therefore we will not give separate figures nor tables for this case.

4.3.3 The effects of parton distribution parametrisations

The size of the various contributions to the DY cross section depends very heavily on the specific set of parton distribution functions. These functions are mainly extracted from the data in deep inelastic lepton hadron scattering, which have been taken for $x \geq 0.01$. However, vector boson production at future high energy colliders require the knowledge of the parton densities at $x \sim M_V/\sqrt{S}$. For LHC and SSC this implies $x \sim 6 \cdot 10^{-3}$ and $x \sim 3 \cdot 10^{-3}$, respectively. A recent analysis [50] has shown that W– and Z–production at these future colliders even probes sea quarks at $x \sim 10 {M_V}^2/S$, which is about $5 \cdot 10^{-5}$ for SSC. Therefore, one has to extrapolate these densities to x–regions, which were not accessible to the deep inelastic experiments carried out up to now. In the future this situation will probably improve, when the HERA machine is put into operation. Moreover, there is some theoretical uncertainty how to parametrise the gluon distribution function at $Q^2 = Q_0^2$. One often assumes that $xG(x, Q_0^2) \to$ constant, for $x \to 0$. However, there are some theoretical reasons to believe that a more correct behaviour for small x would be $xG(x, Q_0^2) \to 1/\sqrt{x}$ [51]. Notice that such a change of the parametrisation of the gluon at Q_0^2 will also strongly influence the small x behaviour of the sea quarks at higher Q^2, because the sea quarks are coupled to the gluons through the Altarelli–Parisi evolution equations. This implies that at high energies considerable differences in the size of the DY cross section can be expected, even at the Born level, if one changes the $x \to 0$ behaviour of the gluon at Q_0^2. To incorporate this kind of uncertainties in our predictions for the W– and Z–production rates we have taken a wide range of different parametrisations. The HMRSE and HMRSB parametrisations [43] correspond with a $xG(x, Q_0^2) \to$ constant behaviour for $x \to 0$. The HMRSE$_+$ and HMRSE$_-$ behave like $\sqrt{x}$ and $1/\sqrt{x}$ for $x \to 0$ and are referred to as the valence-like and singular gluon distribution functions in [50]. For the parametrisation of the gluon densities in the case of MTE and MTB one even has included a logarithmic dependence on x, viz. $xG(x, Q_0^2) \to x^\alpha(-\ln x)^\beta$ for $x \to 0$, with α and β some negative exponents (see tables I2 and I4 of [45]).

	HMRSE$_+$	HMRSE	HMRSE$_-$	HMRSB	MTE	MTB
$\alpha_s(M_W)$	0.107	0.107	0.107	0.117	0.114	0.118
	$Sp\bar{p}S$ ($\sqrt{S} = 0.63$ TeV)					
Born	5.51	5.31	5.20	5.03	4.84	4.93
$\mathcal{O}(\alpha_s)$	6.81	6.60	6.48	6.41	6.13	6.29
$\mathcal{O}(\alpha_s^2)$	7.06	6.86	6.74	6.72	6.41	6.61
	Tevatron ($\sqrt{S} = 1.8$ TeV)					
Born	14.7	15.1	14.7	15.8	15.5	16.0
$\mathcal{O}(\alpha_s)$	17.0	17.6	17.1	18.7	18.3	19.0
$\mathcal{O}(\alpha_s^2)$	17.1	17.7	17.3	18.9	18.5	19.2
	LHC ($\sqrt{S} = 16$ TeV)					
Born	49.3	75.8	112.	104.	114.	120.
$\mathcal{O}(\alpha_s)$	53.7	81.9	122.	114.	128.	132.
$\mathcal{O}(\alpha_s^2)$	52.7	79.5	118.	110.	126.	129.
	SSC ($\sqrt{S} = 40$ TeV)					
Born	85.1	151.	303.	225.	257.	262.
$\mathcal{O}(\alpha_s)$	91.7	161.	324.	244.	288.	287.
$\mathcal{O}(\alpha_s^2)$	90.6	157.	313.	236.	284.	278.

Table 4.3. The total cross section for W-production at $Sp\bar{p}S$, Tevatron, LHC and SSC.

The total cross sections for W-production are displayed in table 4.3 for $\sqrt{S} = 0.63$ TeV ($Sp\bar{p}S$), $\sqrt{S} = 1.8$ TeV (Tevatron), $\sqrt{S} = 16$ TeV (LHC) and $\sqrt{S} = 40$ TeV (SSC). From this table we infer that the $\mathcal{O}(\alpha_s^2)$ correction is much smaller than the $\mathcal{O}(\alpha_s)$ one. Moreover, the cross sections obtained with the different parton densities differ from each other by at least the same order of magnitude as the second order correction. Although at $Sp\bar{p}S$ and Tevatron the results for the various parton distributions do not differ very much, these discrepancies do not allow to discern clearly the $\mathcal{O}(\alpha_s^2)$ corrections. This situation becomes worse at LHC and SSC, where it even might become difficult to identify the first order corrections. For these colliders this is mainly due to the uncertainties present in the small x behaviour of the parton distribution functions. Unless these uncertainties are reduced, it will not be possible

	HMRSE+	HMRSE	HMRSE−	HMRSB	MTE	MTB
$\alpha_s(M_Z)$	0.105	0.105	0.105	0.115	0.112	0.115
	$Sp\bar{p}S$ ($\sqrt{S}$ = 0.63 TeV)					
Born	1.66	1.61	1.58	1.54	1.60	1.55
$\mathcal{O}(\alpha_s)$	2.06	2.00	1.97	1.96	2.02	1.98
$\mathcal{O}(\alpha_s^2)$	2.14	2.08	2.06	2.06	2.12	2.09
	Tevatron ($\sqrt{S}$ = 1.8 TeV)					
Born	4.62	4.66	4.52	4.79	4.74	4.86
$\mathcal{O}(\alpha_s)$	5.38	5.45	5.30	5.69	5.64	5.81
$\mathcal{O}(\alpha_s^2)$	5.44	5.51	5.37	5.78	5.74	5.92
	LHC ($\sqrt{S}$ = 16 TeV)					
Born	15.8	23.5	33.1	31.7	34.6	36.2
$\mathcal{O}(\alpha_s)$	17.2	25.4	35.8	34.9	38.9	40.1
$\mathcal{O}(\alpha_s^2)$	16.9	24.8	34.9	33.9	38.5	39.1
	SSC ($\sqrt{S}$ = 40 TeV)					
Born	27.5	47.4	89.5	69.8	79.2	80.7
$\mathcal{O}(\alpha_s)$	29.6	50.6	95.9	75.7	88.7	88.2
$\mathcal{O}(\alpha_s^2)$	29.3	49.4	93.1	73.6	87.9	86.0

Table 4.4. The total cross section for Z-production at $Sp\bar{p}S$, Tevatron, LHC and SSC.

to learn much about QCD corrections at the future colliders by studying W– and Z–production. In table 4.4 we have listed our results for Z-production. Roughly the same comments apply here as for W-production. However, note the slightly improved possibility to see $\mathcal{O}(\alpha_s^2)$ corrections in the case of Z–production at $\sqrt{S}$ = 0.63 TeV. The reason for this improvement can be attributed to the dominant contribution of the valence $u\bar{u}$ channel in Z–production, whereas the W cross section is mainly determined by the valence $u\bar{d}$ and $\bar{u}d$ subprocesses. It seems that the mutual agreement of the various parton densities for the valence u quark is better than for the valence d quark. Summarising the above we can state that the uncertainty in the cross sections can be estimated to be about 10% for $Sp\bar{p}S$ and Tevatron and 150% and 250% for LHC and SSC, respectively.

To get a better impression of the size of the corrections we give in table 4.5 the first and second order K–factors for W– and Z–production. Notice that for the K–factor a large part of the uncertainty due to the various parametrisations of the parton densities drops out. In this case the main reason for the discrepancies can be traced back to the different values for α_s. Only at very high energies the K–factors

		HMRSE$_+$	HMRSE	HMRSE$_-$	HMRSB	MTE	MTB
$\alpha_s(M_V)$		0.107(5)	0.107(5)	0.107(5)	0.117(5)	0.114(2)	0.118(5)
$Sp\bar{p}S$	K_1	1.24	1.24(5)	1.25	1.27(8)	1.27	1.28
	K_2	1.28(9)	1.29(30)	1.30	1.34	1.32	1.34(5)
Tevatron	K_1	1.16(7)	1.16(7)	1.16(7)	1.18(9)	1.18(9)	1.19(20)
	K_2	1.17(8)	1.17(8)	1.17(9)	1.19(21)	1.20(1)	1.20(2)
LHC	K_1	1.09	1.08	1.08	1.10	1.13	1.11
	K_2	1.07	1.05	1.05	1.06(7)	1.11	1.07(8)
SSC	K_1	1.08	1.07	1.07	1.08	1.12	1.09
	K_2	1.07	1.04	1.03(4)	1.05	1.11	1.06(7)

Table 4.5. K-factors for W-production at $Sp\bar{p}S$, Tevatron, LHC and SSC. The numbers between brackets denote how the K-factors are altered in the case of Z-production. They replace the last 1 or 2 digits.

start depending on the specific choice of the parton distribution function, mainly through the variation of the size of the qg contribution. Therefore, while studying radiative corrections it is better to look at the K-factor than at the cross section. From this table one can also observe that the K-factors are roughly the same for W- and Z-production. This implies that the ratio

$$R = \frac{\sigma_W}{\sigma_Z} \frac{B(W \to \ell\nu_\ell)}{B(Z \to \ell^+\ell^-)} \tag{4.3.11}$$

is hardly affected by QCD corrections.

For $\sqrt{S} = 0.63$ TeV and 1.8 TeV (CERN and FNAL) we compare our predictions with the measurements by the UA1 [52], UA2 [53] and CDF [54, 55] collaborations (see tables 4.6, 4.7 and 4.8). In particular we are interested in the decay channels $W \to \ell\nu_\ell$ and $Z \to \ell^+\ell^-$ for $\ell = e$ or $\ell = \mu$. In this case we have to multiply the total cross sections in tables 4.3 and 4.4 by the branching ratios $B(W \to \ell\nu_\ell)$ and $B(Z \to \ell^+\ell^-)$, respectively. Starting with the CERN collider we find that the central values of the UA1 results for W- and Z-production [52], which were obtained in the muon channel only, are well below our second order predictions. However, due to the large statistical and systematic errors all our approximations are compatible with their data. In case of UA2 [53] we find that for Z-production the second order cross sections are in very good agreement with the experimental values, although the first order corrected ones can accommodate the data rather well, too. However, for W-production the theoretical predictions at $\mathcal{O}(\alpha_s^2)$ lie systematically above the UA2

	HMRSE+	HMRSE	HMRSE−	HMRSB	MTE	MTB
UA1	$\sigma_W\, B(W \to \ell\,\nu_\ell) = 609 \pm 41 \pm 94$ pb					
UA2	$\sigma_W\, B(W \to \ell\,\nu_\ell) = 660 \pm 15 \pm 37$ pb					
Born	600.	579.	567.	549.	528.	538.
$\mathcal{O}(\alpha_s)$	743.	720.	706.	699.	668.	686.
$\mathcal{O}(\alpha_s^2)$	770.	748.	735.	733.	699.	720.
UA1	$\sigma_Z\, B(Z \to \ell^+\,\ell^-) = 58.6 \pm 7.8 \pm 8.4$ pb					
UA2	$\sigma_Z\, B(Z \to \ell^+\,\ell^-) = 70.4 \pm 5.5 \pm 4.0$ pb					
Born	55.4	53.8	52.9	51.4	53.4	51.8
$\mathcal{O}(\alpha_s)$	68.9	67.0	66.1	65.8	67.8	66.4
$\mathcal{O}(\alpha_s^2)$	71.6	69.8	68.9	69.2	71.0	69.9

Table 4.6. The quantities $\sigma_W \cdot B$ and $\sigma_Z \cdot B$ for $Sp\overline{p}S$ [53] ($\sqrt{S} = 0.63$ TeV). We have used $B(W \to \ell\,\nu_\ell) = 0.109$ and $B(Z \to \ell^+\,\ell^-) = 3.35 \cdot 10^{-2}$. The values for $\alpha_s(M_V)$ can be found in tables 4.3 and 4.4.

	HMRSE+	HMRSE	HMRSE−	HMRSB	MTE	MTB
CDF	$\sigma_W\, B(W \to e\,\nu_e) = 2.06 \pm 0.04 \pm 0.34$ nb					
Born	1.60	1.65	1.61	1.73	1.69	1.74
$\mathcal{O}(\alpha_s)$	1.86	1.91	1.87	2.04	1.99	2.07
$\mathcal{O}(\alpha_s^2)$	1.87	1.93	1.88	2.06	2.02	2.10
CDF	$\sigma_Z\, B(Z \to e^+\,e^-) = 0.197 \pm 0.012 \pm 0.032$ nb					
Born	0.155	0.156	0.152	0.160	0.159	0.163
$\mathcal{O}(\alpha_s)$	0.180	0.182	0.178	0.191	0.189	0.195
$\mathcal{O}(\alpha_s^2)$	0.182	0.185	0.180	0.194	0.192	0.198

Table 4.7. The quantities $\sigma_W \cdot B$ and $\sigma_Z \cdot B$ for Tevatron [54] ($\sqrt{S} = 1.8$ TeV). We have used $B(W \to e\,\nu_e) = 0.109$ and $B(Z \to e^+\,e^-) = 3.35 \cdot 10^{-2}$. The values for $\alpha_s(M_V)$ can be found in tables 4.3 and 4.4.

data, but this discrepancy is not dramatical. For the Tevatron collider [54] the Born approximation as well as the higher order results agree with the data due to the large systematic errors in the CDF experiment.

For completeness we give in table 4.8 the values for the ratio R, defined in eq. 4.3.11. As mentioned above the QCD corrections do not change the value of R very much. The theoretical values of R for $Sp\overline{p}S$ tend to be larger than the result obtained

	HMRSE$_+$	HMRSE	HMRSE$_-$	HMRSB	MTE	MTB
UA1	$R = 10.4^{+1.8}_{-1.5} \pm 0.8$					
UA2	$R = 9.38^{+0.82}_{-0.72} \pm 0.25$					
Born	10.8	10.8	10.7	10.7	9.9	10.4
$\mathcal{O}(\alpha_s)$	10.8	10.7	10.7	10.6	9.9	10.3
$\mathcal{O}(\alpha_s^2)$	10.8	10.7	10.7	10.6	9.9	10.3
CDF	$R = 10.2 \pm 0.8 \pm 0.4$					
Born	10.4	10.6	10.6	10.8	10.6	10.7
$\mathcal{O}(\alpha_s)$	10.3	10.5	10.5	10.7	10.6	10.6
$\mathcal{O}(\alpha_s^2)$	10.3	10.4	10.5	10.6	10.5	10.6

Table 4.8. The ratio R (see eq. 4.3.11) for $Sp\bar{p}S$ [53] ($\sqrt{S} = 0.63$ TeV) and Tevatron [55] ($\sqrt{S} = 1.8$ TeV).

by UA2 [53]. This was to be expected, because our results for $\sigma_W \cdot B$ were also larger than the cross section found by the UA2 collaboration. The agreement is better with the UA1 value of R [52], but in this case the experimental errors in R are rather large. For Tevatron we find good agreement with the measurement by CDF [55]. In this case one can observe that by studying the ratio R instead of the separate W– and Z–production rates, as advocated in the literature, the uncertainty due to the choice of the parton distribution functions is reduced. However, this does not apply to the results given for CERN. In this case the spread in the values obtained for the ratio R and the cross sections are of the same order of magnitude.

Summarising the discussion above we conclude that the current experiments carried out at the $Sp\bar{p}S$ and Tevatron do not allow us to distinguish between $\mathcal{O}(\alpha_s)$ and $\mathcal{O}(\alpha_s^2)$ corrected cross sections. This is due to the large systematic errors in the existing data, the uncertainty in the parton distribution functions and the fact that the second order correction is smaller than has originally been expected from the result obtained by the $\mathcal{O}(\alpha_s)$ calculation. Unless the higher order corrections beyond the $\mathcal{O}(\alpha_s^2)$ turn out to be very large, the convergence of the perturbation series does not seem to be a problem for W– and Z–production at the current and future hadron colliders. Therefore, we are now able to give a firm prediction for the total cross section; the main limitations to our predictions are set by the uncertainty in the parton distribution functions.

4.3.4 The effects of the mass factorisation scale

Finally, we want to investigate the dependence of the DY cross section on the chosen mass factorisation scale M. In a previous paper [25] we studied the variations of the cross sections when the mass factorisation scale M is varied independently of the renormalisation scale R. This we will not do in this chapter as there is no distinction between these two scales in the current parton distribution functions. Moreover, the dependence of the cross section on M is much larger than on R, because the Born approximation does not depend on the coupling constant α_s. This is contrary to what one observes in pure hadronic cross sections, like heavy flavour production [34, 46, 47] or dijet production [49], where the Born cross sections do depend on α_s and therefore are much more sensitive to the choice of R. In principle physical (experimentally observable) quantities, like the hadronic structure function $W_V(\tau, Q^2)$ (eq. 4.2.3), should be scale independent. However, the theoretical result for $W_V(\tau, Q^2)$ does depend on the chosen scale. This can be attributed to the fact that the logarithmic terms of the type $\ln(Q^2/M^2)$ (see appendix 4B) in the Wilson coefficient $\Delta_{ij}(x, Q^2, M^2)$ are only calculated up to finite orders of α_s, whereas they are resummed in all orders for the parton densities using renormalisation group methods. This introduces the problem of choosing an appropriate scale. There are many discussions in the literature concerning the choice of the right scale. Some groups prefer PMS [3], whereas other physicists advocate FAC [4]. Another possibility is to vary the scale between some canonical values in order to give an estimate for the theoretical error. The best solution to the problem would be to show that the resulting expressions exhibit a very small variation under a wide range of scale choices. This might be achieved provided the QCD corrections can be computed beyond the leading order in α_s. The Drell–Yan and deep inelastic lepton–hadron cross sections are good candidates for satisfying this condition, since their Born cross sections are independent of α_s and the radiative corrections can be computed up to $\mathcal{O}(\alpha_s^2)$.

Using the HMRSB structure functions we have plotted the DY cross section for the production of W^+ plus W^- in the range 10 GeV $\leq M \leq$ 1000 GeV. Starting with the $Sp\overline{p}S$ ($\sqrt{S} = 0.63$ TeV, see fig. 4.13), we observe a considerable improvement in the scale independence of the cross section σ_W when it is computed in higher order in α_s. Note the maximum at $M = 40$ GeV in σ_2 (PMS point), which is not present in the lower order results σ_0 and σ_1. As has been mentioned before the difference between σ_1 and σ_2 depends on the chosen scale although it never becomes very large (< 0.6 nb). Finally, the difference $\max \sigma_2 - \min \sigma_2$ in the range $10 \leq M \leq 1000$ GeV is about 0.4 nb, which can be considered as a theoretical uncertainty of our

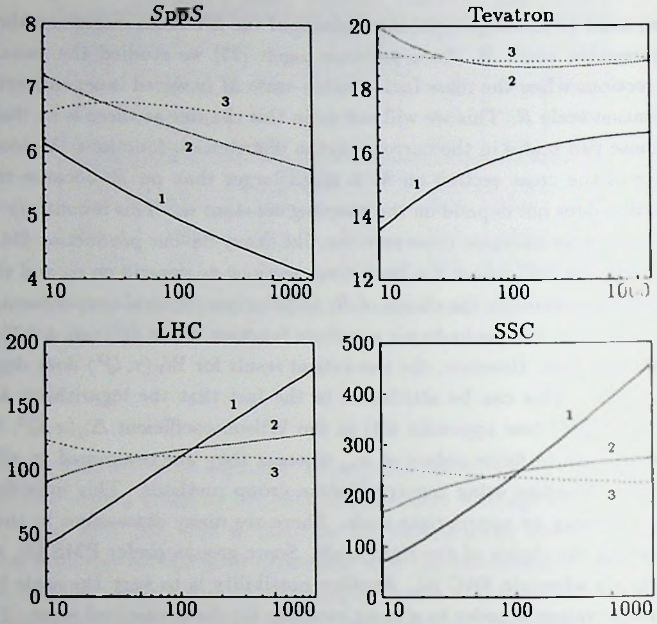

Fig. 4.13. Mass factorization scale (M) dependence of $\sigma_{W^+ + W^-}$ for $Sp\overline{p}S$ ($\sqrt{S} = 0.63$ TeV), Tevatron ($\sqrt{S} = 1.8$ TeV), LHC ($\sqrt{S} = 16$ TeV) and SSC ($\sqrt{S} = 40$ TeV). The total cross section (in nb) is plotted as a function of M (in GeV). The numbering is as follows: 1: Born; 2: $\mathcal{O}(\alpha_s)$; 3: $\mathcal{O}(\alpha_s^2)$.

calculation due to the uncertainty in the scale. The same features are also observed for W–production at the Tevatron ($\sqrt{S} = 1.8$ TeV , see fig. 4.13) although here the difference between the σ_1 and σ_2 is extremely small. The PMS point is at $M = 200$ GeV, where σ_2 exhibits a minimum and $\max \sigma_2 - \min \sigma_2 \sim 0.3$ nb. Notice that at both energies $\sigma_2 - \sigma_1$ becomes zero at a certain M, whereas $\sigma_i - \sigma_0 \neq 0$ $(i = 1, 2)$ over the whole range of scales.

When we study the DY process at higher energies, like $\sqrt{S} = 16$ TeV (LHC, fig. 4.13) or $\sqrt{S} = 40$ TeV (SSC, fig. 4.13), we find that some of the properties of the higher order α_s corrected cross sections change when compared to those obtained for $\sqrt{S} < 2$ TeV. First, we observe that the scale dependence is much stronger at these

		HMRSE+	HMRSE	HMRSE−	HMRSB	MTE	MTB
$Sp\overline{p}S$	S_0	0.31(6)	0.34(8)	0.35(8)	0.41(6)	0.38(42)	0.42(8)
	S_1	0.17(8)	0.18(9)	0.18(9)	0.23(4)	0.20(1)	0.23(5)
	S_2	0.03(4)	0.04	0.04	0.06	0.03(4)	0.06(7)
Tevatron	S_0	0.26(17)	0.22(14)	0.19(1)	0.19(1)	0.27(18)	0.17(09)
	S_1	0.04(6)	0.05(7)	0.05(7)	0.07(9)	0.07(4)	0.06(11)
	S_2	0.03	0.02(1)	0.02(1)	0.02(1)	0.12(0)	0.01(2)
LHC	S_0	1.44(37)	1.30(25)	1.08(4)	1.26(1)	1.27(2)	1.12(06)
	S_1	0.38(6)	0.32(0)	0.24(2)	0.34(1)	0.60(56)	0.27(3)
	S_2	0.16(3)	0.14(2)	0.08(9)	0.13	0.33(1)	0.15
SSC	S_0	1.77(2)	1.60(56)	1.24(2)	1.54(0)	1.53(49)	1.39(5)
	S_1	0.50(49)	0.42	0.28	0.45(4)	0.78(5)	0.38(6)
	S_2	0.17(1)	0.16(2)	0.10(09)	0.15(3)	0.43(1)	0.19(7)

Table 4.9. Scale dependence of the cross section for W–production at $Sp\overline{p}S$, Tevatron, LHC and SSC (see eq. 4.3.12). The numbers between brackets denote the scale dependences of Z–production. They replace the last 1 of 2 digits.

energies. Secondly, the extremum in σ_2 (PMS point) has disappeared, but now there is a value for M where either σ_1 or σ_2 becomes equal to σ_0 (FAC point). Notice that $\sigma_2 = \sigma_0$ near $M = 100$ GeV for LHC as well as SSC energies. The difference between the maximum and minimum value for σ_2 equals 15 nb at $\sqrt{S} = 16$ TeV and 35 nb at $\sqrt{S} = 40$ TeV. The same features discussed for W–production also show up for Z–production, therefore we will not present any figures in this case. In table 4.9 we give the variation of the cross section for the various parton distribution functions when the mass factorisation scale is chosen in the range 10 GeV $\leq M \leq$ 1000 GeV. This variation is expressed by the quantity S_i defined by

$$S_i = \frac{\max \sigma_i - \min \sigma_i}{\langle \sigma_i \rangle}. \tag{4.3.12}$$

where $\langle \sigma_i \rangle$ is the average value of σ_i. In this table one can observe that the scale dependence is roughly the same for all parton distribution functions, except for MTE. In the case of MTE we find at LHC and SSC that the inclusion of the higher order corrections does not improve the scale independence as much as in the case of the other parton densities. Also notice the rather large value of S_2 at Tevatron for MTE. From the values of S_2 one can conclude that the $\mathcal{O}(\alpha_s^2)$ corrected DY cross section depends much less on the scale than on the chosen set of parton distribution functions. Therefore, an important outcome of the $\mathcal{O}(\alpha_s^2)$ computation is that the dependence of the production rates on the scale choice is considerably reduced. The main theoretical uncertainty can now be attributed to the variations in the cross sections when different parametrisations of the parton distribution functions are used. This is especially clear for the future hadron colliders, the LHC and the SSC. At these colliders the parton distribution functions are probed at very small x–values, for which our knowledge of these distribution functions is not very good yet. In particular we want to mention once more the sizable, negative contribution of the qg subprocess to both the first and second order corrections. At very high energies this subprocess is particularly sensitive to the behaviour of the input gluon distribution function at small x–values.

4.3.5 Summary

Summarising the content of this chapter, we have presented the full $\mathcal{O}(\alpha_s^2)$ correction to the K–factor, which is calculated in the $\overline{\text{MS}}$ scheme. To this end the partonic structure functions $\mathcal{W}_{ij}$ (see eqs. 4.2.41–4.2.45) had to be calculated to the second order in α_s. One then encounters new collinear divergences, which have not appeared in any calculation performed until now. To remove these singularities by mass factorisation one needs for the first time the $\mathcal{O}(\alpha_s^2)$ corrected splitting functions calculated in [35, 36, 37, 38, 39]. The calculation reveals that the dominant parton subprocesses are given by the q$\overline{\text{q}}$ (nonsinglet) and qg reactions. This holds for the $\mathcal{O}(\alpha_s)$ as well as for the $\mathcal{O}(\alpha_s^2)$ correction provided the results are presented for $M = R = M_V$. Further the qg contribution to $K^{(1)}$ as well as to $K^{(2)}$ (the $\mathcal{O}(\alpha_s)$ and $\mathcal{O}(\alpha_s^2)$ corrections to the DY K–factor, respectively) is negative. For $K^{(2)}$ it even overwhelms the positive contribution due to the q$\overline{\text{q}}$ subprocess when $\sqrt{S} > 3$ TeV. For this reason the $\mathcal{O}(\alpha_s^2)$ part of the K–factor is much smaller than the $\mathcal{O}(\alpha_s)$ contribution, contrary to what we have observed in a previous paper [25], where the K–factor has been calculated in the DIS scheme. However, in the latter scheme the $\mathcal{O}(\alpha_s^2)$ corrections due to the qg subprocess and the hard gluon part of the q$\overline{\text{q}}$ reaction have not been included yet. Notice that all these comparisons only make sense when the renormalisation scale R and the factorisation scale M are specified. The factorisation scale dependence of the DY cross section has been investigated and we found a considerable improvement by including the $\mathcal{O}(\alpha_s^2)$ correction. Finally, we have seen that the DY cross section heavily depends on the chosen parametrisation for the parton distribution functions. A large part of this dependence can be attributed to our ignorance about their small x behaviour. The main theoretical uncertainties in our predictions are just due to this phenomenon. To complete the study of the DY process it is still necessary to compute the correction term in the DIS scheme in view of the parton densities given in that scheme. Moreover, one also has to investigate the effect of heavy flavour production (massive quarks in the final state). Both calculations will undoubtedly be presented in the near future.

Appendices

4A Basic formulae for the Drell–Yan process

In this appendix we will present the basic notations and some formulae needed for the calculation of the DY cross section. The pointlike cross sections $\sigma_V(Q^2, M_V{}^2)$ defined in eq. 4.2.2 are equal to

$$\sigma_\gamma(Q^2) = \frac{4\pi\alpha^2}{3Q^4}\frac{1}{N}, \tag{4A.1}$$

$$\sigma_Z(Q^2, M_Z{}^2) = \frac{\pi\alpha}{4M_Z\sin^2\theta_W\cos^2\theta_W}\frac{1}{N}\frac{\Gamma_{Z\to\ell\ell}}{(Q^2-M_Z{}^2)^2+M_Z{}^2\Gamma_Z{}^2} \tag{4A.2}$$

and

$$\sigma_W(Q^2, M_W{}^2) = \frac{\pi\alpha}{2M_W\sin^2\theta_W}\frac{1}{N}\frac{\Gamma_{W\to\ell\bar\nu_\ell}}{(Q^2-M_W{}^2)^2+M_W{}^2\Gamma_W{}^2}. \tag{4A.3}$$

For completeness we also give the formula for the γ–Z interference

$$\sigma_{\gamma Z} = \frac{\pi\alpha^2}{6}\frac{1-4\sin^2\theta_W}{\sin^2\theta_W\cos^2\theta_W}\frac{1}{N}\frac{1}{Q^2}\frac{(Q^2-M_Z{}^2)}{(Q^2-M_Z{}^2)^2+M_Z{}^2\Gamma_Z{}^2}. \tag{4A.4}$$

In these formulae Γ_Z and Γ_W denote the total width of the Z- and W-boson, respectively, (sum over all decay channels) and $N=3$. The partial widths due to the leptonic decay of the Z and W are given by

$$\Gamma_{Z\to\ell\ell} = \frac{\alpha M_Z\left(1+(1-4\sin^2\theta_W)^2\right)}{48\sin^2\theta_W\cos^2\theta_W} \tag{4A.5}$$

and

$$\Gamma_{W\to\ell\bar\nu_\ell} = \frac{\alpha M_W}{12\sin^2\theta_W}. \tag{4A.6}$$

In the case of W- and Z-production the total cross section can be obtained using the narrow width approximation in the integrand of eq. 4.3.1, i.e.

$$\frac{1}{(Q^2 - M_V{}^2)^2 + M_V{}^2\Gamma_V{}^2} \to \frac{\pi}{M_V\Gamma_V}\delta(Q^2 - M_V{}^2). \tag{4A.7}$$

We then find

$$\sigma_{V\to\ell_1\ell_2} = \sigma_V\, B(V \to \ell_1\ell_2), \tag{4A.8}$$

where $B(V \to \ell_1\ell_2)$ stands for the branching ratio

$$B(V \to \ell_1\ell_2) = \frac{\Gamma_{V\to\ell_1\ell_2}}{\Gamma_V}, \tag{4A.9}$$

and the total rates σ_V (sum over all leptonic and hadronic decay channels) are given by

$$\sigma_Z = \frac{\pi^2\alpha}{4\sin^2\theta_W\cos^2\theta_W}\frac{1}{N}\frac{1}{S}W_Z\left(\frac{M_Z{}^2}{S}, M_Z{}^2\right), \tag{4A.10}$$

$$\sigma_W = \frac{\pi^2\alpha}{2\sin^2\theta_W}\frac{1}{N}\frac{1}{S}W_W\left(\frac{M_W{}^2}{S}, M_W{}^2\right). \tag{4A.11}$$

Notice that all particles into which the vector bosons decay are taken to be massless. Since the electroweak radiative corrections to $\sin^2\theta_W$ are not negligible it is better to replace $\sin^2\theta_W$ appearing in the denominators of the above expressions by

$$\sin^2\theta_W = \frac{\sqrt{2}M_W{}^2}{\pi\alpha}G_F, \tag{4A.12}$$

where $G_F = 1.166 \cdot 10^{-5}\text{GeV}^{-2}$ (Fermi constant). In the numerators we have put $\sin^2\theta_W = 0.227$.

Combining the various parton densities denoted by PD_{ij}^V with the corresponding DY correction terms Δ_{ij} in eq. 4.2.3, we can construct a compact formula for $W_V(\tau, Q^2)$. Before giving its expression let us first fix the notations. The coefficients v_r^V and a_r^V in eq. 4A.21 are related to the vector and axial couplings of the vector boson V to the quarks (see eq. 4.2.22). For the up and down type quarks they are equal to

$$\begin{aligned}
&v_u^\gamma = \tfrac{2}{3}, && a_u^\gamma = 0,\\
&v_d^\gamma = -\tfrac{1}{3}, && a_d^\gamma = 0,\\
&v_u^Z = 1 - \tfrac{8}{3}\sin^2\theta_W, && a_u^Z = -1,\\
&v_d^Z = -1 + \tfrac{4}{3}\sin^2\theta_W, && a_d^Z = 1,\\
&v_u^W = v_d^W = \tfrac{1}{\sqrt{2}}, && a_u^W = a_d^W = -\tfrac{1}{\sqrt{2}}.
\end{aligned} \tag{4A.13}$$

For the antiquarks the values for v_r^V and a_r^V are the same as for the quarks. Further we introduce three $2n_f \times 2n_f$ matrices C^{ii}, C^{if} and C^{ff}. These matrices contain the information of the coupling of the respective quark flavours to the vector bosons. The indices i and f stand for initial and final; the combination in which they occur with the C indicate the orientation of the quark line to which the vector boson is coupled. For the γ and the Z they are defined by

$$C^{ii}(q_k, q_l) = C^{ff}(q_k, q_l) = \begin{cases} 1 & \text{if } q_k = \overline{q}_l \\ 0 & \text{else} \end{cases} \tag{4A.14}$$

and

$$C^{if}(q_k, q_l) = \begin{cases} 1 & \text{if } q_k = q_l \\ 0 & \text{else} \end{cases} . \tag{4A.15}$$

For the $W^\pm$ they are

$$C^{ii}(q_k, q_l) = \begin{cases} |V_{q_k q_l}|^2 & \text{if } e_{q_k} + e_{q_l} = \pm 1 \\ 0 & \text{else} \end{cases} , \tag{4A.16}$$

$$C^{if}(q_k, q_l) = \begin{cases} |V_{q_k q_l}|^2 & \text{if } e_{q_k} = \pm 1 + e_{q_l} \\ 0 & \text{else} \end{cases} \tag{4A.17}$$

and

$$C^{ff}(q_k, q_l) = \begin{cases} |V_{q_k q_l}|^2 & \text{if } e_{q_k} + e_{q_l} = \mp 1 \\ 0 & \text{else} \end{cases} , \tag{4A.18}$$

where q_k and q_l stand for the (anti)quarks and e_{q_k} is the charge of q_k. The symbol $V_{q_k q_l}$ denotes the Kobayashi–Maskawa KM matrix, which in our calculation is approximated by

$$V_{ud} = V_{cs} = \cos\theta_C, \tag{4A.19}$$

$$V_{us} = -V_{cd} = \sin\theta_C, \tag{4A.20}$$

with $\sin^2\theta_C = 0.05$. The remaining matrix elements are put equal to zero. Using the convention that e.g. $q_u = \overline{q}_{\overline{u}}$ = the up quark density, and $\overline{q}_u = q_{\overline{u}}$ = the anti–up quark density, the hadronic structure function can be written as

$$W_V(\tau, Q^2) = \int_0^1 dx_1 \int_0^1 dx_2 \int_0^1 dx\, \delta(\tau - x x_1 x_2)$$
$$\times \Big\{ \sum_{r,s \in Q, \overline{Q}} \Big[C^{ii}(q_r, \overline{q}_s)(v_r^2 + a_r^2)\Delta_{q\overline{q}}(x)$$

$$+ \delta_{rs} \sum_{k,l \in Q} C^{\rm ff}(q_k, \overline{q}_l)(v_k^2 + a_k^2)\Delta^{(2)}_{q\overline{q},\, B\overline{B}}(x)$$

$$+ \delta_{rs} \sum_{k \in Q,\overline{Q}} \left(C^{\rm if}(q_r, \overline{q}_k) + C^{\rm if}(\overline{q}_r, q_k)\right)(v_r^2 + a_r^2)\Delta^{(2)}_{q\overline{q},\, B\overline{C}}(x)$$

$$+ \delta_{rs} \sum_{k \in Q} C^{\rm ff}(q_k, \overline{q}_k)\left(v_r v_k \Delta^{(2),V}_{q\overline{q},\, A\overline{B}}(x) + a_r a_k \Delta^{(2),A}_{q\overline{q},\, A\overline{B}}(x)\right)\Big]\, q_r(x_1)\overline{q}_s(x_2)$$

$$+ \sum_{r,k \in Q,\overline{Q}} C^{\rm if}(q_r, q_k)(v_r^2 + a_r^2)\Delta_{qg}(x)\left(q_r(x_1)g(x_2) + q_r(x_2)g(x_1) \right)$$

$$+ \sum_{r,s \in Q,\overline{Q}} \Big[\sum_{k \in Q,\overline{Q}} \left(C^{\rm if}(q_r, q_k)(v_r^2 + a_r^2) + C^{\rm if}(q_s, q_k)(v_s^2 + a_s^2)\right)\Delta^{(2)}_{qq,\, C\overline{C}}(x)$$

$$+ C^{\rm if}(q_r, q_r)\left(v_r v_s \Delta^{(2),V}_{q_r q_s,\, C\overline{D}}(x) + a_r a_s \Delta^{(2),A}_{qq,\, C\overline{D}}(x)\right)\Big]\, q_r(x_1)q_s(x_2)$$

$$+ \sum_{r,s \in Q,\overline{Q}} \Big[\left(C^{\rm if}(q_r, q_s)(v_r^2 + a_r^2) + C^{\rm if}(q_s, q_r)(v_s^2 + a_s^2)\right)\Delta^{(2)}_{qq,\, C\overline{E}}(x)$$

$$+ \delta_{rs} \sum_{k \in Q,\overline{Q}} C^{\rm if}(q_r, q_k)(v_r^2 + a_r^2)\Delta^{(2)}_{qq,\, C\overline{F}}(x)\Big]\, q_r(x_1)q_s(x_2)$$

$$+ \sum_{k,l \in Q} C^{\rm ff}(q_k, \overline{q}_l)(v_k^2 + a_k^2)\Delta^{(2)}_{gg}(x)g(x_1)g(x_2) \Big\}, \qquad (4A.21)$$

where

$$\Delta_{q\overline{q}}(x) = \delta(1-x) + \Delta^{(1)}_{q\overline{q}}(x) + \Delta^{(2),\rm NS}_{q\overline{q}}(x), \qquad (4A.22)$$

$$\Delta_{qg}(x) = \Delta^{(1)}_{qg}(x) + \Delta^{(2)}_{qg}(x) \qquad (4A.23)$$

and the sets Q and $\overline{Q}$ are given by

$$Q = \{u, d, s, c\},$$
$$\overline{Q} = \left\{\overline{u}, \overline{d}, \overline{s}, \overline{c}\right\}. \qquad (4A.24)$$

Furthermore, the scale to be used in the parton distribution functions is the mass factorisation scale M. The DY correction terms Δ_{ij} can be found in appendix 4B. They are listed in the same order as they appear in eq. 4A.21. For the γ–Z interference the right combinations of the parton distributions can be found by taking the photon formula and making the following replacements

$$v_r^2 \longrightarrow v_r^{\gamma} v_r^{Z},$$
$$v_r v_s \longrightarrow \tfrac{1}{2}\left(v_r^{\gamma} v_s^{Z} + v_s^{\gamma} v_r^{Z} \right). \qquad (4A.25)$$

Finally, we want to comment on the treatment of the distributions $\mathcal{D}_i(x)$ when they appear in the convolution integral in eq. 4.3.2. In that case one should use the relation

$$\int_0^1 dx \int_0^1 d\xi\ \Phi(\xi, M^2)\mathcal{D}_i(x)\ \delta(\tau - x\xi) = \Phi(\tau, M^2)\frac{\ln^{i+1}(1-\tau)}{(1+i)}$$
$$+ \int_\tau^1 dx \left\{ \frac{1}{x}\Phi(\frac{\tau}{x}, M^2) - \Phi(\tau, M^2) \right\} \frac{\ln^i(1-x)}{1-x}. \qquad (4A.26)$$

Notice that the convolution integral does not depend on the IR cutoff δ.

4B Drell–Yan correction terms

In this appendix we will present the explicit expressions for the DY correction terms Δ_{ij}, the calculation of which is outlined in section 4.2. In order to make the presentation self-contained we also give the lowest order contributions, which were already calculated in the literature [8]–[13]. We distinguish the following contributions to Δ_{ij}:

1. quark–antiquark (non–singlet),
2. (anti)quark–gluon,
3. the quark–antiquark (singlet) and non–identical quark–quark,
4. the identical quark–quark and
5. gluon–gluon.

Before presenting the results of the above mentioned Drell–Yan correction terms, we want to make two remarks. Firstly, in the expressions below the scale in the running coupling constant α_s is always taken to be the renormalisation scale R. Secondly, for the interference terms, we use the convention that $\mathrm{A\overline{C}} = \mathrm{AC^\dagger} + \mathrm{CA^\dagger}$, etc.

4B.1 The quark–antiquark contributions (non–singlet)

The lowest order contribution originating from the Born graph in fig. 4.1 is given by

$$\Delta^{(0)}_{q\bar{q}} = \delta(1-x). \qquad (4B.1)$$

The $\mathcal{O}(\alpha_s)$ correction to the $q\bar{q}$ subprocess, which receives contributions from the graphs in figs. 4.2 and 4.3 has been calculated in the literature [8]–[13]. Choosing the $\overline{\mathrm{MS}}$ scheme the expression for $\Delta^{(1)}_{q\bar{q}}$ can be very easily obtained using dimensional regularisation [8, 12]. From the numerical as well as the theoretical point of view it is convenient to divide it into two pieces, viz.

$$\Delta_{q\bar{q}}^{(1)}(x) = \Delta_{q\bar{q}}^{(1),S+V}(x) + \Delta_{q\bar{q}}^{(1),H}(x), \tag{4B.2}$$

where the $S+V$–part can be obtained by doing the calculation in a soft gluon approximation ($x \to 1$), which means that one only takes the contributions from the soft and virtual gluons into account. To obtain the remaining piece, denoted by H, one has to perform an exact computation. The expressions for $\Delta_{q\bar{q}}^{(1),S+V}$ and $\Delta_{q\bar{q}}^{(1),H}$ are

$$\begin{aligned}\Delta_{q\bar{q}}^{(1),S+V} &= \frac{\alpha_s}{4\pi}C_F\Big\{ \delta(1-x)\Big[6\ln\left(\frac{Q^2}{M^2}\right) + 8\zeta(2) - 16\Big] \\ &\quad +8\mathcal{D}_0(x)\ln\left(\frac{Q^2}{M^2}\right) + 16\mathcal{D}_1(x)\Big\}\end{aligned} \tag{4B.3}$$

and

$$\Delta_{q\bar{q}}^{(1),H} = \frac{\alpha_s}{4\pi}C_F\Big\{-4(1+x)\ln\left(\frac{Q^2}{M^2}\right) - 8(1+x)\ln(1-x) - 4\frac{1+x^2}{1-x}\ln x\Big\}. \tag{4B.4}$$

The distribution $\mathcal{D}_i(x)$ is defined by

$$\mathcal{D}_i(x) = \delta(1-x)\frac{\ln^{i+1}\delta}{(i+1)} + \theta(1-\delta-x)\frac{\ln^i(1-x)}{1-x}. \tag{4B.5}$$

The parameter δ is introduced in order to distinguish between the soft (S) ($x \geq 1-\delta$) and hard (H) ($x \leq 1-\delta$) gluon regions in the phase space integrals, which have to be performed for the contributions from fig. 4.3. The $\ln\delta$ terms arise when the factor $(1-x)^{-1+\epsilon}$ appearing in these integrals is replaced by the distribution

$$(1-x)^{-1+\epsilon} \to \frac{1}{\varepsilon}\delta^\epsilon\delta(1-x) + (1-x)^{-1+\epsilon}\theta(1-x-\delta). \tag{4B.6}$$

In the literature the $\ln\delta$ terms are very often omitted and the distributions $\mathcal{D}_i(x)$ are then denoted by $\left(\ln^i(1-x)/(1-x)\right)_+$, see e.g. [8]. Note that the coefficient of $\delta(1-x)$ in eq. 4B.3 also receives contributions from the virtual gluon graph depicted in fig. 4.2.

The second order correction to the non-singlet part of $\Delta_{q\bar{q}}$ is determined by the diagrams in figs. 4.4–4.9 and the interference between the graphs in figs. 4.7 and 4.8. It can be split into two parts. The first piece is related through mass factorisation to the collinearly singular part of the partonic structure function $\mathcal{W}_{q\bar{q}}$ and will be denoted by

$$\begin{aligned}\Delta_{q\bar{q}}^{(2),NS} &= \Delta_{q\bar{q}}^{(2),S+V} + \Delta_{q\bar{q}}^{(2),C_A} + \Delta_{q\bar{q}}^{(2),C_F} + \Delta_{q\bar{q},A\bar{A}}^{(2)} + 2\Delta_{q\bar{q},A\bar{C}}^{(2)} \\ &\quad + \frac{\alpha_s}{4\pi}\beta_0\Delta_{q\bar{q}}^{(1)}\ln\left(\frac{R^2}{M^2}\right),\end{aligned} \tag{4B.7}$$

where β_0 represents the lowest order coefficient of the β–function (eq. 4.2.12) and $\Delta^{(1)}_{q\bar{q}}$ is given in eq. 4B.2. The symbols M and R stand for the mass factorisation and renormalisation scales, respectively. The appearance of the β_0–term in eq. 4B.7 is a remnant of the fact that the calculation of this part involves coupling constant renormalisation to remove the UV divergences.

The second piece consists of the DY correction terms $\Delta^{(2)}_{q\bar{q},B\bar{B}}$, $\Delta^{(2)}_{q\bar{q},B\bar{C}} = \Delta^{(2)}_{q\bar{q},B\bar{D}}$, $\Delta^{(2),V}_{q\bar{q},A\bar{B}}$ and $\Delta^{(2),A}_{q\bar{q},A\bar{B}}$ originating from those parts of the parton structure function $\mathcal{W}_{q\bar{q}}$, which are collinearly finite and therefore do not need mass factorisation.

First, we will discuss the contributions in eq. 4B.7. As in the case of the first order calculation a part of $\Delta^{(2),NS}_{q\bar{q}}$ can be obtained by a soft gluon approximation [23]. This piece we have again denoted by $S+V$. For the remaining Drell–Yan correction terms in eq. 4B.7 an exact calculation is necessary. The contributions to $\Delta^{(2),S+V}_{q\bar{q}}$ come from the two loop virtual graphs in fig. 4.4, the soft gluon radiative corrections due to figs. 4.5 and 4.6 and soft quark pair production due to diagrams A in fig. 4.7. The expression for this part is equal to

$$\begin{aligned}
\Delta^{(2),S+V}_{q\bar{q}} &= \left(\frac{\alpha_s}{4\pi}\right)^2 \delta(1-x)\Big\{ C_A C_F \Big[\Big[\tfrac{193}{3} - 24\zeta(3) \Big] \ln\left(\frac{Q^2}{M^2}\right) - 11\ln^2\left(\frac{Q^2}{M^2}\right) \\
&- \tfrac{12}{5}\zeta(2)^2 + \tfrac{592}{9}\zeta(2) + 28\zeta(3) - \tfrac{1535}{12} \Big] + C_F{}^2 \Big[\Big[18 - 32\zeta(2) \Big] \ln^2\left(\frac{Q^2}{M^2}\right) \\
&+ \Big[24\zeta(2) + 176\zeta(3) - 93 \Big] \ln\left(\frac{Q^2}{M^2}\right) + \tfrac{8}{5}\zeta(2)^2 - 70\zeta(2) - 60\zeta(3) + \tfrac{511}{4} \Big] \\
&+ n_f C_F \Big[2\ln^2\left(\frac{Q^2}{M^2}\right) - \tfrac{34}{3}\ln\left(\frac{Q^2}{M^2}\right) + 8\zeta(3) - \tfrac{112}{9}\zeta(2) + \tfrac{127}{6} \Big]\Big\} \\
&+ C_A C_F \Big[-\tfrac{44}{3}\mathcal{D}_0(x)\ln^2\left(\frac{Q^2}{M^2}\right) + \Big[(\tfrac{536}{9} - 16\zeta(2))\mathcal{D}_0(x) \\
&- \tfrac{176}{3}\mathcal{D}_1(x) \Big] \ln\left(\frac{Q^2}{M^2}\right) - \tfrac{176}{3}\mathcal{D}_2(x) + \Big[\tfrac{1072}{9} - 32\zeta(2) \Big]\mathcal{D}_1(x) + \Big[56\zeta(3) \\
&+ \tfrac{176}{3}\zeta(2) - \tfrac{1616}{27} \Big]\mathcal{D}_0(x) \Big] + C_F{}^2 \Big[\Big[64\mathcal{D}_1(x) + 48\mathcal{D}_0(x) \Big] \ln^2\left(\frac{Q^2}{M^2}\right) \\
&+ \Big[192\mathcal{D}_2(x) + 96\mathcal{D}_1(x) - (128 + 64\zeta(2))\mathcal{D}_0(x) \Big] \ln\left(\frac{Q^2}{M^2}\right) \\
&+ 128\mathcal{D}_3(x) - (128\zeta(2) + 256)\mathcal{D}_1(x) + 256\zeta(3)\mathcal{D}_0(x) \Big] \\
&+ n_f C_F \Big[\tfrac{8}{3}\mathcal{D}_0(x)\ln^2\left(\frac{Q^2}{M^2}\right) + \Big[\tfrac{32}{3}\mathcal{D}_1(x) - \tfrac{80}{9}\mathcal{D}_0(x) \Big] \ln\left(\frac{Q^2}{M^2}\right) \\
&+ \tfrac{32}{3}\mathcal{D}_2(x) - \tfrac{160}{9}\mathcal{D}_1(x) + (\tfrac{224}{27} - \tfrac{32}{3}\zeta(2))\mathcal{D}_0(x) \Big]. \qquad \text{(4B.8)}
\end{aligned}$$

The hard gluon contribution from figs. 4.5 and 4.6 are denoted by $\Delta_{q\bar{q}}^{(2),C_A}$ and $\Delta_{q\bar{q}}^{(2),C_F}$, where the superscripts C_A and C_F refer to the two colour structures. The expressions for these quantities are

$$\Delta_{q\bar{q}}^{(2),C_A} = \left(\frac{\alpha_s}{4\pi}\right)^2 C_A C_F \Big\{ \tfrac{22}{3}(1+x)\ln^2\left(\frac{Q^2}{M^2}\right)$$
$$+ \Big[\frac{1+x^2}{1-x}\Big[-8\,\mathrm{Li}_2(1-x) + \tfrac{70}{3}\ln x \Big] + (1+x)\Big[8\zeta(2) + \tfrac{88}{3}\ln(1-x)$$
$$- 6\ln x \Big] - \tfrac{4}{9}(19+124x) \Big] \ln\left(\frac{Q^2}{M^2}\right) + \frac{1+x^2}{1-x}\Big[-4\,\mathrm{S}_{1,2}(1-x)$$
$$- 12\,\mathrm{Li}_3(1-x) + \tfrac{4}{3}\,\mathrm{Li}_2(1-x) + 8\,\mathrm{Li}_2(1-x)\ln x - 8\,\mathrm{Li}_2(1-x)\ln(1-x)$$
$$+ 8\zeta(2)\ln x - \tfrac{29}{2}\ln^2 x - \tfrac{104}{3}\ln x + \tfrac{140}{3}\ln x\ln(1-x) \Big]$$
$$+ (1+x)\Big[16\,\mathrm{S}_{1,2}(1-x) - 12\,\mathrm{Li}_3(1-x) - 28\zeta(3) + 8\,\mathrm{Li}_2(1-x)\ln(1-x)$$
$$+ 16\zeta(2)\ln(1-x) + \tfrac{88}{3}\ln^2(1-x) \Big] - \tfrac{4}{3}(7+x)\,\mathrm{Li}_2(1-x)$$
$$- \tfrac{4}{3}(19+25x)\zeta(2) + \tfrac{1}{6}(23-25x)\ln^2 x - 4(3-x)\ln x\ln(1-x)$$
$$- \tfrac{2}{3}(26-57x)\ln x - \tfrac{4}{9}(38+239x)\ln(1-x) - \tfrac{446}{27} + \tfrac{2278}{27}x \Big\} \qquad (4B.9)$$

and

$$\Delta_{q\bar{q}}^{(2),C_F} = \left(\frac{\alpha_s}{4\pi}\right)^2 C_F{}^2 \Big\{ \Big[-16\frac{1+x^2}{1-x}\ln x + 8(1+x)\Big[\ln x - 4\ln(1-x) \Big]$$
$$- 8(5+x) \Big] \ln^2\left(\frac{Q^2}{M^2}\right) + \Big[\frac{1+x^2}{1-x}\Big[16\,\mathrm{Li}_2(1-x) + 24\ln^2 x - 24\ln x$$
$$- 112\ln x\ln(1-x) \Big] + (1+x)\Big[32\,\mathrm{Li}_2(1-x) + 32\zeta(2) - 12\ln^2 x$$
$$+ 32\ln x\ln(1-x) - 96\ln^2(1-x) \Big] + 8(15+2x) + 16(2-3x)\ln x$$
$$- 16(7-x)\ln(1-x) \Big] \ln\left(\frac{Q^2}{M^2}\right) + \frac{1+x^2}{1-x}\Big[-32\,\mathrm{S}_{1,2}(1-x)$$
$$- 8\,\mathrm{Li}_3(1-x) - 24\,\mathrm{Li}_2(1-x)\ln x + 24\,\mathrm{Li}_2(1-x)\ln(1-x) - 12\ln^3 x$$
$$+ 64\zeta(2)\ln x + 72\ln^2 x\ln(1-x) - 124\ln^2(1-x)\ln x + 56\ln x \Big]$$
$$+ (1-x)\Big[64\zeta(2) - 64\ln^2(1-x) \Big] + (1+x)\Big[\tfrac{14}{3}\ln^3 x - 64\ln^3(1-x)$$

$$- 40\,\mathrm{Li}_3(1-x) + 48\,\mathrm{Li}_2(1-x)\ln(1-x) - 32\zeta(2)\ln x + 16\,\mathrm{S}_{1,2}(1-x)$$

$$+ 64\zeta(2)\ln(1-x) - 128\zeta(3) - 24\ln^2 x\ln(1-x) + 32\ln^2(1-x)\ln x\Big]$$

$$+ 8(3-2x)\,\mathrm{Li}_2(1-x) - 16(2-x)\ln^2 x + 16(7-6x)\ln x\ln(1-x)$$

$$- 8(4-13x)\ln x + 4(64+3x)\ln(1-x) - 24(3-2x)\Big\}. \qquad (4B.10)$$

The functions $\mathrm{Li}_n(x)$ and $\mathrm{S}_{n,p}(x)$ denote the polylogarithms and can be found in [56].

The hard part of quark pair production due to the diagrams A in fig. 4.7 is equal to

$$\Delta^{(2)}_{q\bar{q},A\bar{A}} = \left(\frac{\alpha_s}{4\pi}\right)^2 n_f C_F \Big\{ -\tfrac{4}{3}(1+x)\ln^2\left(\frac{Q^2}{M^2}\right) + \Big[-\frac{16}{3}\frac{1+x^2}{1-x}\ln x$$

$$- \tfrac{16}{3}(1+x)\ln(1-x) - \tfrac{8}{9}(1-11x)\Big]\ln\left(\frac{Q^2}{M^2}\right) + \frac{1+x^2}{1-x}\Big[4\ln^2 x$$

$$- \tfrac{4}{3}\mathrm{Li}_2(1-x) + \tfrac{20}{3}\ln x - \tfrac{32}{3}\ln x\ln(1-x)\Big] + (1+x)\Big[\tfrac{4}{3}\mathrm{Li}_2(1-x)$$

$$+ \tfrac{16}{3}\zeta(2) - \tfrac{16}{3}\ln^2(1-x) + \tfrac{2}{3}\ln^2 x\Big] - \tfrac{16}{9}(1-11x)\ln(1-x)$$

$$+ \tfrac{8}{3}(2-3x)\ln x + \tfrac{4}{27}(47-103)\Big\}. \qquad (4B.11)$$

Finally, we have the interference terms corresponding to the combinations $A\overline{C}$ and $A\overline{D}$ in figs. 4.7 and 4.8. For them we find

$$\Delta^{(2)}_{q\bar{q},A\overline{C}} = \Delta^{(2)}_{q\bar{q},A\overline{D}} = \left(\frac{\alpha_s}{4\pi}\right)^2 C_F\left(C_F - \tfrac{1}{2}C_A\right)\Big\{\Big[\frac{1+x^2}{1-x}\Big[-8\,\mathrm{Li}_2(1-x)$$

$$- 4\ln^2 x - 6\ln x\Big] - 14(1+x)\ln x - 4(8-7x)\Big]\ln\left(\frac{Q^2}{M^2}\right)$$

$$+ \frac{1+x^2}{1-x}\Big[16\,\mathrm{Li}_3(1-x) - 36\,\mathrm{S}_{1,2}(1-x) + \tfrac{8}{3}\ln^3 x - 12\,\mathrm{Li}_2(1-x)\ln x$$

$$- 16\,\mathrm{Li}_2(1-x)\ln(1-x) - 6\,\mathrm{Li}_2(1-x) + \tfrac{15}{2}\ln^2 x - 8\ln^2 x\ln(1-x)$$

$$+ 12\ln x - 12\ln x\ln(1-x)\Big] + (1+x)\Big[-8\,\mathrm{Li}_3(1-x) - 26\,\mathrm{Li}_2(1-x)$$

$$+ 4\,\mathrm{Li}_2(1-x)\ln x + \tfrac{2}{3}\ln^3 x + \tfrac{23}{2}\ln^2 x - 28\ln x\ln(1-x)\Big]$$

$$+ 2(22-9x)\ln x - 8(8-7x)\ln(1-x) + 2(47-39x)\Big\}. \qquad (4B.12)$$

Notice that for $V = \gamma$ and Z both the $A\overline{C}$ and $A\overline{D}$ interference terms always contribute, whereas for W–production only one of the two gives a contribution. This is due to the fact that for W–production only one of the sets of diagrams, C or D, is possible for a fixed choice of the initial and final state quark flavours.

The remaining parts of $q\bar{q}$ scattering are free of mass singularities. Therefore, they do not need mass factorisation, which implies that their contributions are scheme and scale independent. The contributions originating from the diagrams B in fig. 4.7 and the interference terms $B\overline{C}$ and $B\overline{D}$ (see figs. 4.7 and 4.8) are

$$\Delta^{(2)}_{q\bar{q},B\overline{B}} = \left(\frac{\alpha_s}{4\pi}\right)^2 C_F \Big\{ (1+x)^2 \Big[-\tfrac{32}{3}\,\mathrm{Li}_2(-x) - \tfrac{16}{3}\zeta(2) + \tfrac{8}{3}\ln^2 x - \tfrac{32}{3}\ln x \ln(1+x) \Big] + \tfrac{8}{3}(3+3x^2+4x)\ln x + \tfrac{40}{3}(1-x^2) \Big\} \tag{4B.13}$$

and

$$\begin{aligned}\Delta^{(2)}_{q\bar{q},B\overline{C}} = \Delta^{(2)}_{q\bar{q},B\overline{D}} = \left(\frac{\alpha_s}{4\pi}\right)^2 C_F \left(C_F - \tfrac{1}{2}C_A\right) \Big\{ &(1+x^2+3x) \Big[32\,\mathrm{S}_{1,2}(1-x) \\ &+ 16\,\mathrm{Li}_2(1-x)\ln x \Big] + (1+x)^2 \Big[-48\,\mathrm{S}_{1,2}(-x) - 8\,\mathrm{Li}_3(-x) + 24\,\mathrm{Li}_2(-x) \\ &+ 24\,\mathrm{Li}_2(-x)\ln x - 48\,\mathrm{Li}_2(-x)\ln(1+x) + 12\zeta(2) - 24\zeta(2)\ln(1+x) \\ &+ 8\zeta(2)\ln x + 20\ln^2 x\ln(1+x) - 24\ln^2(1+x)\ln x + 24\ln x\ln(1+x) \Big] \\ &+ 36(1-x^2)\,\mathrm{Li}_2(1-x) + \tfrac{4}{3}(1+x^2+4x)\ln^3 x + 4(9+11x)\ln x \\ &- 2(-6+15x^2+8x)\ln^2 x - 2(-27+13x^2+14x) \Big\}. \end{aligned} \tag{4B.14}$$

The comment made for the interference terms $A\overline{C}$ and $A\overline{D}$ below eq. 4B.12 also applies to $B\overline{C}$ and $B\overline{D}$.

The matrix element corresponding to the interference term $A\overline{B}$ (fig. 4.7) involves the product of two fermion traces, each containing a vertex of the form $\gamma_\mu(v + a\gamma_5)$. Therefore, it is a type–3 matrix element, described below eq. 4.2.22 and we have to distinguish between the vector–vector and axial–axial parts, which we will denote by $\Delta^{(2),V}_{q\bar{q},A\overline{B}}$ and $\Delta^{(2),A}_{q\bar{q},A\overline{B}}$, respectively. The first part is zero due to Furry's theorem

$$\Delta^{(2),V}_{q\bar{q},A\overline{B}} = 0, \tag{4B.15}$$

whereas the axial–axial contribution is given by

$$\Delta^{(2),A}_{q\bar{q},A\overline{B}} = \left(\frac{\alpha_s}{4\pi}\right)^2 C_F \Big\{ 16\frac{1+x^2}{1-x}\ln x + 32x\ln x + 16(3-x) \Big\}. \tag{4B.16}$$

It is clear from eq. 4B.15 that this interference term does not contribute for $V = \gamma$. It doesn't give a contribution to W–production, either, because the diagrams A and

B can never have the same initial state quarks due to charge conservation. For Z–production the contribution from eq. 4B.15 vanishes by taking complete families of quarks into account.

With the correction terms mentioned above we have exhausted all contributions to $\Delta_{q\bar{q}}$ except those belonging to the singlet part. Since the latter are equal to the corrections Δ_{qq} calculated for the non-identical quark–quark scattering process, we will present them there.

4B.2 The (anti)quark–gluon contribution

At $\mathcal{O}(\alpha_s)$ the qg subprocess shows up for the first time. The Drell–Yan correction term for this reaction has been calculated in [8, 12] and it is given by

$$\Delta_{qg}^{(1)} = \frac{\alpha_s}{4\pi} T_f \left\{ 2(1+2x^2-2x)\ln\left(\frac{(1-x)^2 Q^2}{xM^2}\right) + 1 - 7x^2 + 6x \right\}. \qquad (4B.17)$$

The second order part of Δ_{qg} receives contributions from the graphs in figs. 4.5 and 4.6 and can be written as

$$\Delta_{qg}^{(2)} = \Delta_{\bar{q}g}^{(2)} = \Delta_{qg}^{(2),C_A} + \Delta_{qg}^{(2),C_F} + \frac{\alpha_s}{4\pi}\beta_0 \Delta_{qg}^{(1)} \ln\left(\frac{R^2}{M^2}\right). \qquad (4B.18)$$

The calculation of $\Delta_{qg}^{(2)}$ requires both mass factorisation and renormalisation. The latter gives rise to the β_0–term in eq. 4B.18. The two parts $\Delta_{qg}^{(2),C_A}$ and $\Delta_{qg}^{(2),C_F}$ are equal to

$$\begin{aligned}\Delta_{qg}^{(2),C_A} = \left(\frac{\alpha_s}{4\pi}\right)^2 C_A T_f \Big\{ \Big[& 4(1+4x)\ln x + 4(1+2x^2-2x)\ln(1-x) \\ & + \tfrac{2}{3}(3 - 31x^2 + 24x + 4x^{-1}) \Big] \ln^2\left(\frac{Q^2}{M^2}\right) + \Big[(1+2x^2+2x)\big[-8\,\mathrm{Li}_2(-x) \\ & - 8\ln x\ln(1+x) \big] - 8(1+3x)\ln^2 x + 8(3+2x^2+6x)\,\mathrm{Li}_2(1-x) \\ & - 16(1+2x^2-x)\zeta(2) + 8(1-2x^2+10x)\ln x\ln(1-x) \\ & + 12(1+2x^2-2x)\ln^2(1-x) + \tfrac{4}{3}(9 - 71x^2 + 54x + 8x^{-1})\ln(1-x) \\ & + 4(3+28x^2-2x)\ln x - \tfrac{58}{3} + \tfrac{146}{9}x^2 - \tfrac{8}{3}x + \tfrac{88}{9}x^{-1} \Big] \ln\left(\frac{Q^2}{M^2}\right) \\ & + (1+4x^2+5x)\big[8\,\mathrm{Li}_2(-x) + 8\ln x\ln(1+x) \big] \\ & + (1+2x^2+2x)\Big[-8\,\mathrm{Li}_3(-x) + 16\,\mathrm{Li}_3\left(\frac{1+x}{1-x}\right) - 16\,\mathrm{Li}_3\left(-\frac{1+x}{1-x}\right)\end{aligned}$$

$$
\begin{aligned}
&+ 16\,\mathrm{Li}_2(-x)\ln x - 16\,\mathrm{Li}_2(-x)\ln(1-x) + 12\ln^2 x\ln(1+x) \\
&- 16\ln x\ln(1-x)\ln(1+x)\Big] + 8(9 + 4x^2 + 16x)\,\mathrm{S}_{1,2}(1-x) \\
&- 4(15 + 12x^2 + 34x)\,\mathrm{Li}_3(1-x) - 4(1 + 2x^2 + 4x)\zeta(3) \\
&+ 8(7 - 2x)x\,\mathrm{Li}_2(1-x)\ln x + 8(7 + 5x^2 + 10x)\,\mathrm{Li}_2(1-x)\ln(1-x) \\
&+ \tfrac{4}{3}(33 + 44x^2 + 90x + 16x^{-1})\,\mathrm{Li}_2(1-x) - 16(5 - 2x)x\zeta(2)\ln x \\
&- 32(1 + 2x^2 - x)\zeta(2)\ln(1-x) + \tfrac{4}{3}(15 + 107x^2 - 84x - 8x^{-1})\zeta(2) \\
&+ \tfrac{2}{3}(9 + 20x)\ln^3 x + \tfrac{26}{3}(1 + 2x^2 - 2x)\ln^3(1-x) - (5 + \tfrac{346}{3}x^2)\ln^2 x \\
&- 4(3 - 2x^2 + 14x)\ln^2 x\ln(1-x) + 4(1 - 6x^2 + 22x)\ln^2(1-x)\ln x \\
&+ \tfrac{4}{3}(6 - 77x^2 + 63x + 8x^{-1})\ln^2(1-x) - \tfrac{2}{9}(-354 + 457x^2 + 12x)\ln x \\
&+ 20(1 + 13x^2 - 2x)\ln x\ln(1-x) + \tfrac{539}{9} + \tfrac{1837}{27}x^2 - \tfrac{1226}{9}x + \tfrac{116}{27}x^{-1} \\
&+ \tfrac{2}{9}(-210 + 74x^2 + 75x + 88x^{-1})\ln(1-x)\Big\}
\end{aligned}
\tag{4B.19}
$$

and

$$
\begin{aligned}
\Delta_{q\bar{q}}^{(2),C_F} = {} & \left(\frac{\alpha_s}{4\pi}\right)^2 C_F T_f \Big\{ \Big[12(1 + 2x^2 - 2x)\ln(1-x) - 6(1 + 4x^2 - 2x)\ln x \\
&- 3(1 - 4x)\Big]\ln^2\left(\frac{Q^2}{M^2}\right) + \Big[(1 + 2x^2 - 2x)\big[-8\zeta(2) + 36\ln^2(1-x)\big] \\
&- 48x^2\,\mathrm{Li}_2(1-x) + 8(1 + 4x^2 - 2x)\ln^2 x + 2(5 + 46x^2 - 40x)\ln x \\
&- 8(5 + 16x^2 - 10x)\ln x\ln(1-x) - 4(8 + 23x^2 - 34x)\ln(1-x) \\
&+ 2(12 + 11x^2 - 34x)\Big]\ln\left(\frac{Q^2}{M^2}\right) + (-1 + 3x^2 + 2x)\big[-16\,\mathrm{Li}_2(-x) \\
&- 16\ln x\ln(1+x)\big] + (1 + 2x^2 - 2x)\big[32\,\mathrm{Li}_3(-x) + 100\zeta(3) \\
&- 16\,\mathrm{Li}_2(-x)\ln x - 16\zeta(2)\ln(1-x) + \tfrac{70}{3}\ln^3(1-x)\big] \\
&- 4(11 + 34x^2 - 22x)\,\mathrm{S}_{1,2}(1-x) + 4(-1 + 18x^2 + 2x)\,\mathrm{Li}_3(1-x)
\end{aligned}
$$

$$+ 4(1-2x)\,\mathrm{Li}_2(1-x)\ln x - 4(3+26x^2-6x)\,\mathrm{Li}_2(1-x)\ln(1-x)$$

$$+ 2(3+40x^2-28x)\,\mathrm{Li}_2(1-x) + 24(1+4x^2-2x)\zeta(2)\ln x$$

$$+ 4(5-12x^2+2x)\zeta(2) - \tfrac{1}{3}(17+52x^2-34x)\ln^3 x$$

$$+ 8(3+10x^2-6x)\ln^2 x\ln(1-x) - \tfrac{1}{2}(35+4x^2-68x)\ln^2 x$$

$$- 6(7+22x^2-14x)\ln^2(1-x)\ln x - 2(23+63x^2-80x)\ln^2(1-x)$$

$$+ 4(13+48x^2-50x)\ln x\ln(1-x) - (59+174x^2-245x)\ln x$$

$$+ 2(38+88x^2-147x)\ln(1-x) - \frac{181}{2} - \frac{305}{2}x^2 + 233x \Big\}. \qquad (4B.20)$$

Notice the absence of the functions $\delta(1-x)$ and $\mathcal{D}_i(x)$ in Δ_{qg}, which were present in the expression for $\Delta_{q\bar{q}}$. Although the second order contribution corresponds to graphs with a gluon in the final state, these singular functions do not show up since the lowest order term $\Delta^{(1)}_{qg}$ is integrable in $x = 1$.

4B.3 The non–identical quark–quark contributions

The reaction represented by the diagrams in fig. 4.8 describe quark–antiquark as well as quark–quark scattering (without identical quarks). The contribution to the DY correction term can be split into two parts. The first part, represented by the combinations $C\overline{C}$ and $D\overline{D}$, needs mass factorisation. In this case the contributions for $q\bar{q}$, qq and $\bar{q}\,\bar{q}$ are all equal and are given by

$$\Delta^{(2)}_{q\bar{q},C\overline{C}} = \Delta^{(2)}_{q\bar{q},D\overline{D}} = \Delta^{(2)}_{qq,C\overline{C}} = \Delta^{(2)}_{qq,D\overline{D}} = \Delta^{(2)}_{\bar{q}\bar{q},C\overline{C}} = \Delta^{(2)}_{\bar{q}\bar{q},D\overline{D}} =$$

$$\left(\frac{\alpha_s}{4\pi}\right)^2 C_F T_f \Big\{ \Big[4(1+x)\ln x + \tfrac{2}{3}(3-4x^2-3x+4x^{-1}) \Big] \ln^2\left(\frac{Q^2}{M^2}\right)$$

$$+ \Big[(1+x)\big[16\,\mathrm{Li}_2(1-x) - 8\ln^2 x + 16\ln x\ln(1-x) \big]$$

$$+ 4(3+4x^2+6x)\ln x + \tfrac{8}{3}(3-4x^2-3x+4x^{-1})\ln(1-x)$$

$$- \tfrac{4}{9}(39+22x^2-39x-22x^{-1}) \Big] \ln\left(\frac{Q^2}{M^2}\right)$$

$$+ (3-4x^2-3x+4x^{-1})\big[\tfrac{8}{3}\ln^2(1-x) - \tfrac{8}{3}\zeta(2) \big] + (1+x)\big[48\,\mathrm{S}_{1,2}(1-x)$$

$$- 32\,\mathrm{Li}_3(1-x) + 8\,\mathrm{Li}_2(1-x)\ln x + 32\,\mathrm{Li}_2(1-x)\ln(1-x) - 16\zeta(2)\ln x$$

$$+ 6\ln^3 x - 16\ln^2 x\ln(1-x) + 16\ln^2(1-x)\ln x \Big] + \tfrac{4}{3}(39 + 8x^2$$

$$+ 15x + 16x^{-1})\,\mathrm{Li}_2(1-x) + 8(3 + 4x^2 + 6x)\ln x\ln(1-x)$$

$$- \tfrac{5}{3}(3 + 8x^2 + 15x)\ln^2 x - \tfrac{8}{9}(39 + 22x^2 - 39x - 22x^{-1})\ln(1-x)$$

$$+ \tfrac{2}{9}(345 + 20x^2 - 48x)\ln x + \tfrac{593}{9} + \tfrac{703}{27}x^2 - \tfrac{866}{9}x + \tfrac{116}{27}x^{-1} \Big\}. \qquad (4B.21)$$

The second part, which is collinearly finite, consists of the interference between the graphs C and D in fig. 4.8. The matrix element is of type 3 (see below eq. 4.2.22), therefore we have to distinguish between the vector–vector (V) and the axialvector–axialvector (A) terms, which are represented by $\Delta^{(2),V}_{\mathrm{q\bar{q}},\mathrm{C\bar{D}}}$ and $\Delta^{(2),A}_{\mathrm{q\bar{q}},\mathrm{C\bar{D}}}$, respectively. The contributions to V and A are not equal to each other, like in the $\mathrm{A\bar{B}}$ case (see eqs. 4B.15 and 4B.16). Further notice the relative minus sign between the $\mathrm{q\bar{q}}$ and the qq ($\mathrm{\bar{q}\bar{q}}$) in the V-part. The expressions for these interference terms are

$$\Delta^{(2),V}_{\mathrm{q\bar{q}},\mathrm{C\bar{D}}} = -\Delta^{(2),V}_{\mathrm{qq},\mathrm{C\bar{D}}} = -\Delta^{(2),V}_{\mathrm{\bar{q}\bar{q}},\mathrm{C\bar{D}}} = \left(\frac{\alpha_s}{4\pi}\right)^2 C_F T_f \Big\{ (2 + x + 2x^{-1}) \Big[32\,\mathrm{S}_{1,2}(1-x)$$

$$- 96\,\mathrm{S}_{1,2}(-x) - 48\ln^2(1+x)\ln x - 48\zeta(2)\ln(1+x) + 40\ln^2 x\ln(1+x)$$

$$- 96\,\mathrm{Li}_2(-x)\ln(1+x) \Big] + (1 + x)\Big[80\,\mathrm{Li}_2(-x) + 80\ln x\ln(1+x)$$

$$+ 40\zeta(2) \Big] + 8(3x - 6 + 4x^{-1})\,\mathrm{Li}_3(1-x) - 16(3x - 10 + 10x^{-1})\,\mathrm{Li}_3(-x)$$

$$- 24(x - 6 + 4x^{-1})\zeta(3) + 8(10 - x)\,\mathrm{Li}_2(1-x)\ln x - \tfrac{16}{3}x\ln^3 x$$

$$+ 32(2x + 5x^{-1})\,\mathrm{Li}_2(-x)\ln x + 8(10 + x)\zeta(2)\ln x + 8(5 - 4x)\,\mathrm{Li}_2(1-x)$$

$$- 52x\ln^2 x - 16(5 + 4x)\ln x - 160(1 - x) \Big\} \qquad (4B.22)$$

and

$$\Delta^{(2),A}_{\mathrm{q\bar{q}},\mathrm{C\bar{D}}} = \Delta^{(2),A}_{\mathrm{qq},\mathrm{C\bar{D}}} = \Delta^{(2),A}_{\mathrm{\bar{q}\bar{q}},\mathrm{C\bar{D}}} = \left(\frac{\alpha_s}{4\pi}\right)^2 C_F T_f \Big\{ (2 + x) \Big[32\,\mathrm{S}_{1,2}(1-x)$$

$$- 96\,\mathrm{S}_{1,2}(-x) - 48\ln^2(1+x) - 48\zeta(2)\ln(1+x) + 40\ln^2 x\ln(1+x)$$

$$- 96\,\mathrm{Li}_2(-x)\ln(1+x)\ln x \Big] + (1 + x)\Big[16\,\mathrm{Li}_2(-x) + 16\ln x\ln(1+x)$$

$$+ 8\zeta(2) \Big] + 8(2-x)\,\mathrm{Li}_3(1-x) - 16(6-5x)\,\mathrm{Li}_3(-x) - 24(2-3x)\zeta(3)$$

$$+ 8\,\mathrm{Li}_2(1-x) + 8(2+3x)\,\mathrm{Li}_2(1-x)\ln x + 8(2+5x)\zeta(2)\ln x$$

$$+ 128\,\mathrm{Li}_2(-x)\ln x - \frac{16}{3}x\ln^3 x - 4x\ln^2 x - 16\ln x - 32(1-x) \Big\}. \quad (4B.23)$$

Finally, we want to remark that in case of W–production only one of the two sets of diagrams contributes (C or D, depending on the quark flavours in the initial and final state). This implies that for W–production there is no contribution from the interference term $C\overline{D}$.

The calculation of the expressions in this and the next section can be performed in the off-shell regularisation scheme. This is done in appendix 4C. We agree with the results of Schellekens and van Neerven in [20].

4B.4 The identical (anti)quark–(anti)quark contributions

In case there are identical quarks in the initial and/or final state, we have in addition to the graphs in fig. 4.8 also the ones in fig. 4.9. As the results for $E\overline{E}$, $F\overline{F}$ and $E\overline{F}$ are equal to those for $C\overline{C}$, $D\overline{D}$ and $C\overline{D}$ (of course one has to implement the right statistical factors), we will not discuss them here (see the section on non–identical quark–quark scattering). The new contributions come from the interference terms $C\overline{E}$, $C\overline{F}$, $D\overline{E}$ and $D\overline{F}$. Before giving the results let us explain in some detail how we have taken care of the statistical factors in our calculations.

In case of $V = \gamma$ or Z all four sets of diagrams C, D, E and F contribute and we have a statistical factor $\frac{1}{2}$. However, in the case of $V = W$ we have to distinguish between two cases (recall that for W–production the diagrams C and D cannot contribute simultaneously):

- Identical quarks in the initial state. In this case the contribution comes from either the graphs C and F, or D and E, and there is no statistical factor.

- Identical quarks in the final state. Now only the combinations C and E, or D and F, give contributions. Moreover, in this case there is a statistical factor $\frac{1}{2}$.

For the expression of the hadronic structure function (see eq. 4A.21) it turned out to be convenient to use the statistical factors of the W–production case. Therefore, a statistical factor $\frac{1}{2}$ is included in the results for $C\overline{E}$ and $D\overline{F}$, but this is not the case for $C\overline{F}$ and $D\overline{E}$.

Apart from the statistical factors there is another difference between $C\overline{E}$ ($D\overline{F}$) and $C\overline{F}$ ($D\overline{E}$). The first contains collinear divergences and needs mass factorisation, whereas the latter is free of mass singularities.

The correction corresponding to the interferences $C\overline{E}$ and $D\overline{F}$ is equal to

$$\Delta^{(2)}_{qq,C\overline{E}} = \Delta^{(2)}_{qq,D\overline{F}} = \Delta^{(2)}_{\overline{q}\overline{q},C\overline{E}} = \Delta^{(2)}_{\overline{q}\overline{q},D\overline{F}} =$$

$$\left(\frac{\alpha_s}{4\pi}\right)^2 C_F\left(C_F - \tfrac{1}{2}C_A\right)\Big\{\Big[\frac{1+x^2}{1+x}\Big[4\ln^2 x - 8\zeta(2)$$

$$- 16\,\mathrm{Li}_2(-x) - 16\ln x\ln(1+x)\Big] + 8(1+x)\ln x + 16(1-x)\Big]\ln\left(\frac{Q^2}{M^2}\right)$$

$$+ \frac{1+x^2}{1+x}\Big[32\,\mathrm{S}_{1,2}(1-x) - 16\,\mathrm{S}_{1,2}(-x) - 32\,\mathrm{Li}_3(1-x) - 8\,\mathrm{Li}_3(-x)$$

$$+ 32\,\mathrm{Li}_3\left(\frac{1+x}{1-x}\right) - 32\,\mathrm{Li}_3\left(-\frac{1+x}{1-x}\right) - 4\zeta(3) + 24\,\mathrm{Li}_2(1-x)\ln x$$

$$+ 32\,\mathrm{Li}_2(-x)\ln x - 32\,\mathrm{Li}_2(-x)\ln(1-x) - 16\,\mathrm{Li}_2(-x)\ln(1+x)$$

$$+ 12\zeta(2)\ln x - 16\zeta(2)\ln(1-x) - 8\zeta(2)\ln(1+x) - \tfrac{8}{3}\ln^3 x$$

$$+ 8\ln^2 x\ln(1-x) + 28\ln^2 x\ln(1+x) - 8\ln^2(1+x)\ln x$$

$$- 32\ln x\ln(1-x)\ln(1+x)\Big] + (1-x)\Big[-16\,\mathrm{S}_{1,2}(-x) + 8\,\mathrm{Li}_3(-x)$$

$$+ 8\zeta(3) - 16\,\mathrm{Li}_2(-x)\ln(1+x) + 4\zeta(2)\ln x - 8\zeta(2)\ln(1+x) - \tfrac{2}{3}\ln^3 x$$

$$+ 4\ln^2 x\ln(1+x) - 8\ln^2(1+x)\ln x + 32\ln(1-x) - 34\Big]$$

$$+ (1+x)\Big[8\,\mathrm{Li}_2(-x) + 4\zeta(2) + 16\ln x\ln(1-x) + 8\ln x\ln(1+x)\Big]$$

$$+ 8(3+x)\,\mathrm{Li}_2(1-x) - 4(1+3x)\ln^2 x - 2(9-7x)\ln x\Big\}. \tag{4B.24}$$

The expression for the interference terms $C\overline{F}$ and $D\overline{E}$ is

$$\Delta^{(2)}_{qq,C\overline{F}} = \Delta^{(2)}_{qq,D\overline{E}} = \Delta^{(2)}_{\overline{q}\overline{q},C\overline{F}} = \Delta^{(2)}_{\overline{q}\overline{q},D\overline{E}} = \left(\frac{\alpha_s}{4\pi}\right)^2 C_F\left(C_F - \tfrac{1}{2}C_A\right)\Big\{$$

$$(1-x)^2\Big[16\,\mathrm{Li}_3(1-x) - 16\,\mathrm{S}_{1,2}(1-x) - 24\,\mathrm{Li}_2(1-x) - 16\,\mathrm{Li}_2(1-x)\ln x$$

$$- \tfrac{8}{3}\ln^3 x - 12\ln^2 x\Big] - 4(7-6x)\ln x - 2(15+13x^2-28x)\Big\}. \tag{4B.25}$$

Notice that the above expression is scheme and scale independent.

4B.5 The gluon–gluon contribution

The diagrams for the gluon–gluon subprocess can be obtained from the quark-antiquark annihilation graphs in fig. 4.6 via crossing. This subprocess shows up for the first time at $\mathcal{O}(\alpha_s^2)$. We have divided its Drell–Yan correction term into two parts, i.e.

$$\Delta_{gg}^{(2)} = \Delta_{gg}^{(2),C_A} + \Delta_{gg}^{(2),C_F}. \tag{4B.26}$$

The C_A–contribution is collinearly finite and is therefore scheme and scale independent. It is given by

$$\begin{aligned}
\Delta_{gg}^{(2),C_A} &= \left(\frac{\alpha_s}{4\pi}\right)^2 \frac{N^2}{N^2-1}\Big\{ (1+x)^2 \Big[16\,\mathrm{S}_{1,2}(-x) + 24\,\mathrm{Li}_3(-x) + 16\zeta(3) \\
&+ \tfrac{16}{3}\,\mathrm{Li}_2(-x) - 24\,\mathrm{Li}_2(-x)\ln x + 16\,\mathrm{Li}_2(-x)\ln(1+x) + 8\zeta(2)\ln(1+x) \\
&+ \tfrac{8}{3}\zeta(2) - 12\ln^2 x\ln(1+x) + 8\ln^2(1+x)\ln x + \tfrac{16}{3}\ln x\ln(1+x)\Big] \\
&- 8(1-x)^2\,\mathrm{S}_{1,2}(1-x) + \tfrac{2}{3}(-2+25x^2+2x)\ln^2 x \\
&- \tfrac{2}{3}(6+75x^2+38x)\ln x - \tfrac{47}{3} + \tfrac{191}{3}x^2 - 48x \Big\}.
\end{aligned} \tag{4B.27}$$

The C_F–contribution contains collinear singularities. After mass factorisation in the $\overline{\mathrm{MS}}$ scheme we find

$$\begin{aligned}
\Delta_{gg}^{(2),C_F} &= \left(\frac{\alpha_s}{4\pi}\right)^2 \Big\{ \Big[-2(1+4x^2+4x)\ln x - 4(1-3x^2+2x)\Big]\ln^2\left(\frac{Q^2}{M^2}\right) \\
&+ \Big[(1+4x^2+4x)\Big[-8\,\mathrm{Li}_2(1-x) + 2\ln^2 x - 8\ln x\ln(1-x)\Big] \\
&+ 2(1-4x^2+8x)\ln x - 16(1-3x^2+2x)\ln(1-x) \\
&+ 7 - 67x^2 + 60x\Big]\ln\left(\frac{Q^2}{M^2}\right) + (1+4x^2+4x)\Big[16\,\mathrm{Li}_3(1-x) \\
&- 4\,\mathrm{Li}_2(1-x)\ln x - 16\,\mathrm{Li}_2(1-x)\ln(1-x) + 4\ln^2 x\ln(1-x) \\
&- 8\ln^2(1-x)\ln x\Big] + (1+x)\Big[8\,\mathrm{Li}_2(-x) + 8\ln x\ln(1+x)\Big] \\
&+ (1+x)^2\Big[-16\,\mathrm{S}_{1,2}(-x) - 16\,\mathrm{Li}_2(-x)\ln(1+x) - 8\zeta(2)\ln(1+x) \\
&+ 12\ln^2 x\ln(1+x) - 8\ln^2(1+x)\ln x\Big] - 8(1+7x^2+10x)\,\mathrm{S}_{1,2}(1-x)
\end{aligned}$$

$$- 8(1 - x^2 + 2x)\,\mathrm{Li}_3(-x) - 4(1 - 2x^2 + 2x)\zeta(3)$$

$$- 4(5 - 14x^2 + 4x)\,\mathrm{Li}_2(1-x) + 8(2 + x^2 + 4x)\,\mathrm{Li}_2(-x)\ln x$$

$$+ 4(3 + 10x^2 + 10x)\zeta(2)\ln x + 4(5 - 12x^2 + 9x)\zeta(2)$$

$$- \tfrac{2}{3}(3 + 8x^2 + 8x)\ln^3 x - 2(3 + 4x^2 + 7x)\ln^2 x$$

$$- 16(1 - 3x^2 + 2x)\ln^2(1-x) + 4(1 - 4x^2 + 8x)\ln x \ln(1-x)$$

$$- (23 - 105x^2 + 64x)\ln x + 2(7 - 67x^2 + 60x)\ln(1-x)$$

$$- 2(16 - 49x^2 + 33x)\Big\}. \qquad (4B.28)$$

4B.6 The DY correction terms in the limit $x \to 1$

Before finishing this appendix it is also useful, in view of the discussion of eqs. 4.3.7–4.3.10, to present the behaviour of $\Delta_{ij}(x, Q^2, M^2)$ in the limit $x \to 1$. In this limit the expressions in eqs. 4B.2–4B.28 become

$$\lim_{x\to 1}\Delta_{q\bar{q}}^{(1),H} = \Big(\frac{\alpha_s}{4\pi}\Big)C_F\Big\{ - 16\ln(1-x) - 8\ln\Big(\frac{Q^2}{M^2}\Big) + 8\Big\}, \qquad (4B.29)$$

$$\lim_{x\to 1}\Delta_{q\bar{q}}^{(2),C_A} = \Big(\frac{\alpha_s}{4\pi}\Big)^2 C_A C_F\Big\{ \tfrac{176}{3}\ln^2(1-x) +$$
$$\Big[\tfrac{176}{3}\ln\Big(\frac{Q^2}{M^2}\Big) + 32\zeta(2) - \tfrac{2092}{9}\Big]\ln(1-x) + \tfrac{44}{3}\ln^2\Big(\frac{Q^2}{M^2}\Big)$$
$$+ \Big[16\zeta(2) - \tfrac{1136}{9}\Big]\ln\Big(\frac{Q^2}{M^2}\Big) - 56\zeta(3) - \tfrac{224}{3}\zeta(2) + \tfrac{3128}{27}\Big\}, \qquad (4B.30)$$

$$\lim_{x\to 1}\Delta_{q\bar{q}}^{(2),C_F} = \Big(\frac{\alpha_s}{4\pi}\Big)^2 C_F^2\Big\{ - 128\ln^3(1-x) - \Big[192\ln\Big(\frac{Q^2}{M^2}\Big) - 248\Big]\ln^2(1-x)$$
$$+ \Big[128\ln\Big(\frac{Q^2}{M^2}\Big) - 64\ln^2\Big(\frac{Q^2}{M^2}\Big) + 128\zeta(2) + 316\Big]\ln(1-x)$$
$$- 16\ln^2\Big(\frac{Q^2}{M^2}\Big) + \Big[64\zeta(2) + 216\Big]\ln\Big(\frac{Q^2}{M^2}\Big)$$
$$- 256\zeta(3) - 128\zeta(2) - 152\Big\}, \qquad (4B.31)$$

$$\lim_{x\to 1} \Delta^{(2)}_{q\bar{q},A\bar{A}} = \left(\frac{\alpha_s}{4\pi}\right)^2 n_f C_F \Big\{ -\tfrac{32}{3}\ln^2(1-x) - \Big[\tfrac{32}{3}\ln\left(\frac{Q^2}{M^2}\right) - \tfrac{352}{9}\Big]\ln(1-x)$$

$$-\tfrac{8}{3}\ln^2\left(\frac{Q^2}{M^2}\right) + \tfrac{176}{9}\ln\left(\frac{Q^2}{M^2}\right) + \tfrac{32}{3}\zeta(2) - \tfrac{656}{27}\Big\}, \qquad (4B.32)$$

$$\lim_{x\to 1} \Delta^{(2)}_{q\bar{q},A\bar{C}} = \left(\frac{\alpha_s}{4\pi}\right)^2 C_F\left(C_F - \tfrac{1}{2}C_A\right)\Big\{-16\ln(1-x) - 8\ln\left(\frac{Q^2}{M^2}\right) + 12\Big\}, \qquad (4B.33)$$

$$\lim_{x\to 1} \Delta^{(2)}_{q\bar{q},B\bar{B}} = \left(\frac{\alpha_s}{4\pi}\right)^2 C_F\Big[\tfrac{4}{15}(1-x)^5\Big], \qquad (4B.34)$$

$$\lim_{x\to 1} \Delta^{(2)}_{q\bar{q},B\bar{C}} = \left(\frac{\alpha_s}{4\pi}\right)^2 C_F\left(C_F - \tfrac{1}{2}C_A\right)\Big[-\tfrac{2}{3}(1-x)^3\Big], \qquad (4B.35)$$

$$\lim_{x\to 1} \Delta^{(2),A}_{q\bar{q},A\bar{B}} = \left(\frac{\alpha_s}{4\pi}\right)^2 C_F\Big[\tfrac{16}{3}(1-x)^2\Big], \qquad (4B.36)$$

$$\lim_{x\to 1} \Delta^{(1)}_{qg} = \left(\frac{\alpha_s}{4\pi}\right) T_f\Big\{4\ln(1-x) + 2\ln\left(\frac{Q^2}{M^2}\right)\Big\}, \qquad (4B.37)$$

$$\lim_{x\to 1} \Delta^{(2),C_A}_{qg} = \left(\frac{\alpha_s}{4\pi}\right)^2 C_A T_f\Big\{\tfrac{26}{3}\ln^3(1-x) + 12\ln\left(\frac{Q^2}{M^2}\right)\ln^2(1-x)$$

$$+\Big[4\ln^2\left(\frac{Q^2}{M^2}\right) - 24\zeta(2) + 6\Big]\ln(1-x) + \Big[4 - 12\zeta(2)\Big]\ln\left(\frac{Q^2}{M^2}\right)$$

$$+ 2\zeta(2) - 4\Big\}, \qquad (4B.38)$$

$$\lim_{x\to 1} \Delta^{(2),C_F}_{qg} = \left(\frac{\alpha_s}{4\pi}\right)^2 C_F T_f\Big\{\tfrac{70}{3}\ln^3(1-x) + \Big[36\ln\left(\frac{Q^2}{M^2}\right) - 12\Big]\ln^2(1-x)$$

$$+\Big[12\ln^2\left(\frac{Q^2}{M^2}\right) + 12\ln\left(\frac{Q^2}{M^2}\right) - 16\zeta(2) - 42\Big]\ln(1-x) + 9\ln^2\left(\frac{Q^2}{M^2}\right)$$

$$-\Big[8\zeta(2) + 22\Big]\ln\left(\frac{Q^2}{M^2}\right) + 76\zeta(3) + 12\zeta(2) - 10\Big\}, \qquad (4B.39)$$

$$\lim_{x\to 1} \Delta^{(2)}_{q\bar{q},C\bar{C}} = \left(\frac{\alpha_s}{4\pi}\right)^2 C_F T_f\Big\{8(1-x)\ln^2(1-x)$$

$$+\Big[8\ln\left(\frac{Q^2}{M^2}\right) - 16\Big](1-x)\ln(1-x)$$

$$+\Big[2\ln^2\left(\frac{Q^2}{M^2}\right) - 8\ln\left(\frac{Q^2}{M^2}\right) - 8\zeta(2) + 18\Big](1-x)\Big\}, \qquad (4B.40)$$

$$\lim_{x\to 1} \Delta^{(2),V}_{q\bar{q},\mathrm{C\bar{D}}} = \left(\frac{\alpha_s}{4\pi}\right)^2 C_F T_f \left[7(1-x)^2 \right], \tag{4B.41}$$

$$\lim_{x\to 1} \Delta^{(2),A}_{q\bar{q},\mathrm{C\bar{D}}} = \left(\frac{\alpha_s}{4\pi}\right)^2 C_F T_f \left[7(1-x)^2 \right], \tag{4B.42}$$

$$\lim_{x\to 1} \Delta^{(2)}_{qq,\mathrm{C\bar{E}}} = \left(\frac{\alpha_s}{4\pi}\right)^2 C_F \left(C_F - \tfrac{1}{2}C_A\right) \left\{ 2(1-x) + \tfrac{4}{5}(1-x)^5 \ln(1-x) + \tfrac{2}{5}\ln\left(\frac{Q^2}{M^2}\right)(1-x)^5 \right\}, \tag{4B.43}$$

$$\lim_{x\to 1} \Delta^{(2)}_{qq,\mathrm{C\bar{F}}} = \left(\frac{\alpha_s}{4\pi}\right)^2 C_F \left(C_F - \tfrac{1}{2}C_A\right) \left[\tfrac{16}{3}(1-x)^3 \right], \tag{4B.44}$$

$$\lim_{x\to 1} \Delta^{(2),C_A}_{gg} = \left(\frac{\alpha_s}{4\pi}\right)^2 \frac{N^2}{N^2-1} \left[-\tfrac{2}{3}(1-x)^3 \right], \tag{4B.45}$$

and

$$\lim_{x\to 1} \Delta^{(2),C_F}_{gg} = \left(\frac{\alpha_s}{4\pi}\right)^2 \left\{ 8(1-x)\ln^2(1-x) + \left[8\ln\left(\frac{Q^2}{M^2}\right) - 16 \right](1-x)\ln(1-x) + \left[2\ln^2\left(\frac{Q^2}{M^2}\right) - 8\ln\left(\frac{Q^2}{M^2}\right) - 8\zeta(2) + 16 \right](1-x) \right\}. \tag{4B.46}$$

From the list above we infer that all corrections $\Delta_{ij}(x, Q^2, M^2)$ get zero in the limit $x \to 1$, except for the non-singlet $q\bar{q}$ contribution in eqs. 4B.2 and 4B.7 and the qg correction terms in eqs. 4B.17 and 4B.18. This explains why the bulk of the K-factor can be attributed to these two contributions.

4C Off–shell regularised operator matrix elements and a recalculation of the quark–quark Drell–Yan correction terms

In this appendix three subjects will be discussed. First, we will describe a method to calculate operator matrix elements beyond the pole terms, in contrast to what is done in chapter 3. Such an effort is needed in case one wants to calculate splitting functions, c.q. anomalous dimensions, within the off–shell regularisation procedure. Subsequently, we present the results of two splitting functions in this regularisation scheme. These are needed to factorise mass singularities out of partonic cross sections which were presented in the literature. Thirdly, these splitting functions will be used to recalculate the Drell–Yan correction terms due to the singlet non–identical quark–quark and the non–singlet identical quark–quark subprocesses, which were calculated by off–shell regularisation, as an independent check on the results found in appendix 4B. In order to be able to compare the correction terms, we take Schellekens' results [20], which were calculated in an off–shell scheme, and perform mass factorisation in the $\overline{\text{MS}}$ scheme.

4C.1 Calculation of regular two loop self–energy integrals

The calculation of operator matrix elements up to constant terms differs from the calculation of the pole terms in two ways. The first difference is not so dramatical: all integrals and expansions must be carried out one order further in ε. Secondly, one has to calculate those integrals which are finite. The latter step involves a simple, but smart ingredient. The finite integrals are of the form (cf. eq. 3C.21)

$$I_{\alpha\beta\gamma\delta\epsilon} = \int \frac{d^n k_1}{(2\pi)^n} \frac{d^n k_2}{(2\pi)^n} \frac{N(\Delta\cdot k_1, \Delta\cdot k_2)}{{k_1}^{2\alpha} {k_2}^{2\beta} (p-k_1)^{2\gamma} (p-k_2)^{2\delta} (k_1-k_2)^{2\epsilon}}, \tag{4C.1}$$

where all parameters $\alpha, \dots, \epsilon$ are larger than zero and $N(\Delta\cdot k_1, \Delta\cdot k_2)$ is the numerator of the integral. One can easily show that these integrals never occur in diagrams which involve an operator vertex with 4 legs. As a result, the numerator only contains single sums of the form 3A.17 and no double sums of the form 3A.18. Using this fact and performing suitable transformations $k_1 \to p - k_1$, $k_2 \to p - k_2$ and $k_1 \leftrightarrow k_2$ on the integration variables, the numerator can be brought into one of the following forms

$$N(\Delta\cdot k_1, \Delta\cdot k_2) = \begin{cases} (\Delta\cdot k_2)^i (\Delta\cdot p - \Delta\cdot k_2)^j (\Delta\cdot k_1 - \Delta\cdot k_2)^k \\ \\ (\Delta\cdot k_1)^{m-2} (\Delta\cdot k_2)^{-1} (\Delta\cdot k_1 - \Delta\cdot k_2)^i \end{cases}, \tag{4C.2}$$

where $i, j, k = -1, 0, 1, \dots$. The parameter m is coming from the operator (cf. eqs. 3.1.1–3.1.3). To give an expression for these integrals, we consider the following identity

$$\begin{aligned} 0 &= \int \frac{d^n k_1}{(2\pi)^n} \frac{d^n k_2}{(2\pi)^n} \frac{\partial}{\partial k_1^\mu} \left\{ \frac{(k_1-k_2)^\mu (\Delta\cdot k_1 - \Delta\cdot k_2)^i f(\Delta\cdot k_2)}{{k_1}^{2\alpha} {k_2}^{2\beta} (p-k_1)^{2\gamma} (p-k_2)^{2\delta} (k_1-k_2)^{2\epsilon}} \right\} \qquad (4C.3) \\ &= \int \frac{d^n k_1}{(2\pi)^n} \frac{d^n k_2}{(2\pi)^n} \frac{(\Delta\cdot k_1 - \Delta\cdot k_2)^i f(\Delta\cdot k_2)}{{k_1}^{2\alpha} {k_2}^{2\beta} (p-k_1)^{2\gamma} (p-k_2)^{2\delta} (k_1-k_2)^{2\epsilon}} \\ &\quad \times \left\{ i + n - 2\epsilon - \alpha - \gamma + \alpha \frac{{k_2}^2 - (k_1-k_2)^2}{{k_1}^2} + \gamma \frac{(p-k_2)^2 - (k_1-k_2)^2}{(p-k_1)^2} \right\}, \end{aligned}$$

therefore yielding

$$\int \frac{d^n k_1}{(2\pi)^n} \frac{d^n k_2}{(2\pi)^n} \frac{(\Delta\cdot k_1 - \Delta\cdot k_2)^i f(\Delta\cdot k_2)}{k_1^{2\alpha} k_2^{2\beta} (p-k_1)^{2\gamma} (p-k_2)^{2\delta} (k_1-k_2)^{2\epsilon}}$$

$$= \frac{1}{i+n-2\epsilon-\alpha-\gamma} \int \frac{d^n k_1}{(2\pi)^n} \frac{d^n k_2}{(2\pi)^n} \frac{(\Delta\cdot k_1 - \Delta\cdot k_2)^i f(\Delta\cdot k_2)}{k_1^{2\alpha} k_2^{2\beta} (p-k_1)^{2\gamma} (p-k_2)^{2\delta} (k_1-k_2)^{2\epsilon}}$$

$$\times \left\{ \alpha \frac{(k_1-k_2)^2 - k_2^2}{k_1^2} + \gamma \frac{(k_1-k_2)^2 - (p-k_2)^2}{(p-k_1)^2} \right\}. \qquad (4C.4)$$

This equality is applicable to the integrals with a numerator of the first form in eq. 4C.2. The second form of the numerator in eq. 4C.2 yields an extra contribution upon differentiation with respect to k_1, which is due to

$$(k_1-k_2)^\mu \frac{\partial(\Delta\cdot k_1)^{m-2}}{\partial k_1^\mu} = (m-2)\left((\Delta\cdot k_1)^{m-2} - \Delta\cdot k_2 (\Delta\cdot k_1)^{m-3}\right). \qquad (4C.5)$$

The factor $\Delta\cdot k_2$ of the last term on the right–hand side cancels the $(\Delta\cdot k_2)^{-1}$ of the numerator N. Therefore, the resulting integral can be transformed into an integral with a numerator, which has the first form of eq. 4C.2. By recursion, one can express every integral 4C.1 in simpler ones with only 4 different denominators (see eqs. 3C.22 and 3C.23). This trick was first shown by Tkachov in [17]. In principle we are now able to perform each calculation of a two loop splitting function up to the non–pole terms.

4C.2 The second order singlet quark–quark and non–singlet quark–antiquark splitting functions

In the off–shell regularisation scheme one distinguishes the UV singularities from the mass divergences. The first type appears as factors ε^{-1}, whereas the second type manifests itself as $\ln(-p^2/\mu^2)$ terms. Because the ε^{-1} poles are uniquely related to the logarithms, it is possible to use the operator renormalisation constants as splitting functions in the case of dimensional regularisation of the collinear divergences. In the off–shell scheme the UV poles are really removed by operator renormalisation and the remaining UV finite matrix element is used as splitting function. This makes clear why the non–pole terms of the operator matrix elements are needed in the off–shell regularisation scheme, while they are superfluous in the dimensional regularisation scheme.

The calculation of the singlet part of the quark–quark transition function involves the diagrams, which are shown in figure 4.14. The structure of the operator matrix

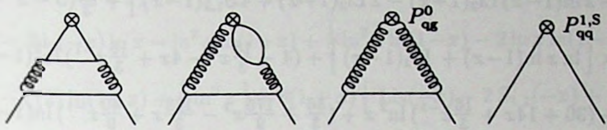

Fig. 4.14. The Feynman diagrams which contribute to Γ^{S}_{qq}.

element is given by

$$\langle 0|T(\overline{\psi}_i(p)O_q(0)\psi_j(-p))|0\rangle =$$
$$\frac{g^4}{(4\pi)^4}C_F T_f \delta_{ij}(\Delta\cdot p)^m \int_0^1 dx\, x^{m-1}\left(\frac{\not\Delta}{\Delta\cdot p}A^S(x) + \frac{\not p}{p^2}B^S(x)\right). \tag{4C.6}$$

The operator O_q is given in eq. 3.1.2 and S_ε in eq. 3.2.11. It is common use to project the structures onto the sum $A^S(x)+B^S(x)$ by applying the projection operator $\frac{1}{4}\mathrm{tr}(\not p\,\cdot)$ to the matrix element. This is equivalent to summing over the polarisations of the external quarks, as one is used to do in calculating cross sections. The counter term that is inserted in the third diagram is the UV pole term of the first order gluon–quark transition function. This diagram is due to the one loop renormalisation of the operators. The fourth diagram contains the second order operator renormalisation constant, which can be deduced from eq. 4.2.37. Its effect is the truncation of all ε-poles in the final answer. Note that the first diagram involves integrals without divergences, which are of the form 4C.1.

The sum of the four diagrams in fig. 4.14 has to be compared to the form of Γ^S_{qq}, given in eq. 4.2.37. However, in the off–shell regularisation method one does not use the ε^{-1}-poles, but the total term which is finite after $\overline{\mathrm{MS}}$ renormalisation of the ε^{-1}-poles (i.e. finite in the limit $\varepsilon \to 0$). The result of our calculation after renormalisation of the operator is

$$A^S(x) + B^S(x) = \Big[\,8(1+x)\ln x + 4 - \tfrac{16}{3}x^2 - 4x + \tfrac{16}{3}x^{-1}\,\Big]\ln^2\left(-\frac{p^2}{\mu^2}\right) + \Big[\,\tfrac{56}{3}$$
$$+\tfrac{176}{9}x^2 - \tfrac{128}{3}x + \tfrac{40}{9}x^{-1} + 16(1+x)\Big[\,\ln^2 x + \ln x\ln(1-x) + \mathrm{Li}_2(1-x)\,\Big]$$
$$+\tfrac{32}{3}(3 - x^2 + x^{-1})\ln x + (8 - \tfrac{32}{3}x^2 - 8x + \tfrac{32}{3}x^{-1})\ln(1-x)\,\Big]\ln\left(-\frac{p^2}{\mu^2}\right)$$
$$+\,8(1+x)\Big[\,\tfrac{5}{6}\ln^3 x + 2\ln^2 x\ln(1-x) + \ln x\ln^2(1-x) + 4\ln x\,\mathrm{Li}_2(1-x)$$

$$+ 2\ln(1-x)\,\mathrm{Li}_2(1-x) - 2\,\mathrm{Li}_3(1-x) + 4\,\mathrm{S}_{1,2}(1-x)\Big] + \tfrac{32}{3}(3 - x^2 + x^{-1})$$

$$\times\Big[\ln x \ln(1-x) + \mathrm{Li}_2(1-x)\Big] + (4 - \tfrac{16}{3}x^2 - 4x + \tfrac{16}{3}x^{-1})\ln^2(1-x)$$

$$+ (30 + 14x + \tfrac{16}{3}x^{-1})\ln^2 x + (\tfrac{56}{3} + \tfrac{176}{9}x^2 - \tfrac{128}{3}x + \tfrac{40}{9}x^{-1})\ln(1-x)$$

$$+ (16 - \tfrac{272}{9}x^2 - 64x + \tfrac{40}{9}x^{-1})\ln x - \tfrac{116}{9} + \tfrac{1064}{27}x^2 - \tfrac{196}{9}x - \tfrac{128}{27}x^{-1}. \quad (4C.7)$$

The mass scale p^2 is the operator renormalisation scale, which will take the role of mass factorisation scale when we recalculate the Drell–Yan correction term. The splitting function 4.2.30 becomes in the off–shell method

$$\Gamma^{\mathrm{S}}_{\mathrm{qq}} = \left(\frac{\hat{\alpha}_s}{4\pi}\right)^2 C_F T_f \left(A^{\mathrm{S}}(x) + B^{\mathrm{S}}(x) \right) \equiv \left(\frac{\hat{\alpha}_s}{4\pi}\right)^2 \Gamma^{(2),\mathrm{S}}_{\mathrm{qq}}. \quad (4C.8)$$

Secondly, we want to present the operator matrix element which represents the non–singlet quark–antiquark transition function. The contributing diagrams are

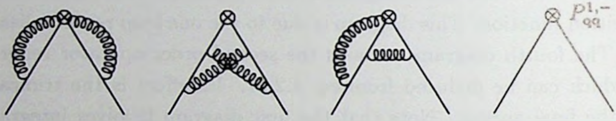

Fig. 4.15. The Feynman diagrams which contribute to $\Gamma^{\mathrm{NS}}_{\mathrm{q\bar{q}}}$.

shown in fig. 4.15, where we only consider the part that is proportional to the factor $(-1)^m$. The latter part of the operator matrix element can be given by (see discussion below eq. 4.2.40)

$$\langle 0|T(\overline{\psi}_i(p)O_{\mathrm{q}}(0)\psi_j(-p))|0\rangle = \quad (4C.9)$$
$$\frac{g^4}{(4\pi)^4} C_F(C_F - \tfrac{1}{2}C_A)\delta_{ij}(-\Delta\cdot p)^m \int_0^1 dx\, x^{m-1}\left(\frac{\not\Delta}{\Delta\cdot p}A^-(x) + \frac{\not p}{p^2}B^-(x)\right).$$

In this case, the finite expression $A^- + B^-$ after operator renormalisation is given by

$$A^-(x) + B^-(x) = 16\left[\frac{1+x^2}{1+x}\left[\tfrac{1}{4}\ln^2 x - \mathrm{Li}_2(-x) - \tfrac{1}{2}\zeta(2) - \ln x\ln(1+x)\right]\right.$$
$$\left. + \tfrac{1}{2}(1+x)\ln x + 1 - x\right]\ln\left(-\frac{p^2}{\mu^2}\right) + 8\frac{1+x^2}{1+x}\Big[\,\mathrm{S}_{1,2}(1-x) - 2\,\mathrm{Li}_3(1-x)$$

$$+ 2\,\mathrm{Li}_3\left(\frac{1+x}{1-x}\right) - 2\,\mathrm{Li}_3\left(-\frac{1+x}{1-x}\right) - 2\,\mathrm{Li}_2(-x)\ln(1-x) + \mathrm{Li}_2(1-x)\ln x$$

$$- \mathrm{Li}_2(-x)\ln x - \ln^2 x\ln(1+x) + \tfrac{1}{2}\ln^2 x\ln(1-x) - 2\ln x\ln(1-x)\ln(1+x)$$

$$- \zeta(2)\ln(1-x) + \tfrac{1}{4}\ln^3 x\Big] + 8(1+x)\Big[\,\mathrm{Li}_3(-x) - 2\,S_{1,2}(-x) + \mathrm{Li}_2(1-x)$$

$$+ \zeta(3) - 2\ln(1+x)\,\mathrm{Li}_2(-x) - \zeta(2)\ln(1+x) - \ln x\ln^2(1+x) + \ln x\ln(1-x)$$

$$+ \tfrac{1}{2}\ln^2 x\ln(1+x)\Big] + (1-x)\Big[\,22 - 12\zeta(2) + 16\ln(1-x)\Big] + 12\ln^2 x$$

$$+ 8(x - x^{-1})\Big[\,\mathrm{Li}_2(-x) + \ln x\ln(1+x)\Big] + 6(5+x)\ln x. \qquad (4C.10)$$

The splitting function 4.2.29 becomes in the off-shell regularisation scheme

$$\Gamma^{NS}_{q\bar{q}} = \left(\frac{\hat{\alpha}_s}{4\pi}\right)^2 C_F(C_F - \tfrac{1}{2}C_A)\left(A^-(x) + B^-(x)\right) \equiv \left(\frac{\hat{\alpha}_s}{4\pi}\right)^2 \Gamma^{(2),NS}_{q\bar{q}}. \qquad (4C.11)$$

The two splitting functions which we have determined up to constant terms, can be used to recalculate the $\overline{\mathrm{MS}}$ factorised quark–quark Drell–Yan correction terms.

4C.3 Mass factorisation of the quark–quark Drell–Yan subprocesses

We have calculated the singlet part of the quark–quark transition function at second order in the coupling constant, using off-shell regularisation. This enables us to recalculate the Drell–Yan correction term, which belongs to the mass singular part of the non-identical quark–quark scattering process. The expression for the structure function, which still contains the collinear divergences, has been given by Schellekens and van Neerven (eq. 3.7 in their first article of [20]). Furthermore, the quark–antiquark transition function at second order enables us to check the Drell–Yan correction term of the mass singular part of identical quark–quark scattering. The expression of the mass singular partonic cross section has also been given by Schellekens and van Neerven (eq. 2.5 in their second article of [20]). However, we do disagree with their result as regards the power of $\hat{\tau}$ in the logarithm: this should be 3 instead of 2. Of course, we have also checked those quark–quark Drell–Yan correction terms which do not need mass factorisation. In the latter case we agree with the results of Schellekens and van Neerven.

In order to factorise the mass singularities, we should consider eqs. 4.2.42 and 4.2.43. The corresponding equalities in the off-shell scheme are

$$\mathcal{W}_{q\bar{q}}^{(2),S} = \left(\frac{\hat{\alpha}_s}{4\pi}\right)^2 \left\{2\Gamma_{q\bar{q}}^{(2),S} + 2P_{gq}^0 \otimes w_{qg}^0 + w_{q\bar{q}}^{1,S}\right\} \tag{4C.12}$$

and

$$\mathcal{W}_{qq}^{(2),NS} = \left(\frac{\hat{\alpha}_s}{4\pi}\right)^2 \left\{2\Gamma_{q\bar{q}}^{(2),NS} + w_{qq}^{1,NS}\right\}, \tag{4C.13}$$

where the convolution symbol $\otimes$ was defined in eq. 4.2.35. The quantities $w_{q\bar{q}}^{1,S}$ and $w_{qq}^{1,NS}$ must be the same as the ones given in eqs. 4.2.42 and 4.2.43, because we consider the same mass factorisation scheme. The second order transition functions were given in eqs. 4C.8 and 4C.11. The singlet quark–quark splitting function contains both the leading and next–to–leading pole terms, which are separately visible in the dimensional regularisation scheme. The $\bar{w}_{qg}^0$ term is absent here, because we work in terms of the off–shell regularised quantities. The quantity that remains to be calculated, is $P_{gq}^0 \otimes w_{qg}^0$. In the off–shell scheme these first order quantities are given by

$$P_{gq}^0 = -4C_F\left\{\frac{(1-x)^2+1}{x}\left[\ln\left(\frac{x(1-x)p^2}{-\mu^2}\right)+1\right]+1\right\}, \tag{4C.14}$$

$$w_{qg}^0 = 2T_f\left\{\left((1-x)^2+x^2\right)\ln\left(\frac{(1-x)^2Q^2}{x\mu^2}\right)+\frac{1}{2}+3x-\frac{7}{2}x^2\right\} \tag{4C.15}$$

where μ denotes an arbitrary mass scale and p^2 is the mass factorisation scale.

If we combine the singlet transition function, the convolution of the two quantities given above and the partonic structure function from [20], we reproduce the correction term, given in eq. 4B.21. The scale p^2, which appears in the expressions of this appendix, must be identified with the scale M^2 of expression 4B.21. Furthermore, if we combine the identical quark–quark result of Schellekens with our expression for the non–singlet quark–antiquark splitting function we reproduce the Drell–Yan correction term 4B.24. These results provide us with a good check on the calculations done in chapter 4.

References

[1] H.D. Politzer, Nucl. Phys. **B129** (1977), 301; C.T. Sachrajda, Phys. Lett. **73B** (1978), 185; D. Amati, R. Petronzio and G. Veneziano, Nucl. Phys. **B140** (1978), 54; **B146** (1978), 29; R.K. Ellis, H. Georgi, M. Machacek, H.D. Politzer and G.G. Ross, Phys. Lett. **78B** (1978), 281; Nucl. Phys. **B152** (1979), 285; S.B. Libby and G. Sterman, Phys. Lett. **78B** (1978), 618

[2] G. Altarelli, Phys. Rep. **81** (1982), 1; Ann. Rev. Nucl. Part. Sci. **39** (1989), 357

[3] P.M. Stevenson, Phys. Rev. **D23** (1981), 2916; Nucl. Phys. **B203** (1982), 472

[4] G. Grunberg, Phys. Lett. **95B** (1980), 70, Erratum: **B110** (1982), 501; Phys. Rev. **D29** (1984), 2315

[5] J.H. Christenson et al., Phys. Rev. Lett. **25** (1970), 1523

[6] S.D. Drell and T.M. Yan, Phys. Rev. Lett. **25** (1970), 316; Ann. Phys. **66** (1971), 578

[7] J.C. Collins, D.E. Soper and G. Sterman, Nucl. Phys. **B261** (1985), 104; Nucl. Phys. **B308** (1988), 833; G.T. Bodwin, Phys. Rev. **D31** (1985), 2616, Erratum: **D34** (1986), 3932

[8] G. Altarelli, R.K. Ellis and G. Martinelli, Nucl. Phys. **B143** (1978), 521, Erratum: **B146** (1978), 544; **B157** (1979), 461

[9] J. Abad and B. Humpert, Phys. Lett. **77B** (1978), 105; **B78** (1978), 627, Erratum: **B80** (1979), 433; **B80** (1978), 115; **B80** (1979), 286

[10] J. Kubar-André and F.E. Paige, Phys. Rev. **D19** (1979), 221

[11] K. Harada, T. Kaneko and N. Sakai, Nucl. Phys. **B155** (1979), 169, Erratum: **B165** (1980), 545

[12] B. Humpert and W.L. van Neerven, Phys. Lett. **84B** (1979), 327, Erratum: **B85** (1979), 471; **B89** (1979), 69; Nucl. Phys. **B184** (1981), 225

[13] J. Kubar, M. le Bellac, J.L. Meunier and G. Plaut, Nucl. Phys. **B175** (1980), 251

[14] J. Badier et al., Phys. Lett. **89B** (1979), 145; R. Barate et al., Phys. Rev. Lett. **43** (1979), 1541

[15] K. Freudenreich, Int. J. Mod. Phys. **A5** (1990), 3643

[16] L. Fayard, '$W^{\pm}$ and Z^0 Production at Hadron Colliders', LAL 90-48

[17] K.G. Chetyrkin, A.L. Kataev and F.V. Tkachov, Phys. Lett. **85B** (1979), 277; M. Dine and J. Sapirstein, Phys. Rev. Lett. **43** (1979), 668; W. Celmaster and R.J. Gonsalves, Phys. Rev. Lett. **44** (1980), 560; Phys. Rev. **D21** (1980), 3112; F.V. Tkachov, Phys. Lett. **100B** (1981), 65; S.G. Gorishny, A.L. Kataev and S.A. Larin, Phys. Lett. **B212** (1988), 238

[18] G. Kramer and B. Lampe, Z. Phys. **C34** (1987), 497, Erratum: **C42** (1989), 504

[19] V.N. Gribov and L.N. Lipatov, Sov. J. Nucl. Phys. **15** (1972), 438, 675; G. Altarelli and G. Parisi, Nucl. Phys. **B126** (1977), 298

[20] A.P. Contogouris and J. Kripfganz, Phys. Rev. **D20** (1979), 2295; A.N. Schellekens and W.L. van Neerven, Phys. Rev. **D21** (1980), 2619; **D22** (1980), 1623; A.N. Schellekens, thesis, University of Nijmegen, 1981

[21] T. Matsuura and W.L. van Neerven, Z. Phys. **C38** (1988), 623

[22] T. Matsuura and W.L. van Neerven, Contribution to the Proc. Int. Europhys. Conf. on High Energy Physics, Vol. 1 (Uppsala, Sweden, 25 June – 1 July, 1987), ed. O. Botner (Uppsala University), p. 198

[23] T. Matsuura, S.C. van der Marck and W.L. van Neerven, Phys. Lett. **B211** (1988), 171; Nucl. Phys. **B319** (1989), 570

[24] T. Matsuura, thesis, University of Leiden, 1989

[25] T. Matsuura, R. Hamberg and W.L. van Neerven, Nucl. Phys. **B345** (1990), 331

[26] F. Bloch and A. Nordsieck, Phys. Rev. **52** (1937), 54; D.R. Yennie, S.C. Frautschi and H. Suura, Ann. Phys. **13** (1961), 379

[27] R. Doria, J. Frenkel and J.C. Taylor, Nucl. Phys. **B168** (1980), 93; A. Andraši, M. Day, R. Doria, J. Frenkel and J.C. Taylor, Nucl. Phys. **B182** (1981), 104; C. Di'lieto, S. Gendron, I.G. Halliday and C.T. Sachrajda, Nucl. Phys. **B183** (1981), 223

[28] T. Kinoshita, J. Math. Phys. **3** (1962), 650; T.D. Lee and M. Nauenberg, Phys. Rev. **133** (1964), B1549; N. Nakanishi, Prog. Theor. Phys. **19** (1958), 159

[29] R.J. Gonsalves, J. Pawlowski and C.-F. Wai, Phys. Rev. **D40** (1989), 2245, and references therein; J. Pawłowski, Phys. Lett. **B246** (1990), 477

[30] W.L. van Neerven, Nucl. Phys. **B268** (1986), 453

[31] R.J. Gonsalves, Phys. Rev. **D28** (1983), 1542

[32] R.K. Ellis, M.A. Furman, H.E. Haber and I. Hinchliffe, Nucl. Phys. **B173** (1980), 397

[33] J. Smith, D. Thomas and W.L. van Neerven, Z. Phys. **C44** (1989), 267

[34] W. Beenakker, H. Kuijf, W.L. van Neerven and J. Smith, Phys. Rev. **D40** (1989), 54

[35] E.G. Floratos, R. Lacaze and C. Kounnas, Phys. Lett. **98B** (1981), 285

[36] E.G. Floratos, D.A. Ross and C.T. Sachrajda, Nucl. Phys. **B129** (1977), 66, Erratum: **B139** (1978), 545; Nucl. Phys. **B152** (1979), 493

[37] A. González-Arroyo, C. López and F.J. Yndurâin, Nucl. Phys. **B153** (1979), 161; A. González-Arroyo and C. López, Nucl. Phys. **B166** (1980), 429

[38] E.G. Floratos, R. Lacaze and C. Kounnas, Phys. Lett. **98B** (1981), 89

[39] W. Furmanski and R. Petronzio, Phys. Lett. **97B** (1980), 437; G. Curci, W. Furmanski and R. Petronzio, Nucl. Phys. **B175** (1980), 27

[40] A.N. Schellekens, Lett. Nuovo Cim. **24** (1979), 513

[41] D.A. Dicus and S.S.D. Willenbrock, Phys. Rev. **D34** (1986), 148

[42] G. Altarelli, M. Diemoz, G. Martinelli and P. Nason, Nucl. Phys. **B308** (1988), 724

[43] A.D. Martin, R.G. Roberts and W.J. Stirling, Phys. Rev. **D37** (1988), 1161; Mod. Phys. Lett. **A4** (1989), 1135; P.N. Harriman, A.D. Martin, W.J. Stirling and R.G. Roberts, Phys. Rev. **D42** (1990), 798

[44] P.N. Harriman, A.D. Martin, W.J. Stirling and R.G. Roberts, Phys. Lett. **B243** (1990), 421

[45] J.G. Morfín and Wu-Ki Tung, "Parton distributions from a global QCD analysis of deep inelastic scattering and lepton-pair production", Fermilab-Pub-90/74

[46] P. Nason, S. Dawson and R.K. Ellis, Nucl. Phys. **B303** (1988), 607; Nucl. Phys. **B327** (1989), 49

[47] W. Beenakker, W.L. van Neerven, R. Meng, G.A. Schuler and J. Smith, Nucl. Phys. B351 (1991), 507

[48] P. Aurenche, R. Baier, M. Fontannaz and D. Schiff, Nucl. Phys. **B286** (1987), 509; Nucl. Phys. **B297** (1988), 661

[49] F. Aversa, P. Chiappetta, M. Greco and J.Ph. Guillet, Phys. Lett. **B210** (1988), 225; Phys. Lett. **B211** (1988), 465; Nucl. Phys. **B327** (1989), 105

[50] A.D. Martin and W.J. Stirling, Phys. Lett. **B248** (1990), 443

[51] J. Kwiecinski, A.D. Martin, W.J. Stirling and R.G. Roberts, Phys. Rev. **D42** (1990), 3645, and references therein

[52] UA1 Collaboration: C. Albajar et al., "Measurement of the ratio $R \equiv \sigma_W Br(W \to \mu\nu)/\sigma_Z Br(Z \to \mu\mu)$ and Γ_W^{tot} at the CERN proton-antiproton collider", CERN-PPE/90-141

[53] UA2 Collaboration: J. Alitti et al., Z. Phys. **C47** (1990), 11

[54] CDF Collaboration: P.F. Derwent, 'Production properties of W, Z bosons', talk presented at the 25th Recontres de Moriond, Les Arcs, Savoie – France, March 1990

[55] CDF Collaboration: F. Abe et al., Phys. Rev. Lett. **64** (1990), 152

[56] L. Lewin, 'Polylogarithms and Associated Functions', North–Holland, 1983; R. Barbieri, J.A. Mignaco and E. Remiddi, Nuovo Cim. **11A** (1972), 824; A. Devoto and D.W. Duke, Riv. Nuovo Cim. **7–6** (1984), 1

Samenvatting

Tweede orde gluonische bijdragen aan fysische grootheden

De algemeen aanvaarde theorie die de sterke wisselwerking tussen quarks en gluonen beschrijft, staat bekend onder de naam Quantum Chromo Dynamica (QCD) en dateert uit het begin van de jaren '70. Quarks en gluonen zijn de bouwstenen van alle tot nu toe bekende hadronen; ze zijn echter nog nooit afzonderlijk waargenomen. Men probeert dit feit, dat opsluiting (confinement) wordt genoemd, met behulp van QCD te verklaren. Terwijl het laatste nog steeds een moeilijk probleem is, bleek QCD veel succesvoller te zijn in de beschrijving van zeer inelastische verstrooiingsprocessen. Dit zijn processen waarbij alle kinematische invarianten, die in de werkzame doorsnede voorkomen, asymptotisch zijn, maar waarbij de onderlinge verhoudingen van deze invarianten eindig gehouden worden. Onder deze voorwaarden kan men storingstheorie toepassen om de werkzame doorsneden uit te rekenen. Dit is geoorloofd omdat in QCD de van de asymptotische invarianten afhankelijke koppelingsconstante naar nul gaat. Dit laatste verschijnsel wordt asymptotische vrijheid genoemd. De theoretische methoden die hier al op vooruit liepen en later in QCD geïmplementeerd werden, de operatorprodukt expansie en het partonmodel, worden geïntroduceerd in hoofdstuk twee van dit proefschrift.

De operatorprodukt expansie, die voor het eerst door K.G. Wilson werd toegepast, beschrijft hoe men een produkt van twee lokale operatoren, gedefinieerd in twee verschillende ruimte–tijd punten, in de buurt van de lichtkegel kan schrijven als een oneindige som van lokale operatoren. De verwachtingswaarden van deze operatoren beschrijven het lange–afstandsgedrag (lage–energiegebied) van de fysische grootheden die men wil onderzoeken. De coëfficiënten van deze lokale operatoren die in de reeks voorkomen zijn singuliere funkties (distributies), die het korte–afstandsgedrag (hoge–energiegebied) van de fysische grootheden zoals werkzame doorsneden beschrijven. Voor deze singuliere funkties, ook wel Wilson coëfficiënten genoemd, bestaat een storingsreeks in de koppelingsconstante. De laagste–orde term van deze reeks wordt gegeven door vrije–veldentheorie en leidt tot schaalonafhankelijk gedrag van de struktuurfunkties die zeer inelastische lepton–hadron verstrooiing beschrijven. De eerste experimenten bevestigden dit gedrag.

Later, toen de experimenten nauwkeuriger uitgevoerd konden worden, ontdekte men afwijkingen van schaalinvariantie. Deze kunnen verklaard worden door hogere–orde QCD–correcties in de operatorprodukt expansie te beschouwen. Het blijkt dat er een intrinsiek verband bestaat tussen het singuliere gedrag van de Wilson coëfficiënten en de dimensies van de hiermee corresponderende lokale operatoren. In een vrije–veldentheorie worden deze dimensies kanoniek genoemd en spelen zij een soortgelijke rol als andere quantumgetallen, zoals bijvoorbeeld spin. Omdat in QCD er een wisselwerking tussen de quarks en gluonen bestaat, veranderen de dimensies van de lokale operatoren. Het verschil tussen een kanonieke dimensie in een vrije–veldentheorie en de dimensie die onstaat in een theorie met wisselwerking wordt anomale dimensie genoemd. Deze laatste kan ook als een oneindige reeks in de koppelingsconstante worden geschreven.

Om de anomale dimensies te berekenen moet men de lokale operatoren renormaliseren. Elke term in de lusexpansie van de verwachtingswaarden van de operatoren geeft een volgende term in de reeks voor de anomale dimensie. Ook de renormalisatiegroepvergelijkingen spelen een grote rol als men het schaalafhankelijke gedrag van de Wilson coëfficiënten wil bepalen. In het begin van de jaren '80 waren alle relevante anomale dimensies van de operatoren, die in de operatorprodukt expansie voorkomen, al tot op tweede orde in de koppelingsconstante berekend. Er was echter één probleem: de uitdrukkingen die gevonden werden voor de anomale dimensie van de gluonoperator kwamen niet overeen. Deze berekening werd door verscheidene groepen uitgevoerd.

Het probleem van de tweede–orde bijdrage aan de anomale dimensie van de gluonoperator is het onderwerp van het derde hoofdstuk. Er wordt beschreven hoe het renormaliseren van een dergelijk ingewikkeld object in een ijkveldentheorie, zoals QCD, zich voltrekt. De eerste–orde berekening wordt gepresenteerd voor twee gevallen, waarin de termen die de ijkkeuze vastleggen respektievelijk axiaal en covariant genomen zijn. De tweede–orde berekening wordt alleen in de covariante ijk gedaan, omdat in dit geval de berekening door eerdere groepen verkeerd is uitgevoerd. Door de constructie van nieuwe operatoren in de Lagrangiaan, die niet voorkomen in de operatorprodukt expansie maar wel een rol spelen bij het renormaliseren van de gluonoperator, is het mogelijk de correcte anomale dimensie te vinden. Deze stemt overeen met het resultaat, dat tien jaar geleden met behulp van de axiale ijk is berekend. Het probleem van de ijkafhankelijkheid van de anomale dimensie van de gluonoperator is door de beschrijving in dit proefschrift definitief opgelost.

De operatorprodukt expansie heeft een beperkt toepassingsgebied en kan het merendeel van zeer inelastische verstrooiingsprocessen zoals hadron–hadron botsingen niet beschrijven. In 1969 introduceerde R.P. Feynman het partonmodel dat ook hadron–hadron processen kan beschrijven. Hierin worden hadronen voorgesteld als bestaand uit een verzameling vrije puntdeeltjes, de partonen. Met behulp van dit model gaven S.D. Drell en T.M. Yan een jaar later een theoretische beschrijving van de produktie van hoog–energetische leptonparen in hadron–hadron processen. Hun model had zoveel succes, dat het proces nog steeds wordt aangeduid met de naam Drell–Yan proces.

Evenals in het geval van lepton–hadron verstrooiing is de laagste–orde struktuurfunktie onafhankelijk van de botsingsenergie. Hogere–orde correcties maken deze funktie schaalafhankelijk, waarbij de eerder genoemde anomale dimensies weer een belangrijke rol spelen. Het renormaliseren van de operatoren uit de operatorprodukt expansie wordt in het partonmodel vervangen door een procedure die massafaktorisatie heet. Massafaktorisatie maakt het mogelijk om divergenties op een zinvolle manier te behandelen door de partondichtheidsfunkties te renormaliseren. Deze funkties beschrijven de kans om een bepaald parton met een bepaalde impuls aan te treffen in een hadron.

Hogere–orde correcties op het Drell–Yan proces geven niet alleen aan hoe de energie–afhankelijkheid verloopt, maar corrigeren ook de absolute werkzame doorsnede. Omdat de eerste–orde correctie bij dit proces nogal groot is, is het van belang om ook de tweede–orde correctie te leren kennen. Dit is noodzakelijk om de nauwkeurigheid van de theoretische voorspelling op hetzelfde niveau te brengen als die van de experimenten. Tot voor kort was het vrijwel onmogelijk om alle bijdragen van tweede orde te berekenen. Daarom werden alleen die bijdragen uitgerekend waarvan men veronderstelde dat ze het meest relevant waren. Ook bedacht men methoden om hogere–orde bijdragen af te schatten op grond van de reeds bekende eerste–orde bijdragen.

In hoofdstuk vier van dit proefschrift wordt de complete tweede–orde correctie op het Drell–Yan proces gepresenteerd. Deze berekening heeft als belangrijk resultaat dat het moeilijkste en tot nu toe altijd verwaarloosde subproces, namelijk quark–gluon verstrooiing, een cruciale rol speelt in die zin dat de tweede–orde correctie zeer klein wordt door zijn negatieve bijdrage. Als tweede resultaat laat de berekening zien dat de afhankelijkheid van de totale werkzame doorsnede van de massafaktorisatie schaal op tweede orde vrijwel verdwijnt. Deze twee feiten geven de indruk dat het totale theoretische tweede–orde resultaat betrouwbaar en nauwkeurig is. De convergentie van de storingsreeks bij hoge botsingsenergieën is goed te noemen. De nu nog resterende fout in de theoretische voorspelling wordt vrijwel geheel bepaald door de keuze van de parametrisatie van de partondichtheidsfunkties.

Curriculum vitae

Op 10 september 1965 ben ik geboren te Hardenberg. Na in 1983 aan de C.S.G. Jan van Arkel te Hardenberg het eindexamen Atheneum te hebben behaald, begon ik aan de studie Technische Natuurkunde aan de Technische Hogeschool Twente te Enschede. In juni 1984 legde ik het propaedeutisch examen af. In 1985 vervolgde ik mijn studie Natuurkunde aan de Rijksuniversiteit te Utrecht. In de experimentele stage onderzocht ik onder begeleiding van dr. W.N.J.C. van Asten en dr. C.C.A.M. Gielen de invloed van visuele–detectiemechanismen op het evenwicht van mensen. Dit vond plaats binnen de vakgroep Medische en Fysiologische Fysica. Het onderwerp van mijn theoretische afstudeerscriptie was een onderzoek naar de beschrijving van chirale anomalieën met behulp van storingstheorie, padintegralen en de connectie met de Atiyah–Singer indexstelling. Dit onderzoek werd eveneens gedaan aan de R.U.U., onder begeleiding van prof. dr. B.Q.P.J. de Wit. Het doctoraalexamen Natuurkunde met als bijvak Wiskunde werd in oktober 1987 afgelegd.

Per 1 december 1987 trad ik in dienst van de Rijksuniversiteit te Leiden om bij prof. dr. F.A. Berends en dr. W.L.G.A.M. van Neerven op het Instituut–Lorentz aan een promotieonderzoek te beginnen. Tijdens mijn promotieperiode bezocht ik het '1989 Cargèse Summer Institute on Particle Physics' te Cargèse, Corsica, wat mede mogelijk werd gemaakt door een subsidie van de Nederlandse Organisatie voor Wetenschappelijk Onderzoek (NWO). Gedurende drie cursusjaren heb ik werkcolleges bij het vak Quantumtheorie II verzorgd.

List of publications

- The contribution of the gluon–gluon subprocess to the Drell–Yan K-factor, T. Matsuura, R. Hamberg and W.L. van Neerven, Nucl. Phys. B345 (1990), 331
- The contribution of the gluon–gluon subprocess to the Drell–Yan K-factor, T. Matsuura, R. Hamberg and W.L. van Neerven, Nucl. Phys. B (Proc. Suppl.) 23B (1991), 3
- A complete calculation of the order α_s^2 correction to the Drell–Yan K-factor, R. Hamberg, W.L. van Neerven and T. Matsuura, Nucl. Phys. B359 (1991), 343
- The correct renormalization of the gluon operator in a covariant gauge, R. Hamberg and W.L. van Neerven, to be published in Nucl. Phys. B

Stellingen

1. Het onafhankelijk testen van de renormalisatie– en faktorisatieschaalafhankelijkheden van werkzame doorsneden is zinloos zolang er in de parametrisaties van de partondichtheidsfunkties maar één schaal geïmplementeerd is.

2. Voor n massieve 4–impulsen p_i kan men $n+1$ lichtachtige 4–impulsen k_i en n positieve parameters α_i vinden zodanig dat

$$p_i^\mu = k_{i-1}^\mu + \alpha_i k_i^\mu, \qquad (i = 1, \ldots, n)$$

waarbij $k_0^\mu = (k_n^0, \pm\vec{k}_n)$. Voor even n bestaat er een 'plus'–oplossing.

3. Beschouw de verzameling V van getallenparen $(s,p) \equiv (a+b, a\cdot b)$, waarbij a en b gehele getallen groter dan 1 zijn. De verzameling $W \subset V$ bestaat uit getallenparen die compatibel zijn met de volgende dialoog tussen twee personen, S en P, die respectievelijk alleen s en alleen p kennen en weten dat $(s,p) \in V$. Persoon P zegt: "Ik ken het getal s niet." Hierop reageert S met: "Dat wist ik al!" Vervolgens zegt P het getal s nu wel te kennen. Persoon S beweert tot slot: "Ik ken nu ook het getal p." De verzameling W kan worden geschreven als

$$W = \Big\{ (s,p) \in V : \Big| X(s) \equiv \Big\{ (s,p') \in V : \Big| \Big\{ (s',p') \in V : s' \bmod 2 = 1 \wedge s'-2 \notin \Pi \Big\} \Big| = 1 \Big\} \Big| = 1 \wedge (s,p) \in X(s) \Big\},$$

waarbij Π de verzameling van priemgetallen voorstelt. Hierbij is het vermoeden van Goldbach voor waar aangenomen. Het kleinste element van deze verzameling is (17,52); de produkten p zijn viervouden en de verzameling bevat oneindig veel elementen.

4. Het feit dat de Atiyah–Singer indexstelling in enkele gevallen bewezen kan worden in de context van supersymmetrische quantummechanische systemen, zegt meer over de mathematische correctheid van het laatstgenoemde dan over de indexstelling zelf.

5. Vanuit fysisch oogpunt gezien is het onwaarschijnlijk dat het Higgs–deeltje uit het standaardmodel elementair is.

6. Voor de volgende dimensioneel geregulariseerde integralen over de Minkowski-ruimte geldt:

$$\int \frac{d^n k}{(2\pi)^n} \frac{\prod_{i=1}^{2\alpha} k_{\mu_i}}{[k^2 + m^2]^\beta} = \frac{i(-1)^{\frac{1}{2}n}\Gamma(\beta-\alpha-\frac{n}{2})m^{n+2\alpha-2\beta}}{\alpha! 2^{2\alpha}(4\pi)^{\frac{1}{2}n}\Gamma(\beta)} \sum_\sigma \prod_{i=1}^{\alpha} g_{\mu_{\sigma(2i-1)}\mu_{\sigma(2i)}}$$

Hierbij wordt gesommeerd over alle permutaties σ van de getallen $1, \ldots, 2\alpha$.

7. Een toonsysteem dat als basiselementen de zuivere intervallen grote terts en quint heeft, kan redelijkerwijs slechts vier opeenvolgende tonen bevatten die alle een quint uit elkaar liggen.

8. Beschouw de logistieke afbeelding $f_c : \mathbb{C} \to \mathbb{C}$, gegeven door

$$f_c : z \to z^2 + c,$$

en laat $f_c^n(z)$ staan voor f_c n maal toegepast op z. Laat z_0 een nulpunt zijn van het polynoom $p(z,n) = f_c^n(z) - z$. De grootheid

$$\sigma = \sum_{i=0}^{n-1} f_c^i(z_0)$$

is een nulpunt van een polynoom waarvan de coëfficiënten rationale funkties zijn in c.

9. (a) Duursport kan dienen als therapie.
   (b) Bij de afweging of sportblessures onder de ziektewet behoren te vallen of niet, dient rekening gehouden te worden met de positieve effecten van sportbeoefening.

10. Een samenleving die als economisch systeem een stelsel heeft dat op enkel kapitalistische beginselen is gebaseerd, kent geen stabiele situaties die aanvaardbaar zijn vanuit het christelijke mensbeeld.

11. De hoge graad van compositorische perfektie en de mate van harmonische toegankelijkheid maken dat een groot deel van de werken van Wolfgang Amadeus Mozart tamelijk oninteressant is, dan wel als zodanig wordt uitgevoerd.

Roelof Hamberg
28 november 1991